PLANT PATHOGEN LIFE-HISTORY TRAITS AND ADAPTATION TO ENVIRONMENTAL CONSTRAINTS

EDITED BY: Christophe Le May, Josselin Montarry, Cindy E. Morris, Omer Frenkel and Virginie Ravigné

PUBLISHED IN: Frontiers in Plant Science and Frontiers in Microbiology

frontiers Research Topics

frontiers

ISSN 1664-8714
ISBN 978-2-88963-530-6
DOI 10.3389/978-2-88963-530-6

About Frontiers

Frontiers is more than just an open-access publisher of scholarly articles: it is a pioneering approach to the world of academia, radically improving the way scholarly research is managed. The grand vision of Frontiers is a world where all people have an equal opportunity to seek, share and generate knowledge. Frontiers provides immediate and permanent online open access to all its publications, but this alone is not enough to realize our grand goals.

Frontiers Journal Series

The Frontiers Journal Series is a multi-tier and interdisciplinary set of open-access, online journals, promising a paradigm shift from the current review, selection and dissemination processes in academic publishing. All Frontiers journals are driven by researchers for researchers; therefore, they constitute a service to the scholarly community. At the same time, the Frontiers Journal Series operates on a revolutionary invention, the tiered publishing system, initially addressing specific communities of scholars, and gradually climbing up to broader public understanding, thus serving the interests of the lay society, too.

Dedication to Quality

Each Frontiers article is a landmark of the highest quality, thanks to genuinely collaborative interactions between authors and review editors, who include some of the world's best academicians. Research must be certified by peers before entering a stream of knowledge that may eventually reach the public - and shape society; therefore, Frontiers only applies the most rigorous and unbiased reviews.
Frontiers revolutionizes research publishing by freely delivering the most outstanding research, evaluated with no bias from both the academic and social point of view. By applying the most advanced information technologies, Frontiers is catapulting scholarly publishing into a new generation.

What are Frontiers Research Topics?

Frontiers Research Topics are very popular trademarks of the Frontiers Journals Series: they are collections of at least ten articles, all centered on a particular subject. With their unique mix of varied contributions from Original Research to Review Articles, Frontiers Research Topics unify the most influential researchers, the latest key findings and historical advances in a hot research area! Find out more on how to host your own Frontiers Research Topic or contribute to one as an author by contacting the Frontiers Editorial Office: researchtopics@frontiersin.org

PLANT PATHOGEN LIFE-HISTORY TRAITS AND ADAPTATION TO ENVIRONMENTAL CONSTRAINTS

Topic Editors:
Christophe Le May, Agrocampus Ouest, France
Josselin Montarry, INRAe Centre Bretagne-Normandie, France
Cindy E. Morris, INRAe Centre Provence-Alpes-Côte d'Azur, France
Omer Frenkel, Agricultural Research Organization (ARO), Israel
Virginie Ravigné, Centre de Coopération Internationale en Recherche Agronomique pour le Développement (CIRAD), France

Citation: Le May, C., Montarry, J., Morris, C. E., Frenkel, O., Ravigné, V., eds. (2020). Plant Pathogen Life-History Traits and Adaptation to Environmental Constraints. Lausanne: Frontiers Media SA. doi: 10.3389/978-2-88963-530-6

Table of Contents

frontiers in Plant Science

EDITORIAL
published: 24 January 2020
doi: 10.3389/fpls.2019.01730

Editorial: Plant Pathogen Life-History Traits and Adaptation to Environmental Constraints

Christophe Le May[1]*, *Josselin Montarry*[1], *Cindy E. Morris*[2], *Omer Frenkel*[3] *and Virginie Ravigné*[4]

[1] IGEPP, INRA, Agrocampus-Ouest, Université de Rennes 1, Le Rheu, France, [2] INRA, UR Pathologie Végétale, Avignon, France, [3] Agricultural Research Organization, Volcani Center, Rishon LeZion, Israel, [4] BIOS Departement, PVBMT Laboratory, CIRAD, Montpellier, France

Keywords: coinfection, epidemic, host resistance, hydric stress, leaf maturity, non-agricultural habitats, survival, temperature

Editorial on the Research Topic

Plant Pathogen Life-History Traits and Adaptation to Environmental Constraints

Life-history is a key concept in evolutionary biology and ecology. It corresponds to the narrative of the various events punctuating the existence of an organism from his birth to his death (Begon et al., 2006; Michalakis et al., 2016). Throughout life, living organisms acquire resources that they actively find or extract from their environment and then allocate to different functions: development, survival, dispersal and reproduction (Roff, 1992; Stearns, 1992; Michalakis, 2009). Traits involved in the timing and amplitude of these allocation dilemmas are defined as life history traits. Life-history traits are often determinant for individuals (Kingsolver and Pfennig, 2007). They influence spatial and temporal disease dynamics, and thus the genetic diversity and structure of pathogen populations (Barrett et al., 2008; Michalakis et al., 2016). These determinants are involved in the ability of pathogens to adapt to varying ecological factors including changes in the biotic and abiotic effect, but also direct or indirect interactions with other strains or species of pathogens co-occurring on the same host (Michalakis et al., 2016; Tollenaere et al., 2016). For plant pathogens, these traits can be grouped into two categories: those involved in the epidemic phase, onto or into the host, and those related to the survival phase, often outside the host. Trade-off can occurred between these two phases, leading to consequences on epidemic dynamics, evolution, and speciation (Pariaud et al., 2009; Hamelin et al., 2011). Understanding processes maintaining variation in plant pathogen life-history traits is a central question in evolutionary ecology and a major challenge for the design of disease control strategies (Galvani, 2003; Grenfell et al., 2004).

The aim of this Research Topic was to collect research papers with vast perspective on plant pathogen life-history traits and adaptation to environmental constraints. Life-history traits of both epidemic and survival phases were considered, and tested environmental constraints included abiotic (temperature, precipitation, hydric stress) and biotic (habitat of origin, cultivar, maturity of leaves, coinfection) factors. Among the 10 accepted papers, three types of plant pathogens were considered: fungi (seven papers), nematodes (two papers), and oomycetes (one paper).

Regarding the epidemic phase, four main topics were covered by the research papers accepted in this special issue: *i)* host adaptation, *ii)* impact of host's physiological status, *iii)* adaptation to climatic conditions, and *iv)* effects of coinfection.

OPEN ACCESS

Edited and reviewed by:
Brigitte Mauch-Mani, Université de Neuchâtel, Switzerland

***Correspondence:**
Christophe Le May
lemay@agrocampus-ouest.fr

Specialty section:
This article was submitted to Plant Microbe Interactions, a section of the journal Frontiers in Plant Science

Received: *07 November 2019*
Accepted: *09 December 2019*
Published: *24 January 2020*

Citation:
Le May C, Montarry J, Morris CE, Frenkel O and Ravigné V (2020) Editorial: Plant Pathogen Life-History Traits and Adaptation to Environmental Constraints. Front. Plant Sci. 10:1730. doi: 10.3389/fpls.2019.01730

How host adaptation affects life history traits evolution was particularly analyzed by studying the effect of resistant cultivars onto several life-history traits. In the ascomycete *Colletotrichum gloeosporioides* the impact of host quantitative resistance on pathogen evolution was studied by evaluating the diversity of populations at the field scale at both neutral markers and pathogenic traits (Frezal et al.). Population genetic structure revealed a significant influence of clonal reproduction in *C. gloeosporioides* evolution and a low migration rate between fields. Results of cross-inoculation tests showed that aggressiveness of the fungal clones seemed to have evolved through an accumulation of components specific to each water yam cultivar, suggesting an adaptation to their host cultivar. Despite the remaining marks of adaptation to the former widely cultivated host, adaptation to current cultivars was clearly depicted. Such pattern of local adaptation to the dominant cultivar was previously highlighted in the potato late blight pathogen *Phytophthora infestans* (Andrivon et al., 2007). In their study, Mariette et al. explored whether the now classical negative relationship between offspring size and number occurred in this oomycete, *P. infestans*, and whether the trade-off was impacted by potato cultivar or host of origin of the pathogen (tomato and potato). They confirmed the existence of a trade-off and showed that it was not affected by any of these biotic factors. The observed polyphenism for these traits in *P. infestans* populations will favor the coexistence of distinct reproductive strategies.

Over the last years, intra-host dynamics has been identified as a major component of epidemiological and evolutionary dynamics of pathogens (Alizon et al., 2009). In plants it is known that host tissue characteristics vary a lot with tissue age. In particular, according the age of tissues, nutrient availability as well as defense levels may vary significantly, with opposing effects on the success of infection (Kus et al., 2002; Al-Naimi et al., 2005). Ontogenic resistance against powdery mildew (*Erysiphe necator)* on *Vitis vinifera* was studied by Calonnec et al. They showed that the three pathogenic traits studied (infection efficiency, sporulation, and mycelium growth) were affected, and their variation was strongly correlated with leaf age. Sporulation was more closely correlated with variations in sugar contents and the infection efficiency with leaf water content, suggesting that ontogenic resistance on grapevine leaves seems to be an immutable physiological process that *E. necator* is able to circumvent by restricting its development to sink tissue. Similarly, Maupetit et al. tested how nutrient availability and defense level impacted the development of *Melampsora larici-populina* (infection efficiency, latent period, uredinia size, mycelium quantity, sporulation rate, sporulation capacity, and spore volume). They showed that *M. larici-populina* was more aggressive on more mature leaves as indicated by wider uredinia and a higher sporulation rate. In contrast, phenolic contents (flavonols, hydroxycinnamic acid esters, and salicinoids) were negatively correlated with uredinia size and sporulation rate suggesting that pathogen's fitness appeared to be more constrained by the constitutive plant defense level than limited by nutrient availability, as evident in the decrease in sporulation.

Like other organisms, pathogens need a particular range of temperature and humidity in order to invade and develop on their host plant (Agrios, 2005). These two parameters particularly can modify spore germination, host colonization, spore production and dispersal of fungal pathogens (Fitt et al., 2006). Decades of research have generated considerable knowledge and greater understanding of the seasonal effects of temperature, rainfall, and humidity on diseases affecting major food crops (Garrett et al., 2011; Pautasso et al., 2011; Donatelli et al., 2017). In this special issue, two main parameters were studied, change in temperature and effect of water stress. Regarding the effect of temperature, Vaumourin and Laine developed a study on *Podosphaera plantaginis* and showed that temperature had a significant effect on all measured life-history traits, suggesting that the effect of temperature on life-history traits was both direct as well as mediated through a genotype-by-temperature interaction. Similarly, Mariette et al. showed on *P. infestans* that the negative relationship between offspring size and number was maintained for all the tested temperatures. Using cyst nematodes, other studies showed an effect of temperature on different life-history traits. Indeed, Fournet et al. showed a strong temperature effect on life-history traits of the beet cyst nematode *Heterodera schachtti*. While nematode multiplication was not differentially affected by temperatures, as favorable conditions for the host are also favorable for the parasite, the effect of temperature on hatching depended on the origin of populations, separating southern from northern European populations. Using a genome scan approach, Gendron St-Marseille et al. evaluated the adaptive potential of the soybean cyst nematode *Heterodera glycines*. The genotyping by sequencing of 64 *H. glycines* populations, allowed identifying 15 loci under selection for climatic or geographic co-variables. Lastly, regarding the effect of water stress, a transcriptomic and metabolomic approach was developed on the *Arabidopsis thaliana/Alternaria brassicicola* pathosystem, to study the level of susceptibility of the fungus to water stress and its impact on its seed transmission ability (N'Guyen et al.). These approaches led to the identification of specific proteins (hydrolipin) implicated in the tolerance toward water stress, and seed transmission, but not in the aggressiveness of the pathogen.

The ability of a pathogen to establish and grow on its host may be drastically altered by simultaneous infection by other pathogens (other strains or species of pathogens co-occurring on the same host). Life-history allocation may change under coinfection, affecting the evolutionary potential and epidemiological dynamics of pathogens (Tollenaere et al., 2016; Laine and Mäkinen, 2018). In their study, Vaumourin and Laine found that coinfection only modified the number of sexual resting structures produced, but did not changed the production of asexual forms. Coinfection studies, assessment of fungi sharing common characteristics, and host species, create a challenge for conventional disease diagnosis and subsequent management strategies. Indeed, lack of powerful tools to simultaneously distinguish and quantify these types of pathogens constitutes a major limitation. In their study, Abdullah et al. developed a duplex real-time PCR assay for

quantifying of co-infecting wheat pathogens, *Pyrenophora tritici-repentis* and *Parastagonospora nodorum*. The utility of the method was demonstrated using field samples of a cultivar sensitive to both pathogens. While visual and culture diagnosis suggested the presence of only one of the pathogen species, the assay revealed not only presence of both co-infecting pathogens (hence enabling asymptomatic detection) but also allowed quantification of relative abundances of the pathogens as a function of disease severity.

Survival stage outside the host has often been much overlooked due to the difficulty of its study. It is a key stage in pathogen's life cycle. Pathogens are all dependent on the life cycle, where despite the existence of dormant forms, evolutionary processes may occur. Thus, according to the status of their host (perennial or annual host plant), pathogens have to develop a wide array of strategies to overcome the alternation of presence/absence (and/or modification of physiological activity) of their host (Agrios, 2005). This survival phase is consequently important as it may affect the population size of the pathogen and lead to a bottleneck process. In this, special issue, research developed by Bardin et al. have investigated the ubiquity of the broad host range necrotrophic fungus *Botrytis cinerea*, outside of agricultural settings and have determined whether the populations in these natural habitats can be distinguished phenotypically and phylogenetically from populations isolated from diseased crops. Their results showed that *B. cinerea* strains sampled on different non-agricultural substrates were genetically and phenotypically similar to strains sampled in agricultural substrates. These results suggest that highly diverse populations of this plant pathogen persist outside of agriculture in association with substrates other than cultivated plants and that this component of their life-history is compatible with its capability to maintain its potential as plant pathogen. The survival phase was also considered in Vaumourin and Laine, as coinfection affects the number of sexual resting structures produced, and in Fournet et al., as they considered also the hatching after storage at different temperatures, simulating survival conditions during the inter-cropping period.

Considering plant pathogen traits in the context of life history trait evolution is a promising research avenue, still in its infancy. We hope that this research topic will help foster this line of research and provide a valuable resource for researchers working in the field of evolutionary ecology of plant pathogen populations.

AUTHOR CONTRIBUTIONS

CL, JM, CM, OF, and VR have made substantial direct contributions to the work, and approved it for publication.

ACKNOWLEDGMENTS

We thank all the authors involved in this research topic for their excellent and varied contributions.

REFERENCES

Agrios, G. N. (2005). *Plant Pathology- 5th ed* (United States: Elsevier Academic Press). 2005.

Alizon, S., Hurford, A., Mideo, N., and van Baalen, M. (2009). Virulence evolution and the trade-off hypothesis: history, current state of affairs and the future. *J. Evol. Biol.* 22, 245–259. doi: 10.1111/j.1420-9101.2008.01658.x

Al-Naimi, F. A., Garrett, K. A., and Bockus, W. W. (2005). Competition, facilitation, and niche differentiation in two foliar pathogens. *Oecologia* 143, 449–457. doi: 10.1007/s00442-004-1814-x

Andrivon, D., Pilet, F., Montarry, J., Hafidi, M., Corbière, R., Achbani, E. H., et al. (2007). Adaptation of *Phytophthora infestans* to partial resistance in potato: evidence from French and Moroccan populations. *Phytopathol* 97, 338–343. doi: 10.1094/PHYTO-97-3-0338

Barrett, L. G., Thrall, P. H., Burdon, J. J., and Linde, C. C. (2008). Life history determines genetic structure and evolutionary potential of host–parasite interactions. *Trends Ecol. Evol.* 23, 678–685. doi: 10.1016/j.tree.2008.06.017

Begon, M., Townsend, C. R., and Harper, J. L. (2006). *Ecology: from individuals to ecosystems* (Malden, MA: Blackwell Pub.).

Donatelli, M., Magarey, R. D., Bregaglio, S., Willocquet, L., Whish, J. P. M., and Savary, S. (2017). Modelling the impacts of pests and diseases on agricultural systems. *Agric. Syst.* 155, 213–224. doi: 10.1016/j.agsy.2017.01.019

Fitt, B. D. L., Huang, Y.-J., van den, Bosch F, and JS, West (2006). Coexistence of related pathogen species on arable crops in space and time. *Ann. Rev. Phytopathol.* 44, 163–182. doi: 10.1146/annurev.phyto.44.070505.143417

Galvani, A. P. (2003). Epidemiology meets evolutionary ecology. *Trends Ecol. Evol.* 18 (3), 132–139.

Garrett, K. A., Nita, M., De Wolf, E. D., Esker, P. D., Gomez-Montano, L., and Sparks, A. H. (2011). "Plant pathogens as indicators of climate change," in *Climate Change (2nd edn): Observed Impacts on Planet Earth*. Ed. Trevor M. Letcher (Amsterdam, The Netherlands: Elsevier BV), 325–338.

Grenfell, B. T., Pybus, O. G., Gog, J. R., Wood, J. L. N., Daly, J. N., Mumford, J. A., and Holmes, E. C. (2004). Unifying the epidemiological and evolutionary dynamics of pathogens. *Science* 303 (5656), 327–332.

Hamelin, F., Castel, M., Poggi, S., Andrivon, D., and Mailleret, L. (2011). Seasonality and the evolutionary divergence of plant parasites. *Ecology* 92 (12), 2159–2166. doi: 10.1890/10-2442.1

Kingsolver, J. G., and Pfennig, D. W. (2007). Patterns and power of phenotypic selection in nature. *BioScience* 57 (7), 561–572. doi: 10.1641/B570706

Kus, J. V., Zaton, K., Sarkar, R., and Cameron, R. K. (2002). Age-related resistance in Arabidopsis is a developmentally regulated Ddfense response to *Pseudomonas syringae*. *Plant Cell* 14, 479–490. doi: 10.1105/tpc.010481

Laine, A.-L., and Mäkinen, H. (2018). Life-history correlations change under coinfection leading to higher pathogen load. *Evol. Lett.* 2, 126–133. doi: 10.1002/evl3.48

Michalakis, Y., Charmantier, A., Gaillard, J.-M., Sorci, G., Tully, T., and Ronce, O. (2016). "Evolution des traits d'histoire de vie," in *Biologie évolutive* (Louvain-la-Neuve: De Boeck Supérieur), 373–422.

Michalakis, Y. (2009). "Parasitism and the evolution of life-history traits," in *Ecology and evolution of parasitism* (Oxford: Oxford University Press), 19–30.

Pariaud, B., Ravigne, V., Halkett, F., Goyeau, H., Carlier, J., and Lannou, C. (2009). Aggressiveness and its role in the adaptation of plant pathogens. *Plant Pathol.* 58, 409–424. doi: 10.1111/j.1365-3059.2009.02039.x

Pautasso, M., Doring, T. F., Garbelotto, M., Pellis, L., and Jeger, M. J. (2011). Impacts of climate change on plant diseases—opinions and trends. *Eur. J. Plant Pathol.* 133, 295–313. doi: 10.1007/s10658-012-9936-1

Roff, D. A. (1992). *The evolution of life histories: theory and analysis* (New York: Chapman and Hall).

Stearns, S. C. (1992). *The evolution of life histories* (Oxford: Oxford University Press).

Tollenaere, C., Susi, H., and Laine, A.-L. (2016). Evolutionary and epidemiological implications of multiple infection in plants. *Trends Plant Sci.* 21, 80–90. doi: 10.1016/j.tplants.2015.10.014

Conflict of Interest: The authors declare that the research was conducted in the absence of any commercial or financial relationships that could be construed as a potential conflict of interest.

frontiers in Plant Science

ORIGINAL RESEARCH
published: 17 July 2018
doi: 10.3389/fpls.2018.00987

Genome Scans Reveal Homogenization and Local Adaptations in Populations of the Soybean Cyst Nematode

*Anne-Frédérique Gendron St-Marseille[1,2], Etienne Lord[1], Pierre-Yves Véronneau[1], Jacques Brodeur[2] and Benjamin Mimee[1]**

[1] Saint-Jean-sur-Richelieu Research and Development Centre, Agriculture and Agri-Food Canada, Saint-Jean-sur-Richelieu, QC, Canada, [2] Institut de Recherche en Biologie Végétale (IRBV), Université de Montréal, Montréal, QC, Canada

Determining the adaptive potential of alien invasive species in a new environment is a key concern for risk assessment. As climate change is affecting local climatic conditions, widespread modifications in species distribution are expected. Therefore, the genetic mechanisms underlying local adaptations must be understood in order to predict future species distribution. The soybean cyst nematode (SCN), *Heterodera glycines* Ichinohe, is a major pathogen of soybean that was accidentally introduced in most soybean-producing countries. In this study, we explored patterns of genetic exchange between North American populations of SCN and the effect of isolation by geographical distance. Genotyping-by-sequencing was used to sequence and compare 64 SCN populations from the United States and Canada. At large scale, only a weak correlation was found between genetic distance (Wright's fixation index, F_{ST}) and geographic distance, but local effects were strong in recently infested states. Our results also showed a high level of genetic differentiation within some populations, allowing them to adapt to new environments and become established in new soybean-producing areas. Bayesian genome scan methods identified 15 loci under selection for climatic or geographic co-variables. Among these loci, two non-synonymous mutations were detected in SMAD-4 (mothers against decapentaplegic homolog 4) and DOP-3 (dopamine receptor 3). High-impact variants linked to these loci by genetic hitchhiking were also highlighted as putatively involved in local adaptation of SCN populations to new environments. Overall, it appears that strong selective pressure by resistant cultivars is causing a large scale homogenization with virulent populations.

Keywords: Bayesian outlier detection, genetic diversity, genotyping-by-sequencing, *Heterodera glycines*, isolation by distance

OPEN ACCESS

Edited by:
Christophe Le May, Agrocampus Ouest, France

Reviewed by:
Yessica Rico, Instituto de Ecología (INECOL), Mexico
Sebastian Eves-van Den Akker, University of Cambridge, United Kingdom

***Correspondence:**
Benjamin Mimee
benjamin.mimee@agr.gc.ca

Specialty section:
This article was submitted to Plant Microbe Interactions, a section of the journal Frontiers in Plant Science

Received: *21 March 2018*
Accepted: *18 June 2018*
Published: *17 July 2018*

Citation:
Gendron St-Marseille A-F, Lord E, Véronneau P-Y, Brodeur J and Mimee B (2018) Genome Scans Reveal Homogenization and Local Adaptations in Populations of the Soybean Cyst Nematode. Front. Plant Sci. 9:987. doi: 10.3389/fpls.2018.00987

INTRODUCTION

The introduction of an organism into a new environment can have unpredictable detrimental consequences, including public health problems, losses in biodiversity and ecosystem services or crop yield losses due to exotic weeds, insects and pathogens, altogether resulting in significant economic impact (Pimentel et al., 2005). Unfortunately, the steady increase in international trade

facilitates the movement and introduction of new invasive species (Hulme, 2009). In addition, climate change is altering environmental conditions and could change the species' distribution range or favor their establishment in previously unsuitable habitats (Early and Sax, 2014). It is therefore imperative to carry out specific risk assessment in order to target species to be controlled. Alien invasive species, by definition, did not evolve in the biogeographic habitat in which they are introduced. Consequently, they are often poorly adapted to their new environment. Generally, the most successful invaders will have a high potential for rapid adaptation through phenotypic plasticity or microevolution (Novak, 2007). Understanding the genetic mechanisms of local adaptation is therefore critical to predict future species distribution.

Plant-parasitic nematodes are microscopic worms that reduce global annual food production by 12.3% and cause more than US$157 billion in economic losses worldwide (Hassan et al., 2013). In North America, one of the most damaging species is the soybean cyst nematode (SCN), *Heterodera glycines* Ichinohe. Since its first detection in 1954 in Hanover County, North Carolina, SCN has been reported in almost every soybean-producing county in the United States (Davis and Tylka, 2000), as well as in southwestern Ontario, Canada (Anderson et al., 1988). During the 2000s, SCN colonized several new northern localities in the United States (North Dakota in 2003; Mathew et al., 2015) and Eastern Canada (northeastern Ontario in 2007 and Québec in 2013; Mimee et al., 2014). A few studies have investigated SCN dispersal, which seems to follow a northward and eastward pathway in North America (Tylka and Marett, 2017). This dispersion pattern correlates with the expansion of soybean cultivation following the introduction of new soybean varieties with shorter maturity periods and improved tolerance to drought and cold (Shurtleff and Aoyagi, 2010; Yu, 2011).

It is expected that SCN would survive and multiply throughout the current North American soybean-growing area and complete at least two generations at its northern limit (Gendron St-Marseille, 2013). Climate warming should also favor the establishment of SCN at higher latitudes and increase the number of generations per year in most regions. However, these predictions are based strictly on temperature requirements and do not account for the intrinsic capacity of SCN to adapt to new environmental conditions. Genetic variations within a population reflect its evolutionary potential and result from four evolutionary forces that affect individual fitness: mutation, gene flow, selection, and genetic drift (Eizaguirre and Baltazar-Soares, 2014). For most organisms, including SCN, the relative weights of these forces can differ significantly. Mutations are rare events that should not contribute significantly to SCN adaptations in a short time frame. Gene flow depends on the dispersal ability of an organism, which for SCN is achieved mainly by means of human activities at the short spatial scale (Kristjansson, 2010). In addition, wind and flooding can carry SCN cysts over very long distances, and contribute to its dispersal at the regional and continental scales. Many different selection pressures can shape the genetic structure of SCN populations, but host plant is probably the strongest selection factor. The ability of SCN to reproduce on a given soybean genotype differs greatly depending on its resistance genes and the nematode's virulence profile (HG type) (Colgrove and Niblack, 2008; Niblack et al., 2008). Thus, management decisions by growers (for example, the systematic use of resistant cultivars) can result in a strong selection pressure. Finally, the influence of genetic drift will also depend on pest control strategies, because they contribute to dictate population size, although it was shown for cyst nematodes that genetic diversity can be very high within a single cyst (Green et al., 1970). Each nematode female can mate with several males and lay hundreds of eggs that can survive for at least a decade in the soil (Slack et al., 1972). Thus, even if the diversity appears reduced due to genetic drift under strong selection by resistant cultivars, most alleles probably persist for several years in the population in a "dormant" state.

In other cyst nematode species, genetic diversity at the population level has been studied by means of several techniques, including microsatellite markers, ITS-RFLP (internal transcribed spacer–restriction fragment length polymorphism), RAPD (random amplified polymorphic DNA), and 2-DGE (two-dimensional gel electrophoresis) (e.g., Blok et al., 1997; Grenier et al., 2001; Plantard et al., 2008; Boucher et al., 2013). However, these methods focus only on specific sections of the genome, yield very few markers, or do not allow precise comparisons among populations. For example, Eves-van den Akker et al. (2015) recently published a metagenetic approach to genotype populations of the pale cyst nematode, *Globodera pallida*. While this method was shown powerful to rapidly evaluate genetic diversity and distribution of specific mitotypes, it is based on very few neutral markers, which prevent any assessment for selection. Genome scan is an interesting approach for the identification of genetic loci involved in adaptation to specific selection pressure. It was notably used in *G. pallida* to identify genomic regions associated with virulence on resistant potato cultivars (Eoche-Bosy et al., 2017).

Despite rapid advances in next-generation sequencing (NGS) technologies, sequencing a large number of individual genomes at high coverage in order to perform population genetic studies remains very expensive and may require important quantities of DNA from individuals. Elshire et al. (2011) developed a genotyping-by-sequencing (GBS) protocol to rapidly identify single-nucleotide polymorphisms (SNPs). The GBS technique and other restriction-site-associated DNA (RAD) sequencing methods produce large quantities of reads that do not cover the entire genome but have higher sequencing depth, thus reducing sequencing errors (Gautier et al., 2013; Anand et al., 2016). Loci generated by GBS can be present in both coding and non-coding regions and will be shared between all populations owing to the conservation of restriction sites (Cariou et al., 2013). Finally, GBS does not require any prior genomic information for the species being studied, which is an important consideration for SCN since there is no reference genome yet. The optimal gene coverage to reduce the amount of missing data depends on the choice of restriction enzyme (Fu et al., 2016). Fortunately, optimal gene coverage was already tested for the closely related species *Globodera rostochiensis* (Mimee et al., 2015).

The main objectives of this study were to (1) investigate the genetic relationships among SCN populations from United States

and Canada, (2) detect isolation by geographical distance (IBD) between SCN populations from United States and Canada, (3) detect genetic loci under selection associated to environmental and climatic parameters, and (4) identify the putative gene functions contributing to the adaptation of SCN populations to specific environmental conditions.

MATERIALS AND METHODS

Soybean Cyst Nematode Populations Sampling and Genotyping-by-Sequencing

A total of 64 field populations of SCN, representative of the area currently infested in North America, were sampled or provided by collaborators from 11 US states (Delaware, Iowa, Illinois, Indiana, Kansas, Michigan, Minnesota, Missouri, North Dakota, Ohio, South Dakota) and one Canadian province (Ontario) (**Figure 1**). For DNA extraction, 40 cysts were randomly chosen from each population and pooled together. Eggs were extracted from each cyst and then washed twice in sterile filtered water. Total genomic DNA of each pool was extracted using the DNeasy Blood and Tissue Kit (Qiagen, Mississauga, ON, Canada) following the manufacturer's instructions. DNA extracts were quantified using Qubit fluorometric quantification (ThermoFisher Scientific, Burlington, ON, Canada) and normalized at 2 ng/μL prior to library preparation and sequencing. These steps were performed following standard protocols (Elshire et al., 2011; Poland et al., 2012) at the Institute for Integrative and Systems Biology (IBIS; Université Laval, Québec City, QC, Canada). Genotyping-by-sequencing was performed using the method described by Mimee et al. (2015) with a combination of two restriction enzymes (PstI/MspI) (New England Biolabs, Whitby, ON, Canada). After the restriction enzyme treatment, all samples (one composite per field population) were barcoded and multiplexed to obtain a single library for the 64 samples, which was sequenced on three Ion Proton chips (ThermoFisher Scientific) at IBIS.

Single-Nucleotide Polymorphism Calling

The UNEAK pipeline (Lu et al., 2013), which is part of the TASSEL 3.0 bioinformatics analysis package (Bradbury et al., 2007), was used to process the raw reads, since no complete reference genome is yet available for *H. glycines*. This pipeline is designed to call SNPs *de novo*, without a reference genome with high stringency. Only sequences containing a single putative SNP (1-bp mismatch) per sequencing read were kept. Before analysis, the SNPs were further filtered with a minimum coverage (minCov) of 20 reads, a maximum coverage (maxCov) of 10,000 reads, and a minimum allele frequency (MAF) of 0.01.

Population Genetics

Clustering of SCN populations using PCA was carried out using the *prcomp* function from the *stats* package in R software (R Core Team, 2017). The *poppr* package (v2.4.1) in R (Kamvar et al., 2014) was used to investigate the genetic relationship between populations and to build a phylogenetic tree (Provesti's distance, 10,000 bootstraps, neighbor-joining algorithm counting missing data as equivalent in the distance computation). Visualization of sample coordinates and phylogenetic relationship analyses were carried out using the *phytools* 0.6–20 package in R (Revell, 2017).

Fixation index (F_{ST}) values (Wright, 1943) were calculated using the classical approach (Hartl and Clark, 2007) with the PoPoolation2 software (Kofler et al., 2011) to evaluate the genetic differentiation between each pair of populations. Furthermore, the effect of isolation by distance on population structure was tested using the correlation between the genetic distance ratio [$F_{ST}/(1–F_{ST})$], as defined by Rousset (1997), and the geographic distance of population pairs in kilometers (km). The geographic distance between each sample location was calculated with the haversine formula using the geosphere package in R. To examine the significance of the relationship between the genetic distance ratio and the pairwise geographic distance distances, we performed a Mantel test (Spearman rank correlation) using the vegan package in R with 999 permutations. To evaluate the effect of time on population genetic differentiation, linear regression analyses were run in R software using pairwise F_{ST} distances based on a point of origin selected on the basis of the first reports of SCN in North America. In our dataset, the closest sample to the oldest population was located in Clarkton, Missouri (MO1) (Hegge, 1957; Tylka and Marett, 2017). To access the genetic isolation from the MO1 location, a Spearman rank correlation (r_s) test was performed at a 0.95 confidence level.

Populations from three states (North Dakota, Minnesota, Illinois) were selected as case studies to evaluate the local (short-scale) genetic differentiation. These states were chosen because there were sufficient samples for comparison and because (i) North Dakota shows a recent introduction of SCN and a continuous northward dispersal of the nematode (Nelson and Bradley, 2003; Mathew et al., 2015); (ii) Minnesota has a longer history of SCN, with the nematode being first detected in 1978 and the infested area still expanding each year (Zheng et al., 2006); (iii) in Illinois SCN has been well established in every county for many years (Riggs, 2004; Tylka and Marett, 2017).

Outlier Detection and Their Association With Environmental Variables

Two geographic and four climatic covariables were investigated as possible factors explaining loci under selection: latitude (LAT), longitude (LONG), annual mean air temperature (BIO1), maximum air temperature of the warmest month (BIO5), annual precipitation (BIO12), and total precipitation of the warmest quarter (BIO18). All climatic variables were retrieved from the WorldClim global climate database, version 1.4 (Fick and Hijmans, 2017), corresponding to historic conditions (1960–1990). The spatial resolution used for the bioclimatic analysis was set at 30 s or 0.86 km^2.

To detect correlations between variations in population allele frequencies of SNPs and environmental factors, we used three different Bayesian methods (software programs): BayPass, version 2.1 (Gautier, 2015), BayeScan, version 2.1 (Foll and Gaggiotti, 2008), and BayeScEnv, version 1.1 (de Villemereuil and Gaggiotti, 2015). For each program, triplicate runs with different random seeds were performed with a pilot run of

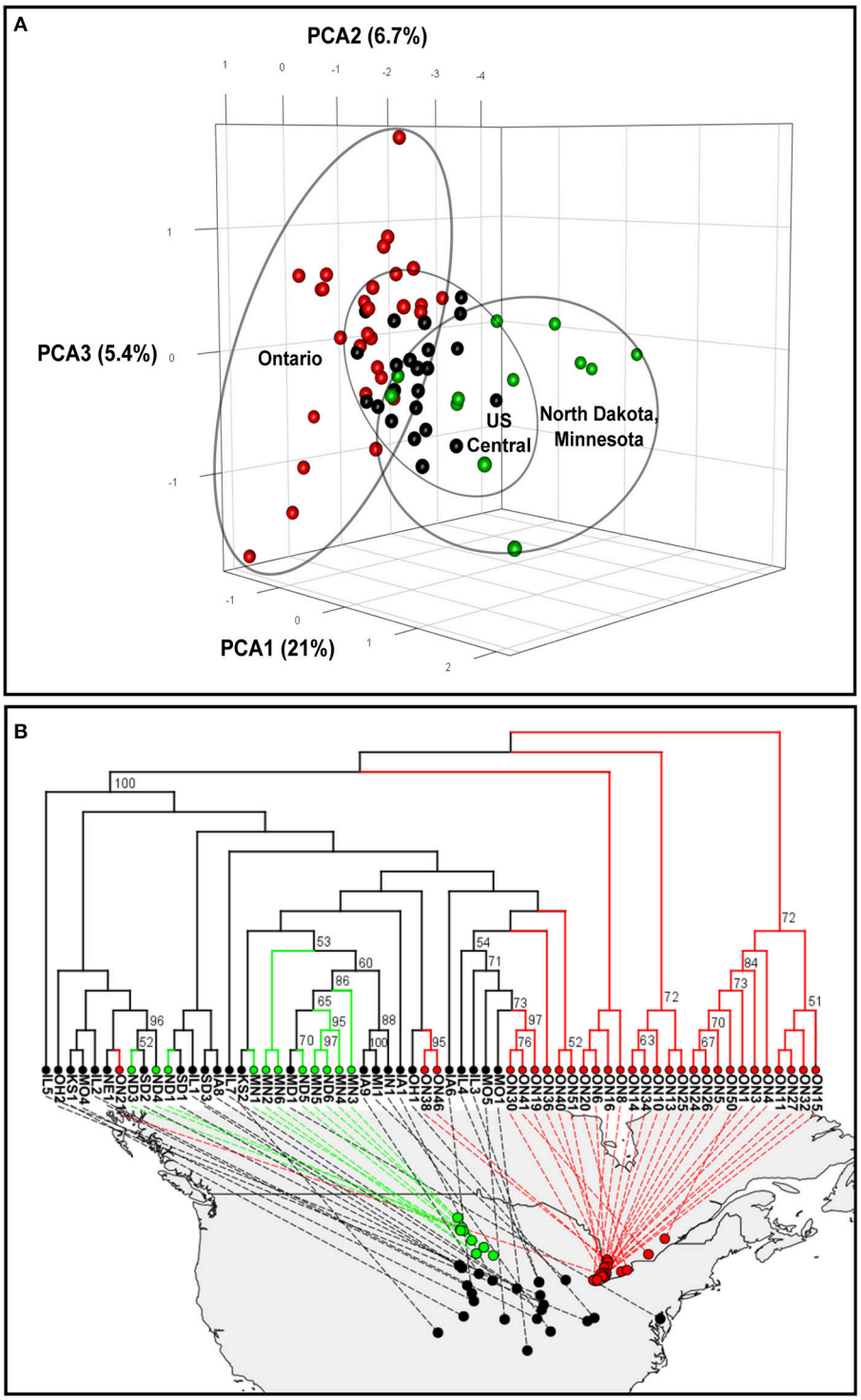

FIGURE 1 | Genetic relationship among North American populations of the soybean cyst nematode. **(A)** Three-dimensional principal component analyses (PCAs). **(B)** Phylogenetic tree plot based on Provesti's absolute genetic distance. Significant bootstrap values (> 50%) are indicated. Soybean cyst nematode populations from Ontario (Canada), North Dakota and Minnesota, and central US states are indicated in red, green and black, respectively.

10,000 iterations to estimate starting parameters, a burn-in length of 50,000 iterations, and a minimum of 50,000 iterations, accounting for the small number of SNPs being investigated. Post-run diagnostics were carried out using the *coda* package in R software in order to ensure sufficient iterations and normality of the Markov chain (Plummer et al., 2006).

The first software, BayPass, identifies genetic markers subject to selection by covariates such as phenotypic or environmental variables associated with the population of interest (Gautier, 2015). This application is based on the BAYENV model proposed by Coop et al. (2010) and Günther and Coop (2013), but with several modifications detailed in Gautier (2015), including the reprogramming of the Markov chain Monte Carlo (MCMC) algorithm. For BayPass, we used a pool-size file with the –d0yij option set at 800 and 20 pilot runs with a length of 10,000 iterations, a burn-in length of 50,000 iterations, and a chain length of 50,000 iterations. For each SNP, BayPass generates a Bayes factor (BF), quantifying evidence against the null hypothesis, and an empirical Bayesian *p*-value (eBPis), a metric measuring the difference between observed data and a simulated set of data (posterior distribution) (Kass and Raftery, 1995; Andraszewicz et al., 2015; Gautier, 2015). To be considered under selection, a SNP had to meet two criteria: a BF greater than 10 (BF $>$ 10) and an eBPis lower than 0.05 (eBPis $<$ 0.05).

The second software, BayeScan, uses a Bayesian likelihood method that assumes a Dirichlet distribution of allele frequencies between populations (Foll, 2012). This program estimates the probability that each locus is subject to selection by using a logistic regression on the two locus-population F_{ST} coefficients. This Bayesian method uses a reversible-jump MCMC algorithm to calculate a posterior probability that each locus is under selection. The decision criterion to determine whether a locus is likely to be under a strong selection is the *q*-value (Foll, 2012), analog to a false discovery rate (FDR) *p*-value, that must be under 0.05. A second decision criterion was applied to further endorse the selected outliers: the ratio of posterior probabilities (PO). The PO threshold to affirm that a locus was under selection, in comparison with a neutral model, was set to 0.91, which corresponds to a strong relationship on the Jeffreys scale (Foll, 2012). We used BayeScan with the default parameters, but we set the minimum number of iterations to 50,000, the length of 20 pilot runs to 10,000 iterations, and the burn-in length to 50,000 iterations.

The third software, BayeScEnv, is similar to BayeScan and uses the F_{ST} index to detect loci with a high level of differentiation in comparison with the entire genome. This program allows a normalization vector to be applied to the environmental data instead of only a binary combination, thus generating a lower number of false positives, according to the creators of the software (de Villemereuil and Gaggiotti, 2015). We used BayeScEnv with the default parameters, with the number of iterations set to 50,000 and 20 pilot runs with a length of 10,000 iterations. We used the reported *q*-value, which is related to the FDR, as our decision criterion, considering only SNPs with a *q*-value less than 0.05.

Localization of Outlier Loci, Gene Function, and Genic Environment

The SNPs identified in short reads were first retrieved from a draft SCN genome available from SCNBase (https://www.scnbase.org/) by means of BLASTN with the default parameters, except for a smaller word size of 4, with the Blast2GO application (Conesa et al., 2005). Many of the identified SNP-containing fragments matched multiple genes or genome locations (see Supplementary Tables 3–5). To assign a putative gene function to each SNP, we compared the aligned sequences to the National Center for Biotechnology Information (NCBI) protein database by means of BLASTX and BLASTP (Altschul et al., 1990) on a subset of sequences (nematodes, taxid: 6231) or to all of the NCBI non-redundant (nr) sequence database with an *E*-value significance cutoff of $1e^{-5}$.

As our GBS sequencing covers approximately 0.8% of the genome (see Results section), we explored the genomic regions around outlier loci for genetic hitchhiking in whole-genome sequences from four populations of different origin and distinct virulence profile (ON1, ON34, IL4, and KS2). Sequencing libraries were prepared using the Nextera XT DNA Library Preparation Kit (Illumina, San Diego, CA) and sequenced on a MiSeq sequencer (Illumina) using the MiSeq Reagent Kit v3 (600-cycle). Reads were demultiplexed using the Sabre software program (https://github.com/najoshi/sabre) and processed with Trimmomatic (v0.32) (Bolger et al., 2014) to remove adapters and barcodes. Alignment on the draft reference genome (see above) was done using SAMtools (v0.1.19) (Li et al., 2009) and BWA (v0.7.12) (Li and Durbin, 2009). Only a window of ± 50 kb around the 15 loci under selection was retained for the genic environment analysis. Variants were called with freebayes (v1.0.2) (Garrison and Marth, 2012) and snpeff (v4.2) (Cingolani et al., 2012). Distribution of allele frequencies in these four populations for each gene variant was compared with the allele frequency of the corresponding loci under selection in the same population in the genotyping-by-sequencing dataset. Only SNPs exhibiting a similar allele frequency and having a high impact on the predicted protein product were retained in our analysis.

RESULTS

Genotyping-by-Sequencing

A total of 192,576,709 short reads were obtained from the sequencing of the DNA from the 64 SCN populations, following digestion by the PstI/MspI restriction enzymes. The *H. glycines* effective genome length was estimated to be 96,752,286 bp, with an average of one PstI restriction site every 12,688 bases (E. Lord, private communication, 2017). On the basis of the sequence size used by the UNEAK (Universal Network-Enabled Analysis Kit) pipeline (first 64 bp of each read), the expected horizontal coverage was approximately 0.8% of the total SCN genome, and the vertical coverage at each locus, considering the number of reads obtained, was 400×. Before filtering, the UNEAK pipeline identified 3,172 variants. After filtering for low coverage and selecting only SNP variants, two datasets were generated. The first dataset contained 245 SNPs without missing data (loci sequenced in all populations), and the second contained 804 SNPs with missing data (Sequences and coverage in Supplementary Table 7).

Population Structure

Principal Component Analysis

A principal component analysis (PCA) was performed using the dataset without missing data, which contained 245 SNPs. The

PCA plot of the 64 North American SCN populations revealed a geographically ordered pattern (**Figure 1A**). Overall, the Ontario populations showed the greatest dispersion, indicating they are more genetically differentiated, while the central regions of the US showed more clustered populations. Also, the group containing populations from Minnesota and North Dakota (in green in **Figure 1A**) was clearly different from the Ontario populations by the first axis, which explained 21% of the total variation. All populations from the central states, although they originated from many states and covered a much wider area, were less diverse and more clustered together.

Phylogenetic Tree

To better understand the population structure of each population, we used the 804-SNP dataset to conduct a phylogenetic analysis based on Provesti's distance. The inferred neighbor-joining phylogenetic tree (**Figure 1B**) showed that most of the Ontario samples (in red in **Figure 1B**) were different from the rest of the North American populations. Some samples from Ontario were found to be different from each others and more similar to those of central states. Such a pattern can also be observed in the PCA analysis (**Figure 1A**).

Genetic Differentiation

Overall, we observed an average value for Wright's fixation index (F_{ST}) of 0.15 ± 0.07. However, pairwise genetic distance was highly variable, with a minimum F_{ST} of 0.005 and a maximum F_{ST} of 0.53 (Supplementary Table 1). The highest F_{ST} value was found between two of the most remote populations, ND6 from North Dakota and ON41 from Ontario, which were separately by approximately 1,720 km. On the other hand, the lowest F_{ST} value was observed between ON3 and ON5, which were separated by only 17.9 km. In general, higher F_{ST} values were found in distant populations, especially between populations from Minnesota (MN4 and MN5), North Dakota (ND3 and ND6), South Dakota (SD2), and Ontario (ON6, ON13, ON25, ON41, and ON46).

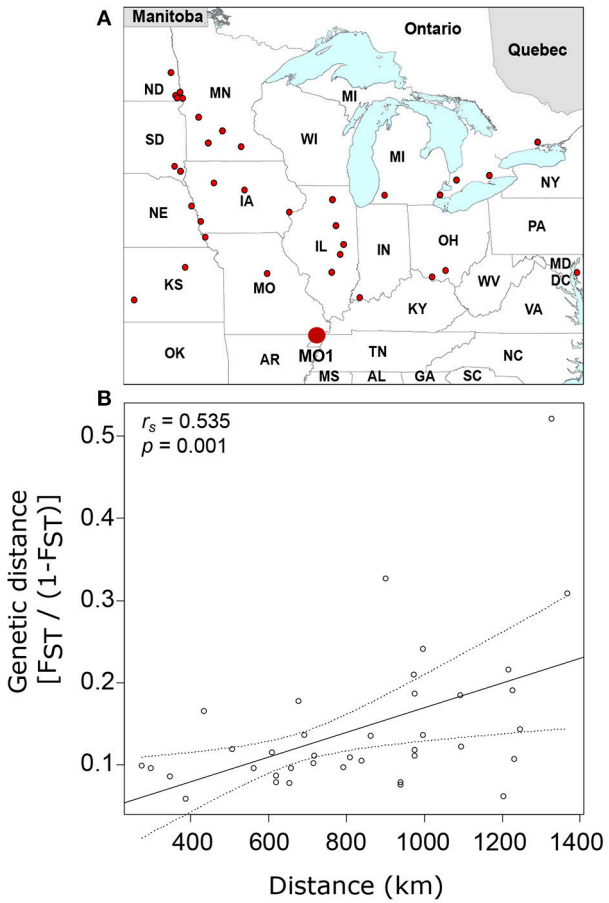

FIGURE 2 | Distribution of soybean cyst nematode populations used in this study (small dots) and identification of the "oldest" sample in the dataset (MO1, large dot) **(A)** as well as the relationship between genetic distance [F_{ST}/(1–F_{ST})] and geographic distance **(B)**. Linear regression line is shown with 95% confidence intervals estimated using 1,000 bootstrap replicates.

Isolation by Distance

The analysis of the relationship between genetic distance [F_{ST}/(1–F_{ST})] and geographic distance (km) for all pairs of populations revealed a significant ($p = 0.012$) but weak effect of isolation by distance, with a Mantel correlation (r) of only 0.135. However, when analyzing the effect of isolation by distance at the local scale, a different pattern was found. With respect to US states with recent SCN history, a strong and significant positive correlation was observed between the genetic and geographic distances in North Dakota ($r = 0.430$, $p = 0.013$) and Minnesota ($r = 0.730$, $p = 0.006$). In contrast, no correlation was found among the populations from Illinois ($r = -0.170$, $p = 0.767$).

To further explore the contribution of isolation by distance to the genetic differentiation of United States and Canada populations of SCN, we compared the genetic distance of each population from a theoretical ancestor population (MO1) using the 245-SNP dataset. This analysis included 38 independent populations that were separated by 273 to 1,367 km from MO1 (**Figure 2A**). The genetic-distance ratio to the "oldest population" varied from 0.06 for IL1 (386 km apart) to 0.52 for ND6 (1,327 km apart) (Supplementary Table 2) and an overall moderate ($r_s = 0.535$) but significant ($p = 0.001$) relationship was observed between genetic distance and geographic distance (**Figure 2B**).

Signature of Genetic Adaptations

Genome Scans

Using three Bayesian inference genome scan approaches, we identified 71 SNPs (out of 804) that were under selection. Among the different computational methods, 48 loci were identified by BayeScan, 23 loci were identified by BayPass, and 16 loci were identified by BayeScEnv (Supplementary Tables 3–5). Out of those 71 SNPs, only one was highlighted by the three methods, while 15 outliers were inferred by at least two of the methods (**Figure 3**). The geographic variables (LAT and LONG) were associated with seven and eight outlier loci, respectively, and the climatic variables (BIO1, BIO5, BIO12, and BIO18) were associated with nine, six, eight, and seven SNPs, respectively (**Table 1**). Three SNPs were strictly associated with

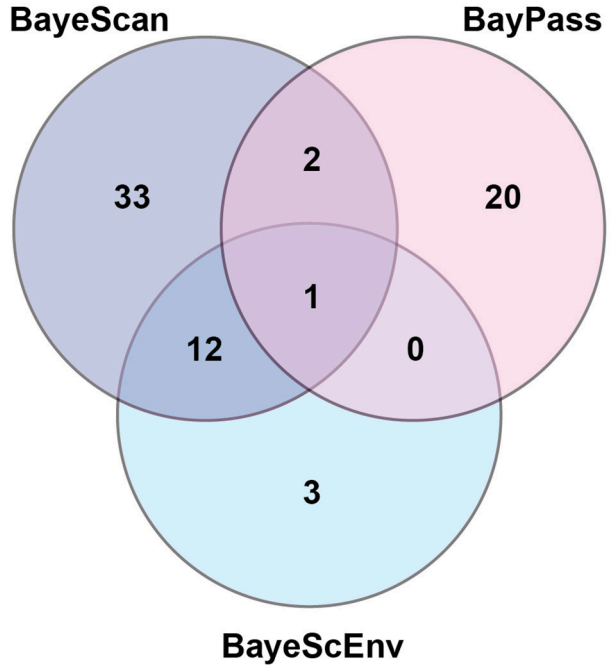

FIGURE 3 | Number of outlier loci identified by three different Bayesian genome scan methods in 64 populations of the soybean cyst nematode from North America.

only one environmental variable: TP188858 was associated with maximum temperature, while TP252086 and TP364091 appeared to be linked to annual temperature. The allele frequencies analysis at these 15 loci revealed SNPs that were specific for a given region, such as TP364091, TP181514, and TP333913 for Minnesota and North Dakota and TP376687, TP146577, and TP226227 for Ontario (**Figure 4**).

Localization, Effect, and Genic Environment of Outlier Loci

Of the 15 SNPs under selection identified by at least two Bayesian approaches, 10 SNPs were located in predicted genes (seven in exons and three in introns), and five SNPs were located in intergenic regions (**Table 2**). Two SNPs (TP380188 and TP364091) correspond to non-synonymous mutations that induce a change in the amino acid sequence of the resulting protein. The annotations of the genes putatively impacted by these modifications are SMAD-4 (mothers against decapentaplegic homolog 4) for TP380188 and DOP-3 (dopamine receptor 3) for TP364091. The sequence corresponding to TP364091 was retrieved in four different genes (g14639.t1, g14642.t1, g14644.t1, and g14654.t1) in the draft reference genome and introduced two different mutations (Supplementary Tables 3–5). All the other SNPs (13/15) were silent mutations (synonymous in exons or located in introns or intergenic regions) and thus probably not the cause of their selection. Among the 42 remaining SNPs that were under selection but identified by only one pipeline, 12 correspond to a non-synonymous modification impacting the predicted protein sequence. These SNPs include the gene UFM1 (Ubiquitin-fold modifier 1), the gene PLA2 (85/88 kDa calcium-independent phospholipase A2), and a pyruvate kinase (Supplementary Tables 3–5).

The whole-genome resequencing of four SCN populations for the exploration of the genic environment of outlier loci highlighted 257 genes containing high-impact variants in a ± 50-kb window around loci under selection. Annotation was available for 148 of these genes, corresponding to 132 different gene functions (Supplementary Table 6). Of these genes, 25 exhibited allele frequencies similar to their neighboring outlier loci (**Table 3**).

DISCUSSION

Since its introduction into North America in 1954, the soybean cyst nematode has spread at a regular pace to most of the soybean-producing areas in the US and reached Canada in 1987. Its northern limit of establishment remains to be determined, as new populations are found each year. Soybean acreage is rapidly increasing in northern latitudes; for example, farmers in the province of Manitoba, Canada, sowed 2.3 million acres with soybean in 2017, a 40% increase in 1 year in a province where soybean was not grown a decade ago (Statistics Canada, 2017). This spectacular change in land use results from a coordinated breeding program for short-season and drought-tolerant soybean cultivars (Tardivel et al., 2014). Although soybean is nowadays very profitable in Canada (Manitoba, Northern Ontario, Québec), managing a pest such as SCN could be challenging, as no resistant cultivars are currently adapted to these regions. Simulations based on thermal development have shown that SCN could theoretically survive in these new soybean growing areas (Gendron St-Marseille, 2013), but actual establishment is a different matter, as initial observations in the province of Québec indicated that even though the nematode is detected in many regions, populations weakly reproduced (Mimee et al., 2016). This phenomenon probably reflects SCN's very recent history in this part of the world and the poor fitness of the introduced populations but does not exclude possible adaptations of the nematode in the future. To better understand the evolution of SCN population genetics in North America, we compared 64 populations originating from 11 US states and the province of Ontario in Canada.

The dynamics of cyst nematode populations are intrinsically complex. Several thousand cysts from different females can form on a single plant, and each cyst contains hundreds of half-sibling individuals as a result of SCN's polyandrous mode of reproduction. Thus, the number of unique genotypes occurring in a field is massive. Isolating individual nematodes, even hundreds of them, to explore the genetic relationship between populations would be an arduous task and the approach would still be biased owing to limited sub-sampling. For these reasons, we opted for a Pool-Seq (sequencing of pooled DNA samples) approach. Sequencing DNA from pooled samples for each population also has the advantage of keeping the number of

TABLE 1 | Association of outlier loci [single-nucleotide polymorphisms (SNPs)] identified by at least two Bayesian genome scan methods in 64 populations of the soybean cyst nematode from North America with geographic or climatic co-variables.

SNP ID	Method	Latitude	Longitude	Temperature (annual)	Temperature (maximum)	Precipitation (annual)	Precipitation (warmest quarter)
TP66981	BayeScan		0.998	0.995			
	BayeScEnv		0.017	0.042			
	BayPass						
TP77825	BayeScan				0.999	0.941	
	BayeScEnv				0.029		
	BayPass						
TP146577	BayeScan	0.952	1.000		1.000	0.997	0.997
	BayeScEnv		0.047		0.038		
	BayPass						
TP173057	BayeScan	0.988					
	BayeScEnv						
	BayPass						13.86
TP181514	BayeScan	0.996	0.940	0.992	0.961		
	BayeScEnv		0.050	0.009			
	BayPass						
TP188858	BayeScan				0.999		
	BayeScEnv				0.050		
	BayPass						
TP226227	BayeScan		1.000		1.000	0.956	0.999
	BayeScEnv				0.044		
	BayPass						
TP252086	BayeScan			0.963			
	BayeScEnv			0.050			
	BayPass						
TP324827	BayeScan	0.999	0.999	0.999		1.000	0.999
	BayeScEnv	0.043	0.023	0.006		0.017	
	BayPass						
TP333577	BayeScan	0.984	0.978			0.999	1.000
	BayeScEnv		0.029	0.015			0.040
	BayPass						14.32
TP333913	BayeScan	0.931	0.978	0.976		0.930	
	BayeScEnv		0.029	0.015			
	BayPass						
TP364091	BayeScan			0.976			
	BayeScEnv			0.020			
	BayPass						
TP376687	BayeScan	0.993	0.999		1.000	0.999	0.999
	BayeScEnv				0.038		
	BayPass						
TP380020	BayeScan			0.998		1.000	
	BayeScEnv			0.030		0.027	
	BayPass						
TP380188	BayeScan			0.968			
	BayeScEnv						
	BayPass						13.97

redundant sequences low (Schlötterer et al., 2014). However, this approach does not allow the assignment of sequences to individuals and prevents some population genetic analyses such as linkage-disequilibrium estimation (Lynch et al., 2014; Anand et al., 2016). Nevertheless, a number of recent studies have overcome these limitations and have proposed new methods to

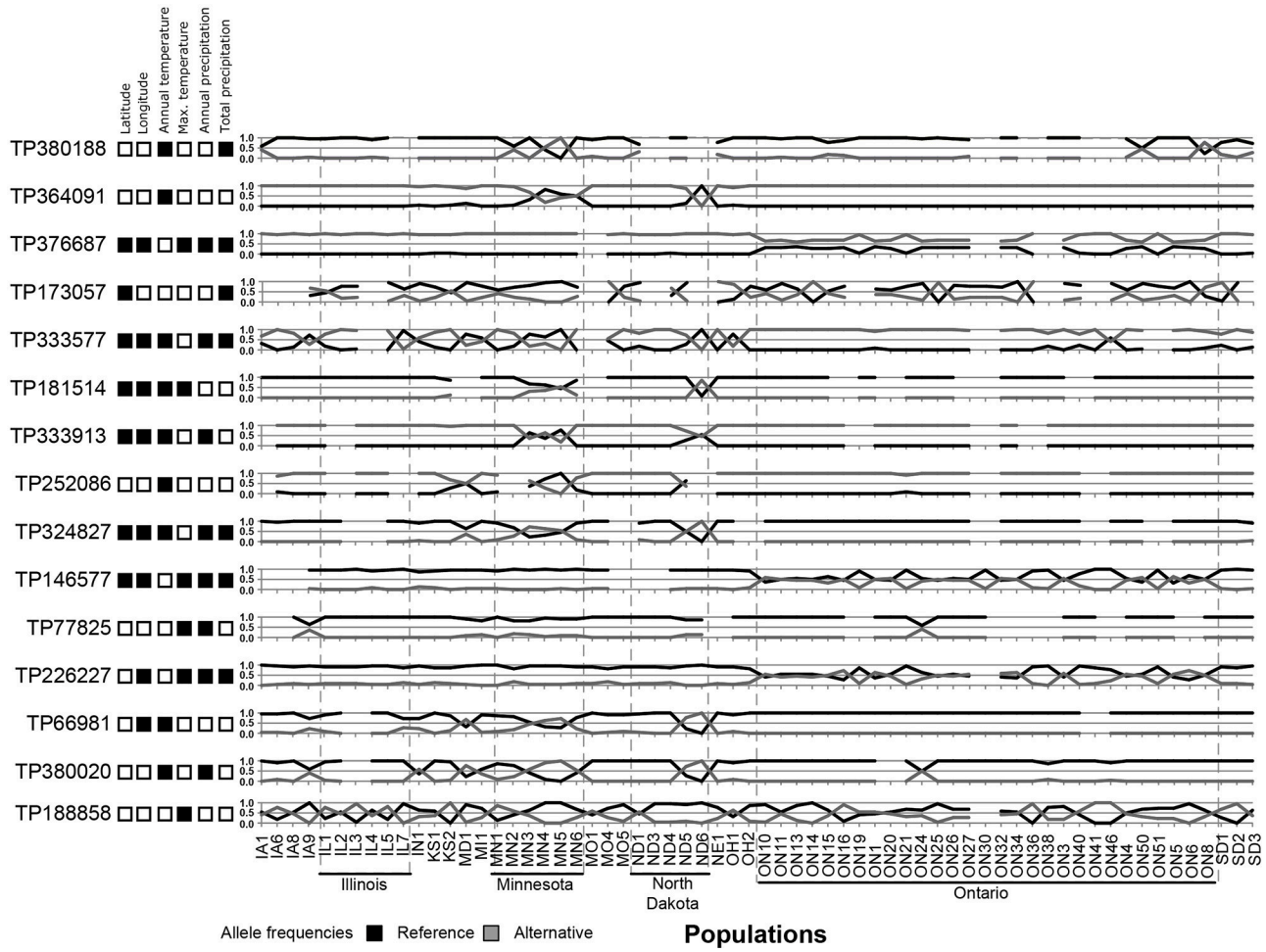

FIGURE 4 | Allele frequencies of 15 outlier loci identified in North American populations of the soybean cyst nematode and associations of the loci with geographic or climatic co-variables. Black squares represent a significant association.

analyze genetic variations among populations based on Pool-Seq data (Van Tassell et al., 2008; Gautier et al., 2013; Navon et al., 2013; Mimee et al., 2015; Anand et al., 2016).

Both the PCA and phylogenetic analyses showed strong clustering of populations based on their geographic origin, which supports the "nearest-neighbor theory" movement as in the stepping-stone model (Kimura and Weiss, 1964; Hutchison and Templeton, 1999). We observed a geographic separation dividing SCN populations into two clusters, a northeastern one (Ontario) and a northwestern one (Minnesota, North Dakota) that both share genetic similarities with central populations. In northeast and northwest regions, SCN populations established only recently, and new detections continue to occur in the northern areas. In the central states, SCN populations have been present for a longer time and resistant soybean cultivars are routinely used. We believed that these two conditions contribute to explain the homogeneity of the central populations. On one hand, the continuous exchange of genetic material would have led to the homogenization of alleles in sympatric populations. On the other hand, the massive use of nematode resistant cultivars that are all derived from a single source of resistance (PI 88788) would have selected for the virulent SCN genotypes, thereby limiting the propagation of some alleles. It is thus surprising to observe a greater genetic differentiation in SCN populations from Ontario since the main assumption is that they originate from central states. These populations should contain less diversity, owing to the founder effect, which would normally result in reduced potential for differentiation. However, the selective pressures mentioned above are not yet present in Ontario, allowing the development of most genotypes. This finding concurs with the results of Faghihi et al. (2010), who observed a much greater diversity in SCN population phenotypes (HG types) in Ontario than in Tennessee, Indiana, or Illinois. A similar pattern was obtained in Minnesota by Zheng et al. (2006) and in China by Liu et al. (1997) when comparing populations from the north to populations from central regions. However, all these authors suggested that climatic conditions or local environmental factors may also play a role.

TABLE 2 | Identification and effect of outlier loci [single-nucleotide polymorphisms (SNPs)] identified by at least two Bayesian genome scan methods in 64 populations of the soybean cyst nematode from North America.

ID	Location	S or N-S[1]	SNP	a.a. subst.[2]	*E*-value	Best annotation
TP380188	Exon	N-S	C/A	Gln/Lys	2.0e-20	SMAD-4 [*Strongyloides ratti*]
TP364091	Exon	N-S	G/A	Asp/Asn	2.6e-104	Dopamine receptor 3 [*Toxocara canis*]
TP376687	Exon	S	T/G	Gly/Gly	4.0e-11	Putative esophageal gland cell protein Hgg-20 [*Heterodera glycines*]
TP173057	Exon	S	C/T	Ile/Ile	2.0e-11	Leucine-rich repeat-containing domain protein, partial [*Necator americanus*]
TP333577	Exon	S	C/T	Leu/Leu	1.0e-110	Cadherin-4 [*Caenorhabditis elegans*]
TP181514	Exon	S	T/C	Gly/Gly	1.6e-100	LET-19 [*Caenorhabditis brenneri*]
TP333913	Exon	S	T/C	Gly/Gly	1.6e-7	EGL-17 [*Brugia malayi*]
TP252086	Intron	–	G/A	–	2.0e-64	Esophageal gland-localized secretory protein 11 [*Heterodera glycines*]
TP324827	Intron	–	C/T	–	3.0e-32	Reverse transcriptase [*Ancylostoma ceylanicum*]
TP146577	Intron	–	T/A	–	2.0e-11	Hypothetical protein Y032_0209g2110 [*Ancylostoma ceylanicum*]
TP77825	Intergenic	–	T/A	–	2.0e-57	Nearest gene: hypothetical protein CRE_19487 [*Caenorhabditis remanei*]
TP226227	Intergenic	–	T/G	–	3.0e-05	Nearest gene: ATP-dependent DNA helicase PIF1, partial [*Toxocara canis*]
TP66981	Intergenic	–	T/G	–	–	*No significant hit*
TP380020	Intergenic	–	G/T	–	–	*No significant hit*
TP188858	Intergenic	–	G/A	–	–	*No significant hit*

[1]*Synonymous (S) or non-synonymous (N-S) mutations in the final protein product.*
[2]*a.a., amino acid substitution.*

According to Hartl and Clark (2007), the overall average F_{ST} value of 0.15 that we obtained by comparing all pairs of SCN populations from North America corresponds to a high level of differentiation. However, when we examined specific pairs of populations, we found that the populations were very similar at the local scale. Also, the differentiation of recent populations (Ontario, Minnesota, North Dakota) from those of the central states was only moderate, whereas comparing these recent populations together generated very high F_{ST} values (up to 0.53). This corroborates results from the PCA analysis and clearly suggests that populations diverged following two distinct routes, one in the northwest toward North Dakota and one in the northeast toward Ontario. This hypothesis is further supported by the isolation-by-distance analysis. Overall, we observed a significant effect of distance on genetic differentiation at the continental scale. The effect of distance was even more noticeable in newly colonized areas like North Dakota and Minnesota or when each population was compared to a common ancestor. On the other hand, the absence of any effect of distance in Illinois and low F_{ST} in the central states clearly suggests that dispersal is frequent enough to weaken signs of isolation by distance after a short period of time. This continuous gene flow combined with the selection of alleles due to the general use of the same resistant soybean lines are thought to cause a rapid homogenization of SCN populations (Mitchum et al., 2007; Niblack et al., 2008; Zheng and Chen, 2011). If SCN is already adapted to environmental conditions prevailing in northern areas, this homogenization process would accelerate the development of virulent genotypes in these regions (in comparison with the central states) and would be independent from the use of resistant cultivars. This concurs with the finding of Faghihi et al. (2010) where 15% of SCN populations in Ontario were able to multiply on PI 548402 and 6% were able to multiply on PI 90763, even though these sources of resistance were not present in commercial cultivars in Ontario.

Although 71 SNPs were found to be under selection among SCN populations, only one SNP was identified by the three Bayesian approaches tested. This SNP (TP333577) was strongly associated with precipitation; but the geographic distribution of allele frequencies (**Figure 4**) at that specific locus did not match with the general pattern of genetic differentiation, instead showing a very local effect (in populations from Minnesota but also in some populations from Iowa, Illinois, North Dakota, and Ohio). Thus, this selection for wetness was either lost in favor of a more stringent pressure or too costly to be maintained in the other regions. Overall, considering the broad range of environmental conditions in which these populations develop, finding only a few genes under selection suggests that SCN possesses an intrinsic capacity to evolve within a large range of temperature and wetness gradients.

Most of the 15 outliers identified by at least two pipelines correlated with temperature, reinforcing that temperature is a key factor that acts on the genetic diversity and natural selection of nematode populations. Nematodes are poikilothermic organisms and depend greatly on temperature to complete their life cycle. Thus, any adaptation that facilitates the development and reproduction of nematodes at lower temperatures would be advantageous. On the basis of the distribution of allele frequencies, however, this adaptation does not seem crucial for survival, as the northern populations did not all exhibit similar patterns. This trait is probably not yet fixed in these populations. Nevertheless, six SNPs under selection and associated with temperature were specific to populations from Ontario (TP376687, TP146577, and TP226227) or only retrieved from Minnesota and North Dakota (TP364091, TP181514, and TP333913), a finding that clearly suggests local adaptations.

TABLE 3 | Putative hitchhiking gene variants with high-impact neighboring loci under selection and exhibiting a similar allele frequency in *Heterodera glycines*.

ID	Gene	Best annotation	*E*-value[1]	Type of variants[2]
TP146577	g15502.t1	G-protein-coupled receptor, partial [*Pristionchus pacificus*]	9.10e-57	complex, insertion
TP173057	g18365.t1	85 kda calcium-independent phospholipase a2 [*Ascaris suum*]	8.50e-46	SNP, insertion
TP173057	g18358.t2	F-box only protein 30 [*Ascaris suum*]	1.10e-33	4 complexes
TP173057	g18327.t1	Protein CBR-CLEC-223 [*Caenorhabditis briggsae*]	5.70e-57	**SNP**
TP173057	g18328.t1	Protein lap1 [*Toxocara canis*]	1.80e-104	6 SNP, 3 insertions, 2 complexes
TP173057	g18332.t1	Protein scribble-like protein, partial [*Stegodyphus mimosarum*]	1.00e-33	2 deletions, **MNP**
TP181514	g3633.t1	Mediator of RNA polymerase II transcription subunit 13-like protein [*Ascaris suum*]	1.20e-133	Deletion
TP226227	g1982.t1	85/88 kDa calcium-independent phospholipase A2 [*Toxocara canis*]	8.00e-29	**SNP**
TP226227	g14545.t1	Glycoside hydrolase domain containing protein [*Haemonchus contortus*]	1.10e-162	deletion, deletion
TP226227	g12205.t1	Kazal domain and organic anion transporter polypeptide (OATP) family and MFS [*Strongyloides ratti*]	3.00e-36	deletion, 3 complexes
TP226227	g1979.t1	Serine/threonine-protein kinase haspin [*Haemonchus contortus*]	1.40e-62	insertion
TP252086	g18812.t1	Bestrophin/UPF0187 family-containing protein [*Strongyloides ratti*]	2.30e-44	deletion
TP252086	g18825.t1	mtN3/saliva family protein [*Oesophagostomum dentatum*]	1.30e-55	deletion, SNP, complex
TP333577	g16696.t2	AFG3-like protein 2 [*Toxocara canis*]	1.30e-286	complex, 2 insertions
TP333913	g14633.t1	Cytohesin-1 [*Trichinella zimbabwensis*]	1.30e-118	SNP
TP333913	g14626.t1	Fibroblast growth factor 17 [*Toxocara canis*]		deletion
TP333913	g14617.t1	Immunoglobulin domain containing protein [*Haemonchus contortus*]	9.60e-42	deletion
TP333913	g14614.t1	Sodium-dependent acetylcholine transporter [*Toxocara canis*]	1.50e-215	SNP
TP364091	g14633.t1	Cytohesin-1 [*Trichinella zimbabwensis*]	1.30e-118	SNP
TP364091	g14656.t1	Major facilitator superfamily MFS-1 domain containing protein, partial [*Haemonchus contortus*]	2.00e-106	deletion
TP380020	g7291.t1	Carboxypeptidase [*Eupolyphaga sinensis*]	1.00e-60	**SNP**
TP380020	g8313.t1	Cell division cycle related [*Caenorhabditis elegans*]	1.10e-254	deletion, SNP
TP380020	g8311.t1	GPI ethanolamine phosphate transferase 3, partial [*Trichinella papuae*]	1.90e-125	deletion
TP380020	g8314.t3	Homeobox protein ceh-6 [*Toxocara canis*]	4.60e-52	insertion, 2 deletions
TP380020	g8309.t1	Immunoglobulin I-set domain containing protein [*Ascaris suum*]	5.50e-31	2 deletions
TP380020	g8305.t1	RecQ-mediated genome instability protein 1 [*Toxocara canis*]	4.60e-28	**SNP**
TP380188	g2288.t1	Cleavage polyadenylation specificity factor domain containing protein [*Haemonchus contortus*]	3.90e-209	insertion
TP380188	g2287.t1	Cytochrome b-c1 complex subunit 2, mitochondrial [*Strongyloides ratti*]	1.20e-63	deletion, SNP

[1] *Expected value for annotations of each putative hitchhiking gene.*

[2] *Variant in bold indicates a stop codon gain. More details on types of variants and position in the gene are provided in Supplementary Table 6. SNP, single-nucleotide polymorphism; MNP, multiple-nucleotide polymorphism.*

The SNP corresponding to TP364091 was retrieved in four out of six populations from Minnesota and in one population from North Dakota. That SNP, which is a non-synonymous mutation in the gene DOP-3 (dopamine receptor 3) that replaces an aspartic acid with an asparagine, was strongly associated with the annual mean temperature and annual precipitation. This modification was retrieved in two distinct gene sequences (g14642.t1 and g14654.t1), and a synonymous mutation (Pro/Pro) was retrieved in two other sequences (g14639.t1 and g14644.t1) but in a different amino acid, indicating a reading frame shift and a putative upstream indel. These four genes were all annotated as DOP-3 and were probably the result of gene duplication. Gene duplication has frequently been hypothesized to play an important role in adaptation to the environment (reviewed in Kondrashov, 2012). In *Caenorhabditis elegans*, the *DOP-3* protein is well known to modulate chemosensory functions, such as mating and foraging, and to be involved in locomotion (Chase et al., 2004; Wood and Ferkey, 2016). The other SNP that introduces a non-synonymous mutation and was highlighted by two genome scan methods, namely, TP380188, was located in the gene SMAD-4 (mothers against decapentaplegic homolog 4) and was retrieved in only a few populations from Minnesota, North Dakota, and Ontario. The *SMAD-4* protein is a regulator of different cellular processes, including cell differentiation, apoptosis, migration, and proliferation (Nikolic et al., 2011). Mutations of *SMAD-2*, *SMAD-3*, *SMAD-4*, or *SMAD-6* were previously shown to result in a 30% reduction in body size in *C. elegans* (Savage-Dunn et al., 2003; Watanabe et al., 2007). Also of interest is the locus TP122360, identified only by BayPass, that was located

in the UFM1 (ubiquitin-fold modifier 1) genes (g7250.t1 and g7228.t1). A deletion in this gene in *C. elegans*, although reducing reproduction rate and life span, increased the survival of this nematode under oxidative or heat stress (Hertel et al., 2013).

For the majority of the loci, their selection probably results from genetic hitchhiking rather than a direct contribution to adaptation. To explore that possibility, we analyzed the genic environment in a ± 50 kb window around each SNP in four SCN populations. Genes containing high-impact genetic variations and exhibiting the same allele frequencies as the associated SNP under selection were of particular interest. Two of these genes (g18327.t1 and g15502.t1) coded for G-protein-coupled receptors (GPCR). These proteins are members of a large and very diverse multigene family with hundreds of occurrences in the *C. elegans* genome (Bockaert and Pin, 1999; Bargmann, 2006). The GCPR are crucial in sensing the local environment and were shown to evolve following alterations in habitat or foraging behavior (Nei et al., 2008). Four genes coding for proteins implicated in metabolite transport into the cell were also identified (g12205.t1, g14656.t1, g18812.t1, and g18825.t1), as was one gene involved in the regulation of those proteins (g18365.t1). All these proteins are required to maintain homeostasis in the cell and to respond to local environmental changes. In a similar study using the fungus *Fagus sylvatica*, Pluess et al. (2016) found that a version of a potassium transporter was associated with lower precipitation and could contribute to the regulation of growth under dry conditions. Structural changes in the body of an organism as a result of microevolution can also confer a significant advantage in terms of resisting more adverse environmental conditions, such as drought or high temperatures (Hazel and Williams, 1990). In our study, mutations were observed in two genes involved in cell-membrane and cell-wall stability (g18328.t1 and g8311.t1). Lastly, modifications in genes involved in the regulation of transcription (g2288.t1 and g3633.t1) and in the maturation of proteins (g14633.t1 and g18358.t2) have the potential to radically change the proteome of the adapted organism.

Although some SCN genes were found to be under selection and local adaptation was found to be underway in this study, our results also indicate that there is no critical adaptive event required for SCN establishment in northern latitudes. Consequently, all populations should theoretically survive and multiply at high latitudes. The risk is thus real for new soybean areas where cultivars resistant to SCN are not available at this time. Of course, the method we used does not explore the entire genome, and a pan-genomic study of these populations could reveal other loci under selection in an evolutionary process.

DATA AVAILABILITY STATEMENT

The raw data supporting the conclusions of this manuscript will be made available by the authors, without undue reservation, to any qualified researcher.

AUTHOR CONTRIBUTIONS

BM, A-FG, and JB conceived and designed the experiments. A-FG, EL, and P-YV performed the experiments and analyzed the data. A-FG, EL, and BM wrote the paper. All the authors revised the manuscript.

ACKNOWLEDGMENTS

The authors thank Drs. Thomas Baum and Andrew Severin for graciously making SCN genome sequences available to us before public release on scnbase.org. The authors also thank Tom Welacky (AAFC) and Terry Niblack (OSU) for providing SCN populations. The authors wish to acknowledge the contribution of Génome Québec, Genome Canada, the Government of Canada, the Ministère de l'Économie, Science et Innovation du Québec, Semences Prograin Inc., Syngenta Canada Inc., Sevita Genetics, La Coop Fédérée, Grain Farmers of Ontario, Saskatchewan Pulse Growers, Manitoba Pulse and Soybean Growers, the Canadian Field Crop Research Alliance and Les Producteurs de grains du Québec.

SUPPLEMENTARY MATERIAL

The Supplementary Material for this article can be found online at: https://www.frontiersin.org/articles/10.3389/fpls.2018.00987/full#supplementary-material

REFERENCES

Altschul, S. F., Gish, W., Miller, W., Myers, E. W., and Lipman, D. J. (1990). Basic local alignment searchtool. *J. Mol. Biol.* 215, 403–410. doi: 10.1016/S0022-2836(05)80360-2

Anand, S., Mangano, E., Barizzone, N., Bordoni, R., Sorosina, M., Clarelli, F., et al. (2016). Next generation sequencing of pooled samples: guideline for variants' filtering. *Sci. Rep.* 6:33735. doi: 10.1038/srep33735

Anderson, T. R., Welacky, T. W., Olechowski, H. T., Ablett, G., and Ebsary, B. A. (1988). First report of *Heterodera glycines* on soybeans in Ontario, Canada. *Plant Dis.* 72:453. doi: 10.1094/PD-72-0453C

Andraszewicz, S., Scheibehenne, B., Rieskamp, J., Grasman, R., Verhagen, J., and Wagenmakers, E.-J. (2015). An introduction to Bayesian hypothesis testing for management research. *J. Manag.* 41, 521–543. doi: 10.1177/0149206314560412

Bargmann, C. I. (2006). Comparative chemosensation from receptors to ecology. *Nature* 444, 295–301. doi: 10.1038/nature05402

Blok, V. C., Phillips, M. S., and Harrower, B. E. (1997). Comparison of British populations of potato cyst nematodes with populations from continental Europe and South America using RAPDs. *Genome* 40, 286–293. doi: 10.1139/g97-040

Bockaert, J., and Pin, J. P. (1999). Molecular tinkering of G protein-coupled receptors: an evolutionary success. *EMBO J.* 18, 1723–1729. doi: 10.1093/emboj/18.7.1723

Bolger, A. M., Lohse, M., and Usadel, B. (2014). Trimmomatic: a flexible trimmer for illumina sequence data. *Bioinformatics* 30, 2114–2120. doi: 10.1093/bioinformatics/btu170

Boucher, A. C., Mimee, B., Montarry, J., Bardou-Valette, S., Bélair, G., Moffett, P., et al. (2013). Genetic diversity of the golden potato cyst nematode *Globodera rostochiensis* and determination of the origin of populations in Quebec, Canada. *Mol. Phylogenet. Evol.* 69, 75–82. doi: 10.1016/j.ympev.2013.05.020

Bradbury, P. J., Zhang, Z., Kroon, D. E., Casstevens, T. M., Ramdoss, Y., and Buckler, E. S. (2007). TASSEL: software for association mapping

of complex traits in diverse samples. *Bioinformatics* 23, 2633–2635. doi: 10.1093/bioinformatics/btm308

Cariou, M., Duret, L., and Charlat, S. (2013). Is RAD-seq suitable for phylogenetic inference? An *in silico* assessment and optimization. *Ecol. Evol.* 3, 846–852. doi: 10.1002/ece3.512

Chase, D. L., Pepper, J. S., and Koelle, M. R. (2004). Mechanism of extrasynaptic dopamine signaling in *Caenorhabditis elegans*. *Nat. Neurosci.* 7, 1096–1103. doi: 10.1038/nn1316

Cingolani, P., Platts, A., Wang, L. L., Coon, M., Nguyen, T., Wang, L., et al. (2012). A program for annotating and predicting the effects of single nucleotide polymorphisms, SnpEff: SNPs in the genome of *Drosophila melanogaster* strain w^{1118}; *iso*-2; *iso*-3. *Fly* 6, 80–92. doi: 10.4161/fly.19695

Colgrove, A. L., and Niblack, T. L. (2008). Correlation of female indices from virulence assays on inbred lines and field populations of *Heterodera glycines*. *J. Nematol.* 40, 39–45.

Conesa, A., Götz, S., García-Gómez, J. M., Terol, J., Talón, M., and Robles, M. (2005). Blast2GO: a universal tool for annotation, visualization and analysis in functional genomics research. *Bioinformatics* 21, 3674–3676. doi: 10.1093/bioinformatics/bti610

Coop, G., Witonsky, D., Di Rienzo, A., and Pritchard, J. K. (2010). Using environmental correlations to identify loci underlying local adaptation. *Genetics* 185, 1411–1423. doi: 10.1534/genetics.110.114819

Davis, E. L., and Tylka, G. L. (2000). Soybean cyst nematode disease. *Plant Health Instr.* doi: 10.1094/PHI-I-2000-0725-01

de Villemereuil, P., and Gaggiotti, O. E. (2015). A new F_{ST}-based method to uncover local adaptation using environmental variables. *Meth. Ecol. Evol.* 6, 1248–1258. doi: 10.1111/2041-210X.12418

Early, R., and Sax, D. F. (2014). Climatic niche shifts between species' native and naturalized ranges raise concern for ecological forecasts during invasions and climate change. *Glob. Ecol. Biogeogr.* 23, 1356–1365. doi: 10.1111/geb.12208

Eizaguirre, C., and Baltazar-Soares, M. (2014). Evolutionary conservation-evaluating the adaptive potential of species. *Evol. Appl.* 7, 963–967. doi: 10.1111/eva.12227

Elshire, R. J., Glaubitz, J. C., Sun, Q., Poland, J. A., Kawamoto, K., Buckler, E. S., et al. (2011). A robust, simple genotyping-by-sequencing (GBS) approach for high diversity species. *PLoS ONE* 6:e19379. doi: 10.1371/journal.pone.0019379

Eoche-Bosy, D., Gautier, M., Esquibet, M., Legeai, F., Bretaudeau, A., Bouchez, O., et al. (2017). Genome scans on experimentally evolved populations reveal candidate regions for adaptation to plant resistance in the potato cyst nematode *Globodera pallida*. *Mol. Ecol.* 26, 4700–4711. doi: 10.1111/mec.14240

Eves-van den Akker, S., Lilley, C. J., Reid, A., Pickup, J., Anderson, E., Cock, P. J., et al. (2015). A metagenetic approach to determine the diversity and distribution of cyst nematodes at the level of the country, the field and the individual. *Mol. Ecol.* 24, 5842–5851. doi: 10.1111/mec.13434

Faghihi, J., Donald, P. A., Noel, G., Welacky, T. W., and Ferris, V. R. (2010). Soybean resistance to field populations of *Heterodera glycines* in selected geographic areas. *Plant Health Prog.* doi: 10.1094/PHP-2010-0426-01-RS

Fick, S. E., and Hijmans, R. J. (2017). WorldClim 2: new 1-km spatial resolution climate surfaces for global land areas. *Int. J. Climatol.* 37, 4302–4315. doi: 10.1002/joc.5086

Foll, M. (2012). *BayeScan v2.1 User Manual*. Available online at: http://cmpg.unibe.ch/software/BayeScan/files/BayeScan2.1_manual.pdf

Foll, M., and Gaggiotti, O. E. (2008). A genome-scan method to identify selected loci appropriate for both dominant and codominant markers: a Bayesian perspective. *Genetics* 180, 977–993. doi: 10.1534/genetics.108.092221

Fu, Y.-B., Peterson, G. W., and Dong, Y. (2016). Increasing genome sampling and improving SNP genotyping for genotyping-by-sequencing with new combinations of restriction enzymes. *G3* 6, 845–856. doi: 10.1534/g3.115.025775

Garrison, E., and Marth, G. (2012). Haplotype-Based Variant Detection from Short-Read Sequencing. *arXiv [preprint] arXiv:*1207.3907.

Gautier, M. (2015). Genome-wide scan for adaptive divergence and association with population-specific covariates. *Genetics* 201, 1555–1579. doi: 10.1534/genetics.115.181453

Gautier, M., Gharbi, K., Cezard, T., Foucaud, J., Kerdelhué, C., Pudlo, P., et al. (2013). The effect of RAD allele dropout on the estimation of genetic variation within and between populations. *Mol. Ecol.* 22, 3165–3178. doi: 10.1111/mec.12089

Gendron St-Marseille, A.-F. (2013). Le nématode à Kyste du Soja (Heterodera glycines) : Enjeux des Changements Climatiques sur sa Distribution, sa Reproduction et sur les Probabilités de Synchronisme Avec le Soja (Glycine max) au Québec. Master's Thesis, Université de Sherbrooke, Sherbrooke, QC. Available online at: http://hdl.handle.net/11143/7214

Green, C. D., Greet, D. N., and Jones, F. G. W. (1970). The influence of multiple mating on the reproduction and genetics of *Heterodera rostochiensis* and *H. schachtii*. *Nematologica* 16, 309–326. doi: 10.1163/187529270X00333

Grenier, E., Bossis, M., Fouville, D., Renault, L., and Mugniéry, D. (2001). Molecular approaches to the taxonomic position of Peruvian potato cyst nematodes and gene pool similarities in indigenous and imported populations of *Globodera*. *Heredity* 86, 277–290. doi: 10.1046/j.1365-2540.2001.00826.x

Günther, T., and Coop, G. (2013). Robust identification of local adaptation from allele frequencies. *Genetics* 195, 205–220. doi: 10.1534/genetics.113.152462

Hartl, D. L., and Clark, A. G. (2007). *Principles of Population Genetics. 4th Edn*. Sunderland, Massachusetts Sinauer Associates.

Hassan, M. A., Pham, T. H., Shi, H., and Zheng, J. (2013). Nematodes threats to global food security. *Acta. Agric. Scand. B. Soil Plant Sci.* 63, 420–425. doi: 10.1080/09064710.2013.794858

Hazel, J. R., and Williams, E. E. (1990). The role of alterations in membrane lipid composition in enabling physiological adaptation of organisms to their physical environment. *Prog. Lipid Res.* 29, 167–227. doi: 10.1016/0163-7827(90)90002-3

Hegge, A. H. (1957). Soybean cyst nematode, *Heterodera glycines*, in Missouri. *Plant Dis. Rep.* 41:201.

Hertel, P., Daniel, J., Stegehake, D., Vaupel, H., Kailayangiri, S., Gruel, C., et al. (2013). The ubiquitin-fold modifier 1 (Ufm1) cascade of *Caenorhabditis elegans*. *J. Biol. Chem.* 288, 10661–10671. doi: 10.1074/jbc.M113.458000

Hulme, P. E. (2009). Trade, transport and trouble: managing invasive species pathways in an era of globalization. *J. Appl. Ecol.* 46, 10–18. doi: 10.1111/j.1365-2664.2008.01600.x

Hutchison, D. W., and Templeton, A. R. (1999). Correlation of pairwise genetic and geographic distance measures: inferring the relative influences of gene flow and drift on the distribution of genetic variability. *Evolution* 53, 1898–1914. doi: 10.1111/j.1558-5646.1999.tb04571.x

Kamvar, Z. N., Tabima, J. F., and Grünwald, N. J. (2014). Poppr: an R package for genetic analysis of populations with clonal, partially clonal, and/or sexual reproduction. *PeerJ* 2:e281. doi: 10.7717/peerj.281

Kass, R. E., and Raftery, A. E. (1995). Bayes factors. *J. Am. Stat. Assoc.* 90, 773–795. doi: 10.1080/01621459.1995.10476572

Kimura, M., and Weiss, G. H. (1964). The stepping stone model of population structure and the decrease of genetic correlation with distance. *Genetics* 49, 561–576.

Kofler, R., Pandey, R. V., and Schlötterer, C. (2011). PoPoolation2: identifying differentiation between populations using sequencing of pooled DNA samples (pool-Seq). *Bioinformatics* 27, 3435–3436. doi: 10.1093/bioinformatics/btr589

Kondrashov, F. A. (2012). Gene duplication as a mechanism of genomic adaptation to a changing environment. *Proc. R. Soc. B.* 279, 5048–5057. doi: 10.1098/rspb.2012.1108

Kristjansson, G. (2010). 09−59.Plant Health Risk Assessment Unit of the Science Advice Division: Canadian Food Inspection Agency. 45p.

Li, H., and Durbin, R. (2009). Fast and accurate short read alignment with Burrows–Wheeler Transform. *Bioinformatics* 25, 1754–1760. doi: 10.1093/bioinformatics/btp324

Li, H., Handsaker, B., Wysoker, A., Fennell, T., Ruan, J., Homer, N., et al. (2009). The sequence alignment/map format and SAMtools. *Bioinformatics* 25, 2078–2079. doi: 10.1093/bioinformatics/btp352

Liu, X. H., Li, J. Q., and Zhang, D. S. (1997). History and status of soybean cyst nematode in China. *Int. J. Nematol.* 7, 18–25.

Lu, F., Lipka, A. E., Glaubitz, J., Elshire, R., Cherney, J. H., Casler, M. D., et al. (2013). Switchgrass genomic diversity, ploidy, and evolution: novel insights from a network-based SNP discovery protocol. *PLoS Genet.* 9:e1003215. doi: 10.1371/journal.pgen.1003215

Lynch, M., Bost, D., Wilson, S., Maruki, T., and Harrison, S. (2014). Population-genetic inference from pooled-sequencing data. *Genome Biol. Evol.* 6, 1210–1218. doi: 10.1093/gbe/evu085

Mathew, F., Markell, S., Jantzi, D., Yan, G., Nelson, B., and Helms, T. (2015). *Soybean cyst nematode. Plant Disease Management.* Fargo, ND: North Dakota State University Extension Service), p. 4.

Mimee, B., Duceppe, M.-O., Véronneau, P.-Y., Lafond-Lapalme, J., Jean, M., Belzile, F., et al. (2015). A new method for studying population genetics of cyst nematodes based on Pool-Seq and genomewide allele frequency analysis. *Mol. Ecol. Resour.* 15, 1356–1365. doi: 10.1111/1755-0998.12412

Mimee, B., Gagnon, A.-È., Colton-Gagnon, K., and Tremblay, É. (2016). Portrait de la situation du nématode à kyste du soja (*Heterodera glycines*) au Québec (2013–2015). *Phytoprotection* 96, 33–42. doi: 10.7202/1038941ar

Mimee, B., Peng, H., Popovic, V., Yu, Q., Duceppe, M.-O., Tétreault, M.-P., et al. (2014). First report of soybean cyst nematode (*Heterodera glycines* Ichinohe) on soybean in the province of Quebec, Canada. *Plant Dis.* 98:429. doi: 10.1094/PDIS-07-13-0782-PDN

Mitchum, M. G., Wrather, J. A., Heinz, R. D., Shannon, J. G., and Danekas, G. (2007). Variability in distribution and virulence phenotypes of *Heterodera glycines* in Missouri during 2005. *Plant Dis.* 91, 1473–1476. doi: 10.1094/PDIS-91-11-1473

Navon, O., Sul, J. H., Han, B., Conde, L., Bracci, P. M., Riby, J., et al. (2013). Rare variant association testing under low-coverage sequencing. *Genetics* 194, 769–779. doi: 10.1534/genetics.113.150169

Nei, M., Niimura, Y., and Nozawa, M. (2008). The evolution of animal chemosensory receptor gene repertoires: roles of chance and necessity. *Nat. Rev. Genet.* 9, 951–963. doi: 10.1038/nrg2480

Nelson, B. D., and Bradley, C. A. (2003). *Soybean cyst nematode (SCN)*. Fargo, ND: North Dakota State University. Available online at: https://www.ndsu.edu/pubweb/$\sim$bernelso/soydiseases/cyst.shtml

Niblack, T. L., Colgrove, A. L., Colgrove, K., and Bond, J. P. (2008). Shift in virulence of soybean cyst nematode is associated with use of resistance from PI 88788. *Plant Health Prog.* doi: 10.1094/PHP-2008-0118-01-RS

Nikolic, A., Kojic, S., Knezevic, S., Krivokapic, Z., Ristanovic, M., and Radojkovic, D. (2011). Structural and functional analysis of SMAD4 gene promoter in malignant pancreatic and colorectal tissues: detection of two novel polymorphic nucleotide repeats. *Cancer Epidemiol.* 35, 265–271. doi: 10.1016/j.canep.2010.10.002

Novak, S. J. (2007). The role of evolution in the invasion process. *PNAS* 104, 3671–3672. doi: 10.1073/pnas.0700224104

Pimentel, D., Zuniga, R., and Morrison, D. (2005). Update on the environmental and economic costs associated with alien-invasive species in the United States. *Ecol. Econ.* 52, 273–288. doi: 10.1016/j.ecolecon.2004.10.002

Plantard, O., Picard, D., Valette, S., Scurrah, M., Grenier, E., and Mugniéry, D. (2008). Origin and genetic diversity of Western European populations of the potato cyst nematode (*Globodera pallida*) inferred from mitochondrial sequences and microsatellite loci. *Mol. Ecol.* 17, 2208–2218. doi: 10.1111/j.1365-294X.2008.03718.x

Pluess, A. R., Frank, A., Heiri, C., Lalagüe, H., Vendramin, G. G., and Oddou-Muratorio, S. (2016). Genome–environment association study suggests local adaptation to climate at the regional scale in *Fagus sylvatica*. *New Phytol.* 210, 589–601. doi: 10.1111/nph.13809

Plummer, M., Best, N., Cowles, K., and Vines, K. (2006). CODA: convergence diagnosis and output analysis for MCMC. *R News* 6, 7–11. Available online at: http://oro.open.ac.uk/22547/

Poland, J. A., Brown, P. J., Sorrells, M. E., and Jannink, J. L. (2012). Development of high-density genetic maps for barley and wheat using a novel two-enzyme genotyping-by-sequencing approach. *PLoS ONE* 7:e32253. doi: 10.1371/journal.pone.0032253

R Core Team (2017). *R: A Language and Environment For Statistical Computing*. Vienna, R Foundation for Statistical Computing. Available online at: http://www.R-project.org/

Revell, L. J. (2017). *Phylogenetic Tools for Comparative Biology (and other things)*. Available online at: https://cran.r-project.org/web/packages/phytools/phytools.pdf

Riggs, R. D. (2004). "History and distribution," in *Biology and Management of Soybean Cyst Nematode*, *2nd Edn*, eds D. P. Schmitt, J. A. Wrather, R. D. Riggs (Marceline, MO: Schmitt and Associates of Marceline), 9–40.

Rousset, F. (1997). Genetic differentiation and estimation of gene flow from *F*-statistics under isolation by distance. *Genetics* 145, 1219–1228.

Savage-Dunn, C., Maduzia, L. L., Zimmerman, C. M., Roberts, A. F., Cohen, S., Tokarz, R., et al. (2003). Genetic screen for small body size mutants in *C. elegans* reveals many TGFβ pathway components. *Genesis* 35, 239–247. doi: 10.1002/gene.10184

Schlötterer, C., Tobler, R., Kofler, R., and Nolte, V. (2014). Sequencing pools of individuals – Mining genome-wide polymorphism data without big funding. *Nat. Rev. Genetics* 15, 749–763. doi: 10.1038/nrg3803

Shurtleff, W., and Aoyagi, A. (2010). *History of Soybeans and Soyfoods in Canada (1831–2010): Extensively Annotated Bibliography and Sourcebook*. Lafayette, CA: Soyinfo Center.

Slack, D. A., Riggs, R. D., and Hamblen, M. L. (1972). The effect of temperature and moisture on the survival of *Heterodera glycines* in the absence of a host. *J. Nematol.* 4, 263–266.

Statistics Canada (2017). *Table 001–0017–Estimated Areas, Yield, Production, Average Farm Price and Total Farm Value of Principal Field Crops, in Imperial Units, Annual, CANSIM (Database)*. [Accessed: November 20, 2017]. Available online at: http://www5.statcan.gc.ca/cansim/a26?lang=eng&id=10017

Tardivel, A., Sonah, H., Belzile, F., and O'Donoughue, L. S. (2014). Rapid identification of alleles at the soybean maturity gene E3 using genotyping by sequencing and a haplotype-based approach. *Plant Genome* 7, 1–9. doi: 10.3835/plantgenome2013.10.0034

Tylka, G. L., and Marett, C. C. (2017). Known distribution of the soybean cyst nematode, *Heterodera glycines*, in the United States and Canada: 1954 to 2017. *Plant Health Prog.* 18, 167–168. doi: 10.1094/PHP-05-17-0031-BR

Van Tassell, C., Smith, T. P., Matukumalli, L. K., Taylor, J. F., Schnabel, R. D., Taylor, L., et al. (2008). SNP discovery and allele frequency estimation by deep sequencing of reduced representation libraries. *Nat. Methods* 5, 247–252. doi: 10.1038/nmeth.1185

Watanabe, N., Ishihara, T., and Ohshima, Y. (2007). Mutants carrying two *sma* mutations are super small in the nematode *C. elegans*. *Genes Cells* 12, 603–609. doi: 10.1111/j.1365-2443.2007.01077.x

Wood, J. F., and Ferkey, D. M. (2016). "GRK roles in C. *elegans*," in *G Protein-Coupled Receptor Kinases*, eds V. V. Gurevich, and J. J. G. Tesmer (New York, NY: Springer), 283–299.

Wright, S. (1943). Isolation by distance. *Genetics* 28, 114–138.

Yu, Q. (2011). "Soybean cyst nematode (*Heterodera glycines* ichinohe)," in *Soybean Physiology and Biochemistry*, ed H. A. El-Shemy (Rijeka: InTech Europe), 461–474. Available online at: http://cdn.intechopen.com/pdfs-wm/22782.pdf

Zheng, J., Li, Y., and Chen, S. (2006). Characterization of the virulence phenotypes of *Heterodera glycines* in Minnesota. *J. Nematol.* 38, 383–390.

Zheng, J. Z., and Chen, S. Y. (2011). Estimation of virulence type and level of soybean cyst nematode field populations in response to resistant cultivars. *J. Entomol. Nematol.* 3, 37–43. Available online at: http://www.academicjournals.org/journal/JEN/article-abstract/791181810204

Conflict of Interest Statement: The authors declare that the research was conducted in the absence of any commercial or financial relationships that could be construed as a potential conflict of interest.

frontiers in Plant Science

METHODS
published: 09 August 2018
doi: 10.3389/fpls.2018.01086

Real-Time PCR for Diagnosing and Quantifying Co-infection by Two Globally Distributed Fungal Pathogens of Wheat

Araz S. Abdullah[1], Chala Turo[1], Caroline S. Moffat[1], Francisco J. Lopez-Ruiz[1], Mark R. Gibberd[1], John Hamblin[2] and Ayalsew Zerihun[1]*

[1] *Centre for Crop and Disease Management, School of Molecular and Life Sciences, Curtin University, Bentley, WA, Australia,* [2] *Institute of Agriculture, University of Western Australia, Crawley, WA, Australia*

Co-infections – invasions of a host-plant by multiple pathogen species or strains – are common, and are thought to have consequences for pathogen ecology and evolution. Despite their apparent significance, co-infections have received limited attention; in part due to lack of suitable quantitative tools for monitoring of co-infecting pathogens. Here, we report on a duplex real-time PCR assay that simultaneously distinguishes and quantifies co-infections by two globally important fungal pathogens of wheat: *Pyrenophora tritici-repentis* and *Parastagonospora nodorum*. These fungi share common characteristics and host species, creating a challenge for conventional disease diagnosis and subsequent management strategies. The assay uses uniquely assigned fluorogenic probes to quantify fungal biomass as nucleic acid equivalents. The probes provide highly specific target quantification with accurate discrimination against non-target closely related fungal species and host genes. Quantification of the fungal targets is linear over a wide range (5000–0.5 pg DNA μl^{-1}) with high reproducibility (RSD $\leq$ 10%). In the presence of host DNA in the assay matrix, fungal biomass can be quantified up to a fungal to wheat DNA ratio of 1 to 200. The utility of the method was demonstrated using field samples of a cultivar sensitive to both pathogens. While visual and culture diagnosis suggested the presence of only one of the pathogen species, the assay revealed not only presence of both co-infecting pathogens (hence enabling asymptomatic detection) but also allowed quantification of relative abundances of the pathogens as a function of disease severity. Thus, the assay provides for accurate diagnosis; it is suitable for high-throughput screening of co-infections in epidemiological studies, and for exploring pathogen–pathogen interactions and dynamics, none of which would be possible with conventional approaches.

Keywords: co-infections, qPCR, hydrolysis probes, molecular disease diagnosis, pathogen interactions

OPEN ACCESS

Edited by:
Christophe Le May, Agrocampus Ouest, France

Reviewed by:
Martin Chilvers, Michigan State University, United States
Syama Chatterton, Agriculture and Agri-Food Canada (AAFC), Canada

****Correspondence:***
Araz S. Abdullah
araz.abdullah@curtin.edu.au

Specialty section:
This article was submitted to Plant Microbe Interactions, a section of the journal Frontiers in Plant Science

Received: *23 April 2018*
Accepted: *05 July 2018*
Published: *09 August 2018*

Citation:
Abdullah AS, Turo C, Moffat CS, Lopez-Ruiz FJ, Gibberd MR, Hamblin J and Zerihun A (2018) Real-Time PCR for Diagnosing and Quantifying Co-infection by Two Globally Distributed Fungal Pathogens of Wheat. Front. Plant Sci. 9:1086. doi: 10.3389/fpls.2018.01086

INTRODUCTION

Co-infections, whereby a host-plant is invaded by multiple pathogens or multiple strains of the same pathogen, are common in the field and can have major consequences for disease ecology and pathogen evolution (Alizon et al., 2013). Despite the recognition of the significance of co-infection (Savary and Zadoks, 1992; Zadoks, 1999; Tack et al., 2012), empirical studies are still few, due mainly to the complexity of distinguishing/quantifying multiple pathogens, which often requires

suitable molecular tools (Tollenaere et al., 2012; Tollenaere et al., 2016). As a result, the theoretical understanding of co-infection has largely outpaced experimental studies in natural and agricultural systems (Hood, 2003; Abdullah et al., 2017) and our capacity to understand and manage the processes and consequences of co-infection is limited until current and future theoretical models can be validated by reliable data.

Methods used for distinguishing multiple pathogens from co-infected tissues involve detection of nucleic acid targets using metagenome sequencing and/or analysis of melt-curves from PCR primers with various annealing properties (Brandfass and Karlovsky, 2006; Tollenaere et al., 2012; Gelaye et al., 2017). Such methods enable multiple pathogen detections but provide limited quantitative information on the relative abundance of each pathogen and their effects on overall disease (Bernreiter, 2017). The quantification of pathogen abundance is critical, as many pathogens are naturally present within plants, but their infection levels, pathogenicity and hence relative impacts can differ vastly (Bakker et al., 2014). At present, real-time quantitative PCR (qPCR) is the most reliable technique for measuring disease load in a sample while providing species specificity (Holland et al., 1991; Bates et al., 2001; Schena et al., 2006). Successful qPCR-based multiplexed assays have been developed for detection of *Phytophthora* diseases of soybean (Rojas et al., 2017), but the accuracy of quantification is often compromised in samples with unbalanced target ratios (Klerks et al., 2004; Atallah et al., 2007). Thus, to ensure reliable quantification, co-infection studies often analyze the abundance of multiple pathogens in separate reactions. Due to the cost of labor and resources required, this approach is limited to small-scale investigations limiting our capacity to investigate co-infections over large-scale host populations.

In order to address the limitations of current approaches, we investigate the use of dual-labeled species-specific probes to simultaneously detect and quantify two globally distributed fungal pathogens of wheat: *Pyrenophora tritici-repentis* and *Parastagonospora nodorum*. These two foliar fungal pathogens cause tan (yellow) spot and septoria nodorum blotch in wheat, respectively, damaging photosynthetically active leaf area and causing substantial yield losses (Bhathal et al., 2003). Symptoms caused by these two diseases are difficult to distinguish and may be misdiagnosed as other unrelated physiological abnormalities (Moffat et al., 2015), creating a challenge for conventional disease diagnosis and subsequent management strategies. Symptoms can also vary markedly depending on host genotype, further hampering accurate disease diagnosis (Lamari and Bernier, 1989). Interestingly, *P. tritici-repentis* carries a pathogenicity/virulence gene, *ToxA*, thought to have been acquired laterally from *Pa. nodorum* (Friesen et al., 2006). This suggests that co-infection by these two fungi is likely to occur in nature and may have consequences for disease management strategies. Despite the high likelihood of co-infection by these two fungi and difficulties of identification, no tools have been developed for the diagnosis of their abundance in co-infected host materials.

Here, we report a duplex assay that distinguishes specific DNA sequences unique to each of these fungi and quantifies their presence by direct comparison to standards amplified in parallel reactions. The basis of this method is the uniquely assigned fluorogenic reporters for each species sequence. The fluorogenic reporters, when bound to the target, quantify fungal b as nucleic acid equivalents. We report on a series of experiments designed to demonstrate the specificity and sensitivity of the method using both a simulated genomic DNA matrix of both fungi at varying ratios as well as naturally infected wheat leaves collected from the field. We also examine the capacity of the technique to show that a species that is present at very low level can be detected and quantified, with very limited interference, in the presence of an abundant species. Finally, we correlate the amount of fungal DNA quantified using the duplex qPCR assay developed here with the level of infection measured by conventional disease scores.

MATERIALS AND METHODS

PCR Primers and Conditions

P. tritici-repentis primers were designed to target a species-specific multicopy genomic region described previously (Moffat et al., 2015; See et al., 2016). Briefly, a 4.65-kb region of the *P. tritici-repentis* isolate Pt-1CBFP carrying the *ToxA* gene (supercontig_1.4) was aligned to an orthologous genomic region of the *Pa. nodorum* isolate SN15 (scaffold_55). All known isolates of the targeted fungi were included in this step to ensure that the primers amplify all known isolates of the pathogens of interest. A pair of primers that target a 99-bp fragment located 701-bp upstream of the *ToxA* coding region was designed to detect *P. tritici-repentis* (**Table 1**). These primers amplify a short fragment (99-bp) within the promoter region of a low molecular weight host-selective toxin. This multicopy region has been detected in a number races of *P. tritici-repentis* isolates collected from around the world (Moolhuijzen et al., 2018). The size of the primer pair was restricted to 99-bp to ensure comparable amplicon sizes between *P. tritici-repentis* and *Pa. nodorum*.

Pa. nodorum DNA was amplified using primers modified from those previously described by Oliver et al. (2008). Additional 3-bp was included at the beginning of each primer sequence to allow the probe to overcome the issue of primer–dimer association (Barbisin et al., 2009). *Pa. nodorum* primers amplify a 112-bp fragment of a highly conserved anonymous

TABLE 1 | List of the oligonucleotides used in this study.

Sequence ID*	5′→3′ sequence	Product length (bp)	GC (%)
Ptr–Forward	GTCTCCTCTGGTGGTATG	99	55.6
Ptr–Reverse	GCTCTTAGTGAAGTTCAATC		
Ptr–Probe	TACCTCTACTCGGTCGCCTATGG		
Pn–Forward	**ACCGCATTACCAAAGTTC**	112	45.8
Pn–Reverse	**ACTGGAACTGGAACAATAAG**		
Pn–Probe	CCTGAATGCTCTTGACACTTGGTT		

**Ptr and Pn refer to P. tritici-repentis and Pa. nodorum, respectively. Sequences in bold are pre-published primers modified from Oliver et al. (2008). Other sequences are designed in this study. Primers and probes were designed to amplify short fragments of the targeted pathogen DNA.*

gene (SNOG_01116·1). This gene has no significant similarity to any other sequences in the publically available genome databases (Oliver et al., 2008). All primers were designed using OligoArchitect™ primer analyzer (Sigma, Life Science) and scanned against the National Center for Biotechnology Information GenBank database using basic local alignment search tools to ensure their specificity.

The designed primers were subjected to conventional PCR to confirm their specificity. Each PCR reaction contained 1xMyTaq buffer, 250 nM forward primer, 250 nM reverse primer, 1 unit MyTaq DNA polymerase (Bioline), and 5 ng DNA template. Reactions were performed as follows: 3 min initial denaturation at 95°C, 35 cycles of 30 s denaturation at 95°C, 30 s of annealing at 58°C and 1 min extension at 72°C. Electrophoresis of PCR products was performed on 2% agarose gels stained with SybrSafe (Life Technologies) and visualized under UV light. Reproducibility of the results was confirmed by running the PCR with negative controls in duplicates. The PCR step also included DNA samples from five common fungal pathogens of cereals as negative controls. Colonies of *Pyrenophora teres* f. sp. *maculata*, *Pyrenophora teres* f. sp. *teres*, *Blumeria graminis* f. sp. *tritici*, *Alternaria alternata,* and *Fusarium graminearum* were kindly provided by Steven Chang, Curtin University/Centre for Crop and Disease Management. Species identity was confirmed by sequencing the internal transcribed spacer of the ribosomal DNA (Schoch et al., 2012). All sequence analyses and multiple sequence alignments were carried out using Geneious version R6.1.6.

Real-Time PCR Probes and Conditions

Two dual-labeled probes were custom-designed and assigned to hybridize with a complementary region between the forward and the reverse primers. The *P. tritici-repentis* and *Pa. nodorum* probes were 23-bp and 20-bp in length, respectively. The length of each probe was chosen to ensure probe-primer hybrids are formed in a complementary manner with the length of the primers. Each probe was labeled with a unique fluorogenic reporter to ensure that target sequences of both pathogens were amplified simultaneously but detected independently. The *P. tritici-repentis* probe was labeled with 6-carboxyfluorescein (FAM™; Sigma-Aldrich). The *Pa. nodorum* probe was labeled with CAL Fluor Gold® (CFG; Sigma-Aldrich). FAM has emission maxima between 494 nm and 518 nm and CFG emission peaks between 538 nm and 559 nm. The fluorogenic reporters were selected based on the capacity of the CFX96 detection system, the instrument used in this study, to resolve overlapping spectra. This was determined prior to carrying out the experiments using a spectra overlay tool available at http://www.Qpcrdesign.com/spectral-overlay. Both probes were paired with the non-fluorescent black hole quencher-1 (BHQ-1®; Sigma-Aldrich).

Probes and their matching primers were run on a 96-well spectrofluorometric thermal cycler (Bio-Rad CFX96) with the following conditions: 15 min at 95°C, 15 s denaturation at 95°C, 20 s at 72°C followed by 40 cycles of 15 s at 95°C and 30 s at 58°C. Each 20 μl reaction volume contained 5 μl of the sample and 12 μl iQ™ Multiplex Powermix (Bio-Rad). For a fixed amount of target template, *P. tritici-repentis* DNA was amplified faster than *Pa. nodorum* DNA. Hence, probe and primers of *P. tritici-repentis* were restricted to obtain comparable quantification cycles (Cq) to that of *Pa. nodorum*. In a preliminary experiment, the concentrations of primers and probes were gradually increased from 50 up to 450 nM at 50 nM intervals. *P. tritici-repentis* DNA was amplified using 200 nM forward primer, 200 nM reverse primer and 100 nM probe. *Pa. nodorum* DNA was amplified using 250 nM forward primer, 250 nM reverse primer and 150 nM probe. Unless specified, reactions were carried out in duplex where primers and probes for both species were applied together. A preliminary experiment showed a comparable amplification efficiency between duplex and singleplex reactions and no evidence of cross-amplification among primers and probes of the two species was observed (**Supplementary Table 1**). Presence of any non-specific amplicon was examined using post-PCR melt curve analysis.

DNA Extraction and Quantification

Pure genomic DNA from fungal colonies was extracted using the Bio-sprint 15 plant DNA kit (Qiagen) as per the manufacturer's protocol. Fungal cultures were maintained on agar plates as described elsewhere (Moffat et al., 2015). Mycelia were harvested from these cultures and ground into a fine powder in liquid nitrogen. Subsamples (40 mg ground tissue) were placed into 1.5-ml microtubes, which were then used for DNA extraction. The concentration of DNA in each subsample was determined using a NanoDrop 2000 UV-Vis spectrophotometer (Thermo Scientific) and diluted to 50 ng μl^{-1} in ultrapure PCR grade water. DNA was stored at −20°C until used. Aerosol protected pipette tips were used throughout the extraction and quantification steps to prevent DNA contamination. DNA from infected wheat leaves was extracted using the same DNA extraction kit and quantified as described above.

DNA Spiking and Field Validation

In two independent experiments, a fixed concentration of fungal DNA of one pathogen (5 ng μl^{-1}) was spiked into a progressively decreasing DNA concentration of the other pathogen (5, 0.5, 0.05, and 0.005 ng DNA μl^{-1}). This generated a ratio of DNA concentration from one pathogen to the other in the sample ranging from 1:1 down to 1:10000. The spiking aimed to simulate the analysis of samples derived from infection conditions whereby the two species occur at different relative abundance, which is typical of many foliar fungal infections. Recovery of fungal DNA for the respective pathogens was expressed as the ratio of the total concentration of fungal DNA quantified using the qPCR method to the amount of DNA added × 100.

In a third experiment, recovery of fungal DNA was measured in fungal DNA samples spiked with abundant wheat DNA. The concentration of fungal DNA in the samples was progressively decreased from 5 down to 0.05 ng μl^{-1} while background wheat DNA was increased from 5 to 100 ng μl^{-1}. The experiment simulated analytical conditions where fungal DNA is present in small concentrations against a background of ample wheat DNA, such as would occur where infection severity and/or incidence are low.

To evaluate how well the assay works for field samples, diseased leaves from the wheat variety Scout were collected from

a site in the southwest of Western Australia (31°.74S, 116°.70E). Scout is rated as susceptible to very susceptible to both *P. tritici-repentis* and *Pa. nodorum* (DAFWA, 2016). Sampled leaves were visually inspected for diseased leaf area and given scores on 0-100 scale. Leaves were then split into two groups; one group (n = 9) was surface-sterilized in 2% chlorine and incubated on agar Petri-dishes in an attempt to characterize the causal agent of the disease. Leaves from the second group (n = 9) were ground in liquid nitrogen and used for DNA extraction. 50 ng μl^{-1} gDNA from the infected leaves, along with 50 ng μl^{-1} gDNA from uninfected leaves from glasshouse-grown plants (negative controls), were first analyzed by conventional PCR. A further 50 ng μl^{-1} gDNA from the same infected leaves and controls were then analyzed using qPCR.

Detection and Quantification of Fungal Biomass

Fluorescence data from the qPCR machine were retrieved during the annealing step of every Cq. Threshold fluorescence was set automatically by the instrument manager system (CFX Manager Version 2.0.8) before carrying out the assay. A log-linear standard curve of a 10-fold dilution series corresponding to 5000 to 0.5 pg μl^{-1} was generated by plotting the logarithms of known concentrations of fungal DNA against the Cq values. The resulting regression equations were used to calculate fungal DNA in unknown samples. No-template controls, where sterile water was added instead of DNA, were included in each reaction. Limit of detection of the duplex assay, the lowest concentration at which reliable detection can be achieved, was determined following Armbruster and Pry (2008). All reactions were run with three replicates and samples that gave positive fluorescence before no-template controls were considered positive.

RESULTS

Specificity of the Assay

To test how well *P. tritici-repentis* and *Pa. nodorum* could be distinguished from each other, as well as from other common wheat pathogens and the host, we carried out two conventional PCR assays each using 5 ng gDNA. Five non-target controls of DNA from closely related cereal fungal pathogens and DNA from the wheat cultivar Scout were included in this step. Reactions were run in separate wells (i.e., singleplex). Conventional PCR provided amplicons of the expected sizes, and *P. tritici-repentis* and *Pa. nodorum* were distinguished based on the size of the amplicons (**Supplementary Figure 1**). *P. tritici-repentis* and *Pa. nodorum* primers only amplified the respective pathogen DNA. None of the five non-target controls or DNA from wheat gave specific amplicons that could be detected by conventional PCR (**Figures 1A,B**).

We then tested the specificity of the probes and their matching primers in two-singleplex real-time qPCR assays each containing 5 ng gDNA. Detection only occurred for probes that were complementary to the expected sequences, and none of the five non-target controls or the wheat DNA had specific amplification during 40 real-time qPCR cycles (**Figures 2A,B**). Samples that included no-template DNA or those that contained wheat DNA were negative during the course of the reaction (**Figures 2A,B**). *P. tritici-repentis* and *Pa. nodorum* were distinguished based on the emission spectra of the fluorogenic reporters that were used to label each pathogen probe.

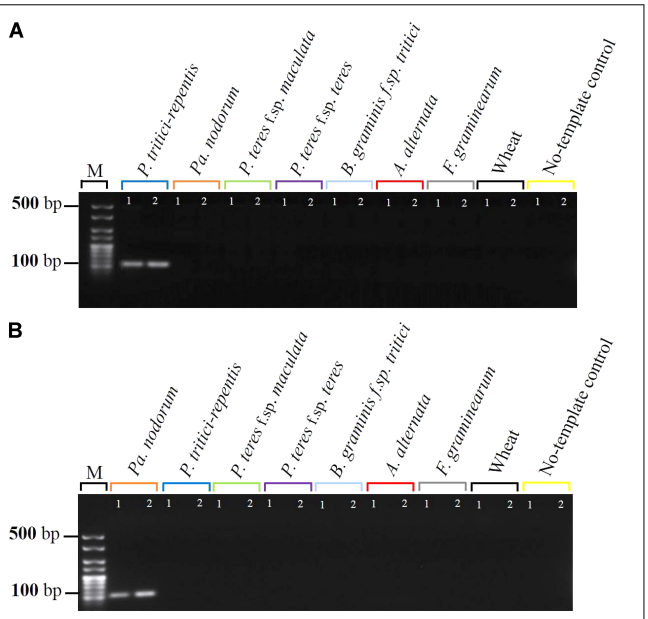

FIGURE 1 | Specificity testing of primers by agarose gel electrophoresis. **(A)** Primers of *P. tritici-repentis, Ptr*-Forward and *Ptr*-Reverse, were tested against *Pa. nodorum* DNA, and **(B)** primers of *Pa. nodorum*, *Pn*-Forward and *Pn*-Reverse, were tested against *P. tritici-repentis* DNA in two separate PCR reactions. Reactions included negative controls of DNA samples from five cereal fungal pathogens. Reactions including positive and negative controls were electrophoresed on 2% agarose with two technical replicates.

Dynamic Range, Efficiency, and Reproducibility of the Assay

We carried out two duplexed standard curve experiments on DNA of *P. tritici-repentis* and *Pa. nodorum* mixed at equal ratios. A 10-fold dilution series in the range of 5000 to 0.5 pg μl^{-1} was generated, analyzed and plotted against the number of Cq required to detect fluorescence signals. Each dilution was prepared with three replicates except the no-template control, which was analyzed using 10 replicates. Fitting log-linear standard curves between Cq and fungal DNA resulted in correlation coefficients (r) −0.997 and −0.996 for *P. tritici-repentis* and *Pa. nodorum*, respectively. The standard curves for both species were linear over 10,000-fold dilution, and the calculated amplification efficiency was 91.28% for *P. tritici-repentis* and 99.25% for *Pa. nodorum* (**Figures 3A,B**). The slopes and intercepts of the log-linear curves were comparable between *P. tritici-repentis* and *Pa. nodorum* ($p > 0.05$). Mean Cq value (±standard deviation bars, where visible) of three replicated reactions was highly reproducible with relative standard deviation $\leq$ 10%

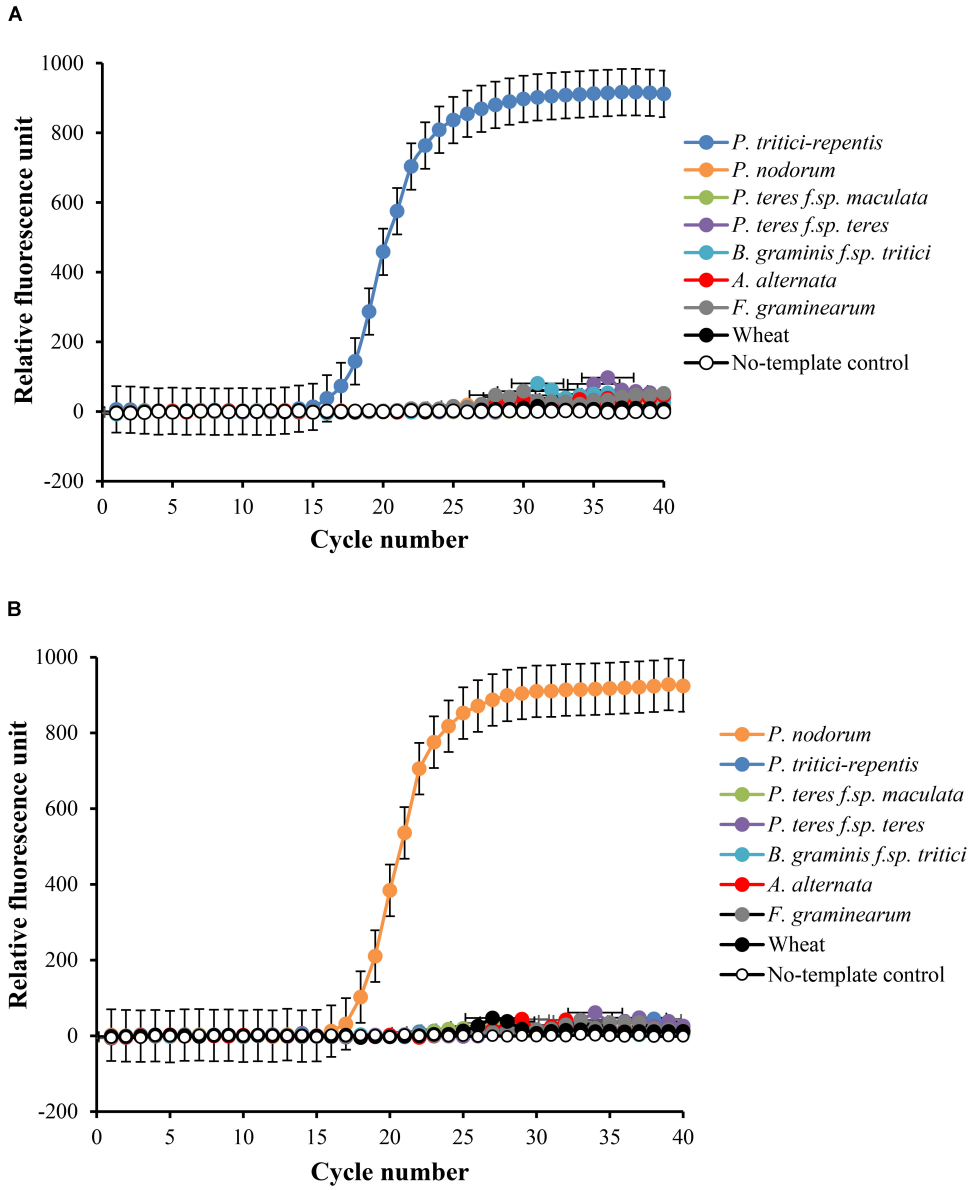

FIGURE 2 | Specificity testing of primers and their matching probes in singleplex real-time qPCR settings. Amplification curve for *P. tritici-repentis* is plotted in blue **(A)** and amplification curve of *Pa. nodorum* is plotted in orange **(B)**. Primers and probes (**Table 1**) were tested against DNA from the five fungal species, a negative wheat control, and a no template control and reactions were run separately. Data represent means ± standard deviation (n = 3).

(**Figures 3A,B**). The variation around the mean was independent of template concentration, and the Cq value for 10 no-template controls averaged 36.618 with a relative standard deviation of 0.35%.

Sensitivity and Limit of Detection of the Assay

We carried out two spiking experiments using a simulated matrix of *P. tritici-repentis* and *Pa. nodorum* DNA mixed at various ratios. Results of the spiking experiments demonstrated that reducing DNA ratio of one species while keeping DNA of the other species constant did not affect the detection limit of the assay. We were able to accurately quantify fungal DNA of either pathogen down to a relative ratio of 1:100 (**Figures 4A,B**). However, further reduction of the DNA ratio to 1:1000 underestimated the amount of *P. tritici-repentis* by 11.75% and *Pa. nodorum* by 18.55%. This underestimation became more pronounced with further dilution, and at 100 ppm (i.e., DNA ratios of 1:10000), neither pathogen was quantifiable in the presence of the other (**Figures 4A,B**). The minimal DNA concentration for detection was 0.059 pg μl^{-1} for *P. tritici-repentis* and 0.036 pg μl^{-1} for *Pa. nodorum*.

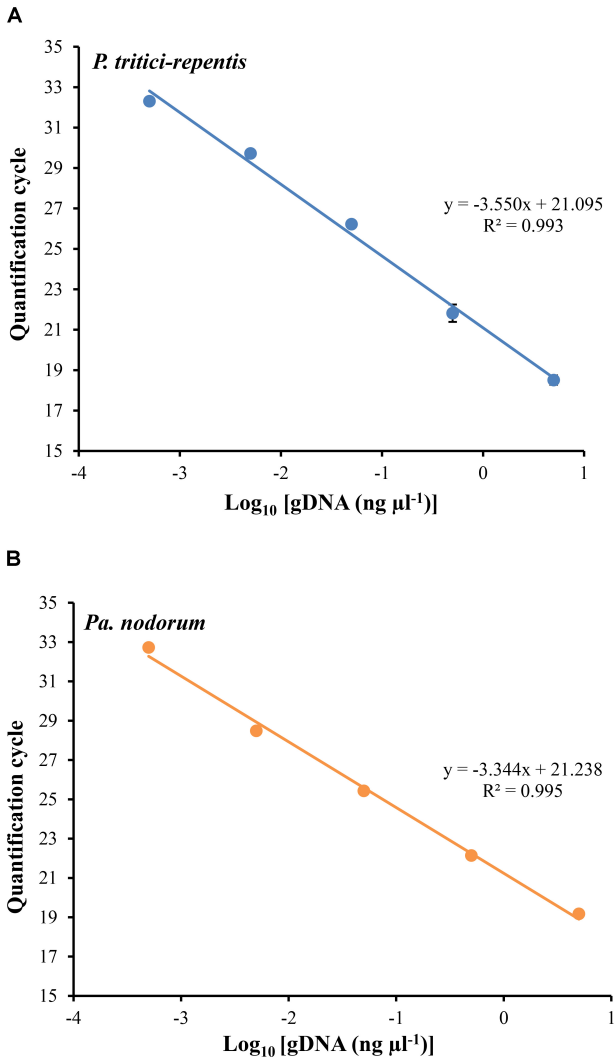

FIGURE 3 | (A) The relationship between quantification cycle and logarithm of the concentration of fungal DNA in duplexed qPCR settings. Triplicate dilution series corresponding to gDNA concentrations of 5000, 500, 50, 5, and 0.5 pg μl^{-1} were prepared. No-template samples were included in every reaction as negative controls (n = 10). The quantification cycle at which fluorescent signals were observed is plotted against the logarithm of DNA concentrations of *P. tritici-repentis* **(A)** and *Pa. nodorum* **(B)**. The corresponding regression equations and coefficient of determinations (R^2) are shown on the plot. Data are means ± standard deviation where visible (n = 3).

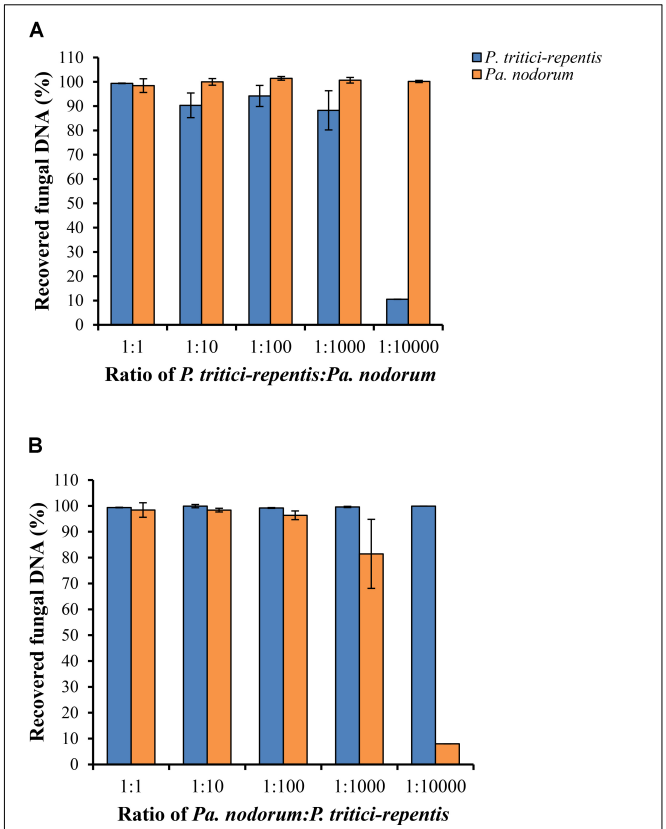

FIGURE 4 | Detection and quantification of P. tritici-repentis and *Pa. nodorum* in a simulated DNA matrix of various ratios. **(A)** *P. tritici-repentis* DNA was spiked with Pa. nodorum DNA at ratios of 1:1, 1:10, 1:100, 1:1000, and 1:10000. **(B)** *Pa. nodorum* was spiked with *P. tritici-repentis* DNA at same ratios. The starting concentration was 5 ng μl^{-1} of each pathogen DNA. The subsequent ratios were sequential 10-fold dilutions (0.5, 0.05, 0.005, and 0.0005 ng μl^{-1}) of one pathogen DNA, with the other held constant at 5 ng μl^{-1}. Data represent means ± standard deviation (n = 6).

We also tested the ability of the assay to detect and quantify fungal DNA in a sample that included abundant wheat DNA. We were able to quantify both species with high accuracy up to a *P. tritici-repentis*: *Pa. nodorum*: wheat DNA ratio of 1:1:200 (**Figure 5**). Recovery of fungal DNA, total amount of DNA quantified using the qPCR method, was high at 95.69% for *P. tritici-repentis* and 94.20% for *Pa. nodorum* when the fungal to wheat DNA ratios dropped to 1:1:2000. At these ratios, however, relative standard deviations were 10.23% and 13.90% for *P. tritici-repentis* and *Pa. nodorum*, respectively, affecting the reliability of fungal DNA quantification.

Field Evaluation of Naturally Infected Plants

We collected eighteen naturally infected wheat leaves from a site in the southwest of Western Australia. These leaves showed typical symptoms of tan spot with distinct yellow halos and tan chlorotic lesions (**Figure 6A**). No apparent symptoms of *Pa. nodorum* were visible on these leaves. Leaves were split into two groups; one group (n = 9) was incubated on agar Petri-dishes in an attempt to characterize the causal agent of the disease. Incubation on agar only yielded colonies typical of *P. tritici-repentis* (data not shown).

DNA was extracted from the second leaf group (n = 9) and analyzed using conventional PCR. Only one out of nine duplicated PCR reactions tested positive to *Pa. nodorum*. All reactions were positive to *P. tritici-repentis*. DNA from the same leaves that were used in the conventional PCR was then analyzed using qPCR. The duplex qPCR assay was able to detect signals corresponding to sequences of *P. tritici-repentis* and *Pa. nodorum* despite the absence of any visible symptoms of

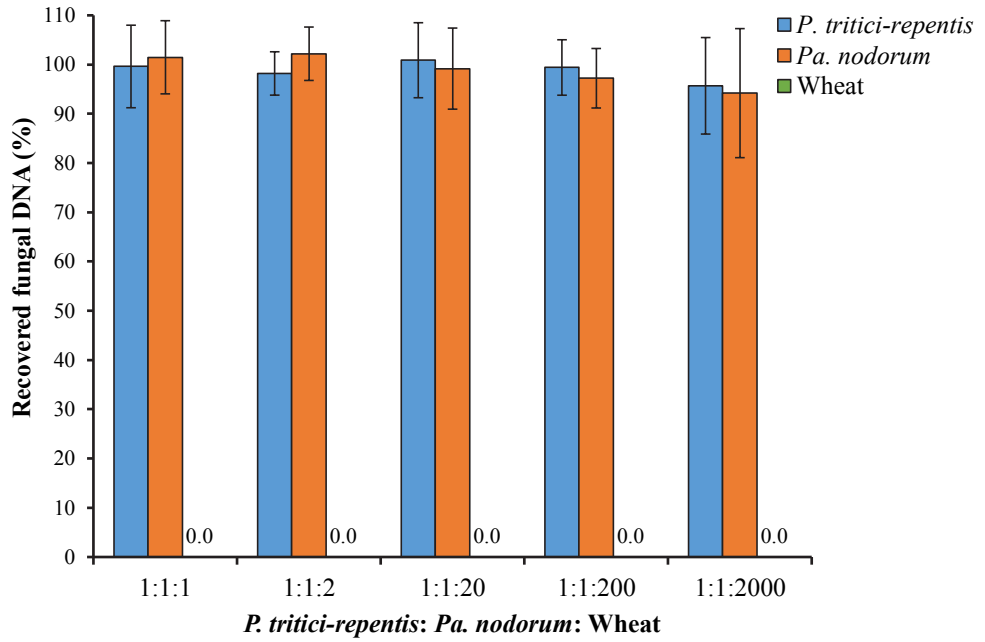

FIGURE 5 | Simulated DNA matrix of various ratios of fungi to wheat DNA. Increasing concentrations (5–100 ng μl^{-1}) of wheat DNA were spiked with decreasing concentrations of fungal DNA (5–0.05 ng μl^{-1}). Quantification was done in real-time quantitative PCR and reactions were duplexed each containing four fungal-specific primers and two complementary probes (**Table 1**). DNA concentrations respectively were 5:5:5, 5:5:10, 5:5:100, 0.5:0.5:100, and 0.05:0.05:100 ng μl^{-1}. Data represent means ± standard deviation (n = 6). Wheat DNA was not quantified/detected.

Pa. nodorum on these leaves (**Figure 6B**). There was a good agreement (r = −0.82) between total fungal DNA quantified by qPCR and conventional disease scores that were collected in the field (**Figure 6B**; black circles/line). Conventional disease scores were significantly correlated with the increase in *P. tritici-repentis* DNA, and *P. tritici-repentis* DNA was greater contributor to the disease scores than *Pa. nodorum* (**Figure 6B**; blue and orange circles/lines).

DISCUSSION

Quantification of the relative abundance of co-infecting pathogens requires selection of primers and probes that are compatible with each other whilst distinguishing between the co-infecting species. Recent work has identified a 235-bp multicopy region present in the *P. tritici-repentis* genome, and primers designed in this region were able to detect *P. tritici-repentis* from wheat leaves, even prior to the visible appearance of tan spot lesions (See et al., 2016). However, these primers cross-hybridized with *Pyrenophora teres* f. sp. *teres*, which the authors suggested may be overcome by the addition of fluorescence-labeled probes in the middle of the amplicon.

In this study, primers were chosen to produce relatively smaller amplicons (99–112 bp) that are more efficient for amplifying specific products than longer primers (Bustin et al., 2009). Our primers successfully distinguished targeted pathogens from non-target closely related fungal species and host genes. However, for increased specificity, fluorogenic probes were designed to hybridize to sequences within the primers enabling the assay to simultaneously distinguish and quantify DNA associated with *P. tritici-repentis* from that associated with *Pa. nodorum*. The length of the probes was designed to ensure that stable primer-probe hybrids were formed at the same annealing temperature for both species, irrespective of the length of the primers. Furthermore, probes were labeled with a unique fluorogenic-reporter allowing DNA sequences from *P. tritici-repentis* and *Pa. nodorum* to be amplified simultaneously but independent of each other. The choice of the fluorogenic reporter was decided based on instrument capability in resolving overlapping spectra. FAM-labeled probes are excited at lower emission spectra than CFG-labeled probes and hence are expected to produce stronger signals. Nevertheless, restricting the concentration of the FAM-labeled probe in the reaction optimized the fraction of the amplicon that is bound to the probe and produced comparable signals for *P. tritici-repentis* and *Pa. nodorum*. In addition to the fluorogenic reporters, probes were labeled with dark-hole quenchers to inhibit probe signals when probes are free in the solution (Holland et al., 1991). The dark-hole quencher was sufficient to inhibit signals from probes that are not in perfect contact with the target, resulting in accurate species-specific quantifications.

A series of experiments were conducted demonstrating the specificity, efficiency, and reproducibility of this assay for simultaneous detection and quantification of *P. tritici-repentis* and *Pa. nodorum*. The method reported here resolved two signals each unique to the assayed fungi. No cross-amplification with either host plant DNA or DNA from other closely related fungal

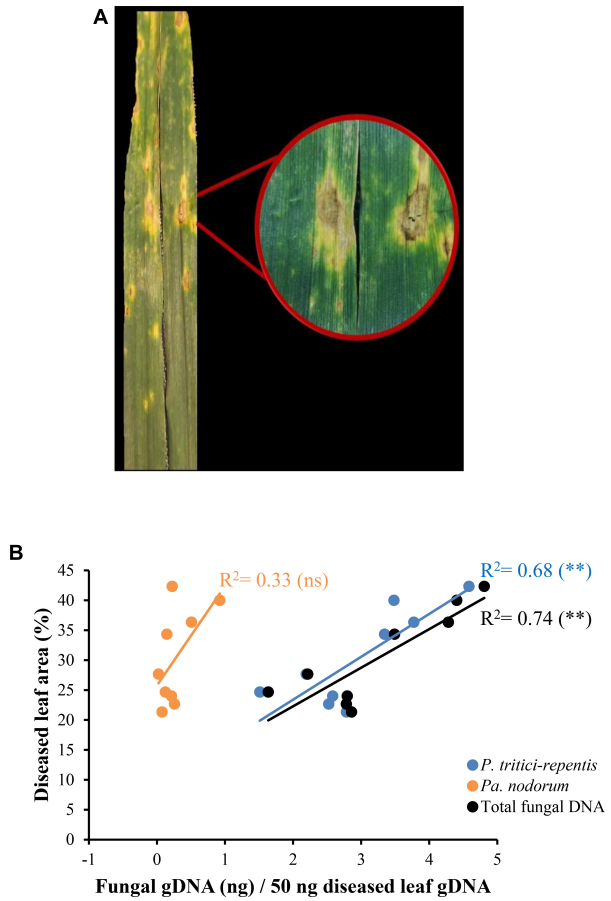

FIGURE 6 | Quantification of fungal DNA in naturally infected wheat leaves. **(A)** Leaves displaying tan spot symptoms with tan necrotic centers and yellow halos. **(B)** A linear model fitted into the relationship between fungal DNA measured in real-time quantitative PCR and conventional disease score. The corresponding regression equation and coefficient of determination (R^2) are shown on the plot. ns and ** refer to not significant and significant ($P < 0.01$), respectively.

pathogens of cereals was observed. The assay amplified the targeted sequences with high specificity, and we were able to detect the presence of *P. tritici-repentis* at 0.059 pg μl^{-1} and *Pa. nodorum* at 0.036 pg μl^{-1} in mixed fungal DNA matrices. Furthermore, in mixed gDNA matrices of both targeted species, the assay was able to detect fungal signals at a relative abundance as low as 1 in 10,000 with ≤10% RSD. Similarly, the assay was able to quantify the presence of *Pa. nodorum* DNA down to 23-pg in leaf samples naturally co-infected by abundant *P. tritici-repentis* up to 2192-pg. Nonetheless, there was a slight interference to the quantification of the less abundant target when DNA of the other target and/or wheat DNA was highly abundant. This may occur because reaction components including DNA polymerase, dNTPs, and $MgCl_2$ become limiting in later qPCR cycles. The more abundant target may compete for reaction components with the less abundant target, delaying its amplification (Bustin et al., 2009). As a result, the quantification of the less abundant target, although remaining specific and within the detection limit, may be compromised. One way to minimize this interference is to optimize concentrations of reaction components sequentially (Bustin et al., 2009). Regardless, the assay is highly stable and reproducible. The reproducibility was confirmed by the small standard deviations of triplicates samples in the standard curves (≤10%). The amplification curves of replicate runs showed strong overlap indicating stability and reproducibility.

A limitation of most nucleic acid-based quantification assays is an inability to distinguish between DNA from living and dead cells (Pinheiro et al., 2016). Although fungal cell viability was not assessed in this work, the high correlation coefficient, 0.826, especially between *P. tritici-repentis* DNA and the conventional disease score, suggests that viability may not have a significant impact on measuring disease as DNA equivalent. Quantification of fungal DNA has been shown to provide accurate measurement of disease severity for *P. tritici-repentis* (See et al., 2016) and *Pa. nodorum* (Oliver et al., 2008). Another limitation more specific to qPCR is that only a few targets can readily be accommodated in a single homogeneous assay. The number of targets that can be fitted in one assay depends on the design of the assay and the ability of the instrument to resolve overlapping spectra. The instrument used in this study has a blue monochromatic laser source for the excitation of fluorophores, and can simultaneously detect five targets on five different channels. This limits the fluorophores that could be efficiently excited by the blue laser to those that are distant from the far-red wavelengths. Instruments with high resolution-detectors and variable-wavelength light sources may allow more targets to be included in an assay. Instruments with such specifications are available and can be employed for detection and quantification of large-scale screening of co-infection by multiple pathogens.

Detection of multiple pathogens has also been achieved by the use of post-PCR dissociation curve analysis. Such methods use a set of primers with different melting temperatures and G + C contents. Using this technique up to 10 microbial pathogens of humans have been distinguished in a single assay (Gelaye et al., 2017; Jiang et al., 2017). Post-PCR methods, although specific and accommodating several targets in a single assay, do not provide quantitative information on the level of disease. Plant tissues can be inhabited by a large number of pathogenic and non-pathogenic microbes. Nevertheless, infection levels of these microbes and the damage they cause to the plant can vary greatly (Bakker et al., 2014). Our assay offers several advantages over the dissociation curve analysis and many other methods for diagnosis of co-infection. First, no post-reaction processing is required. Reactions are driven to completion allowing higher levels of sensitivity even when target sequences are present at low concentrations. Second, the assay provides quantitative data on the level of disease load in a sample, which other methods including metagenome sequencing do not offer. Finally, the cost-effectiveness, although not directly estimated, of testing multiple agents in a single test allows more testing using the same amount of reagents and staff time. When coupled with a 96-well capacity, this assay offers a sensitive and quantitative high throughput methodology for detection of co-infection in plants. The method

can also be used to study epidemiological consequences of co-infection in the field.

AUTHOR CONTRIBUTIONS

AA contributed to the conception of the idea, defined/selected the primers, conducted the experiments, analyzed the data, and drafted the manuscript. CT assisted in setting up the conventional PCR and testing of the primers. CM, FL-R, AZ, MG, and JH supervised the work and provided critical suggestions on the article. All authors read and approved the final version of the article.

FUNDING

AA is a recipient of Research Training Program (RTP), an Australian government funded scholarship for Ph.D. students. The Centre for Crop and Disease Management (CCDM) defrayed the publishing costs for this review. CCDM is a national research centre co-funded by Curtin University and the Grains Research and Development Corporation (project grant CUR00023). The funders had no role in ideas, design, decision to publish, or preparation of the manuscript.

ACKNOWLEDGMENTS

We thank Richard Oliver, Centre for Crop and Disease Management, for critically reading the manuscript and contributing to the genesis of the research. Belinda Cox and Weiwei Deng provided methodological and technical assistance, and Steven Chang shared some of the fungal isolates used in this study.

SUPPLEMENTARY MATERIAL

The Supplementary Material for this article can be found online at: https://www.frontiersin.org/articles/10.3389/fpls.2018.01086/full#supplementary-material

REFERENCES

Abdullah, A. S. A., Moffat, C., Lopez Ruiz, F. J. L., Gibberd, M. G., Hamblin, J., and Zerihun, A. Z. (2017). Host–multi–pathogen warfare: pathogen interactions in co-infected plants. *Front. Plant Sci.* 8:1806. doi: 10.3389/fpls.2017.01806

Alizon, S., De Roode, J. C., and Michalakis, Y. (2013). Multiple infections and the evolution of virulence. *Ecol. Lett.* 16, 556–567. doi: 10.1111/ele.12076

Armbruster, D. A., and Pry, T. (2008). Limit of blank, limit of detection and limit of quantitation. *Clin. Biochem. Rev.* 29(Suppl. 1), S49–S52.

Atallah, Z. K., Bae, J., Jansky, S. H., Rouse, D. I., and Stevenson, W. R. (2007). Multiplex real-time quantitative PCR to detect and quantify *Verticillium dahliae* colonization in potato lines that differ in response to *Verticillium wilt*. *Phytopathology* 97, 865–872. doi: 10.1094/PHYTO-97-7-0865

Bakker, M. G., Schlatter, D. C., Otto-Hanson, L., and Kinkel, L. L. (2014). Diffuse symbioses: roles of plant–plant, plant-microbe and microbe-microbe interactions in structuring the soil microbiome. *Mol. Ecol.* 23, 1571–1583. doi: 10.1111/mec.12571

Barbisin, M., Fang, R., O'shea, C. E., Calandro, L. M., Furtado, M. R., and Shewale, J. G. (2009). Developmental validation of the quantifiler® duo DNA quantification kit for simultaneous quantification of total human and human male DNA and detection of PCR inhibitors in biological samples. *J. Forensic Sci.* 54, 305–319. doi: 10.1111/j.1556-4029.2008.00951.x

Bates, J., Taylor, E., Kenyon, D., and Thomas, J. (2001). The application of real-time PCR to the identification, detection and quantification of *Pyrenophora* species in barley seed. *Mol. Plant Pathol.* 2, 49–57. doi: 10.1046/j.1364-3703.2001.00049.x

Bernreiter, A. (2017). Molecular diagnostics to identify fungal plant pathogens–a review of current methods. *Ecuad. Calid. Rev. Cient. Ecuat.* 4, 26–35.

Bhathal, J., Loughman, R., and Speijers, J. (2003). Yield reduction in wheat in relation to leaf disease from yellow (tan) spot and *Septoria nodorum* blotch. *Eur. J. Plant Pathol.* 109, 435–443. doi: 10.1023/A:1024277420773

Brandfass, C., and Karlovsky, P. (2006). Simultaneous detection of *Fusarium culmorum* and *F. graminearum* in plant material by duplex PCR with melting curve analysis. *BMC Microbiol.* 6:4. doi: 10.1186/1471-2180-6-4

Bustin, S. A., Benes, V., Garson, J. A., Hellemans, J., Huggett, J., Kubista, M., et al. (2009). The MIQE guidelines: minimum information for publication of quantitative real-time PCR experiments. *Clin. Chem.* 55, 611–622. doi: 10.1373/clinchem.2008.112797

DAFWA (2016). *Wheat Variety Guide for Western Australia. Department of Agriculture and Food Western Australia*. Available at: www.agric.wa.gov.au/cropdisease

Friesen, T. L., Stukenbrock, E. H., Liu, Z., Meinhardt, S., Ling, H., Faris, J. D., et al. (2006). Emergence of a new disease as a result of interspecific virulence gene transfer. *Nat. Genet.* 38, 953–956. doi: 10.1038/ng1839

Gelaye, E., Mach, L., Kolodziejek, J., Grabherr, R., Loitsch, A., Achenbach, J. E., et al. (2017). A novel HRM assay for the simultaneous detection and differentiation of eight poxviruses of medical and veterinary importance. *Sci. Rep.* 7:42892. doi: 10.1038/srep42892

Holland, P. M., Abramson, R. D., Watson, R., and Gelfand, D. H. (1991). Detection of specific polymerase chain reaction product by utilizing the 5′–3′exonuclease activity of *Thermus aquaticus* DNA polymerase. *Proc. Natl. Acad. Sci. U.S.A.* 88, 7276–7280. doi: 10.1073/pnas.88.16.7276

Hood, M. (2003). Dynamics of multiple infection and within-host competition by the anther-smut pathogen. *Am. Nat.* 162, 122–133. doi: 10.1086/375539

Jiang, Y., He, L., Wu, P., Shi, X., Jiang, M., Li, Y., et al. (2017). Simultaneous identification of ten bacterial pathogens using the multiplex ligation reaction based on the probe melting curve analysis. *Sci. Rep.* 7:5902. doi: 10.1038/s41598-017-06348-z

Klerks, M., Zijlstra, C., and Van Bruggen, A. (2004). Comparison of real-time PCR methods for detection of *Salmonella enterica* and *Escherichia coli* O157: H7, and introduction of a general internal amplification control. *J. Microbiol. Methods* 59, 337–349. doi: 10.1016/j.mimet.2004.07.011

Lamari, L., and Bernier, C. (1989). Evaluation of wheat lines and cultivars to tan spot [*Pyrenophora tritici-repentis*] based on lesion type. *Can. J. Plant Pathol.* 11, 49–56. doi: 10.1080/07060668909501146

Moffat, C., See, P. T., and Oliver, R. (2015). Leaf yellowing of the wheat cultivar mace in the absence of yellow spot disease. *Australas. Plant Pathol.* 44, 161–166. doi: 10.1007/s13313-014-0335-2

Moolhuijzen, P., See, P. T., Hane, J. K., Shi, G., Liu, Z., Oliver, R. P., et al. (2018). Comparative genomics of the wheat fungal pathogen *Pyrenophora tritici-repentis* reveals chromosomal variations and genome plasticity. *BMC Genomics* 19:279. doi: 10.1186/s12864-018-4680-3

Oliver, R. P., Rybak, K., Shankar, M., Loughman, R., Harry, N., and Solomon, P. (2008). Quantitative disease resistance assessment by real-time PCR using the *Stagonospora nodorum*-wheat pathosystem as a model. *Plant Pathol.* 57, 527–532. doi: 10.1111/j.1365-3059.2007.01787.x

Pinheiro, E. T., Neves, V. D., Reis, C. C., Longo, P. L., and Mayer, M. P. (2016). Evaluation of the propidium monoazide–quantitative polymerase chain reaction method for the detection of viable *Enterococcus faecalis*. *J. Endod.* 42, 1089–1092. doi: 10.1016/j.joen.2016.04.003

Rojas, J. A., Miles, T. D., Coffey, M. D., Martin, F. N., and Chilvers, M. I. (2017). Development and application of qPCR and RPA genus-and

species-specific detection of *Phytophthora sojae* and *P. sansomeana* root rot pathogens of soybean. *Plant Dis.* 101, 1171–1181. doi: 10.1094/PDIS-09-16-1225-RE

Savary, S., and Zadoks, J. (1992). Analysis of crop loss in the multiple pathosystem groundnut-rust-late leaf spot. III. Correspondence analyses. *Crop Prot.* 11, 229–239. doi: 10.1016/0261-2194(92)90042-4

Schena, L., Hughes, K. J., and Cooke, D. E. (2006). Detection and quantification of *Phytophthora ramorum*, *P. kernoviae*, *P. citricola* and *P. quercina* in symptomatic leaves by multiplex real-time PCR. *Mol. Plant Pathol.* 7, 365–379. doi: 10.1111/j.1364-3703.2006.00345.x

Schoch, C. L., Seifert, K. A., Huhndorf, S., Robert, V., Spouge, J. L., Levesque, C. A., et al. (2012). Nuclear ribosomal internal transcribed spacer (ITS) region as a universal DNA barcode marker for Fungi. *Proc. Natl. Acad. Sci. U.S.A.* 109, 6241–6246. doi: 10.1073/pnas.1117018109

See, P. T., Moffat, C. S., Morina, J., and Oliver, R. P. (2016). Evaluation of a multilocus indel DNA region for the detection of the wheat tan spot pathogen *Pyrenophora tritici-repentis*. *Plant Dis.* 100, 2215–2225. doi: 10.1094/PDIS-03-16-0262-RE

Tack, A. J., Thrall, P. H., Barrett, L. G., Burdon, J. J., and Laine, A. L. (2012). Variation in infectivity and aggressiveness in space and time in wild host-pathogen systems: causes and consequences. *J. Evol. Biol.* 25, 1918–1936. doi: 10.1111/j.1420-9101.2012.02588.x

Tollenaere, C., Susi, H., and Laine, A.-L. (2016). Evolutionary and epidemiological implications of multiple infection in plants. *Trends Plant Sci.* 21, 80–90. doi: 10.1016/j.tplants.2015.10.014

Tollenaere, C., Susi, H., Nokso-Koivisto, J., Koskinen, P., Tack, A., Auvinen, P., et al. (2012). SNP design from 454 sequencing of *Podosphaera plantaginis* transcriptome reveals a genetically diverse pathogen metapopulation with high levels of mixed-genotype infection. *PLoS One* 7:e52492. doi: 10.1371/journal.pone.0052492

Zadoks, J. (1999). Reflections on space, time, and diversity. *Annu. Rev. Phytopathol.* 37, 1–17. doi: 10.1146/annurev.phyto.37.1.1

Conflict of Interest Statement: The authors declare that the research was conducted in the absence of any commercial or financial relationships that could be construed as a potential conflict of interest.

frontiers in Plant Science

ORIGINAL RESEARCH
published: 28 September 2018
doi: 10.3389/fpls.2018.01396

Defense Compounds Rather Than Nutrient Availability Shape Aggressiveness Trait Variation Along a Leaf Maturity Gradient in a Biotrophic Plant Pathogen

Agathe Maupetit[1], Romain Larbat[2], Michaël Pernaci[1†], Axelle Andrieux[1], Cécile Guinet[3], Anne-Laure Boutigny[3†], Bénédicte Fabre[1], Pascal Frey[1] and Fabien Halkett[1]*

[1] Université de Lorraine, INRA, IAM, Nancy, France, [2] Université de Lorraine, INRA, LAE, Nancy, France, [3] ANSES, Laboratoire de la Santé des Végétaux, Unité de Mycologie, Malzéville, France

OPEN ACCESS

Edited by:
Christophe Le May,
Agrocampus Ouest, France

Reviewed by:
Sabine Banniza,
University of Saskatchewan, Canada
Fournet Sylvain,
INRA (Paris), France

***Correspondence:**
Fabien Halkett
fabien.halkett@inra.fr

†Present address:
Michaël Pernaci,
PalmElit SAS, Montferriez-sur-Lez, France
Anne-Laure Boutigny,
ANSES – Laboratoire de la Santé des Végétaux, Unité de Bactériologie, Virologie et OGM, Angers, France

Specialty section:
This article was submitted to Plant Microbe Interactions, a section of the journal Frontiers in Plant Science

Received: 20 April 2018
Accepted: 03 September 2018
Published: 28 September 2018

Citation:
Maupetit A, Larbat R, Pernaci M, Andrieux A, Guinet C, Boutigny A-L, Fabre B, Frey P and Halkett F (2018) Defense Compounds Rather Than Nutrient Availability Shape Aggressiveness Trait Variation Along a Leaf Maturity Gradient in a Biotrophic Plant Pathogen. Front. Plant Sci. 9:1396. doi: 10.3389/fpls.2018.01396

Foliar pathogens face heterogeneous environments depending on the maturity of leaves they interact with. In particular, nutrient availability as well as defense levels may vary significantly, with opposing effects on the success of infection. The present study tested which of these factors have a dominant effect on the pathogen's development. Poplar leaf disks of eight maturity levels were inoculated with the poplar rust fungus *Melampsora larici-populina* using an innovative single-spore inoculation procedure. A set of quantitative fungal traits (infection efficiency, latent period, uredinia size, mycelium quantity, sporulation rate, sporulation capacity, and spore volume) was measured on each infected leaf disk. Uninfected parts of the leaves were analyzed for their nutrient (sugars, total C and N) and defense compounds (phenolics) content. We found that *M. larici-populina* is more aggressive on more mature leaves as indicated by wider uredinia and a higher sporulation rate. Other traits varied independently from each other without a consistent pattern. None of the pathogen traits correlated with leaf sugar, total C, or total N content. In contrast, phenolic contents (flavonols, hydroxycinnamic acid esters, and salicinoids) were negatively correlated with uredinia size and sporulation rate. The pathogen's fitness appeared to be more constrained by the constitutive plant defense level than limited by nutrient availability, as evident in the decrease in sporulation.

Keywords: constitutive defense, aggressiveness traits, plasticity, nutrient availability, rust fungus

INTRODUCTION

Plant diseases and pests are responsible for crop damage that may account for up to 40% of yield losses worldwide (Boonekamp, 2012). Pathogen aggressiveness, the quantitative component of pathogenicity (Pariaud et al., 2009a), has been widely studied in order to forecast the evolutionary potential of plant pathogens and to better design disease control strategies (Lannou, 2012). Aggressiveness can be evaluated at different scales: by measuring the epidemic rate at the field scale or through elementary phenotypic traits at the individual scale (Pariaud et al., 2009a). The environment plays a key role in developmental processes of the pathogen and influences the individual's phenotype and the scale of fitness (Scheiner, 1993; Jarosz and Davelos, 1995).

Biotrophic fungal pathogens, such as rust and powdery mildew fungi, spend most of their life cycle within living plant tissues, so their fitness is directly affected by leaf physiology (Agrios, 2005; Gamm et al., 2011; Duplessis et al., 2013). On the one hand the leaf tissue provides the pathogen with the necessary nutrient resources for its development. On the other hand, it impedes pathogen development through a battery of plant defense compounds (Ullah et al., 2017).

Studies on interactions between plants and their foliar pathogens have shown that plant age, and especially leaf age, leads to different responses of the pathogen. Coleman (1986) postulated from a series of experiments that leaves pass through a peak of susceptibility to disease and pest attack. He proposed that for many stresses, including infection by biotrophic fungi, this peak coincides with changes in leaf properties during the transition from metabolite sink to source. This stage corresponds to a maximal nutrient availability. After this sink-source transition, free sugar content and thus nutrient resources decrease with increasing leaf maturity (physiological stage at a relative leaf age). Many studies support this view, demonstrating a maximum disease level before leaves are fully expanded and a decrease of disease severity on older leaves, which is also referred to as ontogenetic resistance (Ficke et al., 2002; Xavier et al., 2015; Farber and Mundt, 2017). In agreement, Merry et al. (2013) demonstrated that the peak in the severity of powdery mildew along a primary shoot of *Vitis vinifera* corresponds to the position of the first leaf that does not import carbohydrates. However, some studies have reported a contrasting pattern, e.g., Knott and Mundt (1991) found that infection efficiency of the wheat leaf rust fungus *Puccinia recondita* f. sp. *tritici* is 25% higher on older than on younger leaves in five wheat cultivars. The opposite trend may involve the dark side of plant-pathogen interaction: defense compounds. Their actions on a pathogen's development have been studied in several pathosystems, including rust fungi infecting poplar (Johnson and Kim, 2005), black currant (Vagiri et al., 2017), and willow (Hakulinen et al., 1999). Phenolic compounds present in leaves appear to highly influence the general plant resistance to fungi (Adandonon et al., 2017; Ullah et al., 2017). Most studies have focused on plant susceptibility to the disease (i.e., infection efficiency of the pathogen) or focused on overall disease severity. To dissect which fungal function is most influenced by leaf maturity and how, we propose to measure a set of elementary traits underlying components of aggressiveness.

Foliar pathogens of woody plants are good biological models to study the influence of leaf age on disease development, because they can infect leaves at various levels of maturity on the same host plant (Cellerino et al., 1978; Sharma et al., 1980; Turechek and Stevenson, 1998). Poplar is particularly well suited for studying the effect of leaf age on pathogens, since poplar plants grown from cuttings in a glasshouse produce new leaves at a constant rate, giving access to a wide range of leaves of increasing maturity on the same plant (Larson and Isebrands, 1971). These authors introduced the concept of leaf plastochron index (LPI) to refer to a position of a leaf along a poplar shoot. The youngest fully expanded leaf corresponds to LPI 1. Older leaves are numbered with increasing LPIs, according to their position along the shoot. In most experimental conditions the sink to source transition in poplar is established around LPI 6 (Coleman, 1986), which thus defines the first mature leaf. The effect of leaf maturity on the development of poplar pathogens (*Marssonina brunnea, Melampsora medusae*, and *M. larici-populina*) has been widely studied (Cellerino et al., 1978; Sharma et al., 1980; Coleman, 1986; Giorcelli et al., 1996). In most of these experiments, leaves were spray-inoculated with spore suspensions. In these conditions, hundreds of spores compete for infection, and as a result, inoculum density has been shown to influence aggressiveness traits (Giorcelli et al., 1996; Pei et al., 2003; Pariaud et al., 2009a). A way to eliminate any possible interaction among spores and to remove the effect of lesion density on trait variation is to use a single-spore inoculation protocol. Moreover, the single-spore inoculation enables the examination of phenotypic variation at the individual lesion level and not by means of average trait values measured on a cohort of lesions.

The aim of this study was to assess the effect of leaf age, and the associated content in nutrients and defense compounds, on the variation in aggressiveness traits in the poplar rust fungus *M. larici-populina.* We quantified trait variation along the leaf maturity gradient using the same fungal genotype to establish a so-called reaction norm (Gavrilets and Scheiner, 1993). We measured the effect of LPI using a single-spore inoculation method for a suite of aggressiveness and morphological traits: infection efficiency, latent period, uredinia size, sporulation rate, sporulation capacity, *in planta* mycelium quantity, and urediniospore volume. In a first step, we examined the differences in pathogen development along a leaf maturity gradient in order to study the variation in fungal traits and to assess the correlations between them. In a second step, we estimated the influence of the most important leaf compounds (sugars, total carbon and nitrogen, and phenolics) on the variation in aggressiveness traits.

MATERIALS AND METHODS

Plant and Fungal Material, and Experimental Design

Characterization of quantitative traits was performed on excised leaf disks of *Populus deltoides* × *P. nigra* 'Robusta'. Poplar plants were grown from dormant cuttings in 10-L pots containing a sand-peat (1:1, v/v) mixture, with an initial fertilization of 3.5 g L^{-1} CaCO3 and 6 g L^{-1} of slow release 13-13-13 N-P-K fertilizer (Nutricote® T100, Fertil). The plants were grown in a growth chamber regulated at 20/22°C (night/day temperatures) and 16 h photoperiod in order to ensure optimal growth, and were watered daily with deionized water. After four months, plants were about 1.2 m high and exhibited 25 to 30 fully expanded leaves.

On the same day, we harvested eight leaves of different maturity (LPI 6, 8, 10, 12, 14, 16, 18, and 20) from each of three plants (total of 24 leaves). From each poplar leaf, 24 disks (12-mm-diameter) were excised, and placed in flotation, each in a different cell culture plate. Each plate consists in 24 wells and thus contained one sample (leaf disk) of all leaves.

A plate thus corresponded to a complete statistical block: Twenty-four replicate plates were prepared, each containing the 24 combinations of LPI and plants. Within plates, the positions of the samples were randomized (**Supplementary Figure S1**). After disk excision, the remaining part of each leaf (about half a leaf) was stored individually in an aluminum wrapper at −80°C for sugar, nitrogen, carbon, and phenolic compound quantification. We hereafter refer to this plant material as "uninfected leaves."

Because the single-spore inoculation protocol is highly time-consuming, we were not able to inoculate more than six plates per day. Inoculations of the 24 plates were thus distributed over four consecutive days (each inoculation day formed a series of six plates). In other words, all leaf disks were excised the same day (day 1), but inoculated after 0 to 3 days depending on the series they belonged to.

Our experimental design (randomized complete block design) thus consisted in three experimental factors: LPI, plant and day of inoculation. Given an infection efficiency of approximately 25%, we expected six replicates per combination.

Single-Spore Inoculation Protocol

Single-spore inoculation was performed with pure *M. larici-populina* isolate 98AG31. This isolate was collected in 1998 in Moÿ-de-l'Aisne (France) on *Populus trichocarpa x Populus deltoides* 'Beaupré' leaves and serves since as a reference isolate (Duplessis et al., 2011). Urediniospores were cryopreserved at −80°C at Institut National de la Recherche Agronomique Nancy (France) and multiplied on fresh poplar leaf disks before inoculation to maximize their germination and infection rates (Pei et al., 2002). To this aim, 1 mg of urediniospores was dispersed in 200 µL of water-agar (0.1 g L^{-1}). The resulting urediniospore suspension was applied as 2 µL droplets on the abaxial surface of two 30-mm-diameter leaf disks of 'Robusta'. Leaf disks were incubated by floating on deionized water in six-well polystyrene cell culture plates, with the abaxial surface upside, at 19 ± 1°C, and under continuous fluorescent light (25 µmol m^{-2} s^{-1}). After a 10 to 13 days incubation period, the sporulating leaf disks were gently tapped over a microscope slide to release and collect urediniospores.

A germination test was performed just before inoculation to ensure the quality of urediniospores used. To this aim, a few hundred urediniospores were dispersed on the surface of a Petri dish containing agar (20 g L^{-1}). After an overnight incubation at 19 ± 1°C, the ratio of germinated/total urediniospores was evaluated under a light microscope (100× magnification) to determine the germination rate. This test ensured that nearly all spores used for the experiment were physiologically able to germinate (mean germination rate of 93%).

For single-spore inoculation leaf disks were inoculated one by one. One single urediniospore was picked with a human eyelash under a stereomicroscope (63× magnification) and deposited into a 5 µL water-agar droplet placed at the center of the poplar leaf disk (abaxial surface). After inoculation the plates were incubated for 13 days in the same conditions as described above.

Quantitative Trait Measurements

Several aggressiveness traits classically studied in plant-pathogen interactions were measured: infection efficiency, latent period, uredinia size, sporulation rate, and sporulation capacity (Lannou, 2012). In addition, we measured *in planta* mycelium quantity, which is less commonly studied.

- *Infection efficiency* is commonly defined as the probability that a urediniospore deposited on a receptive host surface produces a lesion (Lannou, 2012).
- *Latent period* is defined as the time interval between infection and the onset of sporulation from that infection (Lannou, 2012).
- *Uredinia size* is defined as the surface area that produces the urediniospores (Kolmer and Leonard, 1986; Robert et al., 2004) and has been suggested to be an indication of the pathogen capacity for host tissue colonization (Pariaud et al., 2009b; Lannou, 2012). However, the uredinia size is not a proxy of tissue colonization by *M. larici-populina*, as no necrosis is observed. Unlike necrotrophic pathogens, the only visual symptom is the opening in the leaf epidermis, through which urediniospores are extruded.
- *Sporulation rate* is defined as the number of urediniospores produced by the uredinia per unit of time (Leonard, 1969; Clifford and Clothier, 1974; Kardin and Groth, 1989): sporulation rate = urediniospore number/(13 – latent period).
- *Sporulation capacity* is defined as the amount of spores produced per unit area of sporulating tissue per unit of time (Robert et al., 2002; Dowkiw et al., 2003). It characterizes the flux of spores extruded by the uredinia and is calculated as the ratio between sporulation rate and uredinia size.
- *Mycelium quantity* which gives a proxy of the fungal colonization *in planta* is assessed using qPCR analysis on leaf disks (see below).

Beyond these six quantitative aggressiveness traits, we also measured a morphological trait:

- *Volume of urediniospores* was computed from length and width of urediniospores obtained from image analysis (see below).

We monitored the infections for 13 days, allowing measurements of latent period and infection efficiency. Emergence of uredinia was scored twice a day, at 9 a.m. and at 4 p.m. Infection efficiency was assessed for each leaf disk and was recorded as a binary variable: 1 if the deposited urediniospore produced one uredinia, 0 if not.

At day 13 (end of the monitoring period), leaf disks were harvested. We harvested all infected leaf disks (total: 158 samples out of 576 leaf disks inoculated, mean infection efficiency of 27.4%), giving from 4 to 12 biological replicates per LPI and per plant (mean: 6.58 replicates). The first step of the harvest consisted in separating the urediniospores produced

from the leaf disk. Infected leaf disks were placed in 2 mL Eppendorf tubes with 2 mL of Isoton® II isotonic buffered diluent (Beckman Coulter). The tubes were vigorously shaken for 20 s at 4 m s^{-1} on a MP FastPrep®-24 homogenizer, in order to release all urediniospores from the uredinia. The second step consisted in measuring the size of the uredinia (or lesion size): photographs of the spore-free uredinia were taken under a stereomicroscope (25× magnification) coupled to a digital camera. Pictures were analyzed using ImageJ version 1.5i with a dedicated script (**Supplementary Note S1**). To measure the number of yellow pixels corresponding to the sporulating area, the Hue Saturation and Brightness was used: pixels with a hue under 37° were counted. Last, infected leaf disks were stored at −80°C and lyophilized before DNA extraction.

Measurements of both sporulation rate and urediniospore morphological parameters were performed on the urediniospore suspensions using an Occhio® Flowcell FC200+ optical morphogranulometer, which allows simultaneous particle counting and image analysis of the particles. Before counting, urediniospore suspensions were vortexed to disperse clusters of urediniospores. For each sample, counting was performed using the following settings: 0.15 mL of priming, 0.85 mL of volume analysis, and 7% of volume sampling (i.e., 7% within 0.85 mL were really analyzed, evenly distributed along the analyzed volume). Two filters parameter values were applied:

1. For urediniospore counting: bluntness between 0.6 and 1; length of ellipse minor axis between 20 and 60 μm; ellipse elongation between 0.18 and 0.79; and ISO eccentricity higher than 0.15,
2. For urediniospore size measurement: bluntness between 0.6 and 1; inertia Feret elongation between 0.25 and 1; ISO eccentricity higher than 0.1; minimum Feret diameter between 13.5 and 70 μm; and Feret diameter length between 23 and 200 μm.

These filters were applied on the raw data to compute sporulation rate expressed in spores per day, length, and width of urediniospores produced by each uredinia. The volume of urediniospores was computed following the formula of the volume of an ellipsoid (Philibert et al., 2011):

$$Spore\ volume = \frac{4}{3}\pi \times \frac{length}{2} \times \left(\frac{width}{2}\right)^2$$

DNA Extraction and qPCR Quantitation of *in planta* Mycelium

DNA was extracted from infected poplar leaf disks using the DNeasy96® DNA plant kit (Qiagen). The Frozen Plant Tissue protocol (DNeasy 96 Plant Handbook, June 2015) was followed except that 20 1-mm-diameter glass beads were added to one 3-mm-diameter tungsten carbide bead in the 2 mL Eppendorf tubes. The 158 samples were randomly processed in two DNA extraction plates, which were stored at 4°C until qPCR analysis.

In order to correct for amplification differences among qPCR, three technical replicates were performed.

In order to quantify *M. larici-populina* mycelium *in planta*, quantitative Taqman® PCR was performed using new primers and probe designed for the rDNA ITS (Internal Transcribed Spacer). These primers and probe allowed a significant gain in sensitivity compared to a previously used primer pair, which was designed for a single-copy gene (Guinet et al., 2016). Reagent mix contained 3.1 μL of pure water, 6.5 μL of Mastermix®, 0.13 μL of primer ITS-Mlp-F (Primer sequence 5′-3′: TGACTCTTTGTATAAACCATTACCC), 0.13 μL of primer ITS-Mlp-R (TCAAAGTTGCCTTTGAGATACG), and 0.13 μL of probe ITS-Mlp-P (6-FAM-TGCATTGTGGCCCGTCAAAA-BHQ1) per sample. A volume of 3 μL of extracted DNA was added to 10 μL of reagent mix. Standard samples consisted of calibrated quantities of plasmid DNA containing the cloned ITS amplicon. Two series of eight 10-fold dilutions of plasmid DNA (from 1.47×10^7 to 1.47 fg μL^{-1}) were included in each qPCR run to set a standard curve. Quantitative PCR runs were performed on a QuantStudio 6 Flex (Life Technologies) machine and consisted in 10 min at 95°C followed by 45 cycles of 15 s at 95°C and 45 s at 62°C. DNA quantity was analyzed using the QuantStudio™ Real-time PCR software (version 1.1).

Leaf Content Measurements: Total Nitrogen and Total Carbon Contents, Sugars, Phenolic Compounds

All leaf content measurements were conducted on the uninfected leaves, stored at −80°C just after disk excision.

Total nitrogen and total carbon concentrations in uninfected leaves were analyzed using an elemental analyser (Thermo Quest, Type NCS 2500). Measurements, data analysis, data record, and weighing record (Mettler Tolédo MT5 microbalance) were performed using the EAGER 200 software.

Soluble sugars were extracted from 20 mg of dry leaf powder with 1 mL of 70% (v/v) methanol/water for 10 min and then centrifuged at 17,000 *g* for 5 min at 4°C. This step was repeated twice and the resulting supernatants were pooled together. The supernatants, containing soluble sugars, were dried overnight with a vacuum evaporator (Maxi-Dry Plus; Hetomodel DW1, 0-110, Heto-HOLTEN A/S) to eliminate methanol. Dried extracts were rehydrated in 1.5 mL of distilled water, dissolved by sonication and then filtered at 0.2 μm (Acrodisc® Supor® filter; 0.2 μm, Van Waters Rogers). Undiluted aliquots of 20 μL were injected into a high-pressure liquid chromatography system (Dionex™ ICS-5000+ HPLC™) to determine soluble sugar composition. Soluble sugar separation was achieved on a Dionex™ CarboPac™ SA10 IC separation column (6 μm 250 × 4 mm; Thermo Scientific™). The flow rate was maintained at 1 mL min^{-1}, and the column temperature at 40°C. Individual carbohydrates were eluted from 0 to 30 min after injection. The sugar peaks were detected by light scattering (Sedex 45 ELSD system, Seder) then identified according to retention time and commercial standards. Sucrose, glucose, and fructose concentrations (% of dry weight) were determined by peak height and standard calibrations.

Phenolics were extracted from 30 mg dry leaf powder using the method described by Royer et al. (2013). Total phenolic content

was determined according to the Folin–Ciocalteu method. Briefly, each extract was diluted 1:16 in distilled water, and 20 μL of each diluted extract was distributed in a 96-well plate. Then 100 μL of Folin–Ciocalteu's reagent (Sigma), diluted 1:10 in distilled water, and 80 μL of 7.5% sodium carbonate (w/v) were added. The microplate was incubated 30 min at 25°C and shaken 5 s every 10 min. Absorbance of the sample was measured with a microplate-reader (SynergyHT, BioTek) at 760 nm. Quantification of total phenolics was performed according to a calibration curve of gallic acid, and the results were expressed as milligram of gallic acid equivalent per gram of leaf dry weight.

In addition to total phenolic content, the concentration of major phenolics was analyzed on ultra-high performance liquid chromatography (U-HPLC) system (Shimadzu) equipped with a photo diode array detector (DAD) and a mass spectrometer. Each sample (3 μl) was separated on a C18 kinetex (100 mm × 2.1 mm) column (Phenomenex). The mobile phase consisted in 0.1% formic acid in ultra-pure water (solvent A) and 0.1% formic acid in methanol (solvent B). The molecules were eluted with a flow rate of 300 μL min^{-1}, through a gradient elution from 1 to 50% B for 10 min, then to 99% B in 3 min, which was maintained for three additional minutes. The column was then re-equilibrated to 1% B for 4 min prior to the next run. Mass spectrometry analysis was carried out in ESI positive and negative modes. Quantification was performed by measuring the area under each peak at 280, 320, or 350 nm, depending on the lambda max of each molecule. Due to co-eluting signal at 280 nm, catechin quantification was realized by measuring the area under peak at *m/z* 289, corresponding to the [M-H]– of the molecule. Experimental exact masses and MS fragments were compared to metabolomics databases (Respect[1]; MassBank[2], DNP[3]) and data available in the literature in order to identify the nature of the metabolites. Sixteen phenolic compounds were identified. According to their structure, these 16 metabolites could be grouped into four phenolic subclasses, which are Flavan-3-ols (catechin, proanthocyanidin dimer), hydroxycinnamic acid esters (chlorogenic acid, caffeoyl shikimate, caffeoyl glucose isomers (×2), coumaroyl glucose isomers (×2)), flavonols (rutin, quercitrin), and salicinoids (salicine, salicortin, acetylsalicortin, homaloside D, tremulacin, and a putative populoside) (**Supplementary Figure S2**).

Data Analysis

Principal component analyses (PCA) and linear models were used to explore correlations between phenotypic traits. Each independent phenotypic trait was analyzed separately using a generalized linear model evaluating effects of LPI, plant, day of inoculation, and the interaction between LPI and plant. To normalize the error, infection efficiency was analyzed with a binomial error family; latent period and sporulation capacity with a Gamma error family; uredinia size, spore volume, sporulation rate, and mycelium quantity with a Gaussian error family; and uredinia size and sporulation rate were square root transformed. An analysis of variance (ANOVA) with an alpha error <5% was performed on each model. Differences of means were checked with Tukey tests. PCA on leaf characteristics was performed to explore their variations. Spearman correlation coefficients between phenotypic traits and leaf content were computed on mean phenotypic traits per LPI and plant based on 4 to 12 replicates. Spearman correlation coefficients' associated *p*-values were adjusted with a False-Discovery-Rate correction for multiple tests. All data analyses were performed using R version 3.2.5 (see details in the RMARKDOWN document, **Supplementary Note S2**).

[1]http://spectra.psc.riken.jp/

[2]http://massbank.jp/

[3]http://dnp.chemnetbase.com/

RESULTS

Variation in *M. larici-populina* Quantitative Traits

To describe the variation in quantitative traits of *M. larici-populina* in this experiment, a PCA was performed on individual trait measurements assessed for each infected leaf disk (latent period, uredinia size, sporulation rate, sporulation capacity, mycelium quantity, and mean volume of produced spores). Infection efficiency cannot be included in the PCA analysis because it is set to one for infected leaf disk. Experimental factors (LPI, plant harvested, and day of inoculation) were considered as supplementary variables. The first principal component (PC1) explained 31% of the total inertia and was related to uredinia size, sporulation rate and to a lesser extent to sporulation capacity (**Figure 1**). PC2 and PC3 accounted for almost 20% and 17% of the total variance, respectively. PC2 was related to latent period which varied independently from uredinia size and sporulation rate, and PC3 was related to spore volume. However, there was large dispersal of individual measures that remained unexplained by experimental factors (**Supplementary Note S2**).

In accordance with PCA analysis, LPI was the main structuring variable in GLM analyses and had a significant effect on uredinia size ($P_{adjusted} = 1.22 \times 10^{-21}$), sporulation rate ($P_{adjusted} = 7.67 \times 10^{-15}$), and sporulation capacity ($P_{adjusted} = 1.40 \times 10^{-05}$) (**Table 1**). Uredinia size and sporulation rate increased with the LPI, while sporulation capacity decreased (**Figure 2**). Uredinia size exhibited a threefold increase (from 0.272 to 0.737 mm^2) and sporulation rate a twofold increase (from 333 to 611 urediniospores day^{-1}) from LPI 6 to 20 (**Figure 2**). Sporulation capacity was reduced more than twofold from LPI 6 to 20 (from 12,420 to 5,800 urediniospores day^{-1} mm^{-2}) (**Figure 2**). The sporulation rate was also significantly, although less strongly, explained by the plant used for the experiment ($P_{adjusted} = 4.63 \times 10^{-05}$). Sporulation rate was significantly higher on plant No. 3 (mean rate = 526 urediniospores day^{-1}) and lower on plant No. 2 (mean rate = 396 urediniospores day^{-1}) (**Figure 2**), but no interaction was found between plant and LPI (**Table 1**). Other fungal traits varied but not in accordance with LPI, plant and day (**Supplementary Figure S3**).

We found no significant effect of the day of inoculation on any aggressiveness traits. As there was no difference in fungal traits across days of inoculation, we assumed that the incubation

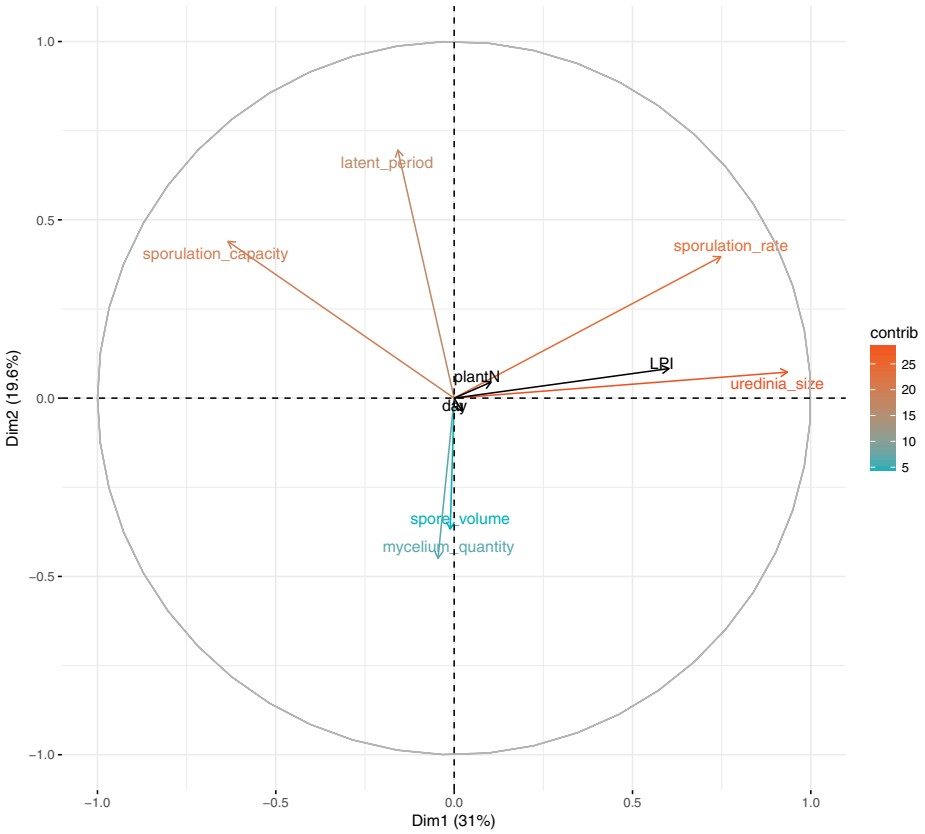

FIGURE 1 | Principal component analysis of fungal phenotypic traits (latent period, uredinia size, sporulation rate, sporulation capacity, spore volume, and mycelium quantity, measured on 4 to 12 replicates per LPI and per plant); LPI, plant and day are supplementary variables. Colors correspond to variables' contribution to the first and second axes.

TABLE 1 | Summary of the analysis of variance of each experimental variable in generalized linear models (Chi-square test probability adjusted with a False-Discovery-Rate correction for multiple tests).

Traits	LPI	Plant	LPI:Plant	Day
Infection efficiency	0.459	0.661	0.346	0.165
Latent period	0.720	0.165	0.720	0.661
Uredinia size	**1.22×10^{-21}**	0.092	0.458	0.346
Spore volume	0.980	0.362	0.720	0.720
Sporulation rate	**7.67×10^{-15}**	**4.63×10^{-05}**	0.497	0.090
Sporulation capacity	**1.40×10^{-05}**	0.379	0.720	0.092
Mycelium quantity	0.866	0.980	0.996	0.720

P-values < 0.05 are indicated in bold characters.

conditions during the pre-inoculation period described above kept the leaf disks in their initial physiological state.

Variation in Leaf Content Characteristics

To assess leaf content variations among the range of leaf maturity, a PCA was performed on leaf characteristics (**Figure 3**). Leaf characteristics were measured on one uninfected half-leaf of each plant and each LPI, so only plant and LPI supplementary variables were taken into account. PC1 explained almost 53% of the total inertia and was highly related to sugars (sucrose, fructose, glucose) and phenolic compounds (total phenolics, and all the phenolic subclasses) variations. Explaining 18% and 12% of the inertia, PC2 and PC3 were associated to sucrose and nitrogen, respectively. The total carbon content of leaves did not vary among the range of leaf maturity studied. Leaf maturity, characterized by the content in phenolic compounds, appeared to structure more leaf characteristics than plant did.

Correlation of Fungal Phenotypic Trait Variation and Leaf Content Characteristics

To assess how fungal and leaf data were correlated, pairwise Spearman's correlation coefficients and their adjusted *p*-values were calculated.

Spearman's coefficient for uredinia size and both sporulation rate and sporulation capacity were highly significant (rhô = 0.87 and −0.73, $P_{\text{adjusted}} = 3.37 \times 10^{-6}$ and 4.66×10^{-4}, respectively) (**Figure 4**), which is consistent with PCA results on individual traits. No other Spearman's coefficient appeared significant between fungal traits.

Spearman coefficients showed a negative correlation between total phenolic content and uredinia size and sporulation rate

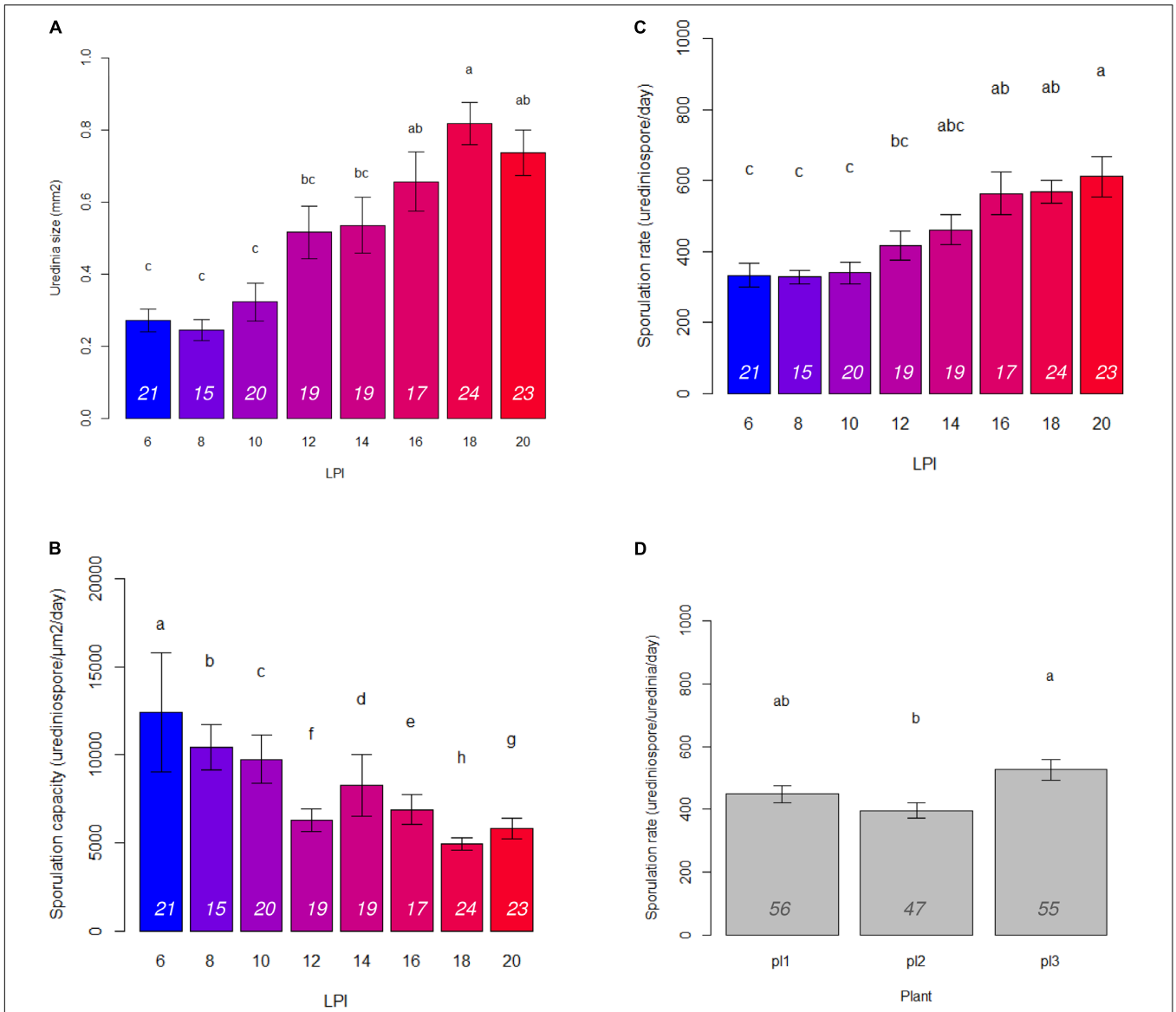

FIGURE 2 | Barplots of means and standard error calculated on three plants and 15 to 24 replicates per LPI (italic numbers at the bottom of the bars) of **(A)** uredinia size, **(B)** sporulation capacity, and **(C)** sporulation rate for each LPI; and **(D)** sporulation rate for each plant. Letters correspond to Tukey test results.

(rhô = −0.77 and −0.61, $P_{adjusted} = 1.62 \times 10^{-4}$ and 1.07×10^{-2}, respectively), as well as a negative correlation between hydroxycinnamic acid esters content and uredinia size and sporulation rate (rhô = −0.83 and -0.68, $P_{adjusted} = 2.25 \times 10^{-5}$ and 1.85×10^{-3}, respectively), and a positive correlation between hydroxycinnamic acid esters content and sporulation capacity (rhô = 0.68, $P_{adjusted} = 1.85 \times 10^{-3}$) (**Figures 4**, **5**). Three of the four phenolic subclasses (salicinoids, hydroxycinnamic acid esters, and flavonols) showed the same trends as total phenolic content, with the exception that the correlation between sporulation rate and sporulation capacity, on one side, and salicinoids and flavonols, on the other side, were not significant ($P_{adjusted} > 0.05$). In accordance with the PCA on leaf characteristics, all sugar contents were correlated with each other. However, no correlation was found between fungal phenotypic traits and sugars, carbon and nitrogen contents. Salicinoids, flavonols, and hydroxycinnamic acid esters were all positively correlated to each other. Flavan-3-ols were, however, negatively correlated to the three other phenolic subclasses, although this was only significant with flavonols.

DISCUSSION

In this study, we analyzed the variation in seven aggressiveness and morphological traits of the poplar rust fungus when inoculated on poplar leaves of varying maturity levels. A single-spore inoculation technique was used, which enabled

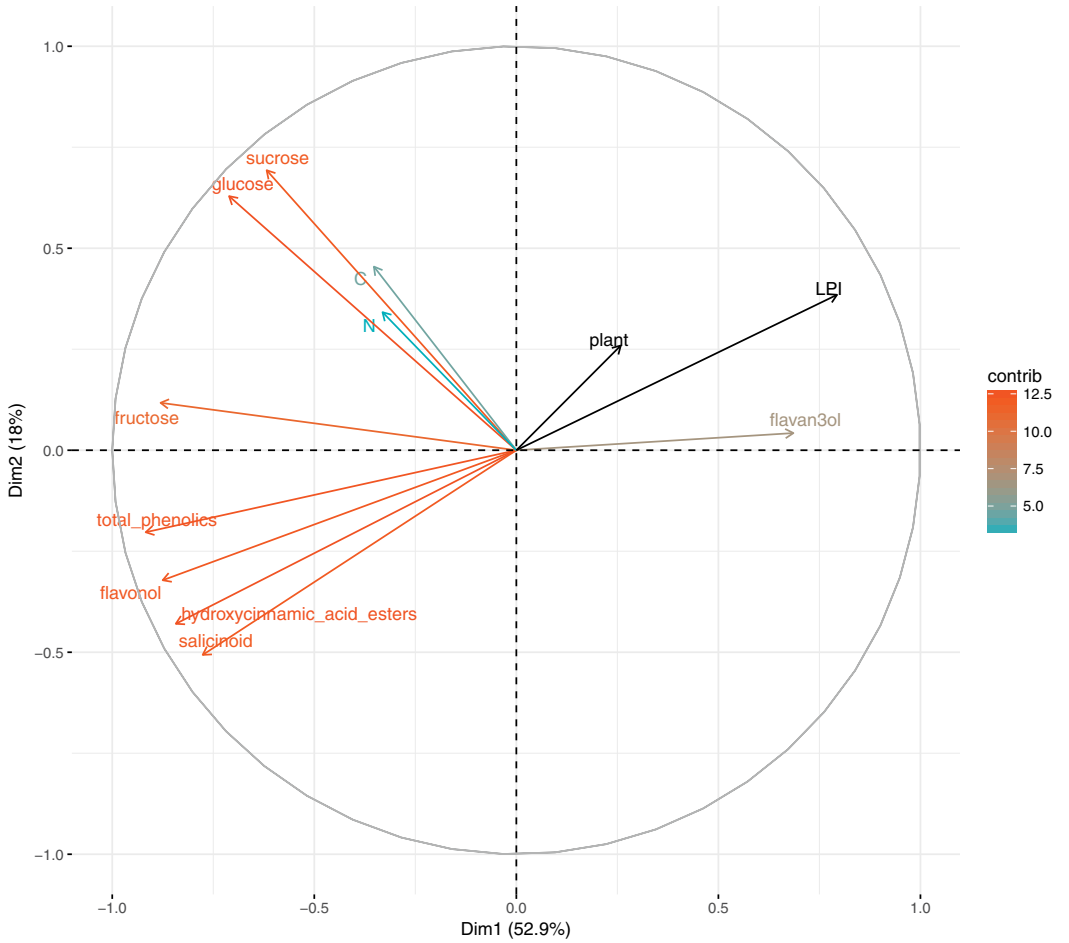

FIGURE 3 | Principal component analysis on leaf chemical content (carbon, nitrogen, glucose, fructose, sucrose, total phenolics, flavan-3-ols, hydroxycinnamic acid esters, flavonols, and salicinoids), LPI and plant are supplementary variables. Colors correspond to variables' contribution to the first and second axes.

us to study trait variance and covariance at the individual lesion level. Applying this method, we aimed at assessing the effect of leaf maturity on aggressiveness traits of *M. larici-populina*. In a second step, we explored correlations between the variation in fungal phenotypic traits and physiological features of the leaves in order to determine whether variation in phenotypic traits was influenced by nutritive or defensive compounds of leaves.

Effect of Leaf Maturity on Aggressiveness and Morphological Traits

Regarding the variation in aggressiveness traits, our first result was a positive correlation between uredinia size and sporulation rate, whereby both increased with leaf maturity. That is, on more mature leaves, uredinia were wider with a higher production of urediniospores. Some authors found that the breaking down of sporulation rate into uredinia size and sporulation capacity enabled to explain differences in aggressiveness levels: an increase in sporulation rate can either be due to wider uredinia or higher sporulation capacity (flux of urediniospores) (Pariaud et al., 2009b). In our study, we found that the increase in sporulation rate is linked to wider uredinia, but not to higher sporulation capacity. The correlation between uredinia size and sporulation rate has already been identified by several authors, including Dowkiw et al. (2003) on poplar rust, Pei et al. (2002) on willow rust and Robert et al. (2002) on wheat leaf rust. Based on our data, we add to this that sporulation capacity is not necessarily even as assumed by Robert et al. (2002). Indeed, sporulation capacity significantly decreased with leaf maturity, in contrast to uredinia size and sporulation rate. Even if the flux of urediniospores was lower on mature leaves, the amount of urediniospores produced was higher, leading to an increased aggressiveness on mature leaves compared to younger ones.

In this study, we also quantified individual variation in mycelium quantity through qPCR analysis. This trait has received little attention as a component of aggressiveness, mostly for methodological reasons. However, it can serve to measure the relative investment in sporulation vs. mycelium growth, the two main functions to which host extracted resources are allocated (Gilchrist et al., 2006; Yegorov et al., 2017). Notably, the quantity of *in planta* mycelium did not vary along the leaf maturity gradient and was correlated to neither sporulation rate nor lesion size. Hence, lesion size does not equate to mycelium

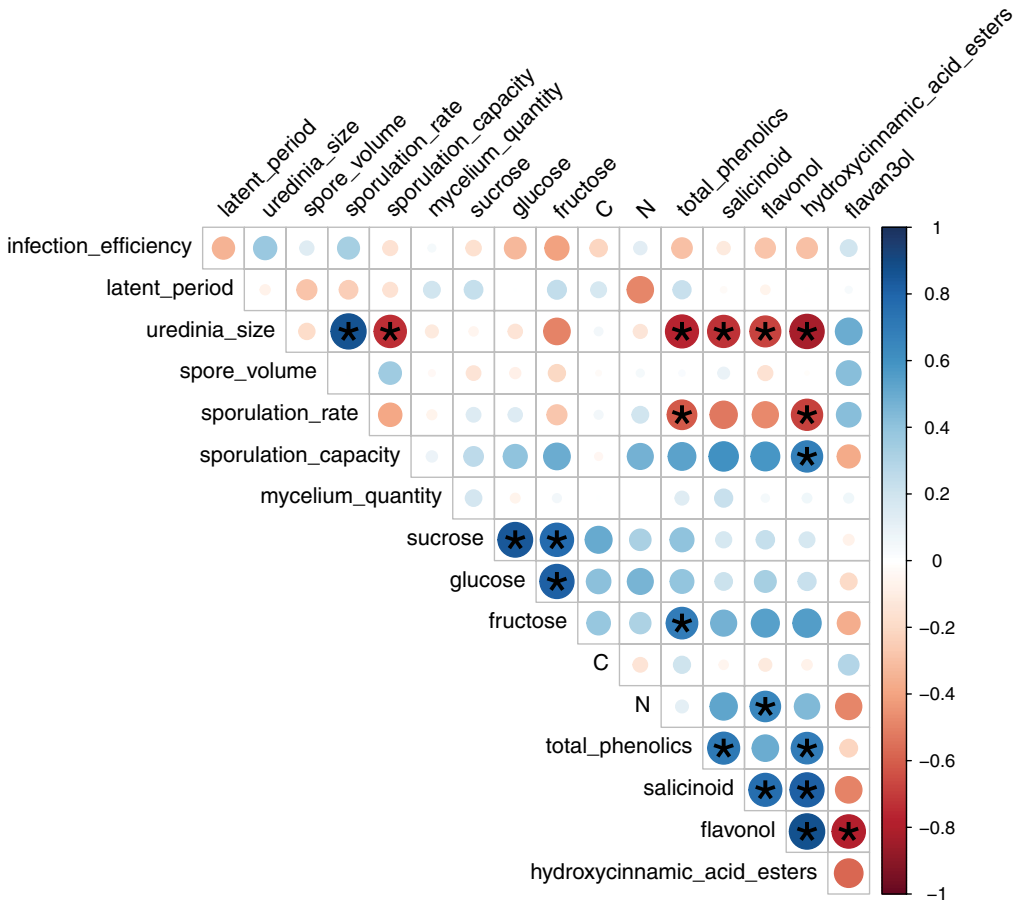

FIGURE 4 | Pairwise Spearman correlation coefficients between leaf chemical content and mean fungal phenotypic traits per LPI and plant based on 4 to 12 replicates. Colors correspond to the sign and dot size to the strength of the correlation. Stars indicate significant correlations according to Student *t*-test adjusted with a False-Discovery-Rate correction for multiple tests.

quantity. This makes sense as for biotrophic fungi like rusts, lesion (uredinia) size is only the size of the aperture through which urediniospores are extruded, and may thus not be directly linked to the size of the area within a leaf that is colonized by the mycelium.

Neither leaf maturity, nor the two other experimental factors (plant and day of inoculation) had an effect on latent period, infection efficiency, mycelium quantity and spore volume, even though substantial variances were observed for those traits. The latent period and spore volume varied independently from each other and independently from the main structuring traits (uredinia size and sporulation rate). Variation in latent period and spore volume might have been affected by an unidentified environmental factor. Even though inoculated leaf disks were incubated under controlled conditions of temperature and light, micro-scale variation may have occurred for these crucial parameters influencing fungal development and infection dynamics (Cochrane, 1959; Rotem et al., 1978; Trapero-Casas and Kaiser, 1992; Turechek and Stevenson, 1998; Turechek et al., 2001; Pap et al., 2013). Moreover, the initial position of the disk in the leaf might have influenced infection outcome (Katsuya and Green, 1967; Johnston et al., 2016). Single-spore inoculation is more prone to inter-replicate variance, in contrast to spray-inoculation which buffers micro-environmental variations. Apart from this drawback, this method allowed us to accurately disentangle the variation in each trait and to properly assess putative correlations. In our study, the dissection of the infection process into elementary traits enabled us to assess that the leaf maturity gradient only influences the sporulation function.

Disentangling Nutritive Limitation vs. Defense Reaction Effects

Two hypotheses were considered to explain variation in uredinia size and sporulation rate. On the one hand, sporulation could be enhanced by a higher nutrient availability in older leaves. On the other hand, higher levels of defense compounds could in contrast prevent fungal development in younger leaves.

Leaf sugars have long been known to be essential to the development of plant pathogenic fungi (Bilgrami and Verma, 1978; Madan and Thind, 1998). Using *Populus deltoides* leaves

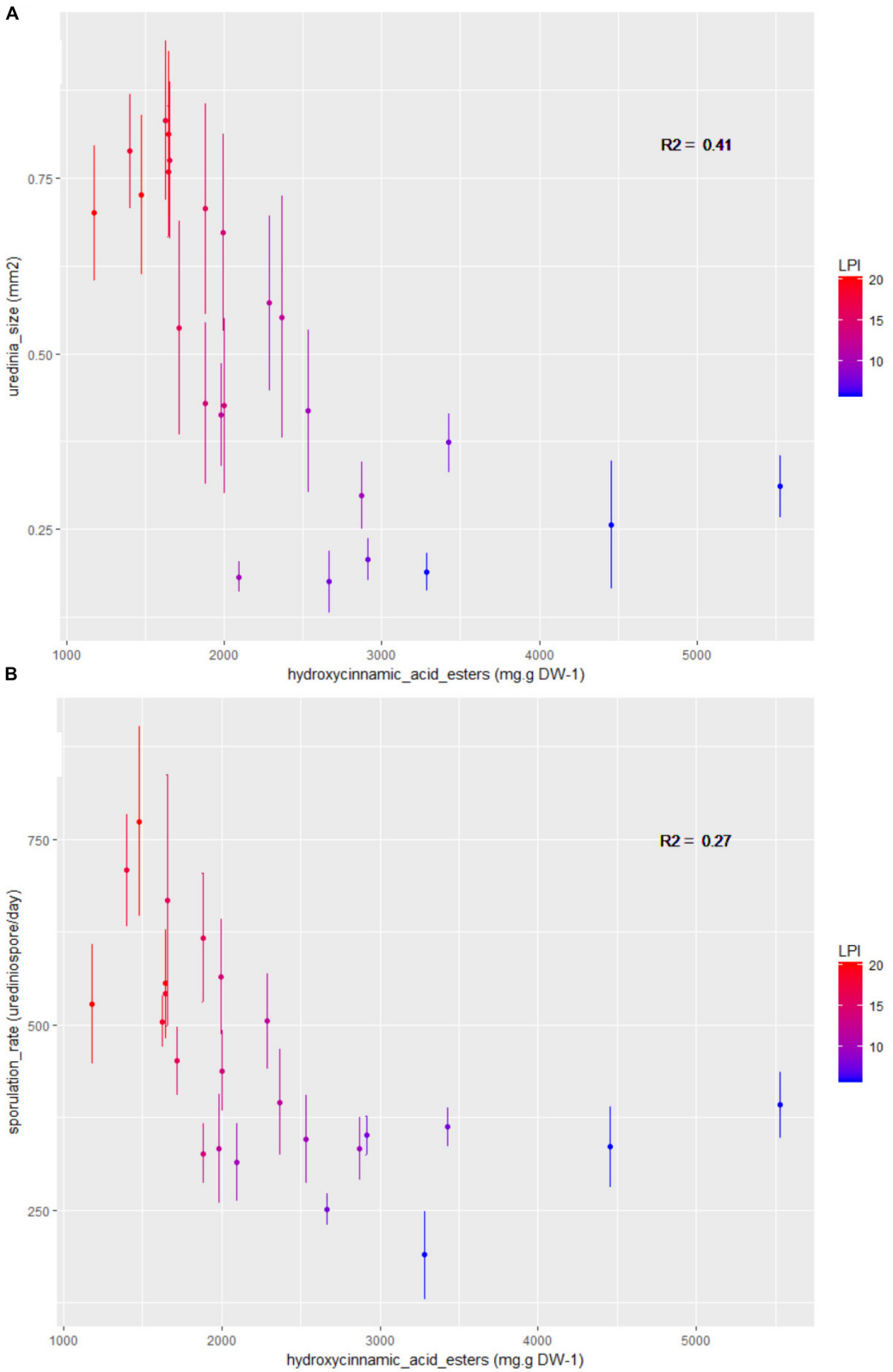

FIGURE 5 | Bivariate plots (LPI and plant mean ± standard error calculated on three plants and 15 to 24 replicates per LPI) showing the variation in **(A)** uredinia size and **(B)** sporulation rate according to the phenolic subclass hydroxycinnamic acid esters content. Colors stand for LPI and R2 gives the coefficients of determination.

inoculated with *Melampsora medusae* f. sp. *deltoidae*, Coleman (1986) showed that the maximum level of susceptibility, measured by the number of lesions (uredinia) as a proxy for infection efficiency, is reached when the sugar availability is maximal, i.e., at a LPI of 5. This finding is inconsistent with our study, in which the infection efficiency did not vary with leaf maturity and the two responsive traits (uredinia size and sporulation rate) steadily increased from LPI 6 to 20. The discrepancy between Coleman (1986) experiments and our results may lie in differences in the growth conditions of poplar plants, which may lead to different levels of nutrient availability. The light quality available in growth chambers has been significantly improved during the last decades. In Coleman (1986), the total sugar content decreased from LPI 6 to 9 (the highest LPI measured). In our experiment, even though sugar contents displayed some variance among leaves, there was no consistent pattern along LPI. Our growth conditions may have led to sugar availability sufficient for steady infection success even at higher LPI. We therefore conclude that leaf sugar content may not be linked to leaf susceptibility *per se*.

Leaf nitrogen content also plays a role in fungal growth and sporulation (Bilgrami and Verma, 1978; Madan and Thind, 1998). Bilgrami and Verma (1978) stated that nitrogen sources are used by fungi for both structural and metabolic functions. These functions require the assimilation of nitrogen into amino acids, proteins, and some peptides. For example, Jensen and Munk (1997) and Robert et al. (2004) found that higher nitrogen fertilization enhanced barley powdery mildew and wheat leaf rust sporulation. In our experiment, although there was a substantial variance in leaf nitrogen contents [same order of magnitude as in Robert et al. (2004)], this variation did not significantly affect *M. larici-populina* development. The leaf nitrogen content only slightly correlated with latent period and sporulation capacity (urediniospores produced par day and per area).

Overall, we did not observe consistent variation in nutrient content along the leaf maturity gradient and, moreover, the variation in nutrient content was not correlated with the two responsive traits, uredinia size, and sporulation rate. Consequently, nutrient availability was apparently not the environmental factor best explaining fungal development in our experiment.

By contrast, the defense hypothesis, tested by assessing the constitutive level of phenolics (total and individual) appeared to better explain fungal development related to leaf age. Indeed, the total phenolic content decreased with leaf age and correlated negatively with uredinia size and sporulation rate. Although higher phenolic concentration in younger leaves is common in poplar and other plants (Coleman, 1986; Johnson and Kim, 2005; Royer et al., 2013; Ullah et al., 2017), the correlation between phenolic concentrations and resistance to fungal infection has not been demonstrated. Coleman (1986) and Coleman et al. (1987) did not detect a correlation between leaf phenolic content and the amount of uredinia produced by *M. medusae* on poplar trees. By contrast, in the same pathosystem, a negative correlation was observed between total phenolic content and urediniospore germination efficiency and hyphae length (Johnson and Kim, 2005). Other studies on black currant (*Ribes nigrum*) and willow (*Salix myrsinifolia*) identified negative correlation between the concentrations of phenolic compounds and development traits of rusts (Hakulinen et al., 1999; Vagiri et al., 2017). By analyzing specific phenolics from poplar leaves, we were able to precisely identify groups of phenolic compounds that correlate with poplar resistance to rust. Among the four phenolic subclasses (from a total of 16 compounds), three subclasses (hydroxycinnamic acid esters, flavonols, and salicinoids) showed the same effect as total phenolic contents and correlated negatively with uredinia size and sporulation rate. The hydroxycinnamic acid ester chlorogenic acid has been shown to correlate to rust resistance in black currant (Vagiri et al., 2017). In addition, several studies highlighted the role of leaf surface flavonoids in the resistance to rust in poplar and birch (Shain and Miller, 1982; Valkama et al., 2005). In our study, we did not address the leaf location (inside or on the surface) of the two flavonols, rutin and quercetrin, however, the fact that they negatively correlate with rust development is in agreement with these previous studies. The only phenolic subclass that did not correlate with resistance to rust was flavan-3-ol which integrates catechin and proanthocyanidin dimers. A role of this phenolic subclass – especially catechin – in resistance to fungal pathogens, including rust fungi, has been proposed in several studies (Brignolas et al., 1998; Hakulinen et al., 1999; Vagiri et al., 2017). Moreover, a recent study on the *M. larici-populina* – *Populus nigra* pathosystem demonstrated that catechin is an effective chemical defense compound against rust (Ullah et al., 2017). This demonstration was based on the fact that (i) catechin is strongly induced upon rust infection, (ii) catechin exhibit a strong antifungal activity against *M. larici-populina* at *in planta* concentration, and (iii) poplar engineered to accumulate high or low levels of catechin were more resistant or more susceptible to rust, respectively. In our study, the concentrations of flavan-3-ols increased with leaf age. The same trend was observed in the study by Ullah et al. (2017) (see **Supplementary Figure S2**). The absence of a correlation between flavan-3-ol concentrations and rust resistance does not indicate that flavan-3-ols are not important factors in leaf rust resistance. Indeed, the compounds were assayed in uninfected leaves; hence reflect constitutive (i.e., non-induced) defense levels. In addition, the concentrations measured in our experiment (from 0.2 to 0.5 mg.g DW^{-1}) were below the concentrations proven to efficiently impair rust development on black poplar leaves (Ullah et al., 2017).

CONCLUSION

Melampsora larici-populina development after single-spore inoculation onto poplar leaf disks was more constrained by the level of plant constitutive defenses than limited by nutrient availability. For the tested strain, uredinia size and sporulation rate, both components of the sporulation function, were the only traits responsive to reaction norms along a gradient of leaf maturity. This experiment – conducted on a single fungal isolate and on a single plant genotype – can nonetheless serve as a pilot study. We report the correlation of a fungal fitness component (sporulation) to an environmental characteristic imposed by the

leaf i.e., the constitutive level of phenolic content. In the future, it would be worthwhile to assess the generality of this finding with more fungal isolates and plant genotypes and decipher further the interplay between constitutive and induced defense compound levels. From a broader perspective, it would be interesting to determine the plasticity and heritability of sporulation-related traits to better assess how the complexity of leaf environment shapes the evolutionary trajectory of a plant pathogen.

AUTHOR CONTRIBUTIONS

FH, PF, and BF designed the study. AM conducted the experiment and analyses. MP developed the single-spore inoculation and trait measurement methods. AA developed the qPCR method based on new primers and probe for *Melampsora larici-populina* in the rDNA ITS (Internal Transcribed Spacer) designed by CG and A-LB. RL conducted leaf phenolics analyses. AM and FH wrote the first draft of the manuscript. PF, MP, and RL contributed to the manuscript. All the authors approved the final version of the manuscript.

FUNDING

This work was supported by grants from the French National Research Agency (Grant No. ANR-13-BSV7-0011, FunFit project; ANR-11-LABX-0002-01, Cluster of Excellence ARBRE). AM and MP were supported by Ph.D. fellowships from the Region Lorraine and INRA, and from the French Ministry of Education and Research (MESR), respectively.

ACKNOWLEDGMENTS

Jérémy Pétrowski is acknowledged for his excellent technical help in poplar plant production. We thank Jacqueline Marchand and Carole Antoine (Université de Lorraine, AgroParisTech, INRA, SILVA, Nancy, France) for the poplar leaf content analyses, Aude Fauvet for the analysis of total phenolics, and Didier Le Thiec for the lyophilization of the samples. We also thank Irène Hummel for advices in statistical analyses, Rantanplan for inspiration, Josselin Montarry, Elisabeth Fournier, Stéphane De Mita, Claire Fourrey, and Katherine Hayden for valuable comments on earlier drafts of this manuscript.

SUPPLEMENTARY MATERIAL

The Supplementary Material for this article can be found online at: https://www.frontiersin.org/articles/10.3389/fpls.2018.01396/full#supplementary-material

REFERENCES

Adandonon, A., Regnier, T., and Aveling, T. A. S. (2017). Phenolic content as an indicator of tolerance of cowpea seedlings to *Sclerotium rolfsii*. *Eur. J. Plant Pathol.* 149, 245–251. doi: 10.1007/s10658-017-1178-9

Agrios, G. N. (2005). *Plant Pathology*. New York, NY: Elsevier Academic Press.

Bilgrami, K. S., and Verma, R. N. (1978). *Physiology of Fungi*. New Delhi: Vikas Publishing House Pvt Ltd.

Boonekamp, P. M. (2012). Are plant diseases too much ignored in the climate change debate? *Eur. J. Plant Pathol.* 133, 291–294. doi: 10.1007/s10658-011-9934-8

Brignolas, F., Lieutier, F., Sauvard, D., Christiansen, E., and Berryman, A. A. (1998). Phenolic predictors for Norway spruce resistance to the bark beetle *Ips typographus* (Coleoptera: Scolytidae) and an associated fungus, *Ceratocystis polonica*. *Can. J. Forest Res.* 28, 720–728. doi: 10.1139/cjfr-28-5-720

Cellerino, G. P., Anselmi, N., and Pinon, J. (1978). Influence de l'âge des feuilles de peuplier sur la sensibilité à *Marssonina brunnea*. *Eur. J. Forest Pathol.* 8, 273–279. doi: 10.1111/j.1439-0329.1978.tb00639.x

Clifford, B. C., and Clothier, R. B. (1974). Physiologic specialization of *Puccinia hordei* on barley hosts with non-hypersensitive resistance. *Trans. Br. Mycol. Soc.* 63, 421–430. doi: 10.1016/S0007-1536(74)80088-4

Cochrane, V. W. (1959). *Physiology of Fungi*. New York, NY: John Wiley & Sons, Inc.

Coleman, J. S. (1986). Leaf development and leaf stress: increased susceptibility associated with sink-source transition. *Tree Physiol.* 2, 289–299. doi: 10.1093/treephys/2.1-2-3.289

Coleman, J. S., Jones, C. G., and Smith, W. H. (1987). The effect of ozone on cottonwood – leaf rust interactions: independence of abiotic stress, genotype, and leaf ontogeny. *Can. J. Bot.* 65, 949–953. doi: 10.1139/b87-131

Dowkiw, A., Husson, C., Frey, P., Pinon, J., and Bastien, C. (2003). Partial resistance to *Melampsora larici-populina* leaf rust in hybrid poplars: genetic variability in inoculated excised leaf disk bioassay and relationship with complete resistance. *Phytopathology* 93, 421–427. doi: 10.1094/PHYTO.2003.93.4.421

Duplessis, S., Cuomo, C. A., Lin, Y. C., Aerts, A., Tisserant, E., Veneault-Fourrey, C., et al. (2011). Obligate biotrophy features unraveled by the genomic analysis of rust fungi. *Proc. Natl. Acad. Sci. U.S.A.* 108, 9166–9171. doi: 10.1073/pnas.1019315108

Duplessis, S., Spanu, P. D., and Schirawski, J. (2013). "Biotrophic Fungi (Powdery Mildews, Rusts, and Smuts)," in *The Ecological Genomics of Fungi*, ed. F. Martin (Hoboken, NJ: John Wiley & Sons, Inc.), 149–168. doi: 10.1002/9781118735893.ch7

Farber, D. H., and Mundt, C. C. (2017). Effect of plant age and leaf position on susceptibility to wheat stripe rust. *Phytopathology* 107, 412–417. doi: 10.1094/PHYTO-07-16-0284-R

Ficke, A., Gadoury, D. M., and Seem, R. C. (2002). Ontogenic resistance and plant disease management: a case study of grape powdery mildew. *Phytopathology* 92, 671–675. doi: 10.1094/PHYTO.2002.92.6.671

Gamm, M., Héloir, M. C., Bligny, R., Vaillant-Gaveau, N., Trouvelot, S., Alcaraz, G., et al. (2011). Changes in carbohydrate metabolism in Plasmopara viticola-infected grapevine leaves. *Mol. Plant Microbe. Interact.* 24, 1061–1073. doi: 10.1094/MPMI-02-11-0040

Gavrilets, S., and Scheiner, S. M. (1993). The genetics of phenotypic plasticity. V. Evolution of reaction norm shape. *J. Evol. Biol.* 6, 31–48. doi: 10.1046/j.1420-9101.1993.6010031.x

Gilchrist, M. A., Sulsky, D. L., and Pringle, A. (2006). Identifying fitness and optimal life-history strategies for an asexual filamentous fungus. *Evolution* 60, 970–979. doi: 10.1554/05-261.1

Giorcelli, A., Vietto, L., Anselmi, N., and Gennaro, M. (1996). Influence of clonal susceptibility, leaf age and inoculum density on infections by *Melampsora larici-populina* races E1 and E3. *Eur. J. Forest Pathol.* 26, 323–331. doi: 10.1111/j.1439-0329.1996.tb01078.x

Guinet, C., Boutigny, A. L., Vialle, A., Hamelin, R. C., Frey, P., and Ioos, R. (2016). Simultaneous monitoring and quantification of *Melampsora allii-populina* and *Melampsora larici-populina* on infected poplar leaves using a duplex real-time PCR assay. *Plant Pathol.* 65, 380–391. doi: 10.1111/ppa.12426

Hakulinen, J., Sorjonen, S., and Julkunen-Tiitto, R. (1999). Leaf phenolics of three willow clones differing in resistance to *Melampsora* rust infection. *Physiol. Plant.* 105, 662–669. doi: 10.1034/j.1399-3054.1999.105410.x

Jarosz, A. M., and Davelos, A. L. (1995). Effects of disease in wild plant populations and the evolution of pathogen aggressiveness. *New Phytolo.* 129, 371–387. doi: 10.1111/j.1469-8137.1995.tb04308.x

Jensen, B., and Munk, L. (1997). Nitrogen-induced changes in colony density and spore production of *Erysiphe graminis* f.sp. hordei on seedlings of six spring barley cultivars. *Plant Pathol.* 46, 191–202. doi: 10.1046/j.1365-3059.1997.d01-224.x

Johnson, J. D., and Kim, Y. (2005). The role of leaf chemistry in *Melampsora medusae* infection of hybrid poplar: effects of leaf development and fungicide treatment. *Can. J. Forest Res.* 35, 763–771. doi: 10.1139/x05-009

Johnston, S. F., Cohen, M. F., Torok, T., Meentemeyer, R. K., and Rank, N. E. (2016). Host phenology and leaf effects on susceptibility of California Bay Laurel to *Phytophthora ramorum*. *Phytopathology* 106, 47–55. doi: 10.1094/PHYTO-01-15-0016-R

Kardin, M. K., and Groth, J. V. (1989). Density-dependent fitness interactions in the bean rust fungus. *Phytopathology* 79, 409–412. doi: 10.1094/Phyto-79-409

Katsuya, K., and Green, G. J. (1967). Reproductive potentials of races 15b and 56 of wheat stem rust. *Can. J. Bot.* 45, 1077–1091. doi: 10.1139/b67-113

Knott, E. A., and Mundt, C. C. (1991). Latent period and infection efficiency of *Puccinia recondita* f. sp. *tritici* populations isolated from different wheat cultivars. *Phytopathology* 81, 435–439. doi: 10.1094/Phyto-81-435

Kolmer, J. A., and Leonard, K. J. (1986). Genetic selection and adaptation of *Cochliobolus heterostrophus* to corn hosts with partial resistance. *Phytopathology* 76, 774–777. doi: 10.1094/Phyto-76-774

Lannou, C. (2012). Variation and selection of quantitative traits in plant pathogens. *Annu. Rev. Phytopathol.* 50, 319–338. doi: 10.1146/annurev-phyto-081211-173031

Larson, P. R., and Isebrands, J. G. (1971). The plastochron index as applied to developmental studies of cottonwood. *Can. J. Forest Res.* 1, 1–11. doi: 10.1139/x71-001

Leonard, K. J. (1969). Selection in heterogeneous populations of *Puccinia graminis* f. sp. *avenae*. *Phytopathology* 59, 1851–1857.

Madan, M., and Thind, K. S. (1998). *Physiology of Fungi*. New Delhi: APH Publishing Corporation.

Merry, A. M., Evans, K. J., Corkrey, R., and Wilson, S. J. (2013). Coincidence of maximum severity of powdery mildew on grape leaves and the carbohydrate sink-to-source transition. *Plant Pathol.* 62, 842–850. doi: 10.1111/j.1365-3059.2012.02691.x

Pap, P., Rankovic, B., and Masirevic, S. (2013). Effect of temperature, relative humidity and light on conidial germination of oak powdery mildew (*Microsphaera alphitoides* Griff. et Maubl.) under controlled conditions. *Arch. Biol. Sci.* 65, 1069–1077. doi: 10.2298/ABS1303069P

Pariaud, B., Ravigné, V., Halkett, F., Goyeau, H., Carlier, J., and Lannou, C. (2009a). Aggressiveness and its role in the adaptation of plant pathogens. *Plant Pathol.* 58, 409–424. doi: 10.1111/j.1365-3059.2009.02039.x

Pariaud, B., Robert, C., Goyeau, H., and Lannou, C. (2009b). Aggressiveness components and adaptation to a host cultivar in wheat leaf rust. *Phytopathology* 99, 869–878. doi: 10.1094/PHYTO-99-7-0869

Pei, M. H., Ruiz, C., Harris, J., and Hunter, T. (2003). Quantitative inoculations of poplars with *Melampsora larici-populina*. *Eur. J. Plant Pathol.* 109, 269–276. doi: 10.1023/A:1022822503139

Pei, M. H., Ruiz, C., Hunter, T., Arnold, G. M., and Bayon, C. (2002). Quantitative relationships between inoculum of *Melampsora larici-epitea* and corresponding disease on Salix. *Plant Pathol.* 51, 443–453. doi: 10.1046/j.1365-3059.2002.00739.x

Philibert, A., Desprez-Loustau, M. L., Fabre, B., Frey, P., Halkett, F., Husson, C., et al. (2011). Predicting invasion success of forest pathogenic fungi from species traits. *J. Appl. Ecol.* 48, 1381–1390. doi: 10.1111/j.1365-2664.2011.02039.x

Robert, C., Bancal, M. O., and Lannou, C. (2002). Wheat leaf rust uredospore production and carbon and nitrogen export in relation to lesion size and density. *Phytopathology* 92, 762–768. doi: 10.1094/PHYTO.2002.92.7.762

Robert, C., Bancal, M. O., and Lannou, C. (2004). Wheat leaf rust uredospore production on adult plants: influence of leaf nitrogen content and *Septoria tritici* blotch. *Phytopathology* 94, 712–721. doi: 10.1094/PHYTO.2004.94.7.712

Rotem, J., Cohen, Y., and Bashi, E. (1978). Host and environmental influences on sporulation in vivo. *Annu. Rev. Phytopathol.* 16, 83–101. doi: 10.1146/annurev.py.16.090178.000503

Royer, M., Larbat, R., Le Bot, J., Adamowicz, S., and Robin, C. (2013). Is the C:N ratio a reliable indicator of C allocation to primary and defence-related metabolisms in tomato? *Phytochemistry* 88, 25–33. doi: 10.1016/j.phytochem.2012.12.003

Scheiner, S. M. (1993). Genetics and evolution of phenotypic plasticity. *Annu. Rev. Ecol. Syst.* 24, 35–68. doi: 10.1146/annurev.es.24.110193.000343

Shain, L., and Miller, J. B. (1982). Pinocembrin: an antifungal compound secreted by leaf glands of eastern cottonwood [*Populus deltoides*]. *Phytopathology* 72, 877–880 doi: 10.1094/Phyto-72-877

Sharma, J. K., Heather, W. A., and Winer, P. (1980). Effect of leaf maturity and shoot age of clones of *Populus* species on susceptibility to *Melampsora larici-populina*. *Phytopathology* 70, 548–554. doi: 10.1094/Phyto-70-548

Trapero-Casas, A., and Kaiser, W. J. (1992). Influence of temperature, wetness period, plant age, and inoculum concentration on infection and development of Ascochyta blight of chickpea. *Phytopathology* 82, 589–596. doi: 10.1094/Phyto-82-589

Turechek, W. W., Mahaffee, W. F., and Ocamb, C. M. (2001). Development of management strategies for hop powdery mildew in the Pacific Northwest. *Plant Health Prog.* 2:8. doi: 10.1094/PHP-2001-0313-01-RS

Turechek, W. W., and Stevenson, K. L. (1998). Effects of host resistance, temperature, leaf wetness, and leaf age on infection and lesion development of pecan scab. *Phytopathology* 88, 1294–1301. doi: 10.1094/PHYTO.1998.88.12.1294

Ullah, C., Unsicker, S. B., Fellenberg, C., Constabel, C. P., Schmidt, A., Gershenzon, J., et al. (2017). Flavan-3-ols are an effective chemical defense against rust infection. *Plant Physiol.* 175, 1560–1578. doi: 10.1104/pp.17.00842

Vagiri, M., Johansson, E., and Rumpunen, K. (2017). Phenolic compounds in black currant leaves – an interaction between the plant and foliar diseases? *J. Plant Interact.* 12, 193–199. doi: 10.1080/17429145.2017.1316524

Valkama, E., Koricheva, J., Salminen, J. -P., Helander, M., Saloniemi, I., Saikkonen, K., et al. (2005). Leaf surface traits: overlooked determinants of birch resistance to herbivores and foliar micro-fungi? *Trees* 19, 191–197. doi: 10.1007/s00468-004-0380-5

Xavier, A. A., da Silva, A. C., da Silva Guimarães, L. M., Matsuoka, K., Hodges, C. S., and Alfenas, A. C. (2015). Infection process of *Puccinia psidii* in *Eucalyptus grandis* leaves of different ages. *Trop. Plant Pathol.* 40, 318–325. doi: 10.1007/s40858-015-0043-7

Yegorov, I., Grognard, F., Mailleret, L., and Halkett, F. (2017). Optimal resource allocation for biotrophic plant pathogens. *IFAC PapersOnline* 50, 3154–3159. doi: 10.1016/j.ifacol.2017.08.328

Conflict of Interest Statement: The authors declare that the research was conducted in the absence of any commercial or financial relationships that could be construed as a potential conflict of interest.

frontiers in Plant Science

ORIGINAL RESEARCH
published: 31 October 2018
doi: 10.3389/fpls.2018.01554

Adaptation of a Fungal Pathogen to Host Quantitative Resistance

*Lise Frézal[1,2], Guy Jacqua[1] and Claire Neema[3]**

[1] INRA-URPV, Guadeloupe, France, [2] CNRS – ENS – INSERM, Institut de Biologie de l'Ecole Normale Supérieure, Paris, France, [3] UMR BGPI, Montpellier SupAgro, Campus International de Baillarguet, Montpellier, France

Impact of host quantitative resistance on pathogen evolution is still poorly documented. In our study, we characterized the adaptation of the pathogenic fungus *Colletotrichum gloeosporioides*, to the quantitative resistance of its host, the water yam (*Dioscorea alata*). Genetic and pathogenic diversities of *C. gloeosporioides* populations were specified at the field scale. We used nuclear markers to describe fungal population structuring within and between six fields of three cultivars differently susceptible to the fungus. Strain aggressiveness was then quantified in the laboratory through cross-inoculation tests. The high level of genetic diversity and significant linkage disequilibrium revealed a significant influence of clonal reproduction in the *C. gloeosporioides* evolution. The recorded fungal migration between fields was weak (evidence for a dispersion mode via tubers rather than splashing dispersal), which provides the first molecular evidence for limited *C. gloeosporioides* migration via yam tuber exchanges. *C. gloeosporioides's* populations are adapted to their host resistance. The aggressiveness of the fungal clones seems to have evolved toward an accumulation of components specific to each host cultivar. Despite the remaining marks of adaptation to the former widely cultivated host, adaptation to current cultivars was clearly depicted.

Keywords: local adaptation, aggressiveness, quantitative resistance, *Colletotrichum gloeosporioides*, *Dioscorea alata*

OPEN ACCESS

Edited by:
Josselin Montarry, INRA Centre Bretagne-Normandie, France

Reviewed by:
Fabien Halkett, INRA Centre Nancy-Lorraine, France
Sébastien Guyader, INRA Centre Antilles-Guyane, French Guiana

****Correspondence:***
Claire Neema
claire.neema@supagro.fr

Specialty section:
This article was submitted to Plant Microbe Interactions, a section of the journal Frontiers in Plant Science

Received: *17 June 2018*
Accepted: *03 October 2018*
Published: *31 October 2018*

Citation:
Frézal L, Jacqua G and Neema C (2018) Adaptation of a Fungal Pathogen to Host Quantitative Resistance. Front. Plant Sci. 9:1554. doi: 10.3389/fpls.2018.01554

INTRODUCTION

Discernment on the adaptive potential of plant pathogen species is essential to designing sustainable integrated pest management framework in which, durability of crop resistance is one crucial point. The adaptive potential of plant pathogen species highly depends on the forces shaping the pathogen evolution. Among these forces, the migration (spatial dispersal), the recombination (reproductive mode), genetic drift and above all, the selection by the host-plant resistances, are of particular importance (McDonald and Linde, 2002). Pathogen populations can either adapt to the most common host (general adaptation), or be divided into several entities, each adapted to one particular host genotype (local adaptation, Gandon et al., 1996; Gandon and Van Zandt, 1998). The theory of polygenic traits' evolution under divergent selection has not been much investigated, especially while investigating host pathogen interactions (Kawecki and Ebert, 2004). The few studies focusing on the host quantitative resistance impact on pathogen populations reported either the local adaptation of pathogen populations (Kaltz and Shykoff, 1998; Zhan et al., 2003), or a directional selection toward an increase in pathogen aggressiveness on all host cultivars (Andrivon, 1993; Andrivon et al., 2007; Montarry et al., 2007). In the present study, we described the population diversity of the plant pathogen *Colletotrichum gloeosporioides* in the Guadeloupean (French West Indies)

agrosystem. We also investigated the pathogen aggressiveness as an adaptive trait of the fungi to the quantitative resistance of its host, *Dioscorea alata*.

The filamentous ascomycete and plant pathogen *C. gloeosporioides* (Penz.) Penz. & Sacc. [telemorph: *Glomerella cingulata* (Stonem.) Spauld. & Schrenk] causes anthracnose disease on various crops (Bailey and Jeger, 1992; strawberry, Freeman et al., 1998; olive, Talhinhas et al., 2005; avocado, mango, stylo, Chakraborty et al., 1999; ornamental lupinines, Elmer et al., 2001; *Salsola tragus*, Berner et al., 2006; peach tree, Kim and Hong, 2008), among which the water yam (*D. alata*). The life cycle of this haploid and hemibiotroph fungus includes both sexual and asexual reproduction. If the two reproductive modes are observed on water yam, the asexual mode prevails during yam anthracnose epidemics. Conidia (asexual spores) disseminate from plant to plant by wind-directed-rain splashing (Green and Simons, 1994; Penet et al., 2014) which limits dispersal to several meters from the source (Ntahimpera et al., 1999).

Sexual reproduction can nevertheless occur at the end of epidemics, on dead leaves or stems, which—when left on the soil surface—may contribute to the primary infection of yam (Ripoche et al., 2007). Ascospores (sexual spores) are produced in dried-perithecia that can eventually be wind-dispersed on a long distance (Abang, 2003). Besides, *C. gloeosporioides* generates quiescent infections in yam tuber epidermis (Simons and Green, 1994); As farmers traditionally save tuber portions from a previous harvest for the new crop propagation, mycelia can pass from one crop season to the next. Thus, commercial exchanges of yam tubers and quiescent infections confer to *C. gloeosporioides* a capacity for long-distance migration and for clonal propagation (Green, 1994).

Dioscorea alata foliar anthracnose has been reported in Oceania and India (Winch et al., 1984; McDonald et al., 1998), in the West and Central Africa (Asiedu et al., 1998; Mignouna et al., 2001) and in the Caribbeans (Coursey, 1967; Green and Simons, 1994; Cowger and Mundt, 2002). In the West Indies, anthracnose disease became the most damaging disease on water yam at the end of the 1970s (McDonald et al., 1998) and was associated with serious yield losses reaching 80–100% for the common cultivars (*cv*) of this time, i.e., *cv* Pacala, in Guadeloupe (Green and Simons, 1994). In the 1970s, the cultivar Plimbite was introduced in the Guadeloupean islands and has been extensively cultivated until it became as susceptible to anthracnose as *cv* Pacala. After the late 1990s, farmers started to use more resistant cultivars such as *cv* Kabusah and *cv* Tahiti, but kept planting previous cultivars (Penet et al., 2016).

Genetic determinants of the interaction between *C. gloeosporioides* and *D. alata* are poorly understood. For a long time, this resistance was thought to be polygenic (Green and Simons, 1994; Abang et al., 2001). More recently, Petro et al. (2011) work based on the Boutou and Pyramide *D. alata* cultivars provided strong evidence for the quantitative inheritance of the components associated with the *D. alata* resistance to *C. gloeosporioides*. Next to this quantitative resistance, a gene-for-gene-like component (Flor, 1971) of the interaction between *C. gloeosporioides* and *D. alata* cultivars has been unraveled (Mignouna et al., 2002; Petro et al., 2011). For instance, the single dominant locus (*Cdg1*) explains the specific resistance of *cv* TDa-95/00328 to moderately virulent *C. gloeosporioides* strains.

The genetic structure of *C. gloeosporioides* populations, causing yam anthracnose, has been mostly studied in Nigeria (Abang et al., 2001, 2004, 2005, 2006), which is the first yam producer in the world (71.5% of the world production, FAOstat 2007). There, *C. gloeosporioides* was shown to exhibit high genetic and phenotypic diversity from the lesion to the region scales (morphotypes, Vegetative Compatibility Groups, RAPD, MP-PCR) and a weak population structure according to the host or to the agroecological areas (Abang et al., 2004, 2006).

Yam breeding and the management of yam resistances in the French West Indies require knowledge about the influence of the migration, the reproductive mode and the yam quantitative resistance on *C. gloeosporioides* evolution. Moreover, the impact of the host quantitative resistance on the evolution of the pathogen aggressiveness has never been investigated. Aiming to document a part or all of these aspects, the objectives of this work were: (i) to estimate genetic diversity and its distribution among fields with neutral markers (AFLP); (ii) to infer the influence of recombination at the field scale; (iii) to study how the degree of host quantitative resistance to anthracnose influences the distribution of fungal aggressiveness diversity.

MATERIALS AND METHODS

Fungal Sampling and Isolation

A total of 222 *C. gloeosporioides* isolates were collected from December 2001 to January 2002, from six yam fields within a 5-km-diameter area of the Guadeloupe (FWI, between Morne à l'eau and Le Moule, 16°15N, 61°35O, **Figure 1** and (**Supplementary Table S1**). Sampling was done on three yam (*D. alata*) cultivars with different levels of resistance to anthracnose: *cv* Pacala (highly susceptible), *cv* Kabusah (moderately susceptible) and *cv* Tahiti (resistant). The study was carried out in six production fields of approximately 0.5 ha, with identical soil composition, topology, crop management and climate (**Supplementary Table S1**). One month before harvest, leaves with typical anthracnose lesions were collected from 50 plots per field, each distant from 2 to 5 m. Fungus isolation was performed from freshly harvested infected yam leaves (on the same day). Circa 1 mm^2 of typical anthracnose lesions were plated on potato dextrose agar medium (PDA). *C. gloeosporioides* isolates were identified according to morphological characteristics (Sutton, 1992), then monoconidial cultures were obtained. The strains were grown on PDA-medium under photoperiodical conditions of 12 h day at 25°C and 12 h night at 23°C. Spores of 7-day-old cultures were suspended in distilled water to reach concentrations of 5.10^5 conidia per mL. Mycelia were dried, thrown in liquid nitrogen and stored at −80°C for DNA extraction.

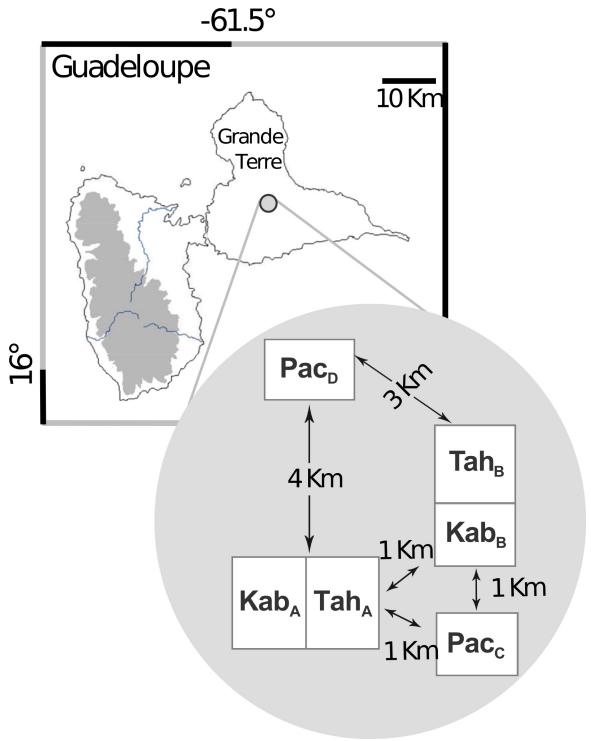

FIGURE 1 | The locations of *Colletotrichum gloeosporioides* sampling sites in Guadeloupe (French West Indies); The relative geographical positions of the six yam (*Dioscorea alata*) fields are represented in the gray circle. The hosts cultivars were *D. alata cv* Kabusah (Kab), *cv* Pacala (Pac) and *cv* Tahiti (Tah). A, B were two locations where two fields were contiguous.

DNA Extraction and AFLP Markers Genotyping

One milliliter of a suspension at 5.10^5 conidia per mL was mixed with 30 mL of potato dextrose broth medium (PDB). After 72 h of incubation at 27°C, the mycelium was harvested, dried on sterile filter paper and stored at −80°C. Total genomic DNA was extracted from frozen mycelium with a phenol/chloroform protocol as described in Villaréal et al. (2002). DNA quality was checked by electrophoresis on 0.8% agarose gel and stored at −20°C in TE 0.1 (10 mM trisHCL, pH8; 0.1 mM EDTA). DNA digestion (*Mse*I and E*co*RI), ligation, pre-amplification, selective amplification and electrophoresis were conducted as described in Villaréal et al. (2002). The primer combinations used for selective amplifications were M*se*I-0 +AT/E*co*RI-0 +AT, M*se*I-0+ AG/E*co*RI +AG and M*se*I-0 +TA/E*co*RI-0 +CAA. The 6%-bisacrylamide-urea gel was stained with silver nitrate as described in Chalhoub et al. (1997). Polymorphic bands between 100 and 500 pb were manually referenced as present ("1") or absent ("0"), which gave a 0–1 combination for each isolate. The AFLP patterns were checked for reproducibility with the two DNA replicates extracted and only clearly repeatable bands were used for further analyses. Co-migrating bands were assumed to be the same locus, and isolates having the same AFLP-pattern were assumed to be one single haplotype.

Plant Material, Inoculation and *in vitro* Aggressiveness Assessment

In order to study the adaptive patterns of *C. gloeosporioides* on its host cv of origin, cross-infection experiments were performed. The diversity for aggressiveness was investigated on a 45-strain subsample composed of six to nine strains per field, randomly chosen in a cloned-corrected sample (i.e., sample containing only single-copy AFLP patterns).

Host-Plant Material

Colletotrichum gloeosporioides strain aggressiveness was tested against the three host-plant cultivars from which they were isolated, i.e., water yam *cv* Pacala (high susceptibility), *cv* Kabusah (moderate susceptibility), *cv* Tahiti (low susceptibility), and also tested on one cultivar of reference for susceptibility to anthracnose, *cv* Plimbite (high susceptibility). Plants were grown from tuber pieces. All the yam tubers were produced in the INRA-URPV experimental center (Guadeloupe, French West Indies) which ensured the origin of the tubers as well as the sanitary control of their production. A total of 15-g tuber pieces were dipped for 24 h into fungicides (Chlorothalonil 550 g L^{-1} and Carbendazim 100 g L^{-1} supplied by Bayer CropScience), air-dried and covered with wood ashes. Tuber pieces were planted into humidified sterile compost in individual pots and put in a greenhouse under the natural conditions of Guadeloupe at the beginning of the wet season (25–30°C, >75% humidity, 12 h-photoperiod). To prevent any leaf infection on the plants used in the *in vitro* tests, we applied pesticides (oxythioquinox at 10 mg/mL supplied by Bayer CropScience) to the compost every 3 weeks until the first leaf emergence. As advised by Simons and Green (1994), fully expanded young leaves were harvested on 3-month old plants. Leaves were then washed with sterilized water and their adaxial surfaces were placed on moistened filter-paper disks in Petri dishes (one leaf per petri dish). Leaves were inoculated on the entire abaxial surface, as described by Toribio and Jacqua (1978).

Inoculation Strains were grown on PDA-medium in 12 h day at 25°C and 12 h night at 23°C conditions. Spores of 7-day old cultures were suspended in distilled water to raise concentrations of 5.10^5 conidia mL^{-1}. For each strain, 22.5 mL of the spore-suspension were sprayed on freshly cut leaves of each cultivar (five leaves per cultivar) using ecospray® atomizer (LCF labo chimie France, Aix en Provence). At the same time, non-inoculated leaves (sprayed with water) of each cultivar were used as controls. Leaves were incubated at 100% humidity and in photoperiodical conditions of 12 h day at 27°C, 12 h night at 22°C. To reproduce the natural conditions of infection of *D. alata* with *C. gloeosporioides*, inoculations were carried out just before night. For all host-strain combination and condition (control and inoculation), five independent repeats were performed simultaneously.

Disease assessment two different symptoms are commonly observed when inoculating *D. alata* leaves with *C. gloeosporioides*: the typical lesion (large necroses, dark brown, coalescent, high expansion rate) and the pinpoint lesion [punctual necroses of less than 2 mm in diameter, black, not coalescent;

Winch et al. (1984)]. Percentages of healthy, typical lesion and pinpoint lesion areas were visually estimated from the first to the 11th day after inoculation. In order to estimate strain aggressiveness, we use the analytical framework detailed in Frézal et al. (2012), which transforms the evolution of disease severity over time into one index, Ag. The construction of the Ag index is based the analysis of the symptom dynamics using a linear mixed-effects regression (PROC MIXED procedure; Laird and Ware, 1982) with two-knots, using SAS software (SAS Institute, 1987). The model is defined with a starting point at day 0 and two changes in slope (at day 6 and day 9). The typical lesion (Na) and total diseased areas (Da) were then defined as:

$$\mathrm{Da}\,(t) = \alpha_{\mathrm{Da}} \cdot t + \beta_{\mathrm{Da}}\,(t-6) + \gamma_{\mathrm{Da}}\,(t-9)$$

$$\mathrm{Na}\,(t) = \alpha_{\mathrm{Na}} \cdot t + \beta_{\mathrm{Na}}\,(t-6) + \gamma_{\mathrm{Na}}\,(t-9)$$

where, $(t-6) = (t-6)$ if $(t-6) > 0$, and 0 otherwise; where $(t-9) = (t-9)$ if $(t-9) > 0$, and 0 otherwise.

Strain aggressiveness index on each cultivar was defined as:

$$\mathrm{Ag} = \frac{3}{10} \cdot 100\left(\left(\alpha_{\mathrm{Da}}\frac{6}{100}\right)^{\frac{1}{4}} \cdot \frac{\mathrm{Da}\,(\mathrm{day}\ 11)}{100}\right) + \frac{7}{10} \cdot 100\left(\left(\alpha_{\mathrm{Na}} \cdot \frac{6}{100}\right)^{\frac{1}{4}} \cdot \frac{\mathrm{Na}\,(\mathrm{day}\ 11)}{100}\right)$$

For each strain, four indices were calculated: Ag-K on yam *cv* Kabusah, Ag-P on *cv* Pacala, Ag-T on *cv* Tahiti and Ag-Pl on *cv* Plimbite. We also focused on the initial lesion expansion rates (i.e., α_{Na}) and the typical lesion area on day 11 (Na) as this provides detailed insight on strain fitness and helps to imagine hypothetic outcomes of the competition between strains.

Data Analysis

Population Genetics Analyses

Diversity at each locus was estimated within subset of isolates grouped by field or cultivar. Unbiased gene diversity (Hd; Nei, 1987) was computed using GENETIX 4.05 (Belkhir et al., 1996/2004) on data sets containing only one copy of each haplotype per subset (i.e., clone-corrected data sets) (Chen and McDonald, 1996). Frequencies at each locus were estimated from each subset and used to calculate standard population statistics. In order to see whether the number of AFLP markers used in this study was sufficient to recover the maximal genotypic diversity, we plotted the genotypic diversity calculated from the multilocus genotype frequencies (Nei, 1987) versus the number of loci: our 23 polymorphic loci were discriminating and powerful enough (**Supplementary Figure S1**).

A minimum spanning tree based on the 23 ALFP markers was constructed for the full sample (222 isolates) using Bionumerics 5.1 with 100,000 resampling and partitioning of two majority trees. To determine population subdivision without any *a priori* knowledge, a second analysis was performed on the clone-corrected dataset using the Bayesian clustering method implemented in the software Structure version 2.3.3 (Pritchard et al., 2000). We used admixture and non-admixture models to identify genetic groups, both with distinct allele frequencies (Falush et al., 2003), and we assumed uniform priors for the vector of proportion (qi) of the individual i's genome in each cluster. The scores of individuals in the genetic groups (i.e., the posterior estimates of the qi) correspond to the probability of ancestry in each one of them. We varied K from 1 to 10, with 10 replicates for each K, and with each simulation consisting in 800,000 Monte-Carlo Markov Chain (MCMC) iterations preceded by a burn-in period of 200,000 iterations. The most probable structure was determined by computing the posterior probability for each K using the distribution of maximum likelihoods and ΔK distribution (Evanno et al., 2005; **Supplementary Figure S2**), which is a quantity, related to the second order rate of change of the log probability of data with respect to the number of genetic clusters. Finally, to determine population subdivision without any *a priori* knowledge and without making any assumptions regarding the population genetics model, we described the genetic clusters from the clone-corrected dataset using the discriminant analysis of principal components (DAPC, Jombart et al., 2010) implemented in the R package adegenet 2.1.1 (Jombart and Ahmed, 2011; R Development Core Team, 2015).

Pairwise Weir and Cockerham (1984) values were calculated between all pairs of populations using GENETIX 4.05 (Belkhir et al., 1996/2004). Populations were defined as field samples and as subsets of individuals collected on the same yam cultivar, i.e., Kabusah, Tahiti and Pacala. Then, the significance of the pairwise-Fst was tested by 10,000 random permutations of the haplotypes (i.e., individuals) between the populations using Multilocus 1.3b software (Agapow and Burt, 2001).

The number of genotypes (Gs) was calculated in the whole sample and per filed from the clone-corrected dataset. As recommended by Arnaud-Haond et al. (2007) we calculated the modified index of clonal diversity, R from Dorken and Eckert (2001) as

$R=(G-1)/(N-1)$, with G, the number of identical multilocus genotypes and N, the number of individuals.

The degree of association between loci was estimated on the clone-corrected dataset by using the index of association, which is the ratio between the observed variance of the number of differences between pairs of strains and the expected variance under the hypothesis of absence of linkage disequilibrium (LD) (Agapow and Burt, 2001). We used a modified version of this index (r_{D}), corrected for the dependence to the number of loci used. r_{D} has an expected value of 0 if there is no association of alleles at unlinked loci, as is expected in a randomly mating population. The significance of r_{D} was tested by a randomization procedure (1,000 times) by comparing the observed value to that expected under the null hypothesis of complete random mating (Agapow and Burt, 2001). Value calculation and tests were performed by Multilocus 1.3b software (Agapow and Burt, 2001). To prevent any effect of the population structure or of the LD between markers, we tested the estimated and tested (LD) between markers and retained 16 loci with no residual LD. We estimated and tested the significance of r_{D} within each genetic cluster using the 16 loci clone-corrected dataset.

Aggressiveness Analysis

Analyses of variance were conducted for the factors host cultivar, field of origin, genetic group using the General Linear Models Procedure of SAS software (SAS Institute, Inc., Cary, NC, United States). A standard analysis of variance (ANOVA) of the aggressiveness indices on each of the four hosts was performed using the SAS software (SAS Institute, Inc., Cary, NC, United States) to test the effect of the host cultivar, the field and the genetic group on strain aggressiveness. Moreover, the mean-values of aggressiveness indices (i.e., Ag-K, Ag-T, Ag-P, Ag-Pl), of initial lesion expansion rate (α_{Na}) and of final lesion area (Na) were compared using the Student's *t*-test. Means values were considered as different for a probability under the threshold of 0.01.

RESULTS

Genetic Diversity

A total of 222 monoconidial strains of *C. gloeosporioides* were isolated from three host cultivars (**Figure 1**). The AFLP analysis generated 89 clearly reproducible bands. Among the 89 clearly reproducible markers, 23 were polymorphic, independent and had a frequency between 0.05 and 0.95, i.e., non-rare alleles. All the markers were amplified from several isolates originating from at least three different fields. Among the 222 isolates, 197 haplotypes were identified, which correlated with high *R* ratios (i.e., modified *G*/*N* ratio, where the number of identical multilocus genotypes, *G*, is divided by the number of individuals, *N*) recorded for the entire dataset, 0.89, and in each field-population, from 0.83 to 0.93 (**Table 1**). Sixteen haplotypes were found in two, three or four copies, but the few isolates sharing the same haplotype were always recovered from a unique field (**Supplementary Figure S3**). Nei (1987) gene diversities were all superior to 0.20 whether they were calculated on field sample or on the entire dataset (**Table 1**).

Population Structure

The population structure analysis with no *a priori*, displayed in the Minimum Spanning Tree (**Figure 2A**) was concordant with the structure analysis using both the Structure software (**Figure 2B**) and the DAPC—adegene package (**Supplementary Figures S4–S6**). According to Evanno's method, the clone-corrected sample (197 isolates) was most likely divided into three genetic groups (**Supplementary Figure S2**). The group 1 (blue in **Figure 2B**, $k = 3$) was composed of more than 98% of strains isolated from yam *cv* Tahiti. This "Tahiti-exclusive" genetic group contained 78.8% of the strains collected on *cv* Tahiti, including 97% of the field Tah_A sample and 61% of the field Tah_B sample. For the groups 2 and 3 (green and orange in **Figure 2B**, $k = 3$) the clustering did not correspond to one host *cv* nor to one geographical location. The group 2 (green in **Figure 2B**, $k = 3$) was composed of isolates from the fields Pac_C (50%), Kab_A (33%), and Tah_B (13.5%). The group 3 (orange in **Figure 2B**, $k = 3$) contained the entire Pac_D sample and 91.6% of Kab_B sample, which represented 93% of the total of strains contained in this genetic group. The genetic grouping was more complex for the group 2. Pac_C strains belonged to one genetic group only, but Kab_A strains belonged to two genetic groups, one common with strains originated from Tah_B and one with strains from Pac_C.

The computed pairwise-Fst proved that populations from different fields were significantly differentiated, whatever the host cultivar, *cv*, and the field (**Table 2**). The pairwise-Fst values were clearly consistent with the genetic clustering given by the analysis with $K = 6$. Indeed, the "Tahiti-private" group and the group 3, respectively, split into two genetic groups corresponding to distinct field of origin (i.e., Tah_A vs Tah_B; Pac_D vs Kab_B). The lowest Fst-value (0.161) was observed between the fields Kab_A (host *cv* Kabusah) and Pac_C (host *cv* Pacala) distant of 1.3 km, whereas higher Fst-values (0.406 and 0.404) were observed between two contiguous fields (Kab_A and Tah_A) and between the two *cv* Pacala fields (Pac_C and Pac_D).

Altogether, the populations sampled on the cultivar Tahiti tend to form a "Tahiti-specific' group, the populations from the fields Pac-D and Kab-B form two clearly distinct genetic groups. The sample from the Kab-A field does not form a uniform genetic group, as to a lesser extent, the sample from the fields Pac-C and Tah-B.

Indices of Association

All indices of association values (r_D) calculated were low (r_D-values ranging from 0.003 to 0.103) but with significant departure to 0 for all populations except cluster 1 (**Table 3**).

TABLE 1 | Genetic diversity indexes within the pooled sample of *Colletotrichum gloeosporioides* and samples from each field.

Origin of the isolates		# isolates	# haplotypes	# loci[(a)]	H n.b.[(b)]	R[(c)]
Field	**Host *cv***					
All	All	222	197	23	0.39 *(0.12)*	0.89
Kab_A	Kabusah	25	21	22	0.23 *(0.19)*	0.83
Kab_B	Kabusah	40	36	18	0.25 *(0.16)*	0.90
Pac_C	Pacala	35	32	22	0.20 *(0.18)*	0.91
Pac_D	Pacala	40	36	21	0.33 *(0.15)*	0.90
Tah_A	Tahiti	41	34	22	0.22 *(0.18)*	0.83
Tah_B	Tahiti	41	38	23	0.31 *(0.17)*	0.93

[(a)]*Number of polymorphic loci out of the 86 loci.* [(b)]*Non-biased Nei's (1987) diversity; standard errors are specified in brackets.* [(c)]*R, the debiased G/N index calculated as (G−1)/(N−1) with G, the number of identical multilocus genotypes and N, the number of individuals.*

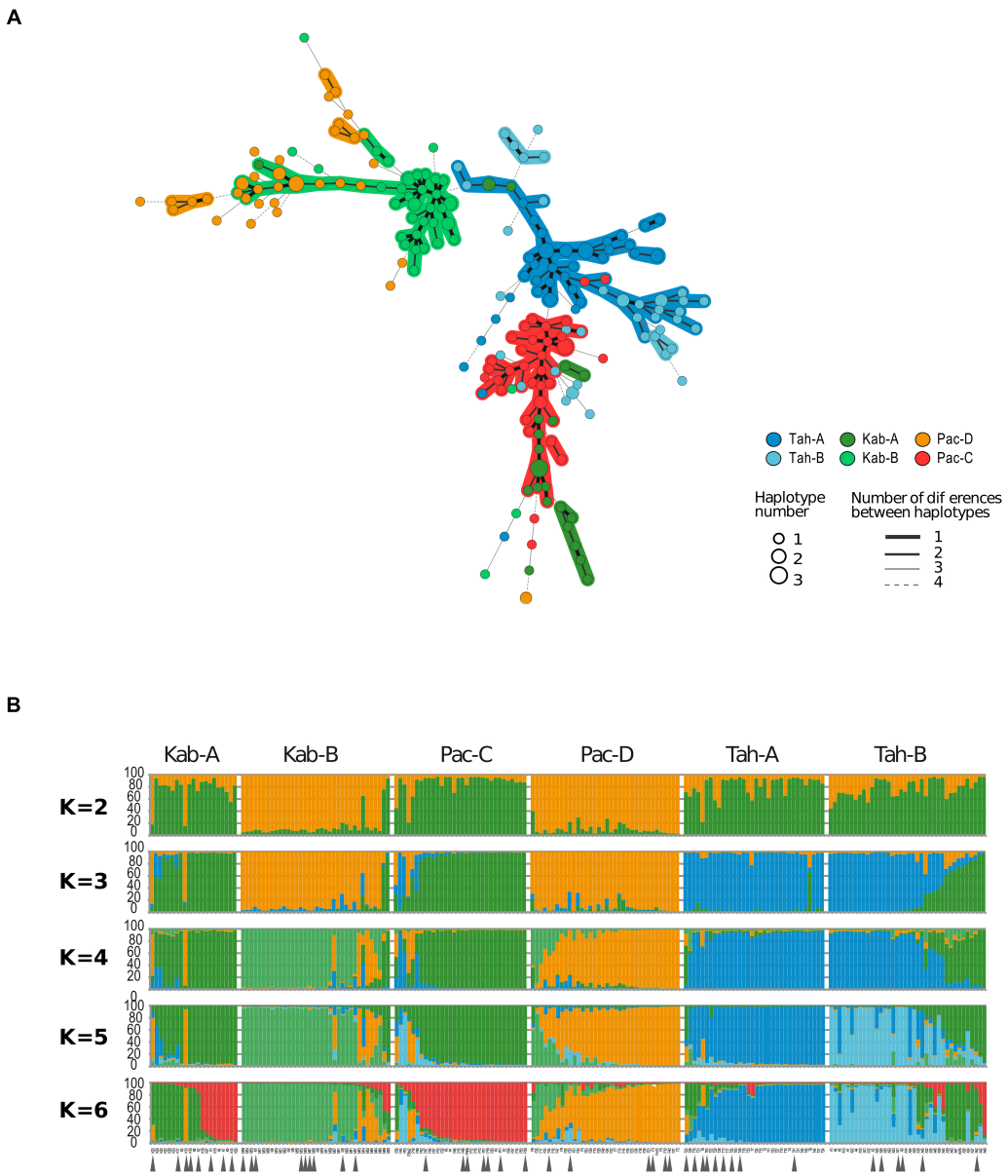

FIGURE 2 | Genetic structure of the 222 *Colletotrichum gloeosporioides* strains sampled on six fields of three different cultivars. **(A)** The minimum-spanning tree based on ALFP markers was constructed using Bionumerics 5.1. Haplotypes collected on *cv* Tahiti are coded in blue, on *cv* Kabusah in green and on *cv* Pacala in Red (bottom right). The size of the circles corresponds to the number of replicates of the same haplotype (bottom right). Numbers of differences between haplotypes are coded by the type of line joining two circles (bottom right). **(B)** Structure software output based on 23 AFLP markers with the number of genetic groups (K) ranging from 2 to 6. Kab, Tah, Pac, respectively, stands for the host, *Dioscorea alata* cultivars Kabusah, Tahiti and Pacala. The letters A, B, C, D stand for the four geographical origins (see **Figure 1**). Gray arrows indicate the strains randomly chosen for the pathogenicity tests.

Strain Aggressiveness Distribution

The diversity for strain aggressiveness was investigated on a 45-strain subsample. These strains belong to the main genetic groups described above (**Figure 3** and **Supplementary Figure S7**). No symptom nor chlorosis appeared on control leaves 11 days after inoculation. We detected an effect of the genetic group (cluster) on strain aggressiveness on the cultivar Tahiti but none on the cultivars Kabusah, Pacala and Plimbite (**Table 4**). Besides, strain aggressiveness on yam *cv* Plimbite (taken as the reference for susceptibility) and on yam *cv* Kabusah (moderate susceptibility) did not depend on the host nor on the field of origin (**Table 4**). Nevertheless, the Student's *t*-test showed that strains collected from *cv* Kabusah were more aggressive on their host *cv* Kabusah (Ag-index mean-value of 47.8) than the strains sampled from *cv* Tahiti (Ag-index mean-value of 20.3). More strikingly, strain aggressiveness, respectively, on the yam *cv* Tahiti (low susceptibility) and *cv* Pacala (high susceptibility), significantly depended on the host cultivar and the field of origin

TABLE 2 | Pairwise-Fst among the six *Colletotrichum gloeosporioides* populations (222 isolates) collected from Yam (*Dioscorea alata*) fields in Morne-à-l'eau (French West Indies, Guadeloupe), estimated with 23 polymorphic AFLP-markers.

Origin of the strains							
Host *cv*	Field	Kab_A	Kab_B	Pac_C	Pac_D	Tah_A	Tah_B
Kabusah	Kab_A	–	*0.0081*	*0.0035*	*0.0090*	*0.0054*	*0.0170*
Kabusah	Kab_B	0.364*	–	*0.0100*	*0.0017*	*0.0000*	*0.0046*
Pacala	Pac_C	0.161*	0.463*	–	*0.0076*	*0.0002*	*0.0250*
Pacala	Pac_D	0.346*	0.282*	0.404*	–	*0.0004*	*0.0045*
Tahiti	Tah_A	0.406*	0.379*	0.244*	0.436*	–	*0.0003*
Tahiti	Tah_B	0.364*	0.341*	0.291*	0.282*	0.243*	–

*Below the diagonal: Pairwise-Fst were calculated following the Weir and Cockerham (1984) indications. *indicates significant Fst ($p < 0.001$) after 1,000 permutations. Above the diagonal: Exact p-values of the exact test of sample differentiation based on haplotype frequencies with Markov chain length of 10,000 steps (Raymond and Rousset, 1995; Goudet et al., 1996).*

TABLE 3 | Standardized index of association within *Colletotrichum gloeosporioides* populations.

Population	$rD^{(a)}$	$rD^{*(b)}$
All	0.031**	
Kab_A	0.056**	
Kab_B	0.103**	
Pac_C	0.032**	
Pac_D	0.036**	
Tah_A	0.049**	
Tah_B	0.029**	
All		0.024***
Cluster 1		0.016
Cluster 2		0.03**
Cluster 3		0.028***

[(a)]rD: standardized index of association calculated on the clone-corrected data set using 23 ploymorphic markers, i.e., with the haplotypes (Haubold et al., 1998; Agapow and Burt, 2001). [(b)]rD: standardized index of association calculated on the clone-corrected data set using 16 polymorphic markers where loci had no significant LD with each others; **indicates significant values with p-values below 0.01 after 1,000 random resampling, ***indicates significant values with p-values below 0.001 after 1,000 random resampling.*

(**Table 4**). The mean aggressiveness on *cv* Tahiti was higher for the strains collected on this cultivar (mean Ag-index value of 44.7) than the strains from other host yam *cv* (mean Ag-index values of 16.6 and 11.7). In the same way, the strains collected on *cv* Pacala displayed the highest level of aggressiveness on *cv* Pacala than the other strains (**Table 4**). Finally, the effect of the host cultivar on the values for the initial lesion expansion rates (α_{Na}; **Figure 3**) and the typical lesion area on day 11 (Na; **Figure 3**) was similar to the effect observed on the Ag-index (aggressiveness). The initial lesion expansion rate seemed critical to explain the adaptive evolution of the aggressiveness.

Patterns of Strain Adaptation to Its Host Cultivar

The pairwise comparison of strain aggressiveness (Ag-indices) on the three host *cv* populations on the same inoculated *cv* (**Table 4** and **Figure 3**) revealed clear pattern of local adaptation on *cv* Tahiti and *cv* Kabusah with high differences in mean aggressiveness values. Local adaptation to the host *cv* Pacala (highly susceptible) was also shown, however, the mean aggressiveness values were all higher on *cv* Pacala than on the other inoculated cultivars which could be seen as a general adaptation to this cultivar. The patterns of local adaptation to the host cultivar were reinforced by the absence of any pattern of differential adaptation of the strains to the cultivar of reference, *cv* Plimbite. Finally, the pattern of *C. gloeosporioides* adaptation to its host cultivar, especially to the cultivar Tahiti, was similar to the pattern expected for locally adapted pathogen populations.

DISCUSSION

Our purpose was to better understand how and in which proportions the migration, recombination and yam quantitative resistance influence the *C. gloeosporioides* evolution, and more particularly the evolution of *C. gloeosporioides* pathogenicity. Does the adaptive pattern of *C. gloeosporioides* correspond to a general adaptation to the most common host cultivar, or to a highly fragmented pathogen population resulting from the adaptation to each cultivar subpopulation (i.e., local adaptation; Gandon et al., 1996; Gandon and Van Zandt, 1998)? Furthermore, can the history of cultivars' succession in Guadeloupe be reflected by the recorded fungal pathogenicity distribution?

Colletotrichum gloeosporioides Diversity and Sexual Reproduction Imprint

The AFLP analysis revealed high genetic diversity. Such levels for neutral molecular diversity were previously recorded for *C. gloeosporioides* collected from different yam hosts in three agro-ecological areas of Nigeria (Abang et al., 2006). The indirect evaluation of the reproductive mode, that is the standardized index of multilocus LD, was in accordance with a significant departure from total panmixia, but not reaching complete clonality. Our results thus revealed significant the impact of clonal reproduction on *C. gloeosporioides*'s evolution, which is in concordance with the role of conidia dispersal in the epidemic expansion and the presence of quiescent mycelia in tubers. However, the influence of recombination (sexuality) was not entirely excluded. Besides previous studies reported the presence of sexual reproductive structures of *C. gloeosporioides* on dead yam leaves at the end of the crop season (Toribio and Jacqua, 1978; Toribio et al., 1980; Degras et al., 1984; Abang et al., 2001, 2006). Therefore, it seems parsimonious to consider that recombination explains the high haplotype diversities observed in every subset. Altogether, the influence of sexual reproduction and the high levels of genetic diversity seem to be general traits in *C. gloeosporioides*'s biology as it was previously suggested for *C. gloeosporioides* populations damaging yams (Mignouna et al., 2002; Abang et al., 2005, 2006) and damaging strawberry (Xiao et al., 2004). To conclude, even if *C. gloeosporioides*, pathogenic on *D. alata*, undergoes weak recombination between two crop seasons, sexuality likely confers this fungus a great opportunity to evolve.

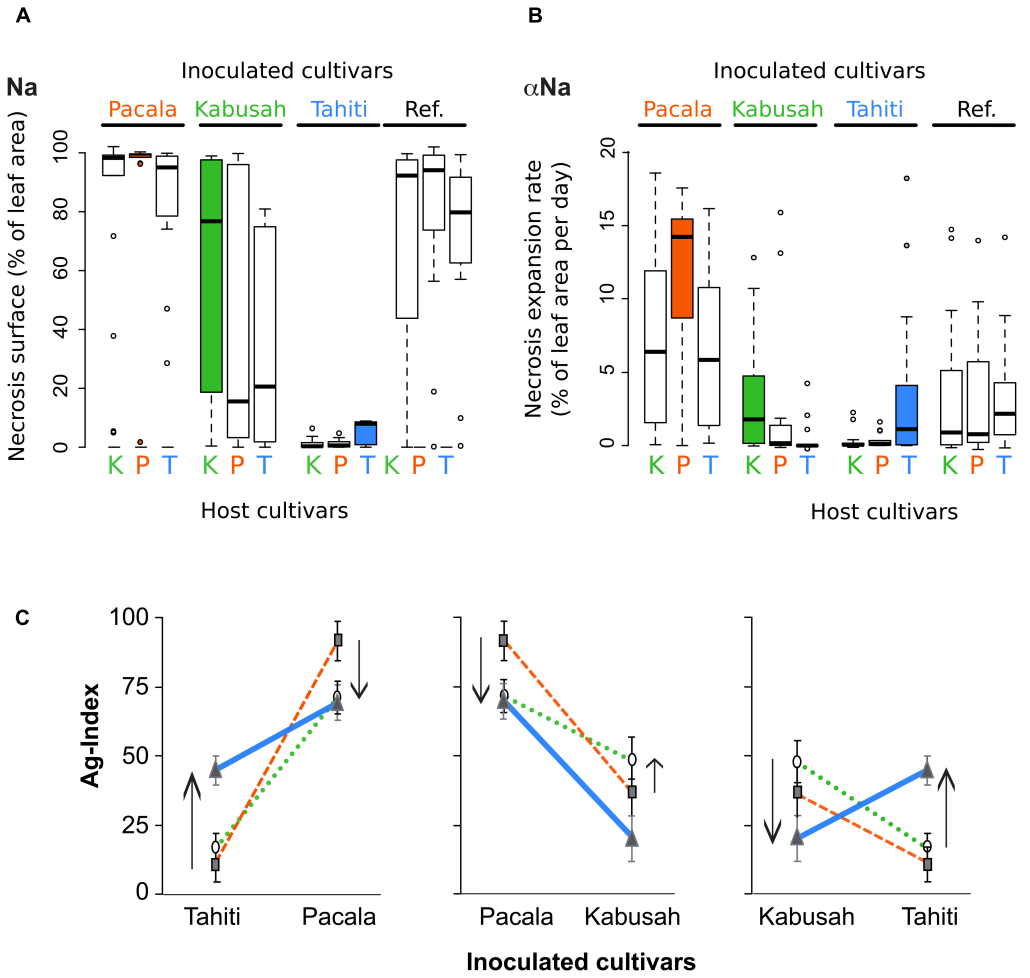

FIGURE 3 | *C. gloeosporioides* local adaptation to its host resistance. A subsample of 45 *C. gloeosporioides* strains isolated from three *D. alata* host cultivars Kabusah (K, moderate susceptibility), Pacala (P, high susceptibility) and Tahiti (T, low susceptibility) were cross-inoculated on these cultivars and on a cultivar of reference (Plimbite, Ref.). **(A)** Boxplot for the necrosis area, Na. **(B)** Boxplot for the initial (i.e., day 0–day 6) necrosis expansion rate, α_{NA} were obtained for each cross-inoculation using R-software. **(C)** Pairwise comparison of the strain aggressiveness inoculated on their local and foreign hosts. Aggressiveness of the strains isolated from *cv* Kabusah are, respectively, represented with black circles (green dotted lines), from *cv* Pacala in black square (red dashed lines) and from *cv* Tahiti in gray triangles (blue lines). Arrows underline the loss or the gain of mean aggressiveness in comparison with the one of strains isolated on *cv* Pacala, the oldest and susceptible cultivar.

Colletotrichum gloeosporioides Migration Rate

The haplotype distribution within one population gives insights into its dispersal potential (McDonald, 1997). In the present study, the AFLP genotyping of the haploid fungus *C. gloeosporioides* revealed a strong population structure: each field sample can be considered as one fungal population. The number of genetic groups revealed with the no *a priori* analyses and the high Fst-values recorded between field populations, whatever their location or host cultivar, suggest a weak influence of *C. gloeosporioides* migration between the fields studied during the crop season. Indeed, no haplotypes were shared between fields. Moreover, the strains from adjoining fields (Kab_A-Tah_A and Kab_B-Tah_B; **Figure 1** and (**Supplementary Figure S3**) belonged to different genetic groups, whereas individuals from the field Pac_C (Pacala) were genetically close to some of the individuals from the field Kab_A (Kabusah). Furthermore, out of the 18 multicopy haplotypes, only seven were sampled from neighboring sampling positions whereas 11 were sampled from dispersed sampling positions within the same field (**Supplementary Figure S3**). In other words, for the fungal populations studied here, the dispersal by splashing during the crop season occurred but had a minor impact at a local scale (i.e., not beyond few meters).

In fact, the population structure recorded here (high diversity and strong structure) corresponds to the one expected for a primary inoculum. It is also consistent with the correlation found between the presence of *C. gloeosporioides* mycelia in the yam tubers planted and the subsequent leaf anthracnose

TABLE 4 | Aggressiveness indices (Ag) of *Colletotrichum gloeosporioides* populations from six *D. alata* yam fields tested on four yam cultivars: Kabusah, Pacala, Tahiti and Plimbite (the cultivar of reference for the susceptibility to anthracnose).

	N	Aggressiveness (Ag-index) estimated on four									*D.alata* cultivars		
Levels		***cv Kabusah***			***cv Pacala***			***cv Tahiti***			***cv Plimbite* (ref)**		
host *cv* Kabusah	17	47.8	*(7.5)*	a	71.1	*(6)*	b	16.6	*(5.2)*	b	51.6	*(7.2)*	a
host *cv* Pacala	13	36.4	*(9)*	ab	91.5	*(7.1)*	a	11.7	*(6.1)*	b	56.6	*(8.6)*	a
host *cv* Tahiti	15	20.3	*(8.3)*	b	69.3	*(6.4)*	b	44.7	*(5.5)*	a	54	*(7.7)*	a
Kab_A – field	8	41.4	*(5.5)*	ab	59.9	*(8.2)*	ab	12.1	*(7.5)*	b	43.4	*(10.4)*	a
Kab_B – field	9	53.4	*(6.3)*	a	81.1	*(7.7)*	ab	20.7	*(7)*	b	59	*(9.8)*	a
Pac_C – field	7	48	*(5.9)*	a	90	*(8.2)*	a	13.5	*(7.5)*	b	65.9	*(10.4)*	a
Pac_D – field	6	13.3	*(5.7)*	b	94.5	*(11.6)*	a	8	*(10.5)*	b	38	*(14.7)*	a
Tah_A – field	9	25.8	*(10.8)*	ab	58.8	*(7.7)*	b	37.1	*(7)*	a	59.7	*(9.8)*	a
Tah_B – field	6	13	*(12.4)*	b	85	*(9.5)*	ab	56.2	*(8.6)*	a	45.5	*(12)*	a
Genetic cluster 1	13	23.3	*(9.3)*	a	66.2	*(6.9)*	a	43.4	*(6.3)*	a	53.3	*(8.3)*	a
Genetic cluster 2	15	42.4	*(5.2)*	a	73.2	*(6.5)*	ab	17.5	*(5.9)*	b	54	*(7.7)*	a
Genetic cluster 3	16	38.6	*(6.1)*	a	86.8	*(6.3*	a	16.8	*(5.7)*	b	54	*(7.5)*	a
prob F, effect = host cultivar		0.061			0.048*			0.000***			0.908		
prob F, effect = field of origin		0.075			0.019*			0.002***			0.472		
prob F, effect = genetic group (cluster)		0.294			0.088			0.005***			0.998		

*Fields $KabA/Tah_A$, and $KabB/Tah_B$ were contiguous (see **Figure 1**). a, b stands for the groups of significant differences of aggressiveness tested using Student's t-test with a p-value $p < 0.01$. Tests were performed considering separately each of the four inoculated cultivars and each of the fungal population grouping levels, host cv, field and genetic cluster. *,***, respectively, indicates significant values with p-values below 0.05 and 0.001. Standard errors are specified in brackets.*

severity (Green and Simons, 1994). Ultimately, as farmers usually divide yam tubers into pieces (seeds) and save them for the next crop season, when a tuber is infected with one isolate, this isolate will be randomly dispersed within a field where seeds are planted. This fully explains the genetic diversity we observed within and between fungal field-populations. More importantly, the spatial distribution of the haplotypes seemed more likely related to seeds distribution than to fungus dispersal by splashing.

Finally, if dead stems and leaves left on the soil after the previous crop season are a potential source of primary inoculum (Ripoche et al., 2007), the impact of such event cannot be detected in this study, as for all the fields the previous crop was sugar cane. Although no strong influence of migration was detected in this study, the pathogen migration can occur between fields of severely damaged plants (Degras et al., 1984; Green, 1994).

Colletotrichum Gloeosporioides Local Adaptive Response to Yam Resistances

Previous works already reported the ability of *C. gloeosporioides* to overcome host resistance (Miles and Lascano, 1997; Chakraborty et al., 1999; Abang et al., 2001; Abang, 2003) or to develop resistance to fungicides (Bayart and Pallas, 1994). The last point of our investigations focused on the adaptation of the field-structured populations to their host quantitative resistance. Are *C. gloeosporioides* field populations adapted to every host cultivar (general adaptation) or are they specifically adapted to their host cultivar?

We can also draw a parallel between the patterns of adaptation recorded and the "age" and intensity of each cultivar's production in Guadeloupe. As a matter of fact, the cultivar Pacala was the most widespread in Guadeloupe until the end of the 1960s, when its resistance to anthracnose was overcome. Despite its susceptibility to anthracnose, *cv* Pacala is still one of the most planted cultivars in Guadeloupe (Penet et al., 2016). The *cv* Plimbite, introduced during the 1970s, was widely cultivated in Guadeloupe but its prevalence decayed when its resistance was overcome in the early 1990s (Ano et al., 2002). The water yam *cv* Kabusah was the last cultivar introduced at the beginning of the 1990s and has been widely cultivated ever since. Finally, *cv* Tahiti has been cultivated from the 1960s but its prevalence increased in the 1990s.

The patterns of adaptation described in the present study are concordant with a general adaptation to the formerly highly prevalent hosts (*cv* Pacala and *cv* Plimbite) and a local adaptation (i.e., diversifying selection) to the cultivars which became abundant more recently (*cv* Kabusah and *cv* Tahiti; **Table 4** and **Figure 3**). Surprisingly a pattern of local adaptation to the old but still widely planted *cv* Pacala was observed despite a strong general adaptation pattern, revealing an ongoing selective pressure of *cv* Pacala on *C. gloeosporioides* populations.

In our sample, strain virulence (not null aggressiveness) on the four yam cultivars prevailed. It is unclear whether this corresponds to an accumulation of virulences within *C. gloeosporioides* populations or to a core virulence component fixed in all populations. The first hypothesis seems more likely as a former survey on Brazilian *C. gloeosporioides* populations infecting *Stylosanthes* showed an increase of fungal race complexity within few years (Chakraborty et al., 2002). The overall virulence of the studied strains reveals that the recorded adaptation for aggressiveness does not depend on the virulence combination. The adaption of *C. gloeosporioides* to its yam host is quantitative. Besides, we did not find any correlation between strain aggressiveness (Ag-values) against the Kabusah, Tahiti

or Pacala cultivars (**Supplementary Figure S8**). This indicates a certain level of specificity in the *C. gloeosporioides–D. alata* interaction, even if it seems minor compared to the quantitative aspect. The evolutionary potential of the *C. gloeosporioides* populations pathogenic on *D. alata* reinforces the necessity to better understand the aggressiveness evolution in time and space in order to efficiently predict the durability of *D. alata* resistance to anthracnose. Further investigations of the in-field population dynamics are needed to evaluate the potential of aggressiveness evolution during one crop season. Finally, as previously mentioned, the yam tuber infection can be crucial for the parasite long-distance dispersal and its survival between crop seasons. The capacity of *C. gloeosporioides* to infect and survive in its host tuber is clearly a determinant aspect of its own fitness thus its evolutionary potential. The pattern of genetic diversity revealed by our study underlines the need to improve the control for seed quality at all cost.

AUTHOR CONTRIBUTIONS

LF, GJ, and CN contributed to conception and design of the study. LF analyzed the results and wrote the first draft of the manuscript. CN supervised the work. All authors contributed to manuscript revision, read and approved the submitted version.

FUNDING

This work was funded by the French National Institute of Agronomical Research (INRA) and the Antilles-Guyane region.

ACKNOWLEDGMENTS

We particularly thank Bruno Le Cam, Bernard Tivoli, Jean Carlier, and Virginie Ravigné for their advices.

SUPPLEMENTARY MATERIAL

The Supplementary Material for this article can be found online at: https://www.frontiersin.org/articles/10.3389/fpls.2018.01554/full#supplementary-material

FIGURE S1 | Power of the number of markers used to detect genotypes and measure diversity.

FIGURE S2 | Evanno's Delta *K* test.

FIGURE S3 | Detailed distribution of haplotypes at the field scale. The relative positions where the haplotypes where sampled are specified. The genetic groups obtained in the Structure analysis with $K = 3$, are color coded in orange, green, and blue. Strains belonging to several genetic groups are specified using dashed color code. The letters T, A, K, M, P, F correspond to the strains, respectively, originating from the fields specified in **Figure 1**, Tah-A, Tah-B, Kab-A, Kab-B, Pac-C, Pac-D. The strains found to be the same haplotype are specified using black boxes, the names of the duplicates are given with the letters a, b, c. No haplotypes were shared between fields.

FIGURE S4 | Principal Component Analysis of the 199 haplotypes. PCA was performed using the adegenet-DAPC software (Jombart and Ahmed, 2011). **(A)** The PCA shows the dispersion of the 197 haplotypes (23 independent AFLP markers). Colors represent the cultivar of origin: Tahiti, Kabusah, Pacala.

FIGURE S5 | Principal Component Analysis of the 199 haplotypes. PCA was performed using the adegenet software (Jombart and Ahmed, 2011). The PCA shows the dispersion of the 197 haplotypes (23 independent AFLP markers) when the number of groups is 6 or 3. For each group defined by the DAPC analysis, the number of haplotypes sampled in each field specified in **Figure 1** (i.e., Tah-A, Tah-B, Kab-A, Kab-B, Pac-C, Pac-D) are specified in the tables.

FIGURE S6 | Principal Component Analysis of the 199 haplotypes. DPCA was performed using the adegenet software (Jombart and Ahmed, 2011). The DPCA shows the dispersion of the 197 haplotypes (23 independent AFLP markers) when the number of groups is, respectively, 4, 5, 7, and 8.

FIGURE S7 | Structure groups for the strains used in the pathogenicity tests. Structure software output based on 23 AFLP markers with the number of genetic groups (K) ranging from 2 to 6. Kab, Tah, Pac, respectively, stands for the host, *Dioscorea alata* cultivars Kabusah, Tahiti, and Pacala. The letters A, B, C, D stand for the four geographical origins (see **Figure 1**).

FIGURE S8 | Pairwise correlation between *C. gloeosporioides* aggressiveness (Ag-Index values) against four *D. alata* cultivars. The psych package (Revelle, 2018) was used to plot and test the pairwise regressions of the 45 *C. gloeosporioides* strains' aggressiveness recorded on four different *D. alata* cultivars, *cv* Kabusah, Pacala, Tahiti, and Plimbite. Below the diagonal: pairwise scatter plots of Ag-indexes, respectively, assessed on *cv* Kabusah (KAB), Pacala (PAC), Tahiti (TAH), and Plimbite (PLI). Diagonal: the histogram and lowess locally fit regression line of the Ag-indexes assessed on each cultivar, respectively. The *x* axis in each scatter plot represents the column Ag-indexes, the *y* axis the row Ag-indexes. Above the diagonal: the Pearson correlation values. The significances of single correlation were tested with multiple comparisons adjustment using the Holm correction and are specified as *** for $p \leq 0.001$ and ** for $p \leq 0.01$.

TABLE S1 | Main characteristics of the six Dioscorea alata fields located in the center of Guadeloupe (Morne-à-l'eau). **(A)** Sugar-cane (sc) and pasture (p); TahA/B and KabA/B refers to the adjoining fields described in **Figure 1**; **(B)** Farm indicates that the tuberpieces (i.e., seeds) planted were harvested during the previous crop-season in the same farm. Imported, means that tuber-pieces planted were obtained from other farms or, more likely imported from Costa Rica.

REFERENCES

Abang, M. M. (2003). *Genetic Diversity of Colletrotrichum Gloeosporioides Penz. Causing Anthracnose Disease of Yam (Dioscorea spp.) in Nigeria*. Ph.D. thesis, Borntraeger Science Publishers, Berlin.

Abang, M. M., Asiedu, R., Hoffmann, P., Wolf, G. A., Mignouna, H. D., and Winter, S. (2006). Pathogenic and genetic variability among *Colletotrichum gloeosporioides* isolates from different yam hosts in the agroecological zones in Nigeria. *J. Phytopathol.* 154, 51–61. doi: 10.1111/j.1439-0434.2005.01060.x

Abang, M. M., Fagbola, O., Smalla, K., and Winter, S. (2005). Two genetically distinct populations of *Colletrotrichum gloeosporioides* penz. causing anthracnose disease of yam (*Dioscorea spp.*). *J. Phytopathol.* 153, 137–142. doi: 10.1111/j.1439-0434.2005.00942.x

Abang, M. M., Green, K. R., Wanyera, N. W., and Iloba, C. (2001). "Characterization of *Colletrotrichum gloeosporioides* penz. from yam (*Dioscorea spp.*) in nigeria," in *Proceedings of the 7th Triennial Symposium of the International Society for Tropical Root Crops*, Cotonou, 613–615.

Abang, M. M., Hoffmann, P., Winter, S., Green, K. R., and Wolf, G. A. (2004). Vegetative compatibility among isolates of *Colletrotrichum gloeosporioides* from Yam (Dioscorea spp.) in Nigeria. *J. Phytopathol.* 152, 21–27. doi: 10.1046/j.1439-0434.2003.00795.x

Agapow, P. M., and Burt, A. (2001). Indices of multilocus linkage disequilibrium. *Mol. Ecol. Notes* 1, 101–102. doi: 10.1046/j.1471-8278.2000.00014.x

Andrivon, D. (1993). Nomenclature for pathogenicity and virulence: the need for precision. *Phytopathology* 83, 889–890. doi: 10.1094/Phyto-83-889

Andrivon, D., Pilet, F., Montarry, J., Hafidi, M., Corbiere, R., Achbani, E. H., et al. (2007). Adaptation of *Phytophthora infestans* to partial resistance in potato: evidence from French and Moroccan populations. *Phytopathology* 97, 338–343. doi: 10.1094/PHYTO-97-3-0338

Ano, G., Anaïs, G., and Chidiac, A. (2002). Création et utilisation de variétés résistantes aux maladies, éléments essentiels de la diversification agricole en Guadeloupe. *Phytoma* 551, 36–37.

Arnaud-Haond, S., Duarte, C. M., Alberto, F., and Serrão, E. A. (2007). Standardizing methods to address clonality in population studies. *Mol. Ecol.* 16, 5115–5139. doi: 10.1111/j.1365-294X.2007.03535.x

Asiedu, R., Ng, S. Y. C., Bai, K. V., Ekanayake, I. J., and Wanyera, N. M. W. (1998). "Genetic improvement," in *Food Yams: Advances in Research IITA and NCRI*, eds G. C. Orkwor, R. Asiedu, and I. J. Ekanayake (Ibadan: IITA), 63–103.

Bailey, J. A., and Jeger, M. J. (1992). *Colletotrichum: Biology Pathology and Control*. Wallingford: CAB international.

Bayart, J. D., and Pallas, B. (1994). Tolerance of yam anthracnose to benzimidazoles: results of the first study conducted in Guadeloupe. *Phytoma* 461, 37–40.

Belkhir, K., Borsa, P., Chikhi, L., Raufaste, N., and Bonhomme, F. (1996/2004). *GENETIX 4.05, Logiciel Sous Windows TM Pour la Genetique des Populations. Laboratoire Genome, Populations, Interactions, CNRS UMR 5000*. Montpellier: Université de Montpellier II.

Berner, D. K., Cavin, C. A., McMahon, M. B., and Loumbourdis, I. (2006). First report of anthracnose of salsola tragus caused by *Colletotrichum gloeosporioides* in Greece. *Plant Dis.* 90, 971–971. doi: 10.1094/PD-90-0971B

Chakraborty, S., Fernandes, C. D., Charchar, M. J. D., and Thomas, M. R. (2002). Pathogenic variation in *Colletrotrichum gloeosporioides* infecting *Stylosanthes spp*. in a center of diversity in Brazil. *Phytopathology* 92, 553–562. doi: 10.1094/PHYTO.2002.92.5.553

Chakraborty, S., Perrott, R., Ellis, N., and Thomas, M. R. (1999). New aggressive *Colletrotrichum gloeosporioides* strains on *Stylosanthes scabra* detected by virulence and DNA analysis. *Plant Dis.* 83, 333–340. doi: 10.1094/PDIS.1999.83.4.333

Chalhoub, B. A., Thibault, S., Laucou, V., Rameau, C., Hofte, H., and Cousin, R. (1997). Silver staining and recovery of AFLP amplification products on large denaturing polyacrylamide gels. *Biotechniques* 22, 216–220. doi: 10.2144/97222bm03

Chen, R. S., and McDonald, B. A. (1996). Sexual reproduction plays a major role in the genetic structure of populations of fungus *Mycosphaerella graminicola*. *Genetics* 142, 1119–1126.

Coursey, D. G. (1967). *Yams. An Account of the Nature, Origins, Cultivation and Utilisation of the Useful Members of the Dioscoreaceae. Tropical Agricultural Series*. Harlow: Longmans.

Cowger, C., and Mundt, C. C. (2002). Aggressiveness of *Mycosphaerella graminicola* isolates from susceptible and partially resistant wheat cultivars. *Phytopathology* 92, 624–630. doi: 10.1094/PHYTO.2002.92.6.624

Degras, L., Arnolin, R., Suard, C., and Poitou, R. (1984). "Selection of D. alata cultivars of low susceptibility to anthracnose (*Colletrotrichum gloeosporioides*)," in *Proceedings of the Sixth Symposium of the International Society for Tropical Root Crops*, Lima, 627–632.

Dorken, M. E., and Eckert, C. G. (2001). Severely reduced sexual reproduction in northern populations of a clonal plant, *Decodon verticillatus* (Lythraceae). *J. Ecol.* 89, 339–350. doi: 10.1046/j.1365-2745.2001.00558.x

Elmer, W. H., Yang, H. A., and Sweetingham, M. W. (2001). Characterization of *Colletotrichum gloeosporioides* isolates for ornamental lupines in Connecticut. *Plant Dis.* 85, 216–219. doi: 10.1094/PDIS.2001.85.2.216

Evanno, G., Regnaut, S., and Goudet, J. (2005). Detecting the number of clusters of individuals using the software structure: a simulation study. *Mol. Ecol.* 14, 2611–2620. doi: 10.1111/j.1365-294X.2005.02553.x

Falush, D., Stephens, M., and Pritchard, J. (2003). Inference of population structure using multilocus genotype data: linked loci and correlated allele frequencies. *Genetics* 164, 1567–1587.

Flor, H. H. (1971). Current status of the gene-for-gene concept. *Annu. Rev. Phytopathol.* 9, 275–296. doi: 10.1146/annurev.py.09.090171.001423

Freeman, S., Katan, T., and Shabi, E. (1998). Characterization of *Colletotrichum* species responsible for anthracnose diseases of various fruits. *Plant Dis.* 82, 596–605. doi: 10.1094/PDIS.1998.82.6.596

Frézal, L., Desquilbet, L., Jacqua, G., and Neema, C. (2012). Quantification of the aggressiveness of a foliar pathogen, *Colletotrichum gloeosporioides*, responsible for water yam (*Dioscorea alata*) anthracnose. *Eur. J. Plant Pathol.* 134, 267–279. doi: 10.1007/s10658-012-9986-4

Gandon, S., Capowiez, A., Dubois, Y., Michalakis, Y., and Olivieri, I. (1996). Local adaptation and gene-for-gene coevolution in a metapopulation model. *Proc. R. Soc. B* 263. doi: 10.1098/rspb.1996.0148

Gandon, S., and Van Zandt, P. A. (1998). Local adaptation and host–parasite interactions. *Trends Ecol. Evol.* 13, 214–216. doi: 10.1016/S0169-5347

Goudet, J., Raymond, M., De Meeus, T., and Rousset, F. (1996). Testing differentiation in diploid populations. *Genetics* 144, 1933–1940.

Green, K. R. (1994). *Studies on the Epidemiology and Control of Yam Anthracnose*. Ph.D. thesis, University of Reading, Reading.

Green, K. R., and Simons, S. A. (1994). 'Dead skin' on yams (*Dioscorea alata*) caused by *Colletrotrichum gloeosporioides*. *Plant Pathol.* 43, 1062–1065. doi: 10.1111/j.1365-3059.1994.tb01660.x

Haubold, B., Travisiano, P. B., and Hudson, R. R. (1998). Detecting linkage disequilibrium in bacterial populations. *Genetics* 150, 1341–1348.

Jombart, T., and Ahmed, I. (2011). *adegenet 1.3-1*: new tools for the analysis of genome-wide SNP data. *Bioinformatics* 27, 3070–3071. doi: 10.1093/bioinformatics/btr521

Jombart, T., Devillard, S., and Balloux, F. (2010). Discriminant analysis of principal components: a new method for the analysis of genetically structured populations. *BMC Genet.* 11:94. doi: 10.1186/1471-2156-11-94

Kaltz, O., and Shykoff, J. A. (1998). Local adaptation in host–parasite systems. *Heredity* 81, 361–370. doi: 10.1046/j.1365-2540.1998.00435.x

Kawecki, T. J., and Ebert, D. (2004). Conceptual issues in local adaptation. *Ecol. Lett.* 7, 1225–1241. doi: 10.1111/j.1461-0248.2004.00684.x

Kim, W. G., and Hong, S. K. (2008). Occurrence of anthracnose on peach tree caused by *Colletotrichum* species. *Plant Pathol. J.* 24, 80–83. doi: 10.5423/PPJ.2008.24.1.080

Laird, N. M., and Ware, J. H. (1982). Random-effects models for longitudinal data. *Biometrics* 38, 963–974. doi: 10.2307/2529876

McDonald, B. A. (1997). The population genetics of fungi: tools and techniques. *Phytopathology* 87, 448–453. doi: 10.1094/PHYTO.1997.87.4.448

McDonald, B. A., and Linde, C. (2002). Pathogen population genetics, evolutionary potential, and durable resistance. *Annu. Rev. Phytopathol.* 40, 349–379. doi: 10.1146/annurev.phyto.40.120501.101443

McDonald, F. D., Alleyne, A. T., O'Garro, L. W., and Delauney, A. J. (1998). Yam anthracnose in the English-speaking islands of the Eastern Caribbean: successes and research advances in disease management. *Trop. Agric. (Trinidad)* 75, 53–57.

Mignouna, H. D., Abang, M. M., Green, K. R., and Asiedu, R. (2001). Inheritance of resistance in water yam (*Dioscorea alata*) to anthracnose (*Colletrotrichum gloeosporioides*). *Theor. Appl. Genet.* 103, 52–55. doi: 10.1007/s001220000531

Mignouna, H. D., Abang, M. M., Onasanya, A., and Asiedu, R. (2002). Identification and application of RADP markers for anthracnose resistance in water yam (*Dioscorea alata*). *Ann. Appl. Biol.* 141, 61–66. doi: 10.1111/j.1744-7348.2002.tb00195.x

Miles, J. W., and Lascano, C. E. (1997). Status of *Stylosanthes* development in other countries. I. *Stylosanthes* development and utilization in South America. *Trop. Grass.* 31, 454–459.

Montarry, J., Corbiere, R., and Andrivon, D. (2007). Is there a trade-off between aggressiveness and overwinter survival in Phytophthora infestans? *Funct. Ecol.* 21, 603–610. doi: 10.1111/j.1365-2435.2007.01252.x

Nei, M. (1987). *Molecular Evolutionary Genetics*. New York, NY: Columbia University Press.

Ntahimpera, N., Wilson, L. L., Ellis, M. A., and Madden, L. V. (1999). Comparison of rain effects on splash dispersal of three *Colletotrichum* species infecting strawberry. *Phytopathology* 89, 555–563. doi: 10.1094/PHYTO.1999.89.7.555

Penet, L., Cornet, D., Blazy, J.-M., Alleyne, A., Barthe, E., Bussière, F., et al. (2016). Varietal dynamics and yam agro-diversity demonstrate complex trajectories intersecting farmers' strategies, networks, and disease experience. *Front. Plant Sci.* 7:1962. doi: 10.3389/fpls.2016.01962

Penet, L., Guyader, S., Peìtro, D., Salles, M., and BussieÌre, F. (2014). Direct splash dispersal prevails over indirect and subsequent spread during rains in *Colletotrichum gloeosporioides* infecting yams. *PLoS One* 9:e115757. doi: 10.1371/journal.pone.0115757

Petro, D., Onyeka, T. J., Etienne, S., and Rubens, S. (2011). An intraspecific genetic map of water yam (*Dioscorea alata* L.) based on AFLP markers and QTL analysis for anthracnose resistance. *Euphytica* 179, 405–416. doi: 10.1007/s10681-010-0338-1

Pritchard, J. K., Stephens, M., and Donnelly, P. (2000). Inference of population structure using multilocus genotype data. *Genetics* 155, 945–959.

R Development Core Team (2015). *R: A Language and Environment for Statistical Computing*. Available at: http://www.r-project.org/

Raymond, M., and Rousset, F. (1995). An exact test for population differentiation. *Evolution* 49, 1280–1283. doi: 10.1111/j.1558-5646.1995.tb04456.x

Revelle, W. (2018). *psych: Procedures for Psychological, Psychometric, and Personality Research, Version 1.8.4.* Available at: https://CRAN.R-project.org/package=psych

Ripoche, A., Jacqua, G., Bussière, F., Guyader, S., and Sierra, J. (2007). Survival of *Colletotrichum gloeosporioides* (causal agent of yam anthracnose) on yam residues decomposing in soil. *Appl. Soil Ecol.* 38, 270–278. doi: 10.1016/j.apsoil.2007.10.015

SAS Institute (1987). *SAS/STAT Guide for personal computers. Version* 6. Cary, NC: SAS Institute Inc.

Simons, S. A., and Green, K. R. (1994). A quantitative method for assessing the severity of anthracnose on yam (*Dioscorea alata*). *Trop. Sci.* 34, 216–224.

Sutton, B. C. (1992). "The genus *Glomerella* and its anamorph *Colletotrichum*," in *Colletotrichum: Biology, Pathology and Control*, eds J. A. Bailey and M. J. Jeger (Wallingford: CAB International Wallingford), 1–26.

Talhinhas, P., Sreenivasaprasad, S., Neves-Martins, J., and Oliveira, H. (2005). Molecular and phenotypic analyses reveal association of diverse *Colletotrichum acutatum* groups and a low level of C. gloeosporioides with olive anthracnose. *Appl. Environ. Microbiol.* 71, 2987–2998. doi: 10.1128/AEM.71.6.2987-2998.2005

Toribio, J. A., Edwige, S., and Jacqua, G. (1980). *Pathologie Des Ignames En Guadeloupe: Maladies Fongiques Colloquium Inra Seminar On Yams Inra, Guadeloupe*, Antilles: INRA 107–114.

Toribio, J. A., and Jacqua, G. (1978). Traitements fongicides contre l'anthracnose de l'igname. *Nouv. Agronomiques Antilles Guyane* 4, 147–152.

Villaréal, L. M. M. A., Lannou, C., Vallavielle-Pope, C., and Neema, C. (2002). Genetic variability in *Puccinia striiformis fsp. Tritici* populations sampled on a local scale during natural epidemics. *Appl. Environ. Microbiol.* 68, 6138–6145. doi: 10.1128/AEM.68.12.6138-6145.2002

Weir, B. S., and Cockerham, C. C. (1984). Estimating F-statistics for the analysis of population structure. *Evolution* 38, 1358–1370.

Winch, J. E., Newhook, F. J., Jackson, G. V. H., and Cole, J. S. (1984). Studies of *Colletrotrichum gloeosporioides* disease on yam, *Dioscorea alata*, in Solomon Islands. *Plant Pathol.* 33, 467–477. doi: 10.1111/j.1365-3059.1984.tb02870.x

Xiao, C. L., Mackenzie, S. J., and Legard, D. E. (2004). Genetic and pathogenic analyses of *Colletotrichum gloeosporioides* isolates from strawberry and non-cultivated hosts. *Phytopathology* 94, 446–453. doi: 10.1094/PHYTO.2004.94.5.446

Zhan, J., Pettway, R. E., and McDonald, B. A. (2003). The global genetic structure of the wheat pathogen *Mycosphaerella graminicola* is characterized by high nuclear diversity, low mitochondrial diversity, regular recombination, and gene flow. *Fungal Genet. Biol.* 38, 286–297. doi: 10.1016/S1087-1845(02)00538-8

Conflict of Interest Statement: The authors declare that the research was conducted in the absence of any commercial or financial relationships that could be construed as a potential conflict of interest.

frontiers in Microbiology

ORIGINAL RESEARCH
published: 16 November 2018
doi: 10.3389/fmicb.2018.02801

Populations of the Beet Cyst Nematode *Heterodera schachtii* Exhibit Strong Differences in Their Life-History Traits Across Changing Thermal Conditions

Sylvain Fournet, Lucile Pellan, Catherine Porte, Christophe Piriou, Eric Grenier and Josselin Montarry*

IGEPP, INRA, Agrocampus Ouest, Université de Rennes 1, Le Rheu, France

It is widely accepted that climate has an essential influence on the distribution of species and that temperature is the major abiotic factor that affects their life-history traits. Species with very restricted active dispersal abilities and a wide geographical distribution are thus expected to encompass distinct populations adapted to contrasted local conditions. The beet cyst nematode *Heterodera schachtii* is a good biological model to study temperature adaptation in populations collected from different environments. Here, we tested the effect of temperature on *H. schachtii* life-history traits using seven field populations from Morocco, Spain, France, Germany, Austria, Poland and Ukraine. We tested hatching and multiplication rates of each population at different temperatures, as well as hatching rates of each population after storage at different temperatures – simulating survival conditions during the inter-cropping period. Results showed a strong temperature effect on the life-history traits explored. Temperature impact on hatching (at different temperatures and after storage at different temperatures) depended on the origin of populations, separating southern from northern ones. Surprisingly, low temperatures influenced hatching less in southern populations. However, for these populations, a storage period at low temperatures strongly reduce subsequent hatching. Conversely, nematode multiplication was not differentially affected by temperatures, as favorable conditions for the host are also favorable for the parasite. Finally, a significant correlation between the genetic diversity and the level of specialization showed that the less diverse populations were more specialized than the more diverse ones.

Keywords: adaptation, genetic diversity, hatching, specialist/generalist, survival

OPEN ACCESS

Edited by:
Brigitte Mauch-Mani, University of Neuchâtel, Switzerland

Reviewed by:
Anna-Liisa Laine, University of Helsinki, Finland
Pablo Castillo, Consejo Superior de Investigaciones Científicas (CSIC), Spain

****Correspondence:***
Sylvain Fournet
sylvain.fournet@inra.fr

Specialty section:
This article was submitted to Plant Microbe Interactions, a section of the journal Frontiers in Microbiology

Received: *02 July 2018*
Accepted: *31 October 2018*
Published: *16 November 2018*

Citation:
Fournet S, Pellan L, Porte C, Piriou C, Grenier E and Montarry J (2018) Populations of the Beet Cyst Nematode Heterodera schachtii Exhibit Strong Differences in Their Life-History Traits Across Changing Thermal Conditions. Front. Microbiol. 9:2801. doi: 10.3389/fmicb.2018.02801

INTRODUCTION

There is no doubt that climate has a major influence on the natural distribution of species (Pearson and Dawson, 2003) and that temperature is the major abiotic factor that affects species phenology (Scranton and Amarasekare, 2017). In a context of ongoing climate change, predicting the temperature impact on life-history traits, such as fecundity, development and survival, and thus on the distribution of species is a very challenging scientific question with implications for conservation biology, ecology, agronomy and pest management.

Species characterized by restricted active dispersal ability and a wide geographical distribution are expected to comprise distinct populations adapted to contrasted local conditions

(Davis and Shaw, 2001). Plant pathogens, being often distributed across a wide range of climates, are good biological models to study the temperature adaptation of populations from different environments. For instance, patterns of local adaptation to temperature have been highlighted in natural (Laine, 2008) and agricultural host-pathogen systems (Zhan and McDonald, 2011; Mboup et al., 2012; Mariette et al., 2016).

The life cycle of many plant pathogens can be split into two alternating phases: the epidemic period, onto or into the host, and the inter-epidemic period, often outside the host. Several investigations have shown the necessity to take into account the inter-epidemic period in order to better describe the evolutionary trajectories of plant pathogens (e.g., Pfender and Vollmer, 1999; Abang et al., 2006; Montarry et al., 2007; Sommerhalder et al., 2011; Suffert et al., 2015; Pasco et al., 2016). Interestingly, temperature regimes are likely to differ across locations much more during the inter-epidemic periods than during the epidemic periods, because optimal temperatures for host growth is quite similar whatever the geographical locality.

The beet cyst nematode *Heterodera schachtii*, which is regarded as the most important pest in sugar beet production worldwide (Müller, 1999; Amiri et al., 2002), is globally distributed with populations living in highly contrasted environments (see Subbotin et al., 2010 for a review). In European wild beets, *H. schachtii* is relatively rare in south of Spain and Portugal, but more frequent from the northern coast of Spain to Denmark (Gracianne et al., 2014). In European sugar beet fields, *H. schachtii* is widely present from east to west, from Portugal to Ukraine, and from south to north, from Morocco to Finland (Subbotin et al., 2010). Also, as for all plant parasitic nematodes, *H. schachtii* has only very limited active dispersal capabilities in the soil (Wallace, 1968), and temperature is one of the most influential environmental factor affecting key steps of its biological cycle (Trudgill et al., 2005; Kakaire et al., 2012; Kaczmarek et al., 2014; Vandenbossche et al., 2015). Indeed, temperature can act on all or part of life-history traits involved in embryogenesis, hatching and development after infection and survival (Wallace, 1955; Thomason and Fife, 1962; Jones, 1975; Griffin, 1988). For *H. schachtii*, such influence is well known and extensively described in many previous studies, but on a limited number of field populations coming from north European fields (e.g., Vandenbossche et al., 2015). Therefore, *H. schachtii* populations may be thus assumed to be differentially adapted to local temperatures, both for traits involved in development within their host plant (sugar beet), and for traits involved in their survival in the soil when plants are not present.

Here, we explored the effect of temperature on *H. schachtii* life-history traits using seven field populations from Morocco, Spain, France, Germany, Austria, Poland, and Ukraine. We tested the hatching and the multiplication rates of each population at different temperatures, as well as the hatching rate of each population after storage at different temperatures, simulating survival conditions during the inter-cropping period. Finally, to test the hypothesis that greater genetic diversity is associated with less ecological specialization, we calculated the level of specialization to the temperature and assessed the genetic diversity using microsatellite markers for each population.

MATERIALS AND METHODS

Nematode Populations

The seven *H. schachtii* populations were sampled between 2014 and 2016 in a single field in seven different countries and localities representing contrasted climatic zone : Morocco (Mor; Al Aroui), Spain (Spa; Lebridja), France (Fra; Prunay), Germany (Ger; Schlanstedt), Austria (Aus; Tadten), Poland (Pol; Radlowek), and Ukraine (Ukr; Teofipol). Each population corresponded to a single soil sample constituted of a minimum amount of 2 kg and a minimum of 10 elementary samples collected randomly in the field between 0 and 20 centimeters deep. The cysts extracted from each of these seven soil samples were multiplied one time in standardized conditions, (20°C, room chamber, 16:8) for two to four generations on the cultivar Ardan. Newly formed cysts were then stored at 5°C in moistened sandy soil.

Genetic Diversity

The seven *H. schachtii* populations were genotyped using eight microsatellite markers developed by Montarry et al. (2015): Hs33, Hs36, Hs55, Hs56, Hs68, Hs84, Hs111, and Hs114. Between 21 and 39 individuals per population were successfully genotyped using only one larva (i.e., 1 s-stage juvenile) per cyst, in order to limit biases due to sibling relationships. DNA of each larva was extracted with a procedure using sodium hydroxide and proteinase K, following Boucher et al. (2013).

Three multiplex panels were defined to genotype the 207 individuals at the eight loci. PCR was performed in a 5 μL volume containing 1X of Type-it Microsatellite PCR kit, 0.4 μM of primer mix and 1 μL of template DNA. Cycling conditions included an initial denaturation at 95°C for 5 min, followed by 30 cycles of denaturation at 95°C for 30 s, annealing at 58°C for 90 s and extension at 72°C for 30 s, followed by a final extension at 60°C for 30 min. PCR products were then diluted to 1:10 in sterile water and 3 μL of this dilution were mixed with 0.05 μL of GeneScan 500 LIZ Size Standard (Applied Biosystems) and 5 μL of formamide (Applied Biosystems). Analyses of PCR products were conducted on a ABI Prism® 3130xl sequencer (Applied Biosystems).

Allele sizes were determined with the automatic calling and binning module of GeneMapper v4.1 (Applied Biosystems), and complemented by a manual examination of irregular results. Samples showing dubious genotypes were tested again.

Genetic diversity in each *H. schachtii* population was estimated using GENETIX 4.05.2 (Belkhir et al., 2004) as the unbiased gene diversity (Hnb) (Nei, 1978). Hnb corresponds to the average probability across loci to draw at random different alleles in the same population.

Hatching at Different Temperatures

For the seven *H. schachtii* populations, larvae emergence was investigated at three temperatures: 11, 17, and 23°C, which cover the range of temperatures encounter by European *H. schachtii* populations, from the North to the South, during the cropping period. For each population and each temperature, six

independent replicates were performed. Each replicate consisted of a pool of four cysts, calibrated in size between 450 and 500 μm. Cysts were placed on a sieve of 250 μm, allowing the active passage of larvae. Each sieve was put in one well of a 24-well plate containing root exudates of sugar beet (cv. Ardan). Plates were placed in the dark in three different climate chambers set at the respective temperatures. Temperature within each climate chamber was recorded every hour using thermo-tracers (ThermoTracer, Oceasoft, Montpellier, France – **Supplementary Figure S1**). The number of hatched larvae was counted after 1, 2, 3, 4, 7, 11, 15, 19, 23, 28, and 33 days, the exudate being changed at each date. The number of unhatched eggs was assessed at the end of the experiment in order to calculate the percentage of hatching.

Multiplication at Different Temperatures

For the seven *H. schachtii* populations, *H. schachtii* multiplication was investigated at three temperatures: 11, 17, and 23°C. For each population and each temperature, 27 independent replicates were performed, i.e., 27 sugar beet plants of the cultivar Ardan. Plants were grown in a 4:1 sand-kaolin mixture watered with a nutrient solution (Hakaphos: NPK 15/10/15). Kaolin was used to aerate the sand and thus to promote the mobility of *H. schahctii* larvae. Each plant was inoculated at the two-leaf stage with 1 mL of a suspension of larvae concentrated at 500 larvae.mL^{-1}. Plants were placed in three different climate chambers set at the respective temperatures with a photoperiod of 16 h. Temperature within each climate chamber was recorded every hour using thermo-tracers (ThermoTracer, Oceasoft, Montpellier, France – **Supplementary Figure S1**). Plants were cut at the end of the cycle, when white females were well formed and contained eggs, i.e., after 4 weeks at 23°C, after 5 weeks at 17°C, and after 9 weeks at 11°C. Plants were kept several weeks in their climatic chamber until the maturation of cysts, i.e., three, four and six additional weeks at 23, 17, and 11°C, respectively. Newly formed cysts were extracted by filtering the soil through two sieves (800 and 250 μm) and counted under a stereomicroscope.

Hatching Following Storage at Different Temperatures

Each *H. schachtii* population was multiplied one generation on the sugar beet cultivar Ardan and newly formed cysts were then stored during 2 months at four temperatures: −3, 4, 10, and 25°C, which cover the range of temperatures encounter by European *H. schachtii* populations, from the North to the South, during the inter-cropping period. For each population and each temperature, six independent replicates were performed. Each replicate consisted of a pool of four cysts, calibrated for their size between 450 and 500 μm, and placed in boxes containing 33 g of sand and 7 mL of water. Boxes were stored in the dark in incubators set at the respective temperatures. Temperature within each incubator was recorded every hour using thermo-tracers (ThermoTracer, Oceasoft, Montpellier, France – **Supplementary Figure S1**). After the storage period, each pool of four cysts was placed on a sieve of 250 μm, allowing the active passage of larvae, and each sieve was put in a 24-well plate containing root exudates of sugar beet (cv. Ardan). Plates were placed in the dark at 20°C (± 1) in an incubator. The number of hatched larvae was counted after 1, 2, 3, 4, 7, 11, 15, 19, 23, and 28 days, the exudate being changed at each date. The number of unhatched eggs was assessed at the end of the experiment in order to calculate the percentage of hatching.

Statistical Analysis

In order to take into account the hatching dynamic in its entirety, and not only the final point of the hatching curve, the Area Under the Hatching Curve (AUHC) was calculated for each replicate. For each population, and for each measured traits (i.e., AUHC, number of produced cysts and AUHC after storage), the temperature effect was tested through a one-way ANOVA and multiple comparisons of means were done with the Tukey contrasts test ($\alpha = 0.05$). Normality and homogeneity of variances were checked using the Shapiro–Wilk and the Leven tests, respectively.

Standardized niche breadth (B_A) – a parameter estimating the level of ecological specialization of a species (or a population) – was calculated for each *H. schachtii* population using the standardized index developed by Levins (1968):

$$B_A = \frac{1}{n-1}\left[\frac{1}{\sum p_i^2} - 1\right]$$

where p_i is the proportion of the measured fitness trait into the environment i and n the total number of tested environments. In this study, $n = 3$ for the hatching and the multiplication at different temperatures (11, 17, and 23°C) and $n = 4$ four for the hatching following storage at different temperatures (−3, 4, 10, and 25°C). The standardized niche breadth varies from 0 to 1. A low niche breadth points to a high level of specialization (i.e., a specialist species) and an high niche breadth to a low level of specialization (i.e., a generalist species).

The relationships between the level of specialization (B_A) and the genetic diversity (Hnb) were tested with the Pearson's product-moment correlation. All statistical analyses were performed using the R software version 3.3.3 (R Development Core Team, 2017).

RESULTS

Hatching and Multiplication at Different Temperatures

ANOVAs revealed a very strong temperature effect for five *H. schachtii* populations, Fra, Ger, Aus, Pol, and Ukr (**Table 1** and **Figure 1**), showing that the hatching pattern was very different at 11°C: larvae emergence was lower at 11°C than at 17 or 23°C, in terms of AUHC (**Figure 1**) but also in terms of cumulative hatching at the end of the experiment (**Supplementary Figure S2**). Conversely, the temperature effect was very small or even non-significant for the two remaining populations, Mor and Spa (**Table 1** and **Figure 1**), for which larvae emergence (i.e., AUHC – **Figure 1** – and cumulative hatching at the end of the experiment – **Supplementary Figure S2**) was similar whatever the temperature.

TABLE 1 | Results from the analyses of variance (ANOVAs) assessing the temperature effect on the three explored life-history traits (AUHC at different temperatures, on the number of cysts produced at different temperatures and on AUHC after storage at different temperatures) for each *Heterodera schachtii* populations.

Population	Source of variation	AUHC			Number of cysts			AUHC after storage		
		df	*F*-value	*P* > *F*	df	*F*-value	*P* > *F*	df	*F*-value	*P* > *F*
Mor	Temperature effect	2	2.00	0.1700	2	12.67	<0.0001***	3	20.31	<0.0001***
	Error	15			74			20		
Spa	Temperature effect	2	10.70	0.0013**	2	4.33	0.0166*	3	12.10	<0.0001***
	Error	15			75			20		
Fra	Temperature effect	2	156.60	<0.0001***	2	0.44	0.6480	3	11.84	0.0001***
	Error	15			74			20		
Ger	Temperature effect	2	407.30	<0.0001***	2	11.15	<0.0001***	3	0.99	0.4170
	Error	15			74			20		
Aus	Temperature effect	2	163.50	<0.0001***	2	4.28	0.0174*	3	4.69	0.0122*
	Error	15			76			20		
Pol	Temperature effect	2	327.60	<0.0001***	2	22.49	<0.0001***	3	15.64	<0.0001***
	Error	15			74			20		
Ukr	Temperature effect	2	69.29	<0.0001***	2	11.16	<0.0001***	3	9.00	0.0006***
	Error	15			75			20		

*The statistically significant effects are indicated as *P < 0.05, **P < 0.01, and ***P < 0.001.*

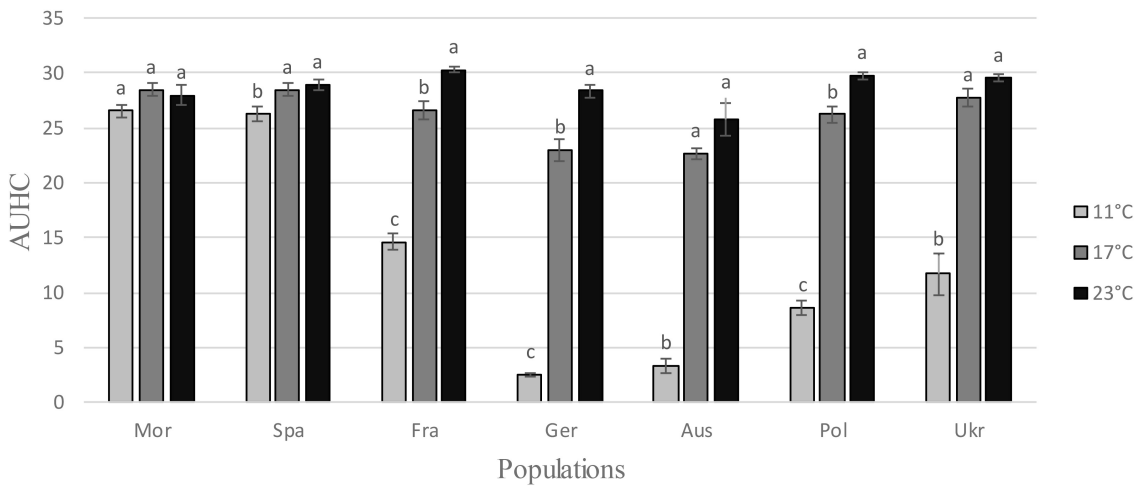

FIGURE 1 | Area Under the Hatching Curve (AUHC) at different temperatures (11, 17, and 23°C) for each *Heterodera schachtii* population (mean values ± standard deviations). Letters represent the homogenous groups identified by the Tukey contrasts test at the 5% threshold.

Regarding the number cysts produced on sugar beet plants at different temperatures, ANOVAs revealed a temperature effect for all populations, except for the French one, showing that *H. schachtii* populations produced more cysts at the intermediary temperature, i.e., 17°C (**Table 1** and **Figure 2**).

Hatching Following Storage at Different Temperatures

After a prior exposure for 2 months to different storage temperatures, the hatching experiment was performed at 20°C (±1) because at this temperature larvae of all populations hatched very well, as showed by the previous experiment (**Figure 1**). Larvae emergence was reduced after storage at −3°C for all populations except the German one (**Table 1** and **Figure 3**). The difference between the storage step at −3°C and the three other temperatures (4, 10, and 25°C) was much higher for the two Mediterranean populations (Mor and Spa) than for the five others (Fra, Ger, Aus, Pol, and Ukr), both for the AUHC (**Figure 3**) or the cumulative hatching at the end of the experiment (**Supplementary Figure S3**).

Relationship Between Genetic Diversity and Ecological Specialization

Regarding the hatching (AUHC) at different temperatures, the standardized niche breadth B_A – a parameter to measure how specialized a population is within a given environment – highlighted the generalist status of *H. schachtii* populations from Morocco and Spain (wide niche breath, $0.98 < B_A < 0.99$) and

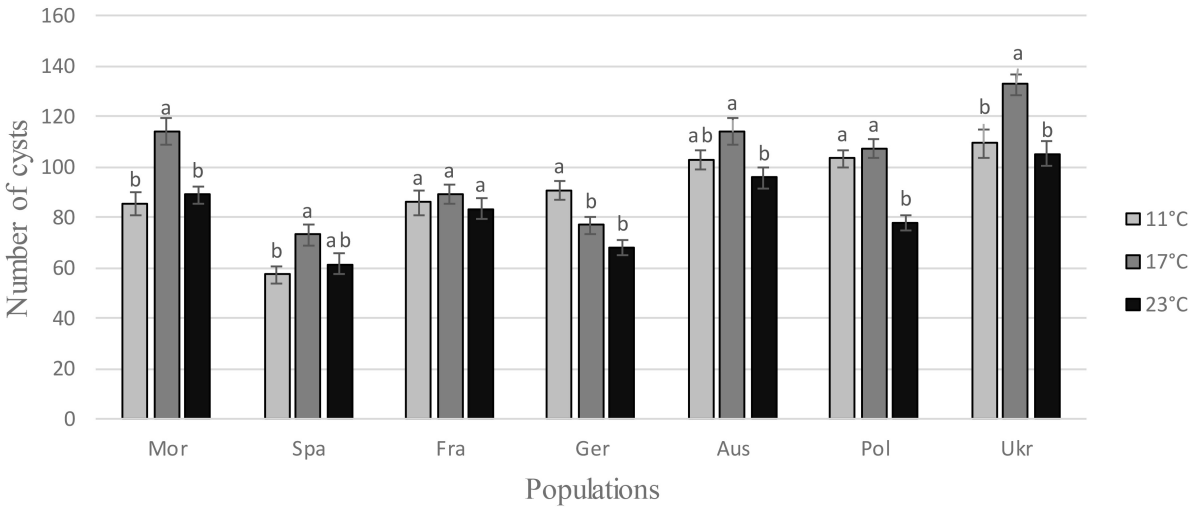

FIGURE 2 | Number of cysts obtained from a multiplication at different temperatures (11, 17, and 23°C) for each *H. schachtii* population (mean values ± standard deviations). Letters represent the homogenous groups identified by the Tukey contrasts test at the 5% threshold.

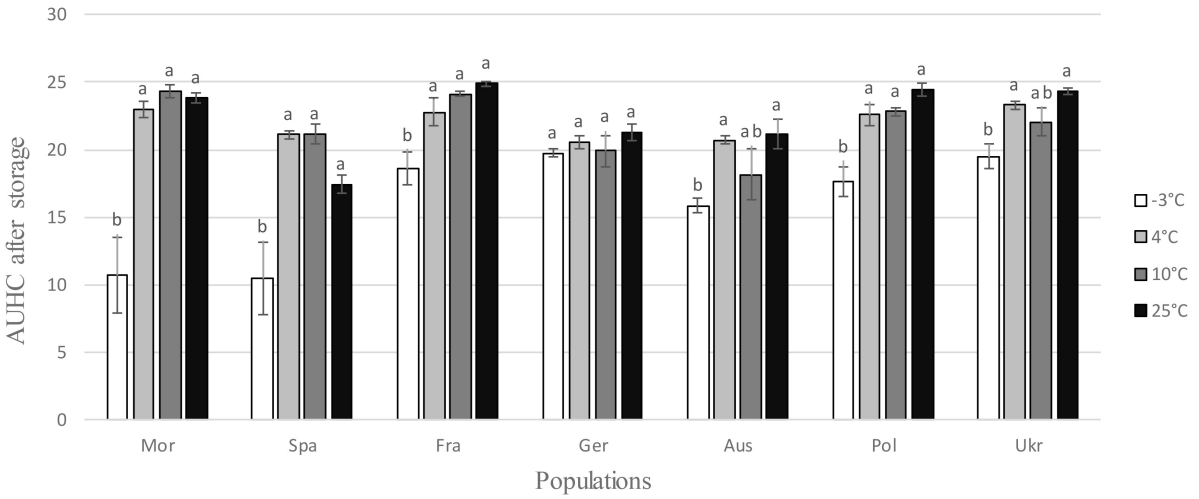

FIGURE 3 | Area Under the Hatching Curve (AUHC) after storage at different temperatures (–3, 4, 10, and 25°C) for each *H. schachtii* population (mean values ± standard deviations). Letters represent the homogenous groups identified by the Tukey contrasts test at the 5% threshold.

TABLE 2 | Genetic diversity (Hnb) and standardized niche breadth (B_A) calculated on AUHC at different temperatures, on the number of cysts produced at different temperatures and on AUHC after storage at different temperatures for each *H. schachtii* populations (Pop).

Pop	*n*	Hnb	B_A on AUHC	B_A on the number of cysts	B_A on AUHC after storage
Mor	38	0.43	0.98	0.97	0.90
Spa	21	0.59	0.99	0.98	0.92
Fra	22	0.48	0.89	0.99	0.98
Ger	37	0.30	0.58	0.98	0.99
Aus	39	0.26	0.63	0.99	0.98
Pol	22	0.53	0.77	0.97	0.98
Ukr	28	0.37	0.83	0.98	0.99

n indicates the number of genotyped individuals.

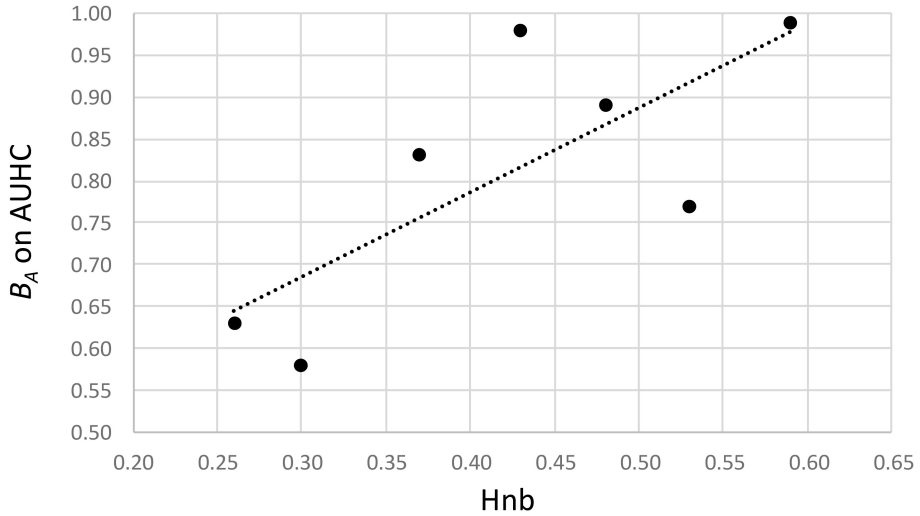

FIGURE 4 | Relationship between the genetic diversity (Hnb) and the standardized niche breadth on the AUHC at different temperatures (B_A on AUHC) calculated of each *H. schachtii* population.

showed a lower niche breadth for the five other populations ($0.58 < B_A < 0.89$), when taking temperatures as different environments (**Table 2**). Moreover, there was a significant correlation between the genetic diversity and the level of specialization (cor = 0.758; $P = 0.048$), showing that the less diverse populations were more specialized than the more diverse ones, and *vice versa* (**Figure 4**).

Regarding the multiplication (number of cysts) at different temperatures and the hatching (AUHC) after storage at different temperatures, the standardized niche breadth B_A highlighted the generalist status of all *H. schachtii* populations ($0.97 < B_A < 0.99$ for the number of cysts and $0.92 < B_A < 0.99$ for the AUHC, **Table 2**) and no correlation with the genetic diversity (cor = −0.373; $P = 0.410$ for the number of cysts and cor = −0.464; $P = 0.294$ for the AUHC).

DISCUSSION

Although the hatching and development of the beet cyst nematode *H. schachtii* have been already studied (e.g., Griffin, 1988), far less is known about the survival abilities of this species under different climate conditions that can be encountered during the inter-cropping season. The main objectives of the present work were thus to test the effect of temperature and to compare the level of specialization of different *H. schachtii* populations for key traits involved in survival and reproduction: hatching, development in the host plant and hatching after a survival period.

Low temperatures strongly reduced both the hatching pattern and the cumulative hatching rate of five populations (France, Germany, Austria, Poland, and Ukraine): at 11°C, hatching was slowly and was incomplete. Previous studies already showed the same behavior in populations from the same geographical areas (e.g., Vandenbossche et al., 2015). Conversely, temperature had only a small effect on the two southern populations, from Spain and Morocco. This was a surprising result: one could imagine that northern populations should be less constrained by lower temperatures than southern ones, which faced much higher temperature levels over the year. In an unexpected way, temperature appeared thus to act differently according to the geographical origin of populations in the sequence leading to the hatch of larvae. Perry and Gaur (1996) showed that differences related to the host, for instance the age of the host plant, on which the nematodes multiplied could strongly affect their subsequent hatching rate. In our study, cysts all came from a single multiplication cycle on the same sugar beet cultivar, and experiments were performed in controlled conditions. The differences observed in hatching behavior could thus not be assigned to the conditions for obtaining cysts used in this study, but would rather be a clear answer of each population to the thermal conditions applied in the experiment. Indeed, cyst nematode species are all obligate parasites, and their reproductive success mainly depends on the synchronization between hatching and host presence. Consequently, it seems that natural selection has optimized the hatching response to enhance fitness in a different way for northern and southern populations (Spain and Morocco). For these last populations, the most important factor driving hatching may rather be the occurrence of favorable conditions (moisture and presence of root exudates), rather than temperature only.

Regarding the development in the host plant, thermal conditions did not affect each population differentially. In all cases, the number of newly formed cysts matched the usual shape of a thermal performance curve (Schulte et al., 2011), and all populations exhibited higher performances at 17°C. This is consistent with what was already described in the literature for field populations (e.g., Griffin, 1988) and for wild populations of *H. schachtii* (Gracianne et al., 2014). This optimum corresponds also to the optimal temperature for sugar beet cropping. Indeed,

even if sugar beet is grown throughout Europe, cropping is always realized under conditions that ensure optimal development and yields. These conditions correspond to the period from April to September in the majority of European countries, but from November to May in Morocco and in the south of Spain.

Most studies only considered the effect of temperature on the multiplication of plant parasites during the epidemic phase, i.e., during the interaction with the host. Here, we also investigated its impact on the survival of the progeny inside the cysts, because the ability to survive when host plants were absent is also an important fitness component submitted to selection (Roff, 1992). In our case study, temperature during the inter-epidemic phases are much more variable than those encountered during the cropping period: they correspond either to very hot summer conditions for the southern populations and to cold winter conditions for the populations of northern and central Europe. In both cases, these periods are characterized by unfavorable conditions for the growth of host plants. We thus exposed cysts of each *H. schachtii* population during 2 months to temperatures from −3 to 25°C, which correspond to the range encountered in natural conditions. The results confirmed the existence of two distinct groups of populations: one (Morocco, Spain) for which survival at a low temperature (−3°C) reduced strongly the subsequent hatching rate, and a second one (all others populations) where survival temperatures had only a limited impact on subsequent hatching. At this point we could therefore conclude, rightly as these populations never encountered such low temperatures, that both southern populations were thus clearly maladapted to survival under cold conditions, while northern populations seemed adapted to survive over a larger range of temperatures, including cold ones.

However, closer examination of the mean standard deviations leads to a more nuanced conclusion. Indeed, southern populations both exhibited greater variation for this trait than northern ones (**Figure 3** and **Supplementary Figure S3**) and seemed to contain some individuals that could survive cold conditions and others that could not (see **Supplementary Figure S4** showing the hatching curves for each independent replicate). This observation makes sense in an evolutionary context, where northern populations can be seen as the result of a gradual northward (re)colonization process of Europe after the Last Glacial Maximum (LGM), with the selection among southern individuals of those able to survive the coldest temperatures. Several studies make this hypothesis relevant. First, the south of the Iberian Peninsula is well known as an historical refuge, climatically stable during geological times (Rodrıguez-Sanchez et al., 2008) and therefore during the LGM which corresponded to the latest coldest conditions encountered in Europe. Second, two recent studies tend to prove that wild populations of *H. schachtii* and of its wild hosts *Beta maritima* recolonized the north of Europe following a northward process of migration from the south of the Iberian Peninsula (Leys et al., 2014; Gracianne, 2015; respectively). After the LGM, the following huge increase of temperature pushes northward favorable conditions to the development of host plants and nematodes and make possible the recolonization of northern Europe. While our study was performed with field populations that share only part of their evolutionary history with wild ones, our results matched this scenario rather well. Indeed, we also observed a northward decrease of genetic diversity in our field populations, as expected in the case of sequential founder events associated to recolonization processes and limited gene flow among population (Austerlitz et al., 1997).

As a last challenge, we explored the link between genetic diversity in populations and their ecological specialization, testing the hypothesis that greater genetic diversity is associated with less ecological specialization. Such a relationship was only demonstrated so far between species: in 11 of 14 studies identified by Li et al. (2014), the specialist species showed lower genetic diversity than related generalists. Here, a similar trend can be observed between populations: Spanish and Morrocan populations were both generalists, with a high niche breath and a higher genetic diversity, while Northern populations appeared to be more specialized and less diverse. The generalist character fitted the independence of the hatching and development according to thermal conditions. The association of this generalist trait with higher genetic diversity fitted also well with Gracianne's scenario, which assumes that Spain and more southern regions kept favorable climate conditions during the LGM, promoting the maintenance of a huge genetic diversity in these areas. The less diversity and the higher specialization to cold climate conditions we observed in northern populations fitted again well with this scenario. The northward recolonization of Europe was associated with the selection for a better capability to survive and a less susceptibility to hatch at low temperatures, maximizing the synchronization between hatching and host presence.

Further investigations are now needed, using wild *H. schachtii* populations, to determine whether the counter-selection of the capability to hatch at low temperatures and the selection of the capability to survive at low temperatures are the result of a fast evolution process in the cultivated compartment (i.e., an adaptation to crop practices in northern Europe), or of a longer process in the wild, associated to the northward recolonization of Europe. Anyway, the high tolerance to contrasted survival conditions observed in northern Europe field populations explains well the presence of *H. schachtii* all around the world where sugar beet is grown (Subbotin et al., 2010). Furthermore, in the framework of global climate change, our data imply that northern populations of *H. schachtii* should not be strongly affected for both survival and development by global warming.

DATA AVAILABILITY

All data used in this article are available at data.inra.fr (doi: 10.15454/ZKGTAH).

AUTHOR CONTRIBUTIONS

LP, CaP, and ChP performed the experiments according to a protocol elaborated jointly by SF, EG, and JM. SF and JM analyzed

the data. SF, EG, and JM wrote the text and prepared the figures. All authors edited the paper and have approved the current version.

ACKNOWLEDGMENTS

We gratefully acknowledge ITB, SES, KWS, Strube, and SYNGENTA who kindly provided the different *Heterodera schachtii* populations. Dr. D. Andrivon is acknowledged for comments on earlier draft of this manuscript.

SUPPLEMENTARY MATERIAL

The Supplementary Material for this article can be found online at: https://www.frontiersin.org/articles/10.3389/fmicb.2018.02801/full#supplementary-material

REFERENCES

Abang, M. M., Baum, M., Ceccarelli, S., Grando, S., Linde, C. C., Yahyaoui, A., et al. (2006). Differential selection on *Rhynchosporium secalis* during parasitic and saprophytic phases in the barley scald disease cycle. *Phytopathology* 96, 1214–1222. doi: 10.1094/PHYTO-96-1214

Amiri, S., Subbotin, S. A., and Moens, M. (2002). Identification of the beet cyst nematode *Heterodera schachtii* by PCR. *Eur. J. Plant Pathol.* 108, 497–506. doi: 10.1023/A:1019974101225

Austerlitz, F., Jung-Muller, B., Godelle, B., and Gouyon, P. H. (1997). Evolution of coalescence times, genetic diversity and structure during colonization. *Theor. Popul. Biol.* 51, 148–164. doi: 10.1006/tpbi.1997.1302

Belkhir, K., Borsa, P., Chikhi, L., Raufaste, N., and Bonhomme, F. (2004). *GENETIX 4.05, A WindowsTM-based Sofware for Population Genetic Analyses. Laboratoire Génome, Populations, Interactions, CNRS UMR 5000*. Montpellier: Université de Montpellier II.

Boucher, A. C., Mimee, B., Montarry, J., Bardou-Valette, S., Bélair, G., Moffett, P., et al. (2013). Genetic diversity of the golden potato cyst nematode *Globodera rostochiensis* and determination of the origin of populations in Quebec, Canada. *Mol. Phylogenet. Evol.* 69, 75–82. doi: 10.1016/j.ympev.2013.05.020

Davis, M. B., and Shaw, R. G. (2001). Range shifts and adaptive response to Quaternary climate change. *Science* 292, 673–679. doi: 10.1126/science.292.5517.673

Gracianne, C. (2015). *De la Génétique des Populations à la Gestion Durable des Résistances: Intérêt de l'étude des Populations sauvages des Pathogènes des Cultures. Cas de deux Nématodes à Kyste et de leur hôte Sauvage Commun*. Thesis, Agrocampus-Ouest, Rennes.

Gracianne, C., Petit, E. J., Arnaud, J. F., Porte, C., Renault, L., Fouville, D., et al. (2014). Spatial distribution and basic ecology of *Heterodera schachtii* and *H. betae* wild populations developing on sea beet, *Beta vulgaris* ssp maritima. *Nematology* 16, 797–805. doi: 10.1163/15685411-00002809

Griffin, G. D. (1988). Factors affecting the biology and the pathogenicity of *Heterodera schachtii* on sugarbeet. *J. Nematol.* 20, 396–404.

Jones, F. G. W. (1975). Accumulated temperature and rainfall as measures of nematode development and activity. *Nematologica* 21, 62–70. doi: 10.1163/187529275X00356

Kaczmarek, A., MacKenzie, K., Kettle, H., and Blok, V. C. (2014). Influence of soil temperature on *Globodera rostochiensis* and *Globodera pallida*. *Phytopathol. Mediterr.* 53, 396–405.

Kakaire, S., Grove, I. G., and Haydock, P. P. J. (2012). Effect of temperature on the life cycle of *Heterodera schachtii* infecting oilseed rape (*Brassica napus* L.). *Nematology* 14, 855–867. doi: 10.1163/156854112X631935

Laine, A. L. (2008). Temperature-mediated patterns of local adaptation in a natural plant-pathogen metapopulation. *Ecol. Lett.* 11, 327–337. doi: 10.1111/j.1461-0248.2007.01146.x

Levins, R. (1968). *Evolution in Changing Environments*. New York, NY: Princeton University Press.

Leys, M., Petit, E. J., El-Bahloul, Y., Liso, C., Fournet, S., and Arnaud, J.-F. (2014). Spatial genetic structure in *Beta vulgaris* subsp. *maritima* and *Beta macrocarpa* reveals the effect of contrasting mating system, influence of marine currents, and footprints of postglacial recolonization routes. *Ecol. Evol.* 4, 1828–1852. doi: 10.1002/ece3.1061

Li, S., Jovelin, R., Yoshiga, T., Tanaka, R., and Cutter, A. D. (2014). Specialist versus generalist life histories and nucleotide diversity in *Caenorhabditis nematodes*. *Proc. R. Soc. B* 281, 2013–2858. doi: 10.1098/rspb.2013.2858

Mariette, N., Androdias, A., Mabon, R., Marquer, B., Corbière, R., Montarry, J., et al. (2016). Local adaptation to temperature within populations and clonal lineages of the Irish potato famine pathogen *Phytophthora infestans*. *Ecol. Evol.* 6, 6320–6331. doi: 10.1002/ece3.2282

Mboup, M., Bahri, B., Leconte, M., De Vallavieille-Pope, C., Kaltz, O., and Enjalbert, J. (2012). Genetic structure and local adaptation of European wheat yellow rust populations: the role of temperature-specific adaptation. *Evol. Appl.* 5, 341–352. doi: 10.1111/j.1752-4571.2011.00228.x

Montarry, J., Corbière, R., and Andrivon, D. (2007). Is there a trade-off between aggressiveness and over-winter survival in *Phytophthora infestans*? *Funct. Ecol.* 21, 603–610. doi: 10.1111/j.1365-2435.2007.01252.x

Montarry, J., Jan, P. L., Gracianne, C., Overall, A. D. J., Bardou-Valette, S., Olivier, E., et al. (2015). Heterozygote deficits in cyst plant-parasitic nematodes: possible causes and consequences. *Mol. Ecol.* 24, 1654–1667. doi: 10.1111/mec.13142

Müller, J. (1999). The economic importance of *Heterodera schachtii* in Europe. *Helminthologia* 36, 205–213.

Nei, M. (1978). Estimation of average heterozygosity and genetic distance from a small number of individuals. *Genetics* 89, 583–590.

Pasco, C., Montarry, J., Marquer, B., and Andrivon, D. (2016). And the nasty ones lose in the end: foliar pathogenicity trades off with asexual transmission in the Irish famine pathogen *Phytophthora infestans*. *New Phytol.* 209, 334–342. doi: 10.1111/nph.13581

Pearson, R. G., and Dawson, T. P. (2003). Predicting the impacts of climate change on the distribution of species: are bioclimate envelope models useful? *Glob. Ecol. Biogeogr.* 12, 361–371. doi: 10.1046/j.1466-822X.2003.00042.x

Perry, R. N., and Gaur, H. S. (1996). Host plant influences on the hatching of cyst nematodes. *Fundam. Appl. Nematol.* 19, 505–510. doi: 10.1186/s12861-016-0144-7

Pfender, W. F., and Vollmer, S. S. (1999). Freezing temperature effect on survival of *Puccinia graminis* subsp. *graminicola* in *Festuca arundinacea* and *Lolium perenne*. *Plant Dis.* 83, 1058–1062. doi: 10.1094/PDIS.1999.83.11.1058

R Development Core Team (2017). *R: A Language and Environment for Statistical Computing*. Vienna: R Foundation for Statistical Computing.

Rodríguez-Sanchez, F., Perez-Barrales, R., Ojeda, F., Vargas, P., and Arroyo, J. (2008). The Strait of Gibraltar as a melting pot for plant biodiversity. *Quatern. Sci. Rev.* 27, 2100–2117. doi: 10.1016/j.quascirev.2008.08.006

Roff, D. A. (1992). *The Evolution of Life Histories: Theory and Analysis*. London: Chapman & Hall.

Schulte, P. M., Healy, T. M., and Fangue, N. A. (2011). Thermal performance curves, phenotypic plasticity, and the time scales of temperature exposure. *Integr. Comp. Biol.* 51, 691–702. doi: 10.1093/icb/icr097

Scranton, K., and Amarasekare, P. (2017). Predicting phenological shifts in a changing climate. *Proc. Nat. Acad. Sci. U.S.A.* 114, 13212–13217. doi: 10.1073/pnas.1711221114

Sommerhalder, R. J., McDonald, B. A., Mascher, F., and Zhan, J. (2011). Effect of hosts on competition among clones and evidence of differential selection between pathogenic and saprophytic phases in experimental populations of the wheat pathogen *Phaeospaeria nodorum*. *BMC Evol. Biol.* 11:188. doi: 10.1186/1471-2148-11-188

Subbotin, S. A., Mundo-Ocampo, M., and Baldwin, J. G. (2010). *Systematics of Cyst Nematodes (Nematoda: Heteroderinae) – Nematology Monographs and Perspectives Volume 8B*. Leiden: Brill.

Suffert, F., Ravigné, V., and Sache, I. (2015). Seasonal changes drive short-term selection for fitness traits in the wheat pathogen *Zymoseptoria tritici*. *Appl. Environ. Microbiol.* 81, 6367–6379. doi: 10.1128/AEM.00529-15

Thomason, I. J., and Fife, D. (1962). The effect of temperature on development and survival of *Heterodera schachtii* Schm. *Nematologica* 7, 139–145. doi: 10.1163/187529262X00873

Trudgill, D. L., Honek, A., Li, D., and Van Straalen, N. M. (2005). Thermal time – concepts and utility. *Ann. Appl. Biol.* 146, 1–14. doi: 10.1111/j.1744-7348.2005.04088.x

Vandenbossche, B. A. B., Niere, B., and Vidal, S. (2015). Effect of temperature on the hatch of two German populations of the beet cyst nematodes, *Heterodera schachtii* and *Heterodera betae*. *J. Plant Dis. Protec.* 122, 250–254. doi: 10.1007/BF03356560

Wallace, H. R. (1955). Factors influencing the emergence of larvae from cysts of the beet eelworm, *Heterodera schachtii* Schmidt. *J. Helminthol.* 29, 3–16.

Wallace, H. R. (1968). The dynamics of nematode movement. *Annu. Rev. Phytopathol.* 6, 91–114. doi: 10.1146/annurev.py.06.090168.000515

Zhan, J., and McDonald, B. A. (2011). Thermal adaptation in the fungal pathogen *Mycosphaerella graminicola*. *Mol. Ecol.* 20, 1689–1701. doi: 10.1111/j.1365-294X.2011.05023.x

Conflict of Interest Statement: The authors declare that the research was conducted in the absence of any commercial or financial relationships that could be construed as a potential conflict of interest.

frontiers in Plant Science

ORIGINAL RESEARCH
published: 20 November 2018
doi: 10.3389/fpls.2018.01670

Role of Temperature and Coinfection in Mediating Pathogen Life-History Traits

Elise Vaumourin and Anna-Liisa Laine*

Research Centre for Ecological Change, University of Helsinki, Helsinki, Finland

Understanding processes maintaining variation in pathogen life-history traits is a key challenge in disease biology, and of importance for predicting when and where risks of disease emergence are highest. Pathogens are expected to encounter tremendous levels of variation in their environment – both abiotic and biotic – and this variation may promote maintenance of variation in pathogen populations through space and time. Here, we measure life-history traits of an obligate fungal pathogen at both asexual and sexual stages under both single infection and coinfection along a temperature gradient. We find that temperature had a significant effect on all measured life-history traits while coinfection only had a significant effect on the number of sexual resting structures produced. The effect of temperature on life-history traits was both direct as well as mediated through a genotype-by-temperature interaction. We conclude that pathogen life-history traits vary in their sensitivity to abiotic and biotic variation in the environment.

Keywords: abiotic interactions, biotic interactions, life-history evolution, overwintering success, pathogen evolution, *Plantago lanceolata*, *Podosphaera plantaginis*

OPEN ACCESS

Edited by:
Cindy E. Morris, Genetics and Improvement of Fruit and Vegetables (INRA), France

Reviewed by:
Remco Stam, Technische Universität München, Germany
Frédéric Suffert, Institut National de la Recherche Agronomique (INRA), France

****Correspondence:***
Elise Vaumourin
elise.vaumourin@helsinki.fi

Specialty section:
This article was submitted to Plant Microbe Interactions, a section of the journal Frontiers in Plant Science

Received: *15 June 2018*
Accepted: *26 October 2018*
Published: *20 November 2018*

Citation:
Vaumourin E and Laine A-L (2018) Role of Temperature and Coinfection in Mediating Pathogen Life-History Traits. Front. Plant Sci. 9:1670. doi: 10.3389/fpls.2018.01670

INTRODUCTION

Pathogens are a major threat to human health and food security (Strange and Scott, 2005; Jones et al., 2008). The success of pathogens may be attributed to their evolutionary potential which allows them to emerge, adapt, and persist in space and time within their host populations (Mundt, 2002; Friesen et al., 2006). Hence, understanding processes maintaining variation in pathogen life-history traits is a key question in evolutionary ecology and a major challenge for the design of disease control programs (Galvani, 2003; Grenfell et al., 2004). Environmental variation may be a powerful process maintaining variation in pathogen populations if infection outcomes depend on conditions directly or through genotype-by-environment interactions, and if variation is spatially and/or temporally structured (e.g., heterogeneous landscapes and seasonality). To understand the role of environmental variation in maintaining variation in pathogen populations, to date most studies have focused on the abiotic environment (e.g., climatic conditions, Harvell et al., 2002). Recently it has become evident that pathogens often occur simultaneously with other strains or species of pathogens colonizing the same host (Tollenaere et al., 2016). Thus, biotic variation in the co-occurring pathogen community may be an overlooked component of the processes maintaining variation in pathogen populations.

The abiotic environment has been shown to affect the evolutionary trajectories of pathogen life-histories (Blanford et al., 2003; Fels and Kaltz, 2006). Variation in temperature represents one of the most ubiquitous sources of environmental variation, and is known to greatly affect biochemical, physiological and behavioral processes of organisms. Pathogens with a free transmission stage are considered particularly vulnerable to variation in temperature (Truscott and Gilligan, 2003). In many pathosystems, temperature has been shown to affect pathogen ability to establish or maintain infection, its latency as well as its aggressiveness (e.g., Burdon, 1987; Thomas and Blanford, 2003; Fels and Kaltz, 2006). There is increasing evidence that the effect of temperature on pathogen fitness may be mediated through genotype-by-environment (G × E) interactions, suggesting that adaptation to biotic and abiotic habitats may be strongly linked (Ferguson and Read, 2002; Thomas and Blanford, 2003; Price et al., 2004; Mitchell et al., 2005; Fels and Kaltz, 2006). For example, it has been shown that the diversity *Arcobacter* populations is modulated by a temperature gradient (Fisher et al., 2014).

More recently, in addition to the surrounding abiotic environment, the biotic environment has been also highlighted to impact the maintenance of the variation in pathogen populations. For example, epidemic outcomes have been shown to change when multiple pathogens are present on a same host (Susi et al., 2015a). Strains under coinfection are generally expected to compete for the same limited resources provided by the host. If this process was acting alone, it could favor higher host exploitation rates (i.e., higher virulence) under coinfection than under single infection (Alizon, 2013). For many pathogens coinfection is also the pre-requisite for sexual reproduction, and thus changes in pathogen growth rates under coinfection may also represent facilitation to increase the probability of generating of new allelic combinations between the coinfecting strains (Otto, 2009; Carter et al., 2013). Thus, coinfection may largely contribute to maintain the genetic variation in pathogen life-history traits and can speed up the adaptation to environmental change (Becks and Agrawal, 2012).

Both abiotic and biotic environments may have strong impacts on infection outcomes, but little is known about their relative importance, and whether outcomes of coinfection are mediated by temperature (but see Marçais et al., 2017). In this study, we investigate how pathogen life-history traits that constitute both asexual and sexual stages are affected by the biotic environment (i.e., coinfection) and abiotic environment (i.e., temperature). Despite its ecological importance, the sexual stage is difficult to study for many pathosystems. Our study is focused on the interaction between *Podosphaera plantaginis* – *Plantago lanceolata* (powdery mildew – ribwort plantain). Given that this pathogen completes its entire life-cycle on the surface of the host plant, we are able to monitor the life-history traits visually in a non-destructive manner. Another advantage of this pathosystem is that *P. plantaginis* is a homothallic fungi (i.e., self-fertile, Tollenaere and Laine, 2013) so the production of the sexual structures (i.e., chasmothecia) can be achieved under both single strain infections as well as in coinfections. Thus, we can evaluate the impact of coinfection and temperature on this critical life-history trait affecting overwinter survival.

MATERIALS AND METHODS

The Pathosystem: *Podosphaera plantaginis – Plantago lanceolata*

We focused our study on the powdery mildew, *Podosphaera plantaginis* (*Erysiphales*, Ascomycota), which is an obligate fungal pathogen naturally infecting host plant *Plantago lanceolata*, the ribwort plantain. The epidemic cycle of the powdery mildew starts with the germination of a spore on a susceptible host resulting in lesion where clonal spores which are wind-dispersed are produced. To survive the winter, resting structures (chasmothecia) are produced. Each resting structure contains eight sexually generated ascospores, which initiate new infections in the spring upon their release. In *P. plantaginis* chasmothecia production can be achieved via haploid selfing of pure strains as well as outcrossing between two different strains infecting the same host plant (Tollenaere and Laine, 2013).

The dynamics of *P. plantaginis* in its fragmented host population network have been intensively studied in the Åland Islands (50 km × 70 km area) in southwest Finland since 2001 (Ojanen et al., 2013). The study system consists of approximately 4 000 host populations that are surveyed annually for the presence of *P. plantaginis*. The powdery mildew infection is visually conspicuous as whitish mycelia on the leaves. Previous studies have shown that prevalence of the pathogen is low in this system, with 2–17% of the host populations being infected each year in the metapopulation. *Podosphaera plantaginis* persists as highly dynamic metapopulation with frequent extinctions and (re)colonizations (Laine and Hanski, 2006; Jousimo et al., 2014). Genotyping has revealed considerable genetic diversity in this pathogen metapopulation, with most of the strains found in only one or few localities with a small subset of strains being common across multiple host populations (Tollenaere et al., 2012). The three strains chosen for our experiment – S1 (genotype i1), S2 (genotype 4000) and S3 (genotype 876-1) – are temporally and spatially widely distributed in the Åland metapopulation (**Supplementary Figure 1**).

Prior to the experiment, we carried out repeated cycles of inoculations to obtain adequate stocks of sporulating fungal material for the inoculation trials. The inoculations were done on petri dishes on detached host leaves of a *P. lanceolata* genotype (*490-15*) that has been characterized as broadly susceptible during previous experimental and maintenance work. For the experiment we used conidial chains from lesions that were 16–18 days old. To have sufficient leaf material for the experiment, we produced multiple clones by placing mother plants growing in pots with a perforated bottom in pots filled with vermiculite. After 9 weeks the mother plant was cut from the roots it had developed in the pot of vermiculite. Roots in the vermiculite yielded new rosettes, which were planted into pots with sand-rich humus. The plants were grown under glasshouse conditions, with 16 h of light and a temperature of +22°C.

Measuring Asexual and Sexual Pathogen Life-History Traits Under Single Versus Coinfection Along a Temperature Gradient

In order to investigate how pathogen life-history traits are impacted by the biotic environment (i.e., coinfection) and by the abiotic environment (i.e., temperature), we conducted an inoculation experiment where we recorded life-history traits of strains on their own (single infection) or with another strain (coinfection). We measured pathogen life-history traits under three different temperatures, +17°C, +20°C and +23°C. This range represent typical growing season temperatures that *P. plantaginis* experiences in the Åland archipelago (Laine, 2008). We measured two life-history traits that constitute the asexual stage (i.e., affecting pathogen growth): time from inoculation to germination and time from germination to sporulation. We also quantified three life-history traits of the sexual stage (i.e., affecting pathogen overwinter survival): time from sporulation to mature chasmothecia, total number of chasmothecia and proportion of viable chasmothecia. Given that this pathogen completes its entire life-cycle on the surface of the host plant, we were able to monitor life-history traits visually in a non-destructive manner. All inoculations were performed on the broadly susceptible host genotype (*490-15*).

To provide single vs. coinfection comparisons under different temperature conditions, each of the three strains was inoculated both individually as well as with another strain in a fully crossed design under the three different temperatures (+17°C, +20°C and +23°C). A cross-inoculation of a strain with itself is considered as a single infection and a cross-inoculation of a strain with another strain is considered as a coinfection. *Plantago lanceolata* leaves were placed on a moist filter paper in a Ø 9 cm Petri dish. Three conidial spore chains of both strains (i.e., six conidial chains at each inoculation site) were carefully placed on the same spot of a *P. lanceolata* leaf by single hair inoculation technique (Tollenaere and Laine, 2013). On each leaf we inoculated three distinct spots resulting in 54 sites of inoculation for each strain pairing per temperature. All inoculated leaves inside Petri dishes were kept at their respective temperatures with a 16L/8D photoperiod in growth chambers. We included non-inoculated leaves as negative controls. All *P. lanceolata* leaves used in the experiment were harvested from same-aged clones that were maintained in the greenhouse.

For each inoculated site, using a dissecting microscope, we measured daily the life-history traits related to the pathogen growth. Then, 14 days after the appearance of the first mature chasmothecia, the number of total chasmothecia produced were counted under a dissecting microscope and the viability of approximately 10 mature randomly collected chasmothecia were measured. To measure their viability, we have used the vital stain fluorescein diacetate (FDA) method (Firstencel et al., 1990; Ficke et al., 2002; Vági et al., 2016). This method consists of gently crushing chasmothecia on microscope slides in a droplet of a solution containing FDA (10 μg/mL). Slides were then scored for fluorescing ascospores under an epifluorescence microscope. FDA is lipophilic, membrane-permeable, non-fluorescent and it is hydrolyzed onto polar fluorescent molecules in the cytoplasm

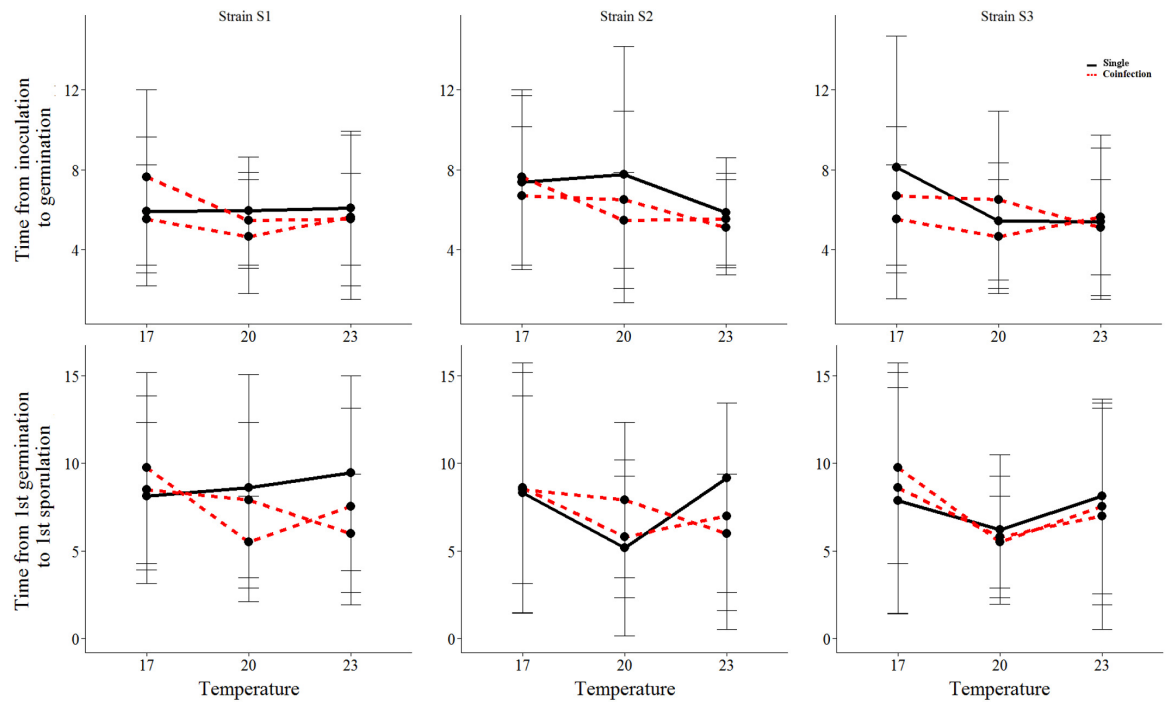

FIGURE 1 | The mean and standard deviation of each asexual life-history trait of the three *Podosphaera plantaginis* strains in single vs. coinfection along a temperature gradient. Single infections are depicted by black lines and coinfection by red lines. The time is indicated in days.

of living cells. These molecules remain in the cytoplasm of viable ascospores with intact cell membranes and exhibit intense green fluorescence when examined under blue light (465–495 nm) thereby signaling chasmothecia viability. A chasmothecium was scored as being viable if it contained any ascospores that exhibited intense green fluorescence.

Statistical Analyses

To understand how temperature and coinfection affected variation in the asexual life-history traits - time from inoculation to germination, time from germination to sporulation and time from sporulation to mature chasmothecia – we used survival models as implemented in R-package survival (Therneau, 2015) with Cox Proportional Hazards model (Cox, 1972). All survival models had temperature, first strain identity, coinfection and their respective interactions with the temperature as fixed explanatory effects. The identity of the second coinfecting strain and the leaf were considered as random factors.

To understand how temperature and coinfection affected variation in the sexual life-history traits – total number of chasmothecia and proportion of viable produced chasmothecia – we fitted generalized linear mixed models. For the model estimating total number of produced chasmothecia we defined a normal error structure and an identity link function, and for the model analyzing proportion of viable chasmothecia we defined a binomial error structure and a logit link function. Then for each model, the temperature, first strain identity, coinfection and their respective interactions with the temperature were fixed explanatory effects and the second coinfecting strain and leaf were considered as random factors.

RESULTS

We found that all measured life-history traits are significantly affected by temperature (**Figures 1**, **2** and **Table 1**). The average timing of each life-history event at each temperature and strain

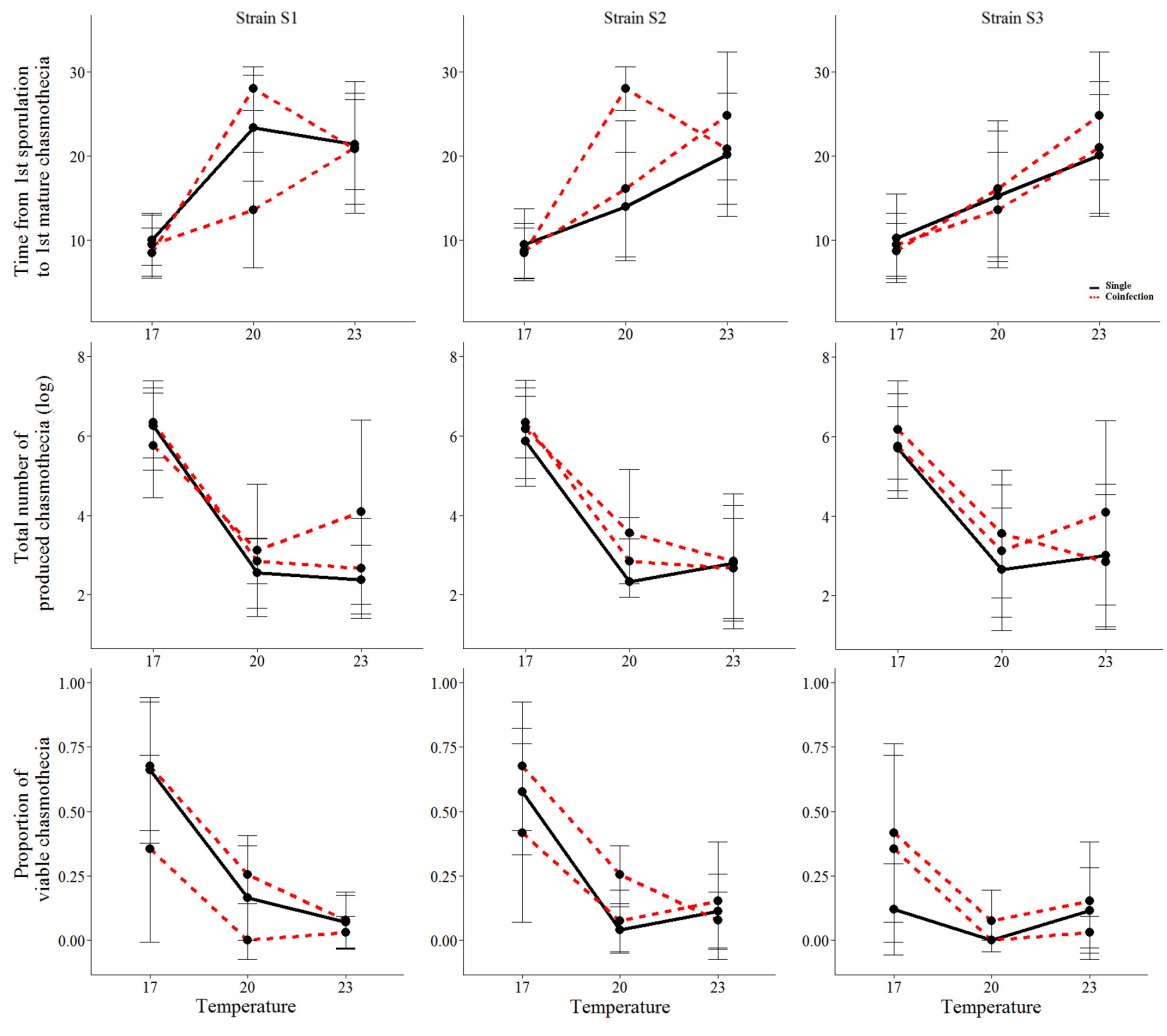

FIGURE 2 | The mean and standard deviation of the sexual life-history traits of the three *Podosphaera plantaginis* strains in single vs. coinfection along a temperature gradient. Single infections are depicted by black lines and coinfection by red lines. The time is indicated in days.

TABLE 1 | Results of the GLMMs analyzing infection development of *Podosphaera plantaginis* measured under single vs. coinfection under a temperature gradient.

Source	χ^2	*P*
Time from inoculation to germination		
First strain identity	1.20	0.548
Coinfection	2.99	0.084
Temperature	14.57	**$<10^{-2}$**
First strain identity × Temperature	7.59	0.108
Temperature × Coinfection	0.31	0.858
Time from first germination to first sporulation		
First strain identity	2.83	0.243
Coinfection	1.26	0.261
Temperature	13.31	**$<10^{-2}$**
First strain identity × Temperature	1.41	0.842
Temperature × Coinfection	4.08	0.130
Time from first sporulation to first mature chasmothecia		
First strain identity	8.51	**0.014**
Coinfection	0.51	0.475
Temperature	149.41	**$<10^{-2}$**
First strain identity × Temperature	17.70	**$<10^{-2}$**
Temperature × Coinfection	2.85	0.241
Total number of produced chasmothecia		
First strain identity	2.08	0.353
Coinfection	6.87	**$<10^{-2}$**
Temperature	386.85	**$<10^{-2}$**
First strain identity × Temperature	12.72	**0.013**
Temperature × Coinfection	1.70	0.428
Proportion of viable chasmothecia		
First strain identity	57.06	**$<10^{-2}$**
Coinfection	1.00	0.317
Temperature	135.64	**$<10^{-2}$**
First strain identity × Temperature	25.77	**$<10^{-2}$**
Temperature × Coinfection	0.39	0.822

Statistically significant results are shown in bold.

is summarized in **Table 2** and in **Supplementary Figure 2**. At the lowest temperature, +17°C, we find all sexual life-history traits to perform better than at higher temperatures (**Table 2**). For example, for strain S1 the time from first sporulation to first mature chasmothecia is 2.1 times faster at +17°C than at +23°C, 2.1 times faster for strain S2 and 2.0 times faster for the strain S3. The total number of produced chasmothecia is 73.3 times higher at +17°C than at +23°C for strain S1, 13.8 times higher for strain S2, and 10.0 times higher for strain S3. The proportion of viable chasmothecia is 9.4 times higher at +17°C than at 23°C for the strain S1, 5.3 times higher for the strain S2 and the same for the strain S3. For the asexual life-history traits studied – time from inoculation to germination and time form germination to sporulation – the effect of temperature tended to be the opposite. Strains were typically faster to germinate and launch spore production at +20°C and +23°C than at +17°C (**Table 2** and **Figure 1**).

Coinfection did not have a significant effect on the asexual life history traits measured. However, we found that under coinfection significantly more chasmothecia are produced (**Figure 2** and **Tables 1**, **3**). For the strain S1 2.0% chasmothecia are produced more under coinfection, 45.6% more for the strain S2 and 63.4% more for the strain S3. The proportion of viable chasmothecia was not significantly different between single infection and coinfection (**Figure 2** and **Table 1**). The interaction between temperature and coinfection was not significant for any of the measured life-history traits (**Table 1**).

We found significant variation among strains in the timing of chasmothecia production and their viability (**Figure 2** and **Table 1**). We also found that for all traits measured, no strain can outperform all others in all temperatures (**Figures 1**, **2**, **Table 2**, and **Supplementary Figure 2**). This trend was most pronounced when measuring the timing and total number of chasmothecia, as well as proportion of viable chasmothecia, as evidenced by the statistically significant strain identity × temperature interaction (**Figure 2** and **Table 1**).

DISCUSSION

Understanding processes maintaining variation in pathogen life-history traits is a long-standing challenge in disease ecology as this variation underlies risks of pathogen emergence and risks of infection (Galvani, 2003; Grenfell et al., 2004). Here, we have measured life-history traits at both asexual and sexual stages of an obligate fungal pathogen. We find that when we simultaneously investigate the effect of abiotic and biotic environmental variation, only temperature had a consistent and significant impact on all measured pathogen life-history. For several of the measured traits, the pathogen strains also differed significantly in how they responded to variation in temperature. Coinfection had a significant direct effect on the number of produced chasmothecia. Our finding suggests that abiotic variation may be more important in maintaining variation in pathogen populations than biotic variation.

In line with a previous study (Laine, 2007), our results demonstrate that the asexual life-history traits leading to infection are significantly affected by temperature. For the asexual life-history traits the optimal temperature depended on the life-history trait as well as strain identity. In general, although the specific effects of temperature vary among pathosystems, it has been shown that temperature may impact all key pathogen life-history traits including the ability to establish infection, subsequent development as well as transmission (Burdon, 1987; Thomas and Blanford, 2003; Fels and Kaltz, 2006). Here, we also find that temperature significantly affects traits linked with the sexual stage. Our inoculation study revealed that at +17°C, the number and viability of produced chasmothecia was the highest for all three strains. This effect of the temperature is in line with the biology of the powdery mildew, as the production of the sexually produced resting structures may be partly triggered by lower temperatures toward the end of the growing season (Tollenaere and Laine, 2013).

Genotype-by-environment interactions are considered an important mechanisms maintaining variation. In support of this, here we find that for nearly all measured life-history

TABLE 2 | The means and standard deviations of the measured life-history traits for each temperature and strain under single infection.

		+17°C			+20°C			+23°C		
		S1	**S2**	**S3**	**S1**	**S2**	**S3**	**S1**	**S2**	**S3**
Time from inoculation to germination	Mean	**5.90**	7.37	8.12	5.94	7.76	**5.42**	6.07	5.85	**5.39**
	SD	*3.71*	*4.34*	*6.55*	*2.70*	*6.41*	*2.93*	*3.87*	*2.76*	*3.69*
Time from 1st germination to 1st sporulation	Mean	8.14	8.33	**7.88**	8.59	**5.18**	6.23	9.45	9.15	**8.12**
	SD	*4.21*	*6.84*	*6.46*	*6.47*	*5.03*	*4.27*	*5.55*	*7.54*	*5.56*
Time from 1st sporulation to 1st mature chasmo	Mean	10.00	**9.47**	10.24	23.33	**14.00**	15.23	21.33	20.13	**20.07**
	SD	*2.98*	*4.24*	*5.26*	*6.28*	*6.44*	*7.76*	*5.33*	*7.29*	*7.25*
Total number of produced chasmo	Mean	**824.19**	546.43	503.12	16.78	**25.00**	18.62	11.25	39.67	**50.33**
	SD	*719.76*	*432.12*	*648.03*	*11.40*	*36.73*	*27.52*	*13.29*	*74.88*	*65.66*
Proportion of viable chasmo	Mean	**0.66**	0.58	0.12	**0.17**	0.04	0.00	0.07	0.11	**0.12**
	SD	*0.28*	*0.25*	*0.18*	*0.24*	*0.09*	*0.00*	*0.10*	*0.14*	*0.17*

The time is indicated in days. The best performing strain at each temperature is indicated in bold.

TABLE 3 | The means and standard deviations of the measured life-history for each temperature and strain under coinfection.

		+17°C			+20°C			+23°C		
		S1	**S2**	**S3**	**S1**	**S2**	**S3**	**S1**	**S2**	**S3**
Time from inoculation to germination	Mean	6.37	7.06	**6.13**	**4.98**	6.07	5.53	5.59	**5.30**	5.36
	SD	*3.58*	*3.84*	*3.14*	*2.68*	*3.68*	*3.74*	*3.33*	*2.32*	*3.29*
Time from 1st germination to 1st sporulation	Mean	9.25	**8.56**	9.16	6.46	6.69	**5.65**	6.81	**6.55**	7.26
	SD	*5.38*	*6.43*	*6.33*	*3.59*	*3.98*	*3.02*	*4.70*	*5.26*	*6.01*
Time from 1st sporulation to 1st mature chasmo	Mean	9.08	**8.62**	9.07	20.00	19.50	**15.27**	**20.92**	23.00	23.34
	SD	*3.45*	*3.12*	*3.51*	*8.88*	*8.65*	*7.40*	*6.91*	*7.25*	*7.68*
Total number of produced chasmo	Mean	765.22	**804.16**	794.07	17.56	**49.86**	46.67	86.42	35.67	**93.79**
	SD	*1211.90*	*784.58*	*1221.78*	*23.27*	*57.86*	*59.14*	*192.60*	*59.00*	*186.34*
Proportion of viable chasmo	Mean	0.48	**0.52**	0.39	**0.17**	0.13	0.06	0.06	**0.12**	0.11
	SD	*0.36*	*0.33*	*0.35*	*0.15*	*0.14*	*0.11*	*0.09*	*0.18*	*0.19*

The time is indicated in days. The best performing strain at each temperature is indicated in bold.

traits, the strains switch ranks along the temperature gradient. Hence, no strain outperforms all others across all temperatures. This trend was statistically significant when measuring all traits linked with sexual reproduction: the timing and number of produced chasmothecia, as well as their viability. These represent core fitness traits in *P. plantaginis*, as chasmothecia production is strongly linked with the ability to survive over winter (Tack and Laine, 2014). Although the experiment only included three strains of *P. plantaginis*, it is in line with previous work demonstrating significant temperature and genotype x temperature effects on asexual life-history traits using a diverse range of *P. plantaginis* strains (Laine, 2004, 2008). An interesting avenue of future work would be to test whether the results we find here – both direct and strain mediated sensitivity to temperature– also holds for a larger number of strains and under more extreme temperature variation.

For pathogens the biotic environment may vary depending on the community of coinfecting pathogens sharing the same host. Coinfection is a common phenomenon across plant pathosystems (Tollenaere et al., 2016). In the *P. plantaginis* metapopulation, approximately half of the local pathogen populations support coinfection (Susi et al., 2015a). Theoretically coinfection has been proposed to change pathogen growth rates as strains compete for the same limited resources of the host, and there is some empirical support for this (Clement et al., 2012; Tollenaere et al., 2016; Suffert et al., 2018). Although previous studies on *P. plantaginis* have revealed coinfection to change both within- and between host dynamics (Susi et al., 2015a,b), here coinfection only had a significant effect on the number of chasmothecia produced. Higher production of resting spores under coinfection is expected to have profound fitness consequences as local pathogen populations go through a severe decline each winter (Tack and Laine, 2014), often resulting in local extinction (Jousimo et al., 2014). As coinfection varies spatially (Susi et al., 2015a), it can be a powerful mechanism maintaining diversity in this natural pathosystem.

Interestingly, we also did not detect a significant coinfection-by-temperature interaction for any of the measured life-history traits. It is likely that the effect of temperature in our experiment was so strong, that most of variation in these data is explained

by the temperature gradient. However, it should also be noted that previous studies have shown strains to vary in how they respond to coinfection (Laine and Mäkinen, 2018). Hence, it is possible that the strains included in this study do not represent those that respond strongly to coinfection. Moreover, the effects of coinfection – either direct or mediated through an interaction with temperature – may not become apparent in the development of a single lesion but accumulate during the epidemic season (Susi et al., 2015a,b). Hence, a future study using more strains and allowing for several cycles of auto- and allo-infection would help elucidate whether coinfection changes infections outcomes also under pronounced abiotic variation.

CONCLUSION

Here, we find both abiotic and biotic environments to impact pathogen life-history traits directly as well as through genotype specific responses. Moreover, we find that the effect of abiotic and biotic variation depends on pathogen life-history traits. Temperature variation affected all studied pathogen life-history traits and hence, we may expect it to be a powerful mechanism maintaining diversity during the epidemic season. We found coinfection to significantly affect the number of produced chasmothecia which is expected to have far-reaching consequences for pathogen survival from one epidemic season to the next (Tack and Laine, 2014). For an epiphytic pathogen such as *P. plantaginis*, it is not surprising to find high sensitivity to ambient temperature. Temperature fluctuations may be gradual (e.g., global warming), seasonal (e.g., summer vs. winter resource availability), or continuously fluctuating (e.g., daily temperatures). Our results suggest that *P. plantaginis* can cope with such variation in the environment, as we documented plastic responses in many life-history traits under temperature variation. We conclude that environmental variation is expected to be an important mechanism maintaining variation in pathogen populations, given that many studies have reported life-history trait plasticity in response to temperature variation (Blanford et al., 2003; Wolinska and King, 2009).

DATA AVAILABILITY STATEMENT

All data associated with this study is available on the Dryad Digital Repository: doi: 10.5061/dryad.fg25kk0.

AUTHOR CONTRIBUTIONS

EV and A-LL conceived and designed the experiments, analyzed the data, and wrote the paper. EV performed the experiments.

FUNDING

This work was funded by grants from the Academy of Finland (296686), and the European Research Council (Consolidator Grant RESISTANCE 724508) to A-LL.

ACKNOWLEDGMENTS

Krista Raveala is acknowledged for assistance in the greenhouse and laboratory.

SUPPLEMENTARY MATERIAL

The Supplementary Material for this article can be found online at: https://www.frontiersin.org/articles/10.3389/fpls.2018.01670/full#supplementary-material

REFERENCES

Alizon, S. (2013). Co-infection and super-infection models in evolutionary epidemiology. *Interface Focus* 3:20130031. doi: 10.1098/rsfs.2013.0031

Becks, L., and Agrawal, A. F. (2012). The evolution of sex is favoured during adaptation to new environments. *PLoS Biol.* 10:e1001317. doi: 10.1371/journal.pbio.1001317

Blanford, S., Thomas, M. B., Pugh, C., and Pell, J. K. (2003). Temperature checks the Red Queen? Resistance and virulence in a fluctuating environment. *Ecol. Lett.* 6, 2–5. doi: 10.1046/j.1461-0248.2003.00387.x

Burdon, J. J. (1987). *Diseases and Plant Population Biology*. Cambridge: CUP Archive.

Carter, L. M., Kafsack, B. F., Llinás, M., Mideo, N., Pollitt, L. C., and Reece, S. E. (2013). Stress and sex in malaria parasites. Why does commitment vary?. *Evol. Med. Public Health* 2013, 135–147. doi: 10.1093/emph/eot011

Clement, J. A., Magalon, H., Glais, I., Jacquot, E., and Andrivon, D. (2012). To be or not to be solitary: *Phytophthora infestans*' dilemma for optimizing its reproductive fitness in multiple infections. *PLoS One* 7:e37838. doi: 10.1371/journal.pone.0037838

Cox, D. R. (1972). Regression Models and Life-Tables. *J. R. Stat. Soc.Series B Stat. Methodol.* 34, 187–220.

Fels, D., and Kaltz, O. (2006). Temperature-dependent transmission and latency of holospora undulata, a micronucleus-specific parasite of the ciliate *Paramecium caudatum*. *Proc. Biol. Sci.* 273, 1031–1038. doi: 10.1098/rspb.2005.3404

Ferguson, H., and Read, A. (2002). Genetic and environmental determinants of malaria parasite virulence in mosquitoes. *Proc. Biol. Sci.* 269, 1217–1224. doi: 10.1098/rspb.2002.2023

Ficke, A., Gadoury, D., and Seem, R. (2002). Ontogenic resistance and plant disease management: a case study of grape powdery mildew. *Phytopathology* 92, 671–675. doi: 10.1094/PHYTO.2002.92.6.671

Firstencel, H., Butt, T. M., and Carruthers, R. I. (1990). A fluorescence microscopy method for determining the viability of entomophthoralean fungal spores. *J. Invertebr. Pathol.* 55, 258–264. doi: 10.1016/0022-2011(90)90061-A

Fisher, J. C., Levican, A., Figueras, M. J., and Mclellan, S. L. (2014). Population dynamics and ecology of arcobacter in sewage. *Front. Microbiol.* 5:525. doi: 10.3389/fmicb.2014.00525

Friesen, T. L., Stukenbrock, E. H., Liu, Z., Meinhardt, S., Ling, H., Faris, J. D., et al. (2006). Emergence of a new disease as a result of interspecific virulence gene transfer. *Nat. Genet.* 38, 953–956. doi: 10.1038/ng1839

Galvani, A. P. (2003). Epidemiology meets evolutionary ecology. *Trends Ecol. Evol.* 18, 132–139. doi: 10.1645/13-414.1

Grenfell, B. T., Pybus, O. G., Gog, J. R., Wood, J. L., Daly, J. M., Mumford, J. A., et al. (2004). Unifying the epidemiological and evolutionary dynamics of pathogens. *Science* 303, 327–332. doi: 10.1126/science.1090727

Harvell, C. D., Mitchell, C. E., Ward, J. R., Altizer, S., Dobson, A. P., Ostfeld, R. S., et al. (2002). Climate warming and disease risks for terrestrial and marine biota. *Science* 296, 2158–2162. doi: 10.1126/science.1063699

Jones, K. E., Patel, N. G., Levy, M. A., Storeygard, A., Balk, D., Gittleman, J. L., et al. (2008). Global trends in emerging infectious diseases. *Nature* 451, 990–993. doi: 10.1038/nature06536

Jousimo, J., Tack, A. J., Ovaskainen, O., Mononen, T., Susi, H., Tollenaere, C., et al. (2014). Ecological and evolutionary effects of fragmentation on infectious disease dynamics. *Science* 344, 1289–1293. doi: 10.1126/science.1253621

Laine, A.-L. (2004). A powdery mildew infection on a shared host plant affects the dynamics of the *Glanville fritillary* butterfly populations. *Oikos* 107, 329–337. doi: 10.1111/j.0030-1299.2004.12990.x

Laine, A. L. (2007). Pathogen fitness components and genotypes differ in their sensitivity to nutrient and temperature variation in a wild plant–pathogen association. *J. Evol. Biol.* 20, 2371–2378. doi: 10.1111/j.1420-9101.2007.01406.x

Laine, A. L. (2008). Temperature-mediated patterns of local adaptation in a natural plant–pathogen metapopulation. *Ecol. Lett.* 11, 327–337. doi: 10.1111/j.1461-0248.2007.01146.x

Laine, A.-L., and Hanski, I. (2006). Large-scale spatial dynamics of a specialist plant pathogen in a fragmented landscape. *J. Ecol.* 94, 217–226. doi: 10.1111/evo.12239

Laine, A. L., and Mäkinen, H. (2018). Life-history correlations change under coinfection leading to higher pathogen load. *Evol. Lett.* 2, 126–133. doi: 10.1002/evl3.48

Marçais, B., Piou, D., Dezette, D., and Desprez-Loustau, M.-L. (2017). Can oak powdery mildew severity be explained by indirect effects of climate on the composition of the erysiphe pathogenic complex? *Phytopathology* 107, 570–579. doi: 10.1094/PHYTO-07-16-0268-R

Mitchell, S. E., Rogers, E. S., Little, T. J., and Read, A. F. (2005). Host-parasite and genotype-by-environment interactions: temperature modifies potential for selection by a sterilizing pathogen. *Evolution* 59, 70–80. doi: 10.1111/j.0014-3820.2005.tb00895.x

Mundt, C. (2002). Use of multiline cultivars and cultivar mixtures for disease management. *Annu. Rev. Phytopathol.* 40, 381–410. doi: 10.1146/annurev.phyto.40.011402.113723

Ojanen, S. P., Nieminen, M., Meyke, E., Pöyry, J., and Hanski, I. (2013). Long-term metapopulation study of the *Glanville fritillary* butterfly (*Melitaea cinxia*): survey methods, data management, and long-term population trends. *Ecol. Evol.* 3, 3713–3737. doi: 10.1002/ece3.733

Otto, S. P. (2009). The evolutionary enigma of sex. *Am. Nat.* 174, S1–S14. doi: 10.1086/599084

Price, J. S., Bever, J. D., and Clay, K. (2004). Genotype, environment, and genotype by environment interactions determine quantitative resistance to leaf rust (*Coleosporium asterum*) in *Euthamia graminifolia* (Asteraceae). *New Phytol.* 162, 729–743. doi: 10.1111/j.1469-8137.2004.01082.x

Strange, R. N., and Scott, P. R. (2005). Plant disease: a threat to global food security. *Annu. Rev. Phytopathol.* 43, 83–116. doi: 10.1146/annurev.phyto.43.113004.133839

Suffert, F., Delestre, G., and Gélisse, S. (2018). Sexual reproduction in the fungal foliar pathogen *Zymoseptoria tritici* is driven by antagonistic density dependence mechanisms. *Microb. Ecol.* doi: 10.1007/s00248-018-1211-3 [Epub ahead of print].

Susi, H., Barrès, B., Vale, P. F., and Laine, A.-L. (2015a). Co-infection alters population dynamics of infectious disease. *Nat. Commun.* 6:5975. doi: 10.1038/ncomms6975

Susi, H., Vale, P. F., and Laine, A.-L. (2015b). Host genotype and coinfection modify the relationship of within and between host transmission. *Am. Nat.* 186, 252–263. doi: 10.1086/682069

Tack, A. J., and Laine, A. L. (2014). Ecological and evolutionary implications of spatial heterogeneity during the off-season for a wild plant pathogen. *New Phytolo.* 202, 297–308. doi: 10.1111/nph.12646

Therneau, T. (2015). *A Package for Survival Analysis in S. version 2.38*. Available at: http://CRAN.R-project.org/package=survival

Thomas, M. B., and Blanford, S. (2003). Thermal biology in insect-parasite interactions. *Trends Ecol. Evol.* 18, 344–350. doi: 10.1016/S0169-5347(03)00069-7

Tollenaere, C., and Laine, A. L. (2013). Investigating the production of sexual resting structures in a plant pathogen reveals unexpected self-fertility and genotype-by-environment effects. *J. Evol. Biol.* 26, 1716–1726. doi: 10.1111/jeb.12169

Tollenaere, C., Susi, H., and Laine, A.-L. (2016). Evolutionary and epidemiological implications of multiple infection in plants. *Trends Plant Sci.* 21, 80–90. doi: 10.1016/j.tplants.2015.10.014

Tollenaere, C., Susi, H., Nokso-Koivisto, J., Koskinen, P., Tack, A., Auvinen, P., et al. (2012). SNP design from 454 sequencing of podosphaera *Plantaginis* transcriptome reveals a genetically diverse pathogen metapopulation with high levels of mixed-genotype infection. *PLoS One* 7:e52492. doi: 10.1371/journal.pone.0052492

Truscott, J., and Gilligan, C. (2003). Response of a deterministic epidemiological system to a stochastically varying environment. *Proc. Natl. Acad. Sci. U.S.A.* 100, 9067–9072. doi: 10.1073/pnas.1436273100

Vági, P., Caffi, T., Váczy, K. Z., Németh, M. Z., and Kiss, L. (2016). Refining a method for ascospore viability testing in overwintering chasmothecia of *Erysiphe necator*. *Eur. J. Plant Pathol.* 144, 799–802. doi: 10.1007/s10658-015-0797-2

Wolinska, J., and King, K. C. (2009). Environment can alter selection in host–parasite interactions. *Trends Parasitol.* 25, 236–244. doi: 10.1016/j.pt.2009.02.004

Conflict of Interest Statement: The authors declare that the research was conducted in the absence of any commercial or financial relationships that could be construed as a potential conflict of interest.

frontiers in Plant Science

ORIGINAL RESEARCH
published: 05 December 2018
doi: 10.3389/fpls.2018.01820

Striking Similarities Between *Botrytis cinerea* From Non-agricultural and From Agricultural Habitats

Marc Bardin, Christel Leyronas, Claire Troulet and Cindy E. Morris*

Pathologie Végétale, INRA, Montfavet, France

Investigations into life history of microorganisms that cause plant diseases have been limited mostly to contexts where they are in interaction with plants, and with cropped or otherwise managed vegetation. Therefore, knowledge about the diversity of plant pathogens, about potential reservoirs of inoculum and about the processes that contribute to their survival and adaptation is limited to these contexts. The agro-centric perspective of plant pathogen life histories is incoherent with respect to the capacity of many of them to persist as saprophytes on various substrates. In this context we have investigated the ubiquity of the broad host range necrotrophic fungus *Botrytis cinerea*, outside of agricultural settings and have determined if the populations in these natural habitats can be distinguished phenotypically and phylogenetically from populations isolated from diseased crops. Over a period of 5 years, we isolated *B. cinerea* from 235 samples of various substrates collected in France including rainfall, snowpack, river, and lake water, epilithic biofilms in mountain streams, leaf litter and plant debris, rock surfaces, bird feathers and healthy wild plants from outside of agricultural fields. All substrates except rock surfaces harbored *B. cinerea* leading us to establish a collection of purified strains that were compared to *B. cinerea* from diseased tomato, grapes and various other crops in France. Phylogenetic comparisons of 321 strains from crop plants and 100 strains from environmental substrates based on sequences of 9 microsatellite markers revealed that strains from crops and the environment could not be distinguished. Furthermore, the genetic diversity of strains outside of agriculture was just as broad as within agriculture. In tests to determine the aggressiveness of strains on tomato stems, the mean disease severity caused by strains from environmental substrates was statistically identical to the severity of disease caused by strains from tomato, but was significantly greater than the severity caused by strains from grape or other crops. Our results suggest that highly diverse populations of this plant pathogen persist outside of agriculture in association with substrates other than plants and that this part of their life history is compatible with its capacity to maintain its potential as plant pathogen.

Keywords: microbial ecology, epidemiology, gray mold, polyphagous, diversity, aggressiveness, fitness, selection

OPEN ACCESS

Edited by:
Jeremy Astier,
INRA UMR1347 Agroécologie, France

Reviewed by:
Renaud Travadon,
University of California, Davis,
United States
Michelina Ruocco,
Istituto per la Protezione Sostenibile
delle Piante (IPSP), Italy

****Correspondence:***
Marc Bardin
marc.bardin@inra.fr

Specialty section:
This article was submitted to Plant Microbe Interactions, a section of the journal Frontiers in Plant Science

Received: *28 August 2018*
Accepted: *22 November 2018*
Published: *05 December 2018*

Citation:
Bardin M, Leyronas C, Troulet C and Morris CE (2018) Striking Similarities Between Botrytis cinerea From Non-agricultural and From Agricultural Habitats. Front. Plant Sci. 9:1820. doi: 10.3389/fpls.2018.01820

INTRODUCTION

Investigations into the life history of microorganisms that can cause disease to plants have been limited mostly to contexts where they are in interaction with plants, and even more frequently with cropped or otherwise managed vegetation (Morris et al., 2009). Therefore, knowledge about the diversity of plant pathogens, about potential reservoirs of inoculum and about the processes that contribute to survival and adaptation of plant pathogens is limited to these contexts. By contrast, there are many examples of human pathogens for which habitats and biological activities are known outside the strictly medical context (Morris et al., 2009). The agro-centric perspective of plant pathogen life histories is incoherent with respect to the capacity of many plant pathogens to persist as saprophytes on various substrates. Thus, various plant pathogens, including bacteria, fungi and viruses have been detected in non-agricultural habitats or in the absence of host plants (Morris et al., 2009). For instance, recently the fungal species *Fusarium oxysporum*, a major fungal plant pathogen, has been isolated in tap water (Edel-Hermann et al., 2016). However, apart from the bacterial species *Pseudomonas syringae* (Morris et al., 2013), and the oomycete genera *Phytophthora* (Hansen et al., 2012), the ecology and evolutionary history of plant pathogens at spatiotemporal scales wider than their strict interaction with plants (either cultivated or wild) has not been extensively studied.

The aerially disseminated fungus *Botrytis cinerea* is considered to be a broad-host range necrotrophic pathogen able to attack about 586 plant genera, mostly dicots (Elad et al., 2016). It is also capable of growing as a saprophyte on dead and decaying plant matter (Williamson et al., 2007) and it probably has an underestimated facultative endophytic behavior, i.e., it survives in host plant tissue without generating disease symptoms (Van Kan et al., 2014). Additionally this fungus has been detected in non-agricultural contexts such as outdoor or indoor air in agricultural or urban settings (Bartlett et al., 2004; Lugauskas and Krikstaponis, 2004; Leyronas and Nicot, 2013), in clouds (Amato et al., 2007), in precipitation (Monteil et al., 2014), in agricultural or non-agricultural soils (Azmi and Seppelt, 1998; Leyronas et al., 2015c), on rocks and monuments (Gaylarde and Morton, 1999), in stocks of hydrocarbons (Gaylarde et al., 1999), on external or in internal parts of insects (Fermaud and Lemenn, 1989; Louis et al., 1996), on pelage of small mammals (Shchipanov et al., 2006) and human hairs (Ali-Shtayeh et al., 2001). However, to our knowledge, the genetic diversity and the pathogenic potential of saprophytic *B. cinerea* strains isolated from non-agricultural habitats have never been studied.

Recent research is revealing that natural environments harbor strains of microorganisms that have likely given rise to strains that have emerged in plant disease epidemics (Hansen et al., 2012; Monteil et al., 2016). In this context, we have assessed the ubiquity of the fungus *B. cinerea* outside of agricultural settings and have determined if the populations in these natural habitats can be distinguished phenotypically and phylogenetically from populations isolated from diseased crops. The objectives of the present study were (i) to determine the presence and the abundance of *B. cinerea* in various non-agricultural habitats, (ii) to evaluate the genetic diversity and the phenotypic diversity of the strains collected, and (iii) to compare this diversity with strains collected from crops.

MATERIALS AND METHODS

Isolation of *B. cinerea* From Non-agricultural Habitats

Over a period of 5 years (2005–2010), we collected 235 samples of various substrates, including rainfall, snowpack, fresh water from rivers and lakes, epilithic biofilms in mountain streams, rocks, leaf litter and plant debris, healthy wild plants from outside of agricultural fields and feathers from the great tit (*Parus major*) (**Table 1**). Most of samples originated from the Provence-Alpes-Côte d'Azur region in France. Some of the strains obtained from rainfall and snowfall were part of a previous study (Monteil et al., 2014).

Each sample was plated on Petri plates containing the semi-selective *Botrytis* Spore Trap Medium (BSTM) (Edwards and Seddon, 2001). The Petri plates were sealed with parafilm and incubated at 20°C in daylight for 14 days to allow the development of fungal colonies. The colonies with mycelium resembling that of *B. cinerea* were individually sub-cultured on Potato Dextrose Agar (PDA) and their identity was confirmed 7 days after transplanting by observing characteristic asexual sporulation of *B. cinerea* (Barnett, 1998). Dry sterile cotton swabs were rubbed on sporulating plates to collect *B. cinerea* spores. The swabs were stored at −20°C until isolate purification.

All isolates were purified and single-spored in a classical way (Leyronas et al., 2012) prior to their genotypic and phenotypic characterization. Hereafter these characterized single spore isolates will be referred to as "environmental strains."

Strain Genotyping

A subset of 109 strains collected from non-agricultural habitats were genotyped (**Table 1**). They were compared to 327 agricultural strains sampled from lettuce and tomato plants grown in several greenhouses in the South of France (Leyronas et al., 2015a,b,c).

Genomic DNA was extracted from aliquots of 15 mg lyophilized fungal material (harvested from two-week old cultures on Potato Dextrose Agar), following the DNeasy Plant extraction Kit protocole (Qiagen). The nine microsatellite markers designed for *B. cinerea* by Fournier et al. (2002) were amplified following the protocol described by Leyronas et al. (2015b). To determine the size of the microsatellites, the PCR products were scanned with the help of an ABI 3730 sequencer (Applied Biosystems). GeneMapper software version 4.1 (Applied Biosystems) was then used for the microsatellite size analysis. Complete microsatellite size profiles (referred to as "haplotypes" hereafter) were obtained for 109 environmental strains and 327 agricultural strains.

Genetic Characteristics of Strains

In a first step, the strains with the private allele at microsatellite locus BC6 associated with the cryptic species *B. pseudocinerea*

TABLE 1 | Quantification of the number of *Botrytis cinerea* strains collected in non-agricultural habitats (environmental strains) and number of strains tested for different traits.

Origin of samples	Number of samples collected	Number of samples containing *B. cinerea*	Number of *B. cinerea* strains detected on medium	Number of genotyped strains	Number of strains tested for their aggressiveness on tomato	Number of strains tested for other phenotypic traits
Precipitation	35	18	84	69	84	11
Snowpack	35	7	13	10	13	5
Fresh water	56	14	18	12	11	3
Epilithic biofilm	18	3	3	2	0	0
Litter	33	4	4	3	1	1
Rock surfaces	6	0	0	0	0	0
Plant debris	9	1	1	1	1	1
Asymptomatic wild plants	37	6	10	7	10	2
Bird feather	6	3	8	5	8	1
Total	235	56	141	109	128	24

(Walker et al., 2011) were removed from further analyses. This private allele is found only in *B. pseudocinerea* strains and never in *B. cinerea* strains. Then, in order to compare the *B. cinerea* strains sampled from the different reservoirs, several indices of genetic diversity were used. The software FSTAT version 2.9.3 (Goudet, 1995) was used to compute allelic richness (corrected for the smallest sample size) and unbiased gene diversity per locus. Unbiased gene diversity (Hnb) and allelic richness (average over the nine loci) were computed separately for the strains collected in the different reservoirs with the Genetix software (Belkhir et al., 1996–2004). The number of different multilocus haplotypes (MLH) was computed with GenClone 1.0 software (Arnaud-Haond and Belkhir, 2007). We used the index of haplotypic diversity (based on the number of individuals and the number of distinct MLH), which estimates the proportion of haplotypes present in a population and takes a value of 1 when a population is composed exclusively of unique haplotypes (Arnaud-Haond et al., 2007).

Phylogenetic Relationships Between Strains From Non-agricultural Habitats and From Crops

To assess the relationships between the different strains, we computed a neighbor-joining (NJ) tree with the program POPULATIONS (version 1.2.32 provided by Olivier Langella, Quantitative Genetics and Evolution, Gif-sur-Yvette, France). The NJ-tree was based on the distances of Cavalli-Sforza and Edwards (1967), computed from our microsatellite loci. The tree was visualized and edited with TREEVIEW (Page, 1996). All analyses were conducted on data sets excluding clone replicates.

In addition, Arlequin version 3.5 (Excoffier et al., 2005) was used to assess genetic differentiation between strains collected from non-agricultural habitats (NH) and from crops by computing RST values as suggested by Slatkin (1995) for microsatellite data. The clonally corrected data set was used.

Aggressiveness of Strains on Tomato Plants

The aggressiveness of a subset of 128 environmental strains (**Table 1**) was assessed on 8-week old tomato plants cv. Monalbo (INRA). Tomato plants were grown in a greenhouse and watered daily with a nutrient solution as described previously (Decognet et al., 2009). Each strain was inoculated on three plants. On each plant, three leaves were removed, leaving 1 cm petiole stubs on the stems and the wounds were inoculated with 10 μL aliquots of spore suspension. The spore suspensions were prepared from two-week old cultures on PDA and were adjusted to 10^6 spores mL^{-1}. All plants were incubated in a growth chamber with a photoperiod of 14 h, with a light intensity of 162 μmol m^{-2} s^{-1}, maintained at 21°C with a relative humidity above 90%. The length of resulting stem lesions was monitored daily from the 3rd to the 7th day after inoculation and these data were used to compute the area under the disease progress curves (AUDPC). Due to a limited place in the growth chamber, strains were tested in series of 10–15 strains, and in each series, strain BC1 was used as a reference to calculate an index of aggressiveness (IA) for each strain, relative to that of this strain (Decognet et al., 2009), as follows:

$$IA = 100^* (AUDPC_{strain}/AUDPC_{BC1})$$

with $AUDPC_{strain}$ being the value of AUDPC computed for the tested strain and $AUDPC_{BC1}$ the value of AUDPC obtained for the reference strain BC1. Two to three independent repetitions of the test were realized for each strain.

The aggressiveness of environmental strains was compared to that of 156 single-spored agricultural strains having a wide diversity regarding year, region of isolation and host plants. All these strains were collected from 1988 to 2008 with a majority collected after 2000 (108 strains). Regarding their geographical origin, 149 strains were sampled from France, of which 122 were from the southern part of the country. In addition, four strains came from Italy, two from Syria and one from Portugal. They were collected from various diseased plants: 101 from tomato, 33 from grape, and 22 from other plants including rose, cucumber,

strawberry, artichoke, pepper, carrot, onion, asparagus, peach fruit, cherry fruit, kiwifruit, hydrangea, gerbera, cyclamen, and poinsettia.

Traits of *B. cinerea in vitro*

Mycelial growth, sporulation and sclerotia production were evaluated for a sub-sample of 31 agricultural strains and 24 environmental strains of *B. cinerea* (**Table 1**), which represent the full range of aggressiveness of the tested strains. Mycelial growth was evaluated by inoculating PDA with a 5 mm-diameter mycelial plug of each *B. cinerea* strain and incubating in a growth chamber (21°C, photoperiod 14 h, 114 μmol m^{-2} s^{-1}). Two perpendicular measurements of the diameter of the mycelial colony were performed every day for 3 days and the rate of mycelial growth between the first and the third day of incubation was calculated for each strain. Three plates were inoculated for each strain and the whole experiment was repeated two times. The spore production was determined 14 days after inoculation on PDA medium (21°C, photoperiod 14 h, 114 μmol m^{-2} s^{-1}). Spores were scrapped from the media, suspended in water and spore concentration was determined using a hemacytometer. The number of sclerotia produced by each strain of *B. cinerea* on PDA was recorded after five weeks of incubation at 21°C (1 week with a photoperiod of 14 h at 114 μmol m^{-2} s^{-1} and 4 weeks in the dark) and 5 weeks of incubation at 4°C in the dark. For the sporulation and sclerotia production experiments, three replicates were realized for each strain.

Statistical Analyses

Statistical analyses were performed with Statistica (version 12, Statsoft). Non-parametric tests (Mann and Whitney) were used to determine significant differences between gene diversity and allelic richness of environmental and agricultural strains. To compare the different phenotypic traits evaluated, analysis of variance (ANOVA) were performed. In the case of a significant effect of the tested factor, a comparison of mean was realized using the Newman–Keuls test. The relationship between the various phenotypic traits tested (mycelial growth, sporulation, sclerotia production) and aggressiveness was realized using linear regressions. Statistical inferences were made at the 5% level of significance, unless indicated otherwise.

RESULTS

B. cinerea Is Ubiquitous in Non-agricultural Habitats

Botrytis cinerea was recovered in 56 samples out of the 235 samples collected (**Table 1**). From these 56 samples, we were able to purify 141 strains of *B. cinerea*. All substrates except rock surfaces harbored *B. cinerea*. The fungus was detected at a rate of 51% in precipitation, 50% from feathers of Great Tits, 21% in fresh water and 20% in snowpack. Detection rates were between 11 and 17% in the other substrates including epilithic biofilm, litter, plant debris and asymptomatic plants.

Environmental and Agricultural Strains Cannot Be Significantly Differentiated Based on Their Genetic Diversity

Among the 109 genotyped environmental strains and 327 genotyped agricultural strains, 9 and 6 strains, respectively, carried the private allele at microsatellite locus BC6 associated with the cryptic species *B. pseudocinerea* (Walker et al., 2011) and were removed from further analyses. We thus compared the indices of genetic diversity based on the haplotypes obtained for the 100 and 321 remaining strains considered to be *B. cinerea* (**Table 2**). There was no significant difference between the number of alleles in each microsatellite locus and the gene diversity per locus of environmental strains and agricultural strains (respectively, $P_{\text{Mann and Whitney}} = 0.60$, $P_{\text{Mann and Whitney}} = 0.79$) (**Table 3**). The global gene diversity and the mean number of alleles per locus were in the same range for both population of strains (**Table 2**). However, environmental strains had higher haplotypic diversity than agricultural strains (**Table 2**). Two hundred and seventy different multilocus haplotypes (MLH) were found among the 423 strains analyzed but none of these was shared by environmental strains and agricultural strains.

The distribution of the strains collected from crops and those collected from non-agricultural habitats in the NJ tree shows that they were widely intermixed in the tree regardless of their origin (**Figure 1**). This result is supported by the low level of genetic differentiation ($R_{ST} = 0.021$, $P = 0.019$) between these two groups of strains.

Environmental Strains Represent a Greater Variability in Aggressiveness and an Overall Greater Mean Aggressiveness Than Agricultural Strains

Based on the lesion expansion on the stem of the tomato plants, different levels of aggressiveness were observed within the 128 environmental strains and the 156 agricultural strains of *B. cinerea* tested (**Figure 2**). For each of the population of strains (agricultural strains and environmental strains), significant differences were observed among strains (ANOVA, $P < 0.0001$). MOP7-4 isolated in rainfall in 2010, and H6 and BC25 isolated on diseased tomato plants in 1991 were not able to generate symptoms on the stem of the plant, suggesting that they are hypo-aggressive on tomato stems. However, these strains were able to infect the tomato petiole stubs (data not shown). The index of aggressiveness for the 284 strains of *B. cinerea* ranged from 0 to 144% on potted tomato plants with the wider range of aggressiveness for environmental strains compared to agricultural strains (**Table 4**). The mean disease severity caused by strains from environmental substrates was statistically identical to the severity of disease caused by strains from tomato, but was significantly greater than the severity caused by strains from grape or other crops. Globally, environmental strains are significantly more aggressive than agricultural strains on plants (58.9% vs. 50.4%, $P = 0.009$).

TABLE 2 | Indices of genetic diversity among strains collected from non-agricultural habitats (environmental strains) and from crops (agricultural strains).

Origin of strains	Number of strains genotyped	Number of *B. pseudocinerea* strains	Number of *B. cinerea* strains	Gene diversity (Hnb)	Mean number of alleles per locus	Number of distinct MLH	Haplotypic diversity
Total environment	109	9	100	0.77 (0.16)	13.6	83	0.82
Precipitation	69	6	63	0.78 (0.14)	12.3	54	0.85
Snowpack	10	3	7	0.69 (0.18)	4	6	0.83
Fresh water	12	0	12	0.64 (0.29)	4.5	9	0.75
Epilithic biofilm	2	0	2	0.44 (0.33)	1.6	2	1
Litter	3	0	3	0.62 (0.26)	2.4	3	1
Plant debris	1	0	1	0	1.0	1	nd
Wild plants	7	0	7	0.57 (0.27)	3.3	7	1
Bird feather	5	0	5	0.38 (0.27)	2.1	5	1
Agricultural strains	327	6	321	0.76 (0.18)	15.6	186	0.58

TABLE 3 | Allelic richness (AR) and unbiased gene diversity (Hnb) of environmental and agricultural strains of *B. cinerea*, at each of the nine microsatellite loci (corrected for the smallest sample size: 100).

	BC1		BC2		BC3		BC4		BC5		BC6		BC7		BC9		BC10	
	AR	Hnb	AR	Hnb	AR	Hnb	AR	Hnb	AR	Hnb	AR	Hnb	AR	Hnb	AR	Hnb	AR	Hnb
Environmental	21.0	0.91	15.0	0.87	11.0	0.84	11.0	0.84	12.0	0.87	25.0	0.83	11.0	0.81	10.0	0.55	14.0	0.86
Agricultural	21.2	0.87	15.8	0.89	15.2	0.84	15.2	0.84	12.4	0.81	21.4	0.84	11.0	0.85	9.6	0.47	16.8	0.86

Environmental Strains Grow Faster and Sporulate Less Abundantly but Do Not Differ in Sclerotial Production Compared to Agricultural Strains

Among the 31 agricultural and 24 environmental strains tested, the mycelial growth between the first and the third day after the plating of mycelial plug varied widely among strains (**Figure 3**; ANOVA, $P < 0.0001$ for each set of strains). Four strains (BC83, 06C12, 06C163, and S381) had a mycelial growth rate significantly lower than the other strains. These four strains were all isolated from diseased plants (rose, grape and tomato). Globally, mycelial growth rate was significantly higher for environmental strains compared to agricultural strains (29.8 ± 0.4 vs. 25.7 ± 0.4; $P < 0.0001$). A significant correlation was detected between aggressiveness of strains on tomato plants and their mycelial growth on PDA medium ($r^2 = 0.12$, $P = 0.009$ for all the strains). However, this correlation is not significant for each set of strains taken independently ($r^2 = 0.09$, $P = 0.17$ for environmental strains and $r^2 = 0.11$, $P = 0.08$ for agricultural strains).

All strains of *B. cinerea* tested were able to sporulate on PDA medium but the number of spores produced varied widely among strains, both for environmental and for agricultural strains (**Figure 4**; ANOVA, $P < 0.0001$ for each population of strains). Globally, sporulation was significantly lower for environmental strains compared to agricultural strains (12.9 ± 1.1 vs. 17.4 ± 1.1 million spores/mL; $P = 0.005$). There was no significant correlation between aggressiveness of strains on tomato plants and sporulation ($r^2 = 0.00001$, $P = 0.98$ for all strains).

The number of sclerotia produced on PDA medium varied greatly among strains (**Figure 5**; ANOVA, $P < 0.0001$ for both environmental and agricultural strains) and the average number of sclerotia produced was not different between the two sets of strains (41.1 ± 5.5 and 65.5 ± 12.6 for environmental and agricultural strains, respectively, $P = 0.11$). Twelve strains of *B. cinerea* (7 from diseased plants and 5 from non-agricultural context) were not able to produce sclerotia under the conditions used here and one strain (BC96 isolated from hydrangea) produced a significantly higher number of sclerotia than all the other strains. We found a significant negative relationship for all strains between the aggressiveness and the number of sclerotia produced ($r^2 = 0.09$, $P = 0.031$). This correlation is highly significant for the 24 non-agricultural strains ($r^2 = 0.47$, $P = 0.0002$) while it was not significant for the 31 agricultural strains ($r^2 = 0.03$, $P = 0.33$), suggesting that the relationship between aggressiveness and sclerotial production differ among these two populations of strains.

DISCUSSION

This study is the first systematic census of the fungal plant pathogen *B. cinerea* in diverse non-agricultural environments that could come into contact with agriculture such as snowpack, fresh water from river and lake, epilithic biofilms in mountain streams, leaf litter, plant debris and bird feathers. These results complement the prior detection of *B. cinerea* in the diverse substrates described in the introduction. It also contributes to information about sources of *B. cinerea* in precipitation (Monteil et al., 2014) and corroborates reports about its capacity to

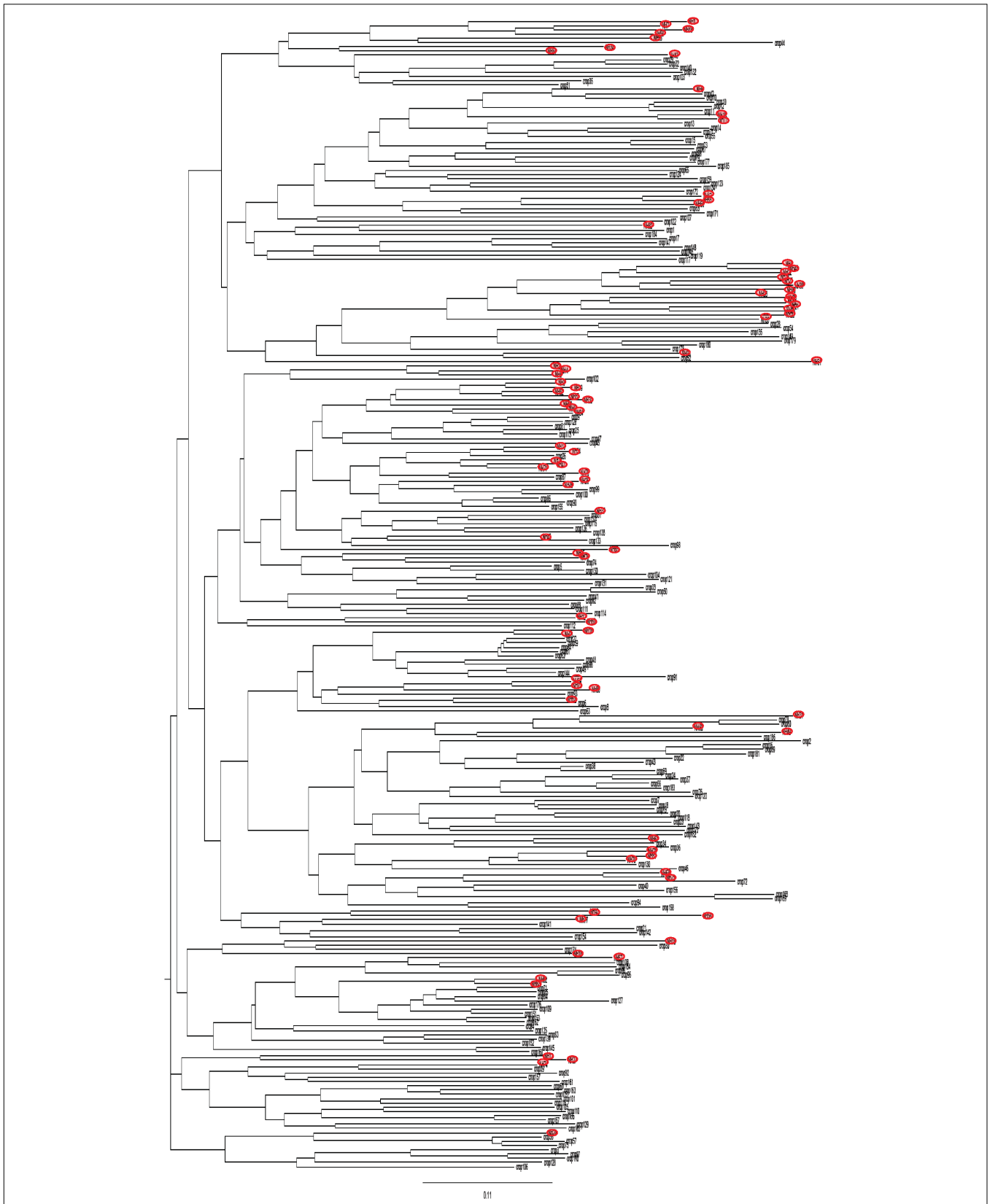

FIGURE 1 | Neighbor-joining tree showing the genetic distance between strains from non-agricultural habitats (red circle) and from crops, based on microsatellite markers.

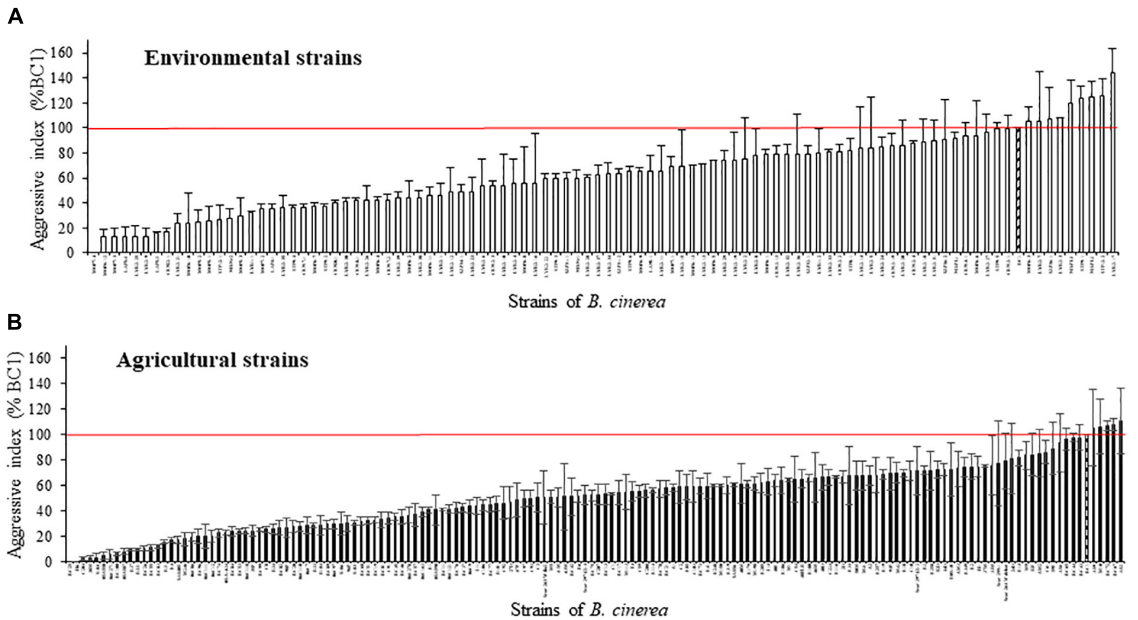

FIGURE 2 | Aggressiveness of 128 environmental strains **(A)** and 156 agricultural strains **(B)** of *B. cinerea* on tomato plant in controlled condition (21°C, RH > 80%, photoperiod 14 h, 114 μmol m^{-2} s^{-1}). Index of aggressiveness (in %) was calculated for each strain, relative to the reference strain BC1 (hatched). The horizontal red bar corresponds to an index of aggressiveness of 100% (value of BC1). Each value represents the mean of two or three independent repetitions. The vertical bar associated to each histogram correspond to SE.

TABLE 4 | Mean and range of aggressiveness of strains of *B. cinerea* collected on various substrates.

Substrate	Number of strains	Mean Ia* ± SE	Minimum	Maximum	Median
Total	284	54.2 ± 1.6	0.0	144.3	54.8
Environmental	128	58.9 ± 2.5[a]	0.0	144.3	58.2
Tomato	101	59.5 ± 2.4[a]	0.0	110.9	61.7
Grape	33	25.8 ± 2.5[c]	3.1	72.5	25.7
Other plants	22	45.7 ± 4.7[b]	11.8	97.6	43.4
ANOVA (*p*-value)		<0.0001			

**Ia (index of aggressiveness) is expressed in % relative to the reference strain BC1. Values with the same uppercase letter are not significantly different according to Newman-Keuls multiple range test (P < 0.05).*

colonize and survive internally in plants without causing any symptoms (Van Kan et al., 2014), traits that are essential for an endophytic phase. Our results illustrate that *B. cinerea* can survive in environmental reservoirs outside of agriculture *sensu stricto* and possibly in the absence of susceptible plants. This knowledge contributes to the growing notion that the life history of plant pathogens should be viewed from a wider angle than their direct interaction with plants in contexts that are favorable for disease. Furthermore, the relative ease with which we found strains of *B. cinerea* in environmental reservoirs highlights how defining this fungus as a plant pathogen skews research questions on its life history and ecology in spite of the numerous previous reports of its presence in a wide range of diverse habitats.

Our results also suggest that the environmental reservoirs are probable sources of inoculum. Previous reports of the genetic diversity of *B. cinerea* from wild plants (e.g., primrose, bramble, dandelion, *Hypochaeris radicata*, *Plantago lanceolata*, and *Sonchus asper*), illustrated the potential reservoirs of inoculum for crops on wild plants and weeds in agricultural systems (Fournier and Giraud, 2008; Rajaguru and Shaw, 2010; Walker et al., 2015; Wessels et al., 2016), but there have been no studies on non-agricultural sources. Phylogenetic comparisons of strains from crop plants and from environmental substrates presented in this study revealed that strains from crops and from the environment could not be distinguished, thereby supporting the hypothesis that strains from these different sources mix. Furthermore, the genetic diversity of strains outside of agriculture was just as broad as within agriculture (**Table 5**; Bardin et al., 2014), suggesting that there are no strong selective pressures that remarkably distinguish these two categories of habitats. These results are consistent with those previously published for *B. cinerea* in different agricultural contexts, using the same genotyping tools developed by Fournier et al. (2002). In such studies, the haplotypic diversity (ratio of the number of different haplotypes over the total number of characterized strains) varied from 0.37 to 1.00. In the present study, this index was

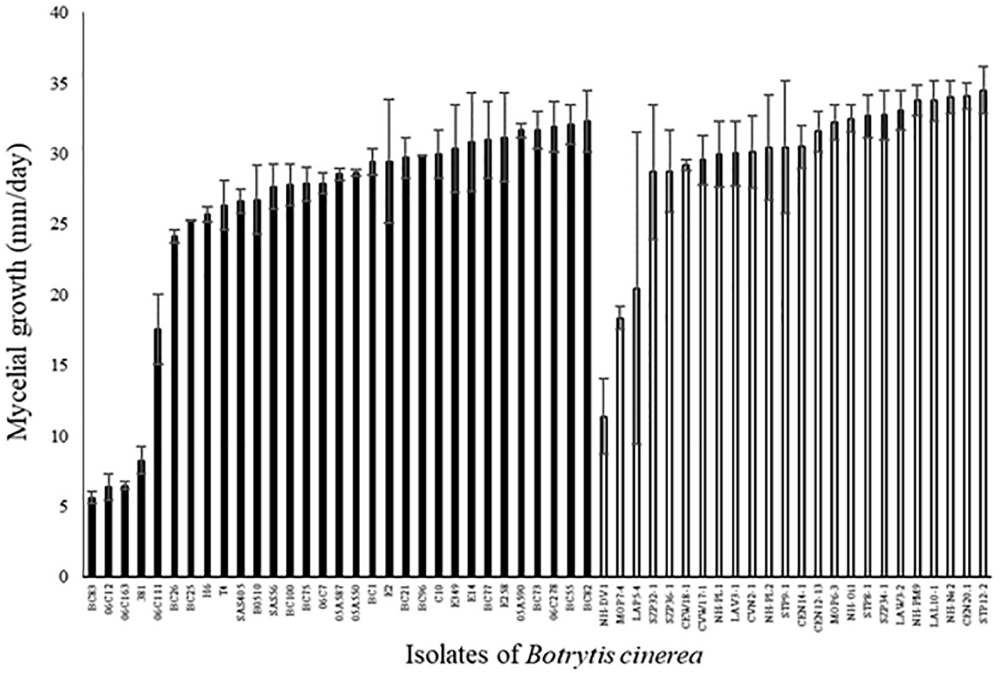

FIGURE 3 | Mycelial growth (mm/day) of 31 agricultural (black) and 24 environmental (white) strains of *B. cinerea* on PDA medium in controlled condition (21°C, photoperiod 14 h, 114 μmol m^{-2} s^{-1}). Each value represents the mean of two independent repetitions. The vertical bar associated to each histogram correspond to SE.

FIGURE 4 | Number of spores produced on PDA medium after 14 days of incubation in controlled condition (21°C, photoperiod 14 h, 114 μmol m^{-2} s^{-1}) by 30 agricultural (black) and 24 environmental (white) strains of *B. cinerea*. Each value represents the mean of three replicates. The vertical bar associated to each histogram correspond to SE.

high, with a value of 0.82, comparable to what is observed in populations of *B. cinerea* collected on diseased plant in open field situations. It reflects the scarcity of strains with identical genotypic profiles in the non-agricultural context. Although we have demonstrated that strains from a non-agricultural context cannot be genetically distinguished from strains from diseased plants, various questions remain about the rate of flux of strains between non-agricultural environment and crops and on the contribution of environmental reservoirs to epidemics.

In tests to determine the severity of disease that strains could induce on tomato stems, the mean disease severity caused by strains from environmental substrates was statistically

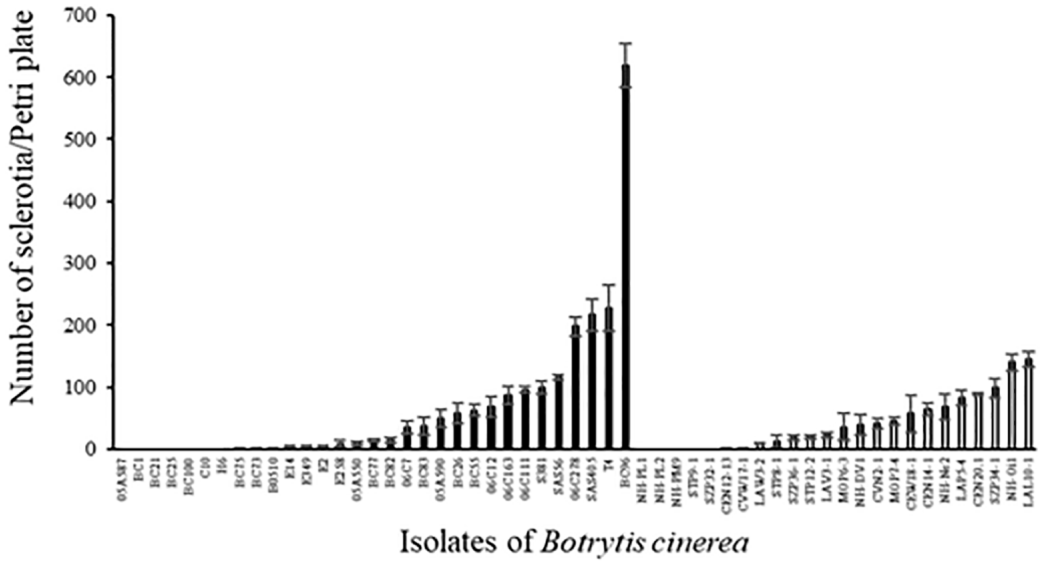

FIGURE 5 | Number of sclerotia produced by 31 agricultural (black) and 24 environmental (white) strains of *B. cinerea* on PDA medium after 5 weeks of incubation in controlled condition at 21°C (1 week with a photoperiod of 14 h at 114 μmol m^{-2} s^{-1} and 4 weeks in the dark) and 5 weeks of incubation at 4°C in the dark. Each value represents the mean of three replicates. The vertical bar associated to each histogram correspond to SE.

TABLE 5 | Genetic diversity reported for strains of *B. cinerea* collected from different origins and characterized using the same microsatellite markers developed by Fournier et al. (2002), as in this study.

Strain origin[a]	Localization	Number of isolates	Gene diversity	Mean number of alleles per locus	Haplotypic diversity[b]	Reference
Environmental	France	100	0,77	13.6	0,82	Present study
Pear orchard (OF)	South-Africa	181	0.69	5.49–7.76	0.50	Wessels et al., 2016
Grapevine (OF)	Italy	317	na[c]	na	0.92	Campia et al., 2017
Grapevine (OF)	China	135	0.29	na	0.94	Zhang et al., 2018
Tomato, lettuce (G)	France	86	0.62–0.77	4.70–9.20	0.37–0.69	Leyronas et al., 2015b
Tomato (G)	France	170	0.76–0.77	11.6–11.3	0.55–0.65	Leyronas et al., 2015a
Tomato (G)	Algeria	170	0.57	8.22	0.63	Adjebli et al., 2015
Soil (G)	France	66	0.68	8.5	0.58	Leyronas et al., 2015c
Air (OF)	France	616	0.71	19.11	0.72	Leyronas et al., 2015d

The References presented here range from 2015 to 2018. For information on previous references, see Bardin et al. (2014). [a]*Indication between brackets indicates the type of crop. OF, open field; G, greenhouse.* [b]*Haplotypic diversity index directly available or computed (on the basis of reported information) as the ratio of (number of distinct MLG – 1) over (sample size – 1).* [c]*na, data not available.*

greater than the severity caused by strains from diseased crops (P = 0.009). It suggests that there are no selective pressures for strains of *B. cinerea* to lose pathogenicity while they are in contexts where they do not cause plant disease or are not even colonizing plants. On the other hand, the environment seems to select for more rapid mycelial growth whereas cropping contexts select for more abundant sporulation. This suggests that there are fitness or survival benefits for these traits in each of the respective environments. This hypothesis is reinforced by the fact that mycelial growth is positively correlated with aggressiveness. Therefore, it suggests that the non-agricultural environment could select strains for factors that would facilitate their pathogenicity on plants. It would be interesting to determine how much time is needed for mycelial growth and sporulation rates to change under the selection pressures of each environment and if in fact these traits are fixed or due to epigenetic processes. This could give clues to the amount of time that strains from these habitats have been localized in one habitat or another. Interestingly, a trade-off between the aggressiveness and the number of sclerotia produced was observed for the environmental strains of *B. cinerea*. This suggests that the least aggressive environmental strains compensate this low level of aggressiveness by their high ability to survive in the environment in the absence of host plants.

Our results are consistent with those concerning the life history of the bacterial plant pathogen *P. syringae* (Morris et al., 2013) in that highly diverse populations of strains that maintain their pathogenic potential can persist outside of agriculture in association with substrates other than plants. These findings set the stage for new perspectives on factors that foster to

the evolution and emergence of pathogenic potential in microorganisms, on disease epidemiology and on the factors that contribute to the durability of disease control methods. They also beg for the development of systematic approaches to widen our understanding of the life history of plant pathogens in general beyond the context of agriculture.

AUTHOR CONTRIBUTIONS

MB, CT, and CM achieved the sampling of environmental strains. MB and CT realized the phenotypic experiments and the associated data analysis. CL carried out microsatellite genotyping and the genetic data analysis. MB coordinated the writing of the manuscript. MB, CL, and CM wrote the manuscript. All authors reviewed the manuscript.

ACKNOWLEDGMENTS

The research leading to these results has received funding from INRA department of Plant Health and Environment. We are grateful to Dr. Philippe Nicot for extremely useful discussions throughout this research project and to Dr. Caroline Monteil, Jean-Charles Bouvier, Caroline Guilbaud, Charlotte Chandeysson, and Magali Duffaud for their valuable help in samples collection. Part of this work was carried out by using the resources of the Molecular Biology Platform of INRA-PACA center. Research on plant biology depends heavily on the cultivation of plants under experimental conditions that are controlled, monitored, and repeatable. For ensuring a perfect plant production, the contribution of the Plant Production and Environmental Management Service of the Plant Pathology Research Unit was greatly appreciated.

REFERENCES

Adjebli, A., Leyronas, C., Aissat, K., and Nicot, P. C. (2015). Comparison of *Botrytis cinerea* populations collected from tomato greenhouses in northern algeria. *J. Phytopathol.* 163, 124–132. doi: 10.1111/jph.12289

Ali-Shtayeh, M. S., Salameh, A. A. M., Abu-Ghdeib, S. I., and Jamous, R. M. (2001). Hair and scalp mycobiota in school children in Nablus area. *Mycopathologia* 150, 127–135. doi: 10.1023/a:1010989431375

Amato, P., Parazols, M., Sancelme, M., Laj, P., Mailhot, G., and Delort, A. M. (2007). Microorganisms isolated from the water phase of tropospheric clouds at the Puy de Dome: major groups and growth abilities at low temperatures. *FEMS Microbiol. Ecol.* 59, 242–254. doi: 10.1111/j.1574-6941.2006.00199.x

Arnaud-Haond, S., and Belkhir, K. (2007). Genclone: a computer program to analyse genotypic data, test for clonality and describe spatial clonal organization. *Mol. Ecol. Notes* 7, 15–17. doi: 10.1111/j.1471-8286.2006.01522.x

Arnaud-Haond, S., Duarte, C. M., Alberto, F., and Serrao, E. A. (2007). Standardizing methods to address clonality in population studies. *Mol. Ecol.* 16, 5115–5139. doi: 10.1111/j.1365-294X.2007.03535.x

Azmi, O. R., and Seppelt, R. D. (1998). The broad-scale distribution of microfungi in the windmill islands region, continental antarctica. *Polar Biol.* 19, 92–100. doi: 10.1007/s003000050219

Bardin, M., Decognet, V., and Nicot, P. C. (2014). Remarkable predominance of a small number of genotypes in greenhouse populations of *Botrytis cinerea*. *Phytopathology* 104, 859–864. doi: 10.1094/PHYTO-10-13-0271-R

Barnett, H. L. (1998). *Illustrated Genera of Imperfect Fungi*, 4th Edn. Saint Paul, MN: American Phytopathological Society.

Bartlett, K. H., Kennedy, S. M., Brauer, M., Van Netten, C., and Dill, B. (2004). Evaluation and a predictive model of airborne fungal concentrations in school classrooms. *Ann. Occup. Hyg.* 48, 547–554. doi: 10.1093/annhyg/meh051

Belirkh, K., Borsa, P., Chikhi, L., Raufaste, N., and Bonhomme, F. (1996–2004). *Genetix 4.05, Logiciel Sous Windows Tm Pour La Génétique Des Populations*. Montpellier: Université de Montpellier.

Campia, P., Venturini, G., Moreno-Sanz, P., and Casati, P. L. T. S. (2017). Genetic structure and fungicide sensitivity of *Botrytis cinerea* populations isolated from grapevine in northern Italy. *Plant Pathol.* 66, 890–899. doi: 10.1111/ppa.12643

Cavalli-Sforza, L. L., and Edwards, A. W. F. (1967). Phylogenetic analysis: models and estimation procedures. *Am. J. Hum. Genet.* 19, 233–257.

Decognet, V., Bardin, M., Trottin-Caudal, Y., and Nicot, P. C. (2009). Rapid change in the genetic diversity of *Botrytis cinerea* populations after the introduction of strains in a tomato glasshouse. *Phytopathology* 99, 185–193. doi: 10.1094/PHYTO-99-2-0185

Edel-Hermann, V., Sautour, M., Gautheron, N., Laurent, J., Aho, S., Bonnin, A., et al. (2016). A clonal lineage of *Fusarium oxysporum* circulates in the tap water of different French hospitals. *Appl. Environ. Microbiol.* 82, 6483–6489. doi: 10.1128/AEM.01939-16

Edwards, S. G., and Seddon, B. (2001). Selective media for the specific isolation and enumeration of *Botrytis cinerea* conidia. *Lett. Appl. Microbiol.* 32, 63–66. doi: 10.1046/j.1472-765x.2001.00857.x

Elad, Y., Pertot, I., Cotes Prado, A. M., and Stewart, A. (2016). "Plant hosts of *Botrytis* spp," in *Botrytis - The Fungus, the Pathogen Ans Its Management in Agricultural Systems*, eds S. Fillinger and Y. Elad (Berlin: Springer), 413–486. doi: 10.1007/978-3-319-23371-0_20

Excoffier, L., Laval, G., and Schneider, S. (2005). Arlequin ver. 3.0: an integrated software package for population genetics data analysis. *Evol. Bioinform.* 1, 47–50. doi: 10.1177/117693430500100003

Fermaud, M., and Lemenn, R. (1989). Association of *Botrytis cinerea* with grape berry moth larvae. *Phytopathology* 79, 651–656. doi: 10.1094/Phyto-79-651

Fournier, E., and Giraud, T. (2008). Sympatric genetic differentiation of a generalist pathogenic fungus, *Botrytis cinerea*, on two different host plants, grapevine and bramble. *J. Evol. Biol.* 21, 122–132. doi: 10.1111/j.1420-9101.2007.01462.x

Fournier, E., Giraud, T., Loiseau, A., Vautrin, D., Estoup, A., Solignac, M., et al. (2002). Characterization of nine polymorphic microsatellite loci in the fungus *Botrytis cinerea* (Ascomycota). *Mol. Ecol. Notes* 2, 253–255. doi: 10.1046/j.1471-8286.2002.00207.x

Gaylarde, C. C., Bento, F. M., and Kelley, J. (1999). Microbial contamination of stored hydrocarbon fuels and its control. *Rev. Microbiol.* 30, 1–10. doi: 10.1590/s0001-37141999000100001

Gaylarde, C. C., and Morton, L. H. G. (1999). Deteriogenic biofilms on buildings and their control: a review. *Biofouling* 14, 59–74. doi: 10.1080/08927019909378397

Goudet, J. (1995). FSTAT (Vers.1.2): a computer program to calculate F-statistics. *J. Heredity* 86, 485–486. doi: 10.1093/oxfordjournals.jhered.a111627

Hansen, E. M., Reeser, P. W., and Sutton, W. (2012). *Phytophthora* beyond agriculture. *Annu. Rev. Phytopathol.* 50, 359–378. doi: 10.1146/annurev-phyto-081211-172946

Leyronas, C., Bardin, M., Duffaud, M., and Nicot, P. C. (2015a). Compared dynamics of grey mould incidence and genetic characteristics of *Botrytis cinerea* in neighbouring vegetable greenhouses. *J. Plant Pathol.* 97, 439–447.

Leyronas, C., Bryone, F., Duffaud, M., Troulet, C., and Nicot, P. C. (2015b). Assessing host specialization of *Botrytis cinerea* on lettuce and tomato by genotypic and phenotypic characterization. *Plant Pathol.* 64, 119–127. doi: 10.1111/ppa.12234

Leyronas, C., Duffaud, M., Pares, L., Jeannequin, B., and Nicot, P. C. (2015c). Flow of *Botrytis cinerea* inoculum between lettuce crop and soil. *Plant Pathol.* 64, 701–708. doi: 10.1111/ppa.12284

Leyronas, C., Halkett, F., and Nicot, P. C. (2015d). Relationship between the genetic characteristics of *Botrytis* sp. airborne inoculum and meteorological parameters, seasons and the origin of air masses. *Aerobiologia* 31, 367–380. doi: 10.1007/s10453-015-9370-x

Leyronas, C., Duffaud, M., and Nicot, P. C. (2012). Compared efficiency of the isolation methods for *Botrytis cinerea*. *Mycol. Int. J. Fungal Biol.* 3, 221–225.

Leyronas, C., and Nicot, P. C. (2013). Monitoring viable airborne inoculum of *Botrytis cinerea* in the South-East of France over 3 years: relation with climatic parameters and the origin of air masses. *Aerobiologia* 29, 291–299. doi: 10.1007/s10453-012-9280-0

Louis, C., Girard, M., Kuhl, G., and LopezFerber, M. (1996). Persistence of *Botrytis cinerea* in its vector *Drosophila melanogaster*. *Phytopathology* 86, 934–939. doi: 10.1094/Phyto-86-934

Lugauskas, A., and Krikstaponis, A. (2004). Microscopic fungi found in the libraries of vilnius and factors affecting their development. *Indoor Built Environ.* 13, 169–182. doi: 10.1177/1420326x04045274

Monteil, C. L., Bardin, M., and Morris, C. E. (2014). Features of air masses associated with the deposition of *Pseudomonas syringae* and *Botrytis cinerea* by rain and snowfall. *ISME J.* 8, 2290–2304. doi: 10.1038/ismej.2014.55

Monteil, C. L., Yahara, K., Studholme, D. J., Mageiros, L., Méric, G., Swingle, B., et al. (2016). Population-genomic insights into emergence, crop-adaptation, and dissemination of *Pseudomonas syringae* pathogens. *Microb. Genom.* 2:e000089. doi: 10.1099/mgen.0.000089

Morris, C. E., Bardin, M., Kinkel, L. L., Moury, B., Nicot, P. C., and Sands, D. C. (2009). Expanding the paradigms of plant pathogen life history and evolution of parasitic fitness beyond agricultural boundaries. *PLoS Pathog.* 5:e1000693. doi: 10.1371/journal.ppat.1000693

Morris, C. E., Monteil, C. L., and Berge, O. (2013). The life history of *Pseudomonas syringae*: linking agriculture to Earth system processes. *Annu. Rev. Phytopathol.* 51, 85–104. doi: 10.1146/annurev-phyto-082712-102402

Page, R. D. M. (1996). Treeview: an application to display phylogenetic trees on personal computers. *Comp. Appl. Biosci.* 12, 357–358.

Rajaguru, B. A. P., and Shaw, M. W. (2010). Genetic differentiation between hosts and locations in populations of latent *Botrytis cinerea* in southern England. *Plant Pathol.* 59, 1081–1090. doi: 10.1111/j.1365-3059.2010.02346.x

Shchipanov, N. A., Aleksandrov, D. Y., and Aleksandrova, A. V. (2006). Dispersal of micromycete spores by small mammals. *Zool. Zhurnal.* 85, 101–113.

Slatkin, M. (1995). A measure of population subdivision based on microsatellite allele frequencies. *Genetics* 139, 1463–1463.

Van Kan, J. A. L., Shaw, M. W., and Grant-Downton, R. T. (2014). *Botrytis* species: relentless necrotrophic thugs or endophytes gone rogue? *Mol. Plant Pathol.* 15, 957–961. doi: 10.1111/mpp.12148

Walker, A. S., Gautier, A., Confais, J., Martinho, D., Viaud, M., Le Pêcheur, P., et al. (2011). *Botrytis pseudocinerea*, a new cryptic species causing gray mold in French vineyards in sympatry with *Botrytis cinerea*. *Phytopathology* 101, 1433–1445. doi: 10.1094/PHYTO-04-11-0104

Walker, A. S., Gladieux, P., Decognet, V., Fermaud, M., Confais, J., Roudet, J., et al. (2015). Population structure and temporal maintenance of the multihost fungal pathogen *Botrytis cinerea*: causes and implications for disease management. *Environ. Microbiol.* 17, 1261–1274. doi: 10.1111/1462-2920.12563

Wessels, B. A., Linde, C. C., Fourie, P. H., and Mostert, L. (2016). Genetic population structure and fungicide resistance of *Botrytis cinerea* in pear orchards in the Western Cape of South Africa. *Plant Pathol.* 65, 1473–1483. doi: 10.1111/ppa.12523

Williamson, B., Tudzynski, B., Tudzynski, P., and van Kan, J. A. L. (2007). *Botrytis cinerea*: the cause of grey mould disease. *Mol. Plant Pathol.* 8, 561–580. doi: 10.1111/j.1364-3703.2007.00417.x

Zhang, Y., Li, X., Shen, F., Xu, H., Li, Y., and Liu, D. (2018). Characterization of *Botrytis cinerea* isolates from grape vineyards in China. *Plant Dis.* 102, 40–48. doi: 10.1094/PDIS-01-17-0062-RE

Conflict of Interest Statement: The authors declare that the research was conducted in the absence of any commercial or financial relationships that could be construed as a potential conflict of interest.

frontiers in Plant Science

ORIGINAL RESEARCH
published: 11 December 2018
doi: 10.3389/fpls.2018.01808

Pathogenicity Traits Correlate With the Susceptible *Vitis vinifera* Leaf Physiology Transition in the Biotroph Fungus *Erysiphe necator*: An Adaptation to Plant Ontogenic Resistance

Agnes Calonnec[1]*, *Jerome Jolivet*[1], *Philippe Vivin*[2] and *Sylvain Schnee*[1†]

[1] UMR1065 SAVE Santé et Agroecologie du Vignoble, INRA, ISVV, Villenave d'Ornon, France, [2] EGFV, Bordeaux Sciences Agro, INRA, University of Bordeaux, ISVV, Villenave d'Ornon, France

OPEN ACCESS

Edited by:
Omer Frenkel,
Agricultural Research Organization (ARO), Israel

Reviewed by:
Andreia Figueiredo,
Universidade de Lisboa, Portugal
Courtney Coleman,
University of Missouri, United States

***Correspondence:**
Agnes Calonnec
agnes.calonnec@inra.fr

†Present Address:
Sylvain Schnee,
Station de Recherche Agroscope Changins-Wädenswil ACW, Nyon, Switzerland

Specialty section:
This article was submitted to Plant Microbe Interactions, a section of the journal Frontiers in Plant Science

Received: 15 June 2018
Accepted: 20 November 2018
Published: 11 December 2018

Citation:
Calonnec A, Jolivet J, Vivin P and Schnee S (2018) Pathogenicity Traits Correlate With the Susceptible Vitis vinifera Leaf Physiology Transition in the Biotroph Fungus Erysiphe necator: An Adaptation to Plant Ontogenic Resistance. Front. Plant Sci. 9:1808. doi: 10.3389/fpls.2018.01808

How and when the pathogen cycle is disrupted during plant development is crucial for harnessing ontogenic resistance in sustainable agriculture. Ontogenic resistance against powdery mildew (*Erysiphe necator)* was quantified on *Vitis vinifera*. Shoots were sampled in the vineyard at several dates during seasonal growth and processed in the laboratory under controlled conditions. Experiments were conducted on two susceptible *Vitis vinifera* Cabernet Sauvignon and Merlot. The process of leaf ontogenic resistance was investigated by measuring three quantitative traits of pathogenicity: the infection efficiency, sporulation and mycelium growth. Morphological and physiological plant indicators were used to identify leaf changes that resulted in ontogenic resistance and to predict pathogen variations that were linked to pathogenicity traits. The process of ontogenic resistance was established early in correspondence with the physiological transition of the leaf from sink to source status and was characterized by its increase in sugar content. The three traits of pathogenicity that we measured were affected, and their variation was strongly correlated with leaf age. Using leaf age, we were able to accurately predict the susceptibility of the leaf: a leaf aged, on average, 13.3 days had a very high probability (0.8) of being susceptible, while this probability decreased to 0.5 one week later. Sporulation was more closely correlated with variations in sugar and the infection efficiency in leaf water. The results for both cultivars were consistent. Ontogenic resistance on grapevine leaves is thus interpreted to be a strong, immutable physiological process that *E. necator* is able to circumvent by restricting its development to sink tissue. Future research should explore how this native plant resistance can be incorporated into grape management strategies to better control powdery mildew (PM) epidemics with reduced amounts of fungicides.

Keywords: powdery mildew, ontogenic resistance, sink-source transition, traits of pathogenicity, grapevine

INTRODUCTION

Biotrophs totally depend on their hosts to complete their life cycles, deriving their nutrients from living host cells through the development of specialized infection structures (O'Connell and Panstruga, 2006). *Erysiphe necator* Schwein, the powdery mildew of grapevines, is very efficient and can adopt highly sophisticated mechanisms to invade living plant cells successfully, such as upregulating the expression of cell wall invertase and plant hexose transporter genes or downregulating vacuolar invertase genes (Hayes et al., 2010).

Powdery mildew of grapevine is a ubiquitous disease that affects common cultivars of *Vitis vinifera* L., and it is responsible for significant damage (Calonnec et al., 2004) if no protective measures are used. While fungicide-based strategies are generally effective in reducing disease (Delière et al., 2010; Deliere et al., 2015; Valdés-Gómez et al., 2017), finding alternative methods that consider practitioners and the environment and that are economically feasible remains a challenge for sustainable viticulture. One solution relies on the exploitation of resistant grape varieties, in which sources of resistance coming from other *Vitis* of American or Asian origin are introgressed (Calonnec et al., 2013b). The difficulty for breeders in associating traits of agronomical and oenological values and genes of pathogen resistance leads also to exploration of the native potential of plant defenses in cases of a susceptible *V. vinifera* host. Innovative strategies to counteract pathogen efficiency could rely on integration into the management of the disease of the time-course evolution of the plant (i.e., leaves and berries) resistance during the season (Burie et al., 2011; Valdes-Gomez et al., 2011; Gadoury et al., 2012; Calonnec et al., 2013a).

In many plant-pathogen interactions, a susceptible host can acquire resistance to a pathogen at a certain developmental stage (Develey-Rivière and Galiana, 2007). This age-related resistance, commonly called ontogenic resistance (when young tissues are susceptible) or receptivity (when old tissues are susceptible), could be defined as the dynamic modification of tissue receptivity during organ development, triggering resistance/tolerance to pathogenic micro-organisms. Ontogenic resistance has been described for many plant-pathogen systems [e.g., strawberry-powdery mildew (Carisse and Bouchard, 2010), cucurbit fruit—*Phytophthora capsici* (Ando et al., 2009), tobacco—*Phytophthora parasitica* (Hugot et al., 1999), apple-apple scab (Li and Xu, 2002), cocoa—*Phytophthora megakarya* (Takam Soh et al., 2012), pea-powdery mildew (Fondevilla et al., 2006), pea-aschochyta blight (Richard et al., 2012)]. They are therefore common traits but remain underexploited in disease management, principally because of a lack of understanding of the underlying mechanisms and of the potential variability linked to the physiological responses of the host to environmental factors. The phenomenon of ontogenic resistance or receptivity to the main pathogens of grapevines has been highlighted and assessed on bunches for *Plasmopara viticola* (Kennelly et al., 2005), *Guignardia bidwellii* (Molitor and Berkelmann-Loehnertz, 2011), and *Botrytis cinerea* (Deytieux-Belleau et al., 2009). Botrytis susceptibility is known to increase with fruit maturity. Although the mechanisms involved remain speculative, they might differ from those involved in response to infection in the classical defense system (Develey-Rivière and Galiana, 2007; Gee et al., 2008). For powdery mildew, the process has been underscored for berries, on which infection stops when berry sugar content reaches 8% (Delp, 1954), and it is characterized by a low penetration rate of infectious structures following potential modification of the structure and chemical composition of the cuticle (Ficke et al., 2002). The level of irradiance received before inoculation can strengthen ontogenic resistance through modifications of berry physiology, such as decreases in pH and K concentration and increases in polyphenol and anthocyanin concentrations (Zahavi and Reuveni, 2012). Ontogenic resistance also exists in mature leaves, which suffer less infection (Doster and Schnathorst, 1985). Experiments on cuttings grown in a glasshouse under a controlled temperature showed that infection is maximal for leaves that have just ceased importing assimilates (Merry et al., 2013). Simulations have shown that, depending on its parameter value, ontogenic resistance could significantly reduce the severity of late epidemics (Calonnec et al., 2008, 2011). However, little information is available regarding the behavior of the pathogen at each step of its sequential development for a broad range of crop development, and no information is available for field-grown material.

In our study, leaf ontogenic resistance to powdery mildew in *V. vinifera* was investigated using the susceptible cultivars Cabernet Sauvignon and Merlot. They are the two most commonly grown cultivars in the world for wine grapes (OIV, 2018). Shoots were characterized and sampled in the field, and leaves were processed in the laboratory. Our questions were: When is ontogenic resistance established? How does it vary with variety, crop development and climatic environment? Which pathogenicity traits are the most affected, and how variable is the effect? We used leaf age, leaf surface, sugars and LWC to identify changes in leaf physiology linked to ontogenic resistance and to determine whether they could be used to predict variations in pathogenicity.

MATERIALS AND METHODS

Plants

Vitis vinifera Cabernet cv. Sauvignon and Merlot were grown on two INRA experimental vineyards near Bordeaux, France, at Cadaujac and Latresne, respectively. Plantation density was 5,050 vines/10,000 m^2; the vinestocks were between 7 and 12 years old. The experimental plots were regularly protected with fungicides from natural infection by downy ("Remiltine or Dauphin" (cymoxanil, mancozeb) and powdery mildews (powder or wettable sulfur). Treatments were applied between 6 and 20 days before sampling. Plant phenological stages were monitored from bud break until ripening (Baillod and Baggiolini, 1993). Each new fully expanded primary leaf (width from 3 cm) was tagged by a set of plastic color markers to indicate the date of leaf appearance and subsequently to calculate leaf age. These color markers allowed leaf age (LA) and the sum of temperatures (above 10°C) accumulated by the leaf during its development (LAdev) to be determined.

Bioassays

Shoots were sampled at different dates during the vegetative growth of grapevines (May 12, May 26 and June 10 for Cabernet Sauvignon) in 2005; June 4, 2009, and May 27 and June 24, 2010, for Merlot). Selected shoots were cut early in the morning and immediately brought to the laboratory, with the base of the shoots kept in water. No more than one shoot per vine. Before leaf sampling, petioles were marked with a color code to specify their respective positions on the shoot and to maintain traceability throughout the whole experiment. An approximation of the leaf extension rate (LER) per day was calculated by measuring leaf dimensions 3 days (t-3) and the day before (t-1) sampling with. $LER = \frac{(LS_{t\text{-}3} - LS_{t\text{-}1})/2}{(LS_{t\text{-}3} - LS_{t\text{-}1})/2}$ The maximum leaf width (W) and maximum leaf length (L) of each leaf were measured to calculate the leaf surface (LS) in accordance with Montero et al. (2000) ($LS = L \times W \times 0.6$). For each shoot, the leaves were detached, abundantly washed under permuted water and then dried on filter paper. Under axenic conditions, the leaves were disinfected in a 5% (w/v) aqueous calcium hypochlorite at 65% for 10 min, rinsed in sterile water and dried in sterile filter paper. Three leaf discs (Ø 22 mm) were cut into each leaf and distributed in three different Petri dishes prepared for the pathogenicity tests. The leaf discs were disposed abaxial face down on an agar medium (20 g L^{-1}) supplemented with benzimidazole (30 mg L^{-1}). Each Petri dish contained six discs from an identical leaf level (not necessarily the same LA, as shoots are not synchronous in their growth) from six different shoots (replicates). Petri dishes corresponding to the infection efficiency test and to the total production of spores per cm² were randomly placed in a settling tower and then artificially inoculated by blowing conidia from a leaf infected 14 days earlier (4–5 conidia on each conidiophore), in accordance with Cartolaro and Steva (1990). All leaf levels were inoculated together in one tower. Two towers were necessary to inoculate all of the replicates for each experiment. The average density of spores inoculated was 120, 388, and 610 spores/cm² for 2005, 2009, and 2010, respectively. The dishes were placed in a growth chamber at 22°C (12:12 h light:dark photoperiod) for pathogen development. One different monospore isolate was used each year. It was sampled from vinestock leaves from a vineyard in the Bordeaux area or in the greenhouse before each annual experiment and was bulked on Cabernet Sauvignon leaves from greenhouse-grown cuttings. Infection efficiency was assessed at 72 hpi (hours post-infection) by counting the conidia that reached the branching hyphae stage (stage 5–6 according to Leinhos et al., 1997) after removing tape from leaves and then applying a cotton blue staining procedure (Cartolaro and Steva, 1990). The total production of spores per infected disc was measured at 14–15 dpi. For colony growth and spores per colony tests, the leaf discs were inoculated by the deposit, with a needle, of a few conidia (from 1 to 10) in their centers. Colony growth was assessed at ∼4, 7, 10, 14, and 18 dpi (days post-infection) and the production of spores per colony at 14 or 18 dpi. Sporulating disks were placed in a vial filled with 20 mL of isotone 2 and one drop of non-ionic dispersant (Nacconol *90F*), shaken, and the spore production was assessed by counting the number of particles between 15 and 38 µm diameter on a sample of 500 µl using a particle counter (Coulter Counter® Multisizer™ 3—Beckman Coulter©, U.S). The disease variables calculated were: Inf (% of infectious spores as defined above), Spo (number of spores per cm^2 of infected leaf disc), Spoc (number of spores per isolated colony), and Diam (final colony diameter in mm). A total of 12–20 shoots (120–220 leaves) were tested depending on the experiments. The experimental conditions and variables measured are summarized in **Tables 1**, **2**, respectively and experimental design in **Supplementary Figure S1**.

Physiological Indicators

For each sampled leaf, six discs (Ø 6 mm) were collected into a 2-ml Eppendorf tube, fresh weighed, dried in a hood (60–70°C for 72 h) and then weighed again. Leaf water content (LWC) was calculated from fresh (FW) and dry mass measurements (DW) (LWC = (FW − DW)/FW). The total non-structural carbohydrates were extracted and dosed as described by Gomez et al. (2007). Briefly, two metallic balls (Ø 5 mm) were added to each disc leaf samples, and the Eppendorf tube was submitted to intense shaking (3 min at 30 swings sec-1, Retsch Mixer Mill MM200). An ethanolic solution (80%, v/v) was added to the finely ground tissue, sonicated for 10 min at 60°C and centrifuged (3,700 trs min^{-1} for 5 min). The pellet containing soluble starch (ST) was rinsed three times with nanopure water, autoclaved and then hydrolysed in the presence of 200 µl of amyloglucosidase at 55°C for 1 h. The supernatant representing soluble sugars (including glucose, fructose and sucrose) (SS) was dried and then hydrolysed by addition of 200 µl of invertase (Sigma 19253) at 55°C for 1 h. After drying, 800 µl of nanopure water were added to the two types of extracts and vigorously shaken by vortex agitation and sonication to ensure total carbohydrate solubilisation. Soluble sugars and starch solutions were prepared (kit LISA 200C, CETIM, France) and measured spectrophotometrically at 340 nm, with an ELx800UV automated micro-plate reader (Biotek Instruments Inc., Vermont, USA). Glucose (Sigma G8270) was used for the standard range, and all of the obtained data were expressed in glucose equivalents.

Environmental Growing Conditions

The sum of degree-days above 10°C (growing degrees) was used to determine grapevine organogenesis (Schultz, 1992). Five variables were calculated to characterize the environmental conditions of vine growth: the sum of GD at the day of sampling, which is also an indicator of the time of the experiment; the sum of GD during the 10 days before sampling; the average evapotranspiration rate, according to the Penman formula for this period (ETPP in $mm.day^{-1}$); and the sum of rainfall for the 10 days before the experiments. The environmental conditions are summarized in **Table 1**.

Data and Statistical Analyses

For infection efficiency (Inf), only data based on more than 30 counted spores were analyzed, and for all variables, only shoots with more than 3 validated samples were considered. To lessen the variation between shoots and to emphasize the variation between leaves of different ages, relative infection (RInf) and sporulation (RSpo) rates were also calculated by dividing the value obtained for a given leaf by the maximum value on its own shoot.

TABLE 1 | Conditions of the experimentations.

					Climatic conditions before the experiment						
				Phenological stage	During the 10 days before D				at D-1	at D-1	
Experiments	**Variety**	**Date of sampling = D**	**Nb sampled shoots**	**mean Nb leaf/shoot ± σ**	**Average T°C**	**GD**	**Sum Rain mm**	**Average ETPP**	**Average global radiance J.cm^2**	**GD**	**Average T°C**
Exp. 1	Cabernet Sauvignon	12-May	20	6.05 ± 0.74	15.2	51.9	1.5	3.82	2481	212.4	16.8
Exp. 2	Cabernet Sauvignon	26-May	20	9.5 ± 1.43	16.2	61.6	0.5	4.34	2868	295.7	20.7
Exp. 3	Cabernet Sauvignon	9-Jun	15	14.73 ± 1.34	18.3	83	0.5	4.9	3049	423.7	19.1
Exp. 4	Merlot	4-Jun	12	14.33 ± 1.37	18.7	86.9	11	3.78	4677	323.5	22.3
Exp. 5	Merlot	27-May	6	12.50 ± 0.96	18.1	84.2	5	4.03	2290	271	17.6
Exp. 6	Merlot	24-Jun	6	20.17 ± 1.10	15.9	58.9	48	3.09	4792	474.3	19.4

Nb, number; σ, standard deviation; ETPP, Evapotranspiration rate; GD, growing degrees, sum of degrees above 10°C.

TABLE 2 | Measured variables for the experiments.

Variables	**Abbr.**	**Units**	**Experiments**					
			Exp. 1	**Exp. 2**	**Exp. 3[a]**	**Exp. 4**	**Exp. 5**	**Exp. 6**
PLANT GROWTH VARIABLES								
Leaf age	LA	Day	•	•	•	•	•	•
Leaf temperature of development	LAdev	Sum of °C days above 10	•	•	•	•	•	•
Leaf surface	LS	cm²	•	•	•	•	•	•
Leaf extension rate	LER	Day^{-1}	•	•	•	•	•	•
PHYSIOLOGICAL INDICATORS								
Soluble sugars	SS	(glucose + fructose + saccharose) in % of dry weight	•	•		•	•	•
Complex sugars	CS	Starch expressed in equivalent glucose in % of dry weight	•	•		•	•	•
Leaf water content	LWC	–	•	•		•	•	•
DISEASE								
Infection efficiency	Inf	Rate of branched conidia at 72 hpi	•	•	•	•	•	•
Relative infection	RInf	Relative rate	•	•	•	•	•	•
Maximal colony diameter	Diam	mm	•	•	•	•	•	•
Sporulation per colony	Spoc	Number of spores generated per colony	•	•	•	•	•	•
Sporulation per leaf area	Spo	Number of spores generated per cm² of inoculated leaf area	•	•	•	•	•	•
Relative sporulation	RSpo	Relative rate	•	•	•	•	•	•

[a]*No physiological indicators available.*

Variance analyses (general linear modeling procedure in SAS) were performed on different variables, such as infection efficiency (Inf), sporulation (Spo), maximum diameter (Diam), and the number of spores produced per colony (Spoc), with leaf age as a factor. For Diam and Spoc, some of the age classes were grouped to allow for statistical comparison when the sample numbers were too low (<5) due to a failure of the infection process related to ontogenic resistance (only a few spores are deposited) (**Table 2**). The effect of leaf age on the independent variables was measured by performing Tukey-Kramer's multiple comparisons test adapted for unbalanced designs. The mean number of spores produced per area of a colony (Spoc/[(Diam/2)².π]), a proxy of the sporulation capacity according to Lannou (2012), was compared by permutation testing (5000 permutations) for two classes of leaf age.

The disease data functions of leaf age were fitted to models using ordinary least squares methods. The choice of one specific model was based on Akaike's information criterion, which selects the model most likely to have generated the data. Goodness of fit was measured by R^2 and the adequacy of the model by replicate testing. A fitting procedure was performed using Prism software (version 5.04).

Relationships among experimental conditions, leaf growth characteristics, leaf physiological indicators and disease were studied by a partial least squares path model analysis (PLS-PM) (Tenenhaus et al., 2005). The PLS-path model was described by six unobservable or latent variables (LVs): "Variety," "Climate," "Leaf growth," "Leaf physiology," "Inoculum," and "Disease." This analysis provides how much variation of "Disease" can be predicted by the other latent variables. Each LV was constructed by a set of observable variables called manifest variables (MVs). "Variety" and "Inoculum" were constructed in a formative way by qualitative variables (CS and M for variety, 2005–2009–2010 for inoculum), corresponding either to the varieties Cabernet Sauvignon and Merlot or to the year using different isolates. "Climate" was described in a reflexive way by the average temperature over the 10 days before the experimentation (STJ-10) and the sum of rain (SRJ-10). "Leaf growth" was described in a reflexive way by leaf age (LA), the sum of GD temperature during leaf development (LAdev) and the leaf surface (LS). It is worth noting that, for one experiment, leaves sharing the same leaf age encountered the same climatic conditions, but they do not necessarily have the same plastochron index, which is a function of the rate of growth of the shoot, nor do they have the same LS, which is dependent on the variety, vigor and environmental conditions. An identical leaf age yields various LAdev depending on experiments. "Leaf physiology" was described by the leaf soluble carbohydrates (SS), starch (ST) concentrations and LWC. The "Disease" variable was described by the variables characterizing the two basic pathogen processes: the infection efficiency (Inf) and the sporulation per colony (Spoc). The standardized latent variables were estimated as linear combinations of their centered MVs. Collinearity between manifest variables was allowed. The PLS-path model was described by the measurement model, which related the different MVs to their own LVs, and the structural model, which linked the endogenous LV "Disease" to the other LVs: "Leaf growth," "Leaf physiology," and "Year." The inner estimate was performed using a path weighting scheme algorithm. Confidence intervals on regression coefficients are estimated by bootstrap methods (500 random sampling of 280 individuals of the observed data set). Two criteria of the goodness of fit of the model (GoF) are provided to evaluate the external model (relationship between MVs and LVs) and the internal model (relationship between LVs). Altogether, 321 observations (leaves) were considered (49 from 2005_exp1, 64 from 2005_exp2, 117 from 2009_exp4, 50 from 2010_exp5, and 41 from 2010_exp6). Observations on leaves older than 31 days were not considered to avoid introducing bias between the early and late experiments. Missing values were estimated using NIPALS procedures. The analysis was performed using the XLstat PLS-PM module (version 2012.2.02).

Finally, logistic regression was performed on the whole data set, including old leaves. The Spo variable was transformed into binary form with a value of 1 for Spo >3000 (significant peak with the particle counter) and 0 for less. Then, a model was fitted to describe how the chance of the event of a "diseased" leaf occurring depends on a maximum of one or two covariables, among which are "LA," "LAdev," "LS," "SS," "ST," and "1/LWC." The regression assumes that $P(Y = 1/X = exp(\beta_0 + \beta_1 X_1 + \beta_2 X_2)/exp(\beta_0 + \beta_1 X_1 + \beta_2 X_2)$ with Y the outcome and X the covariates. The model parameters β are estimated by the method of maximum likelihood. The analysis was performed on 497 individuals from the 5 experiments [261 leaves classified as "healthy" = "non-sporulating"; and 236 classified as "diseased"; null hypothesis P(D) = 0.47]. Among these leaves, 30 were randomly sampled for model validation. The ability of the model to distinguish between low and high risk for a leaf to be diseased was tested by ROC (receiver operating curve) curve analysis. The ROC curve plots the sensitivity (proportion of truly "positive," here "diseased," observations classified as such by the model) function of the 1-specificity (the specificity is the probability of the model predicting the sample "negative," given that the observation is "negative," here "healthy"). The area under the curve yields the ability of the model to correctly distinguish between healthy and diseased leaves. When the AUC is high (>0.8), the model has high discrimination ability.

RESULTS

Environmental Growing Conditions

The first leaves were marked on April 29 for Cabernet Sauvignon (2005, exp. 1–2–3), corresponding to a sum of 138.7°C growing degrees (GDs) and on April 14 and April 19 for Merlot, corresponding to 52.1°C GD (2009 exp. 4), and 66.2°C (2010 exp. 5–6), respectively. For each experiment, there was a linear relationship between leaf age (LA) and the sum of GD for a leaf during its development (LAdev), with an increased difference for older leaves. The GD globally explained the number of leaves per shoot for each experiment, with ∼21°C for each newly expanded leaf. For Cabernet Sauvignon, the leaves sampled for experiment 1 (early May 2005) were those developed at the coldest temperature: a 13-day-old leaf developed under a similar GD as a 10-day-old leaf from experiment 2 (**Figure 1**). In comparison, for Merlot, the leaves sampled for exp. 6 (late June) encountered the coldest period: 13-day-old leaves developed under a similar GD as 10-day-old leaves from exp. 5 (end of May).

Infection Rate Function of Leaf Age

In 2005, for the first sampling date (exp. 1), no significant difference in infection efficiency was observed between the different leaf ages of Cabernet Sauvignon (**Table 3**), whereas for the second (exp. 2), and third experiments (exp. 3), which occurred later in the season, the youngest leaves up to 6 days old displayed significantly higher infection rates. For experiments 2 and 3, we could adjust the data of infectious efficiency to the same exponential decrease model (**Figure 2A**, **Table 4**-M1). In such a model, 10-day-old leaves had an infection efficiency that decreased to 0.25. When the data were standardized (data divided

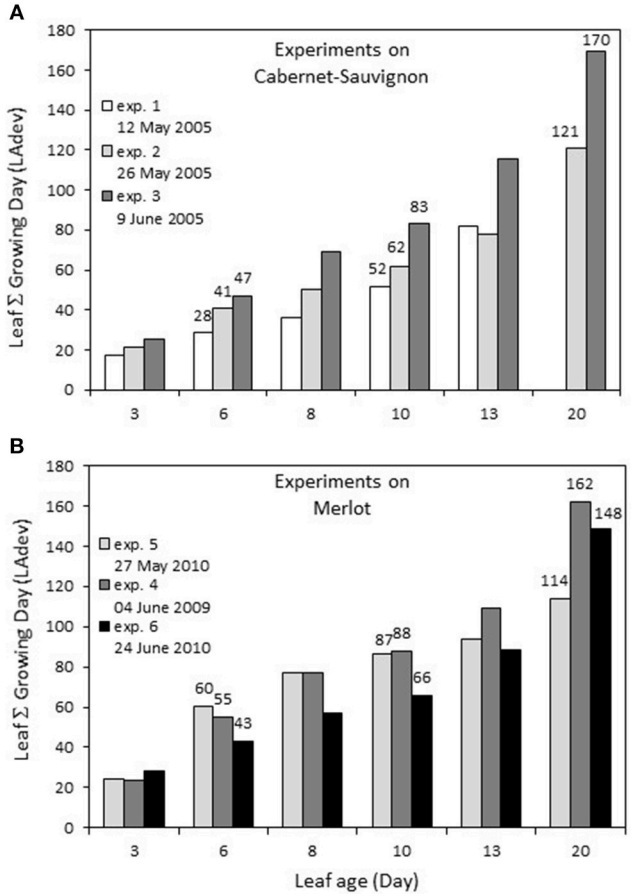

FIGURE 1 | Sum of growing days (Sum of daily temperature >10°C) encountered by a leaf during its development depending on its age, for experiments on Cabernet Sauvignon **(A)** and Merlot **(B)**. Experiments on Cabernet-Sauvignon were conducted on 12, 26, May and 9 June 2005 (exp. 1, 2, 3) and experiments on Merlot were conducted on 4 June 2009, 27 May and 24 June 2010 (exp. 4, 5, 6).

by the maximum % of infection on the shoot), the whole set of data could be adjusted to a decreasing exponential model with an R^2 of 0.59 (**Figure 2B**, **Table 4**-M1). Thus, a 10-day-old leaf lost approximately half of its infectivity, compared to the most susceptible ones. For the Merlot cultivar, the rate of infection efficiency also showed an exponential decrease with leaf age. Very young leaves were excluded from the analysis since we could not exclude that the tape test was not disturbed on particularly hairy young leaves (**Figure 5A**, **Table 5**-M1). For experiment 4 (4 June 2009) and 5 (27 May 2010), with similar environmental conditions, the decrease with leaf age was quite similar, despite a higher rate of infection for very young leaves (I_0) in experiment 4. For experiment 6 (24 June 2010), leaves up to 16 days old that developed at cooler temperatures showed a high rate of infection, and then the rate decreased very quickly.

Colony Growth Function of Leaf Age

The maximum diameter of a colony produced by single conidia was, on average, smaller on leaves older than 10 days for Cabernet Sauvignon (**Table 3**). A model with a decreased diameter at the inflection point of 8.35 days (a_{50}), a maximum diameter (M) on young leaves of 6.8 mm and a minimum diameter (m) of 4.6 mm for older leaves, fit the data with an $R^2 = 0.41$ (**Table 4**-M2, **Figure 3A**). On average, the sporulation of a colony was exponentially correlated with the maximal diameter attained by the mycelium network (**Table 4**-M4, **Figure 3B**), but at <5 mm, the level of sporulation was low and constant, indicating that a colony with only a two-millimeter difference in diameter (e.g., between 5 and 7 mm) will generate twice as many more spores. For Merlot, the trends and models were the same but with different parameters depending on the experimentation. In experiments 4 and 6, the maximum diameters were greater than in experiment 5. Similar to infection efficiency, slower growth appeared for older leaves in experiment 6 (a50 = 16.93 vs. 12.6 or 12.17 for exp. 5 and 4) (**Table 5**-M4, **Figure 5B**). Sporulation per colony was much higher for experiment 4 (**Figure 5D**).

Sporulation Function of Leaf Age

The variable sporulation (Spo) measured on inoculated leaf discs results from three successive processes: infection efficiency, mycelium growth and sporulation. From this point of view, it could be considered an integrative variable of susceptibility. The Spo variable followed a clearly bell-shaped curve function of leaf age for experiments 1 and 2, with higher levels of spores produced on 3- to 6-day-old leaves and a decrease for 8-day-old leaves (**Figure 4A**, **Tables 3**, **4**-M3). For experiment 3, on average, the youngest leaves had the highest level of sporulation. When the three experiments were pooled and standardized to homogenize the shoots, the same bell-shaped curve was obtained (**Figure 4B**, **Table 4**-M3) with a high level of sporulation for leaves aged between 3 and 8 days, corresponding to a plastochron index (LPI) between 1.3 and 1.7 (first to second leaf expended). Sporulation per colony (Spoc), which is independent of infection efficiency, also had this bell-shaped curve (**Figure 4C**, **Table 4**-M3). For experiment 2, for which the data were most numerous, the number of spores produced per area of sporulating colony (the sporulation capacity) was significantly higher (P = 1) for very young, susceptible leaves (1–6 days), compared to older leaves (≥10 days) (295 sp.mm² against 167 sp.mm²). This finding is consistent with the hypothesis that, for very young leaves, the higher sporulation results from an increase rate in the hypha branching combined with an increased number of spores produced per conidiophore. For Merlot, the sporulation curve with leaf age was similar to that observed on Cabernet Sauvignon, but the stage of high sporulation (Spo and Spoc) lasted longer, with increased sporulation for 5- to 16-day-old leaves with a peak at 6, 9, or 14 days, depending on the experiment (**Figure 5C**, **Table 5**-M3). This outcome matched an LPI of 2.5 (exp. 6) to 3.3 (exp. 4).

Leaf Physiological Evolution

Total non-structural carbohydrate (TNC) concentrations tended to follow sigmoid curves regarding leaf age. The soluble sugars concentration (SS) displayed a strong and rapid increase for young leaves, followed by a plateau for older ones. For Cabernet Sauvignon, this change appeared on 8- to 12-day-old leaves (LPI

TABLE 3 | Effect of leaf age of Cabernet Sauvignon on the disease variables tested by variance analyses and mean comparisons for each leaf age level.

	Exp.1				Exp.2				Exp.3			
Leaf age	**Inf**	**Spo**	**Spoc**	**Diam**	**Inf**	**Spo**	**Spoc**	**Diam**	**Inf**	**Spo**	**Spoc**	**Diam**
1	0.373^{a}	20569.8^{ab}	8447.9^{a}	6.31^{ac}	0.534^{a}	16675.5^{b}	14935^{a}	7.15^{a}	0.442^{a}	34328.6^{a}	12920^{a}	8.06^{a}
3	0.476^{a}	24806.9^{ab}			0.467^{a}	45861.6^{a}			0.468^{ab}	25283.1^{a}		
6	0.436^{a}	32483.6^{a}	8600.0^{a}	5.90^{ac}	0.434^{ac}	53627.0^{a}	12108^{ac}	7.8^{a}	0.387^{ab}	19720.7^{ab}	18280^{ab}	7.39^{ab}
8	0.474^{a}	21340.9^{b}	8431.9^{a}	6.50^{a}	0.292^{ab}	13138.9^{b}	6965^{bc}	6.58^{ac}	0.299^{abc}	18105.5^{abc}	12600^{abc}	6.96^{ab}
10	0.457^{a}	7438.0^{c}	4112.4^{b}	5.34^{bc}	0.214^{b}	8294.5^{b}	3673^{b}	4.41^{bc}	0.249^{bc}	8992.7^{bcd}	5655^{c}	4.63^{c}
13	0.349^{a}	1974.5^{c}	3915.6^{b}	5.25^{bc}	0.173^{b}	7739.5^{b}	4518^{b}	4.88^{bc}	0.170^{bcd}	4010.196^{d}	6664.3^{c}	4.78^{c}
15					0.090^{b}	8752.4^{b}			0.103^{cd}	1227.4^{d}		
17					0.149^{b}	1864.4^{b}			0.143^{cd}	3362.370^{d}		
20					0.238^{bc}	5820.6^{b}			0.105^{cd}	3518.1^{d}		
22					0.113^{b}	8394.9^{b}			0.033^{d}	3324.0^{d}		
24					0.176^{b}	4857.2^{b}	3510^{b}	4.62^{bc}	0.121^{cd}	4363.1^{bcd}	7590^{bc}	3.75^{c}
27					0.134^{b}	4857.2^{b}			0.003^{d}			
29–39									0.048^{d}	4275.05^{cd}	7850^{bc}	5.75^{bc}
df model, error	5, 43	5, 88	5, 37	4, 44	11, 95	11, 114	5, 43	6, 56	12, 144	11, 76	6, 16	6, 36
F fisher	1.71	27.54	8.41	4.49	10.73	48.24	16.93	8.72	13.35	8.37	11.03	14.1
P-value	0.154	<0.0001	<0.0001	0.0039	<0.0001	<0.0001	<0.0001	<0.0001	<0.0001	<0.0001	<0.0001	<0.0001

Inf, percentage of infectious spores; Spo, sporulation of inoculated leaf disks; Spoc, sporulation of the colony; Diam, maximal colony diameter. Different letters near the average indicate significant difference at P < 0.05 according to the Tukey-Kramer multiple comparison test.

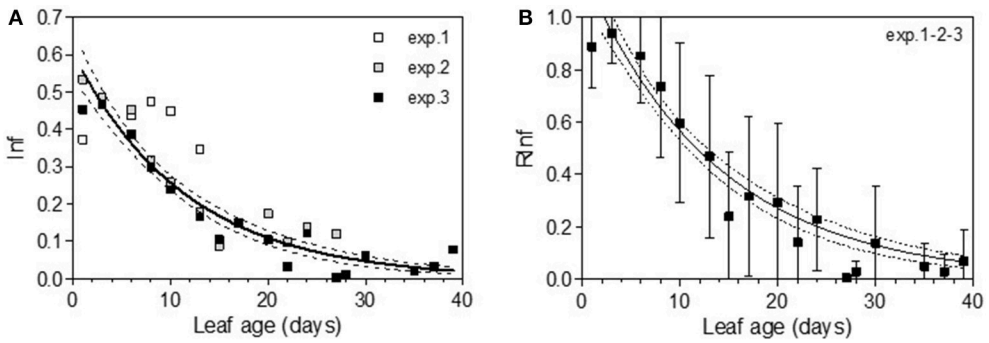

FIGURE 2 | Infection efficiency rate (Inf) **(A)** and relative infection efficiency rate (RInf) **(B)** as a function of leaf age for experiments on Cabernet Sauvignon. Bars indicate standard deviations. Plain lines correspond to the fitted model M1 in **Table 4**. Dashed lines correspond to the 95% confidence bands on the models.

= 2.7 to 3.4), while for Merlot, it appeared later: 10- to 14-day-old leaves (exp. 4 and 5, LPI = 3.9) to 14-to 16-day-old leaves (exp. 6, LPI = 3.7) (**Figures 6A,C**). The level reached for old leaves depended on the experiments. The leaf starch concentration was also highly variable with leaf age, but no starch was detected within the youngest leaves (<10 days) (**Figures 6B,D**). Leaves showing an increase in SS reached ∼50% of their final size (∼150 and 270 cm^2 for, respectively, CS and M), consistent with the time for transition between sink-to-source tissue (**Figures 7A,C**). The increases in the leaf soluble sugar content and leaf age were associated with a decrease in leaf water content (**Figures 7B,D**).

Thus, the processes of infection efficiency, sporulation and colony growth associated with leaf age showed similarities between the experiments on Cabernet Sauvignon and Merlot: a lower rate of mycelium growth and the end of the peak of a high level of sporulation matching an increase of sugar (SS); in comparison, the decrease in infection efficiency was more gradual with leaf age, as was the decrease in leaf water content. Infection efficiency is more closely correlated with leaf age (−0.68), leaf water content (−0.41), and starch (−0.32) than is sporulation (−0.54, −0.32, −0.30). Sporulation per colony was also significantly correlated with soluble sugar (−0.25), although it was more influenced by the experiments on Cabernet Sauvignon, for which we had more colonies for a wider range of leaf ages. For Cabernet Sauvignon, the proxy of the sporulation capacity (number of spores produced per unit area of sporulating colony) was significantly correlated with leaf age (−0.52) and with the amount of sugar (−0.64), indicating that colonies on

TABLE 4 | Results of model fitting for disease variables for experiments on Cabernet Sauvignon.

Model equation	$Y = I_0 \exp^{-kX}$			$Y = m + \frac{M-m}{1+10^{(X-q50)}}$		$Y = B + A\exp\left[-\left(\frac{(X-c)}{D}\right)\right]^2$					$Y = a\exp^{bX}$	
	with Y = Dependent variable and X = leaf age variable			**with Y = Dependent variable and X = leaf age variable**		**with Y = Dependent variable and X = leaf age variable**					**with Y = Dependent variable and X = leaf age variable**	
Dependant variable		Inf	RInf		Diam		Spo	Spo	Spo	Spoc	RSpo		Spoc
Model identification		M1	M1		M2		M3	M3	M3	M3	M3		M4
Experimentation		exp.2-3	exp.1-2-3		exp.1-2-3		exp.1	exp.2	exp.3	exp.1-2	exp.1-2-3		exp.2
df		209	231		120		56	91	66	64	182		41
Parameter value	I_0	0.606	1.181	m	4.64	A	34357	54676	32600	12673	0.95	a	515.5
	k	0.086	0.073	M	6.86	B	2124	7498	3628	3029	0.12	b	0.4
				$a50$	8.35	c	5.151	4.769	0.699	4.455	4.659		
						D	3.479	2.957	6.666	3.566	3.65		
Goodness of fit R^2		0.57	0.59		0.41		0.76	0.85	0.79	0.72	0.88		0.74
P-value for Replicates tests		0.7	0.1		0.71		0.7	0.6489	0.96	0.68	0.26		0.81
Evidence of inadequate model		No	No		No		No	No	No	No	No		No
Outliers		0	0		0		4	1	6	0	0		0

Inf, rate of infectious spores (branched conidia at 72hpi); RInf, relative rate of infectious spores; Diam, colony diameter (mm); Spo, number of spores generated per cm^2 of inoculated leaf area; Spoc, number of spores generated per colony; RSpo, relative rate of spores generated per cm^2 of inoculated leaf.

TABLE 5 | Results of model fitting for comparison of infection rate (Inf), colony diameter (Diam), and sporulation rate (Spo) for experiment on Merlot.

Model equation	$Y = I_0 \exp^{-kX}$			$Y = m + \frac{M-m}{1+10^{(X-q50)}}$			$Y = B + A\exp\left[-\left(\frac{(X-c)}{D}\right)\right]^2$						$Y = a\exp^{bX}$	
				With *Y* = Dependent variable and *X* = leaf age			**With *Y* = Dependent variable and *X* = leaf age**						**With *Y* = Dependent variable and *X* = colony diameter**	
Dependant variable		**Inf**	**Inf**	**Inf**		**Diam**	**Diam**	**Diam**		**Spo**	**Spo**	**Spo**	**Spoc**	**Spoc**	**Spoc**		**Spoc**	**Spoc**
Model identification		M1	M1	M1		M2	M2	M2		M3	M3	M3	M3	M3	M3		M4	M4
Experimentation		exp 4	exp 5	exp 6		exp 4	exp 5	exp 6		exp 4	exp 5	exp 6	exp 4	exp 5	exp 6		exp 4	exp 5-6
df		137	56	85		40	22	24		131	63	91	139	61	94		43	45
Parameter value	I_0	0.63	0.38	2243	m	4.91	5.15	2.67	A	73207	55842	62308	20134	2895	7240	a	883.7	241.3
	k	0.095	0.067	0.615	M	9.93	8.15	10.3	B	2606	2312	449.5	807.6	756.9	210.2	b	0.29	0.26
					$a50$	12.17	12.61	16.93	c	8.93	6.51	13.29	8.36	6.28	11.99			
									D	5.14	3.68	3.47	4.68	3.13	3.24			
Goodness of fit R^2		0.74	0.54	0.75		0.66	0.24	0.69		0.81	0.72	0.89	0.6	0.21	0.67		0.54	0.5
P-value for Replicates		0.55	0.11	0.79		0.35	0.45	0.72		0.37	0.98	0.34	0.99	1	0.99		0.89	0.21
Evidence of inadequate model		No	No	No		No	No	No		No	No	No	No	No	No		No	No

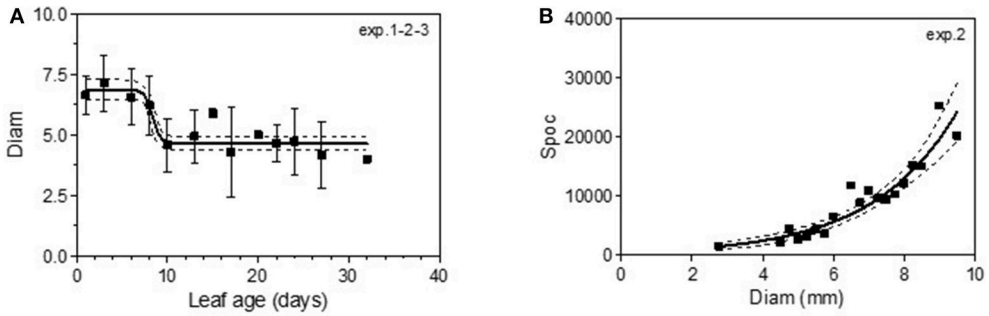

FIGURE 3 | Colony diameter in mm (Diam) as a function of leaf age after 14 days of colony growth **(A)** and number of spores produced per colony (Spoc) as a function of the colony diameter **(B)** for Cabernet-Sauvignon. **(A)** correspond to the average colony diameter from experiments 1–3 whereas Panel **(B)** to the spores per colony from experiment 2. Plain lines correspond to the fitted models M2 **(A)** and M4 **(B)** in **Table 4**. Dashed lines correspond to the 95% confidence bands on the models, and bars correspond to the standard deviation.

young leaves with smaller amounts of sugar are significantly able to produce more spores per colony. When a period of cold is encountered, processes are delayed (increased sugar, leaf development, decreased leaf water content), and the duration of the sensitivity period is lengthened (exp. 6). Very early in the growing season (exp. 1), all of the leaves are as susceptible as each other to infection.

Disease Severity Prediction

Partial least-squares path modeling allowed for highlighting the relative contributions of the studied composite variables ("Leaf growth" and "Leaf physiology") in the global explanation of the global "Disease" variable, depending on the experimental conditions ("Variety," "Climate," "Year"). The "Disease" variable was explained at $R^2 = 0.61$ by "Leaf growth," "Leaf physiology," and "Year," with relative contributions of 57.3, 19.5, and 23.2%, respectively (**Figure 8**). Variations in leaf physiology were explained at $R^2 = 0.50$, mainly by leaf growth (87%) (leaf age, leaf temperature for development and leaf surface). "Variety" and "Climate" only poorly contributed to leaf physiology level. When considering total effects (indirect plus direct effects) on the disease, "Leaf growth" had a higher effect on "Disease" (−0.68) compared with "Leaf Physiology" (−0.27), due to the correlation between variables. Leaf water content (1/LWC) and simple sugars (SS) made the greatest contributions to "Leaf physiology" (w = 0.62 and 0.38, respectively), indicating that, regardless of whether sugar (SS) increases or water content decreases, the "Disease" variable decreases. The "Year" effect certainly reflects the variation of isolate aggressiveness that was obvious when considering the level of sporulation per colony diameter. The relative goodness of fit of the model was high ($GoF_{rel} = 0.85$) with moderate absolute goodness of fit ($GoF_{abs} = 0.55$), indicating that the predictors used only partly explained disease variation.

Logistic regression showed that, with a maximum of one co-variable, leaf age was the best predictor ($Pr > LR < 0.0001$, $\beta_0 = 4.12$, $\beta_1 = -0.20$), with sensitivity of 86.02% (73.3% for the validation sample) and very high discrimination (AUC = 0.927) of "diseased" vs. "not diseased" leaves. The individuals not well assigned were those at the transition state or very young leaves that were not sufficiently sporulating but that were considered susceptible by the model. If we analyzed the probability after model fitting, there was a probability for a leaf to be susceptible of 0.8 for an average leaf age of 13.3 days [11.4; 14.9] and a probability decrease at 0.5 for a leaf age of 20 days [18.7; 21.4]. With two co-variables, leaf age and starch content were the best predictors, but the model was only slightly improved (AUC = 0.936) with slightly higher specificity (prediction that the leaf is healthy given that it is observed to be healthy).

DISCUSSION

Understanding and quantifying the process of ontogenic resistance of the grapevine leaf of the two susceptible, first widely cultivated wine cultivars Cabernet Sauvignon and Merlot to one of the major fungal pathogens, *E. necator* is a prerequisite to promote more sustainable pest management strategies in viticulture. Although ontogenic resistance on grapevine bunches has been well documented (Ficke et al., 2002; Gee et al., 2008), little evidence is available of similar processes for leaves, although leaves are the primary targets for the onset of epidemics. In this study, we attempted to analyse and quantify how the life traits of the pathogen were impacted by ontogenetic resistance and find predictors on the plant side associated with them. To obtain a generic view of the phenomenon, we used shoots coming from vinestocks grown in vineyards under different environmental conditions, and we used several predictable variables that were more or less easy to measure and relevant to analyse leaf state change.

Pathogen behavior was analyzed in relation to leaf age and was characterized by: (i) highly infectious colony growth and sporulation rates for young leaves (<10 days for Cabernet Sauvignon and <16 days for Merlot), with significantly higher sporulation on very young leaves; and (ii) lower colony growth, with a strong decrease in the sporulation rate and in the relative infection rate for older leaves (>10–16 days). Then, all of the chronologic infectious steps of the pathogen—infection efficiency, mycelium growth and sporulation—are affected by the leaf age. The sporulation capacity is even increased on very

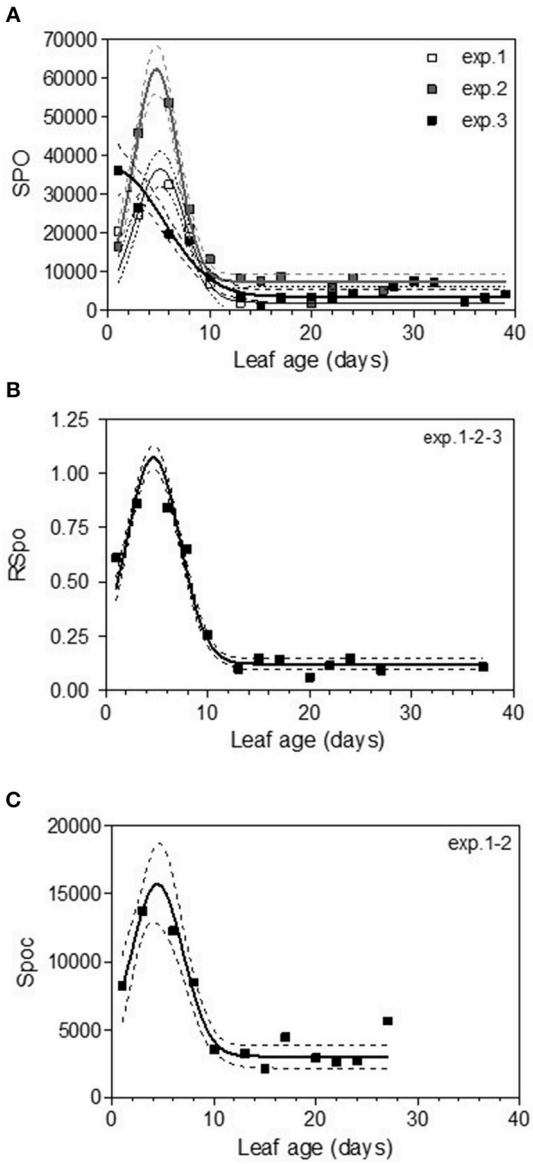

FIGURE 4 | Sporulation (number of spores produced per cm² of infected leaf disk) (Spo) **(A)**, relative sporulation (RSpo) **(B)** and number of spores generated per colony (Spoc) **(C)** as a function of leaf age for experiments on Cabernet Sauvignon. Plain lines correspond to the fitted model M3 in **Table 4**. Dashed lines correspond to the 95% confidence bands on the models, and bars indicate standard deviation.

young leaves, at least for Cabernet Sauvignon. This increase in sporulation was correlated to low sugar content, whereas the decrease in infection efficiency was more closely correlated with a decrease in leaf water content and an increase of starch. If we consider the leaf plastochron index, instead of leaf age, compared with other studies, the peak of sporulation was 1.4 for Cabernet Sauvignon and 2.7 for Merlot. These values of LPI varied by less than one point for the average temperature encountered during the experiments (15.9–18.7°C), indicating that, at each time during the growing season, very few leaves are potentially highly susceptible (∼2 to 3 per shoot), and the landscape of susceptibility should be higher for Merlot than for Cabernet Sauvignon. In a previous study (Merry et al., 2013), Cabernet Sauvignon leaves showing the maximum severity were those at LPI 3.7 at 18°C (constant temperature in the glasshouse), and the range of maximum severity was for leaf positions 2.1- 4.8. At 25°C, for a higher rate of leaf emergence, the mean modal leaf position for maximum severity was 4.4. Comparatively, in our study with leaves coming from field shoots under natural irradiance and fluctuating temperatures, the maximum severity (corresponding more or less to Spo) was earlier (1.4), with the decrease of leaf susceptibility even sharper. In another study performed on cuttings in growth chambers, colony hyphal length and infection efficiency decreased on both resistant and susceptible cultivars as leaves matured (LPI 1 to LPI 8), with, however, high variations between cultivars (Doster and Schnathorst, 1985).

The high infection rate and increased colony growth on young leaves resulted in an increase in penetration sites and haustoria formation favoring pathogen nutrient uptake and, consequently, a higher sporulation rate. In our study, the very young, susceptible leaves were characterized by a small amount of glucose content, higher water content and a high leaf extension rate. These expanding leaves reached only ∼1/3 of their final size, consistent with the status of sink tissues for grapevines (Lebon et al., 2008; Scott, 2008). Sink leaves depend on other leaves for their energy supply, and the carbohydrates that they receive from source plant parts are immediately used for respiration, growth and the synthesis of new cell components and are therefore not stored. Sink leaves correspond to leaf plastochron indices of 1–3, showing maximal photosynthetic activity (30% for LPI 3) (Zufferey et al., 2000) and higher day respiratory rates (Rd) over the whole growing period. Rd values in young leaves (LPI 3-5) on primary shoots were two times greater than those of mature leaves (Zufferey, 2016). The leaves in transition from sink to source showed a high increase in sugar levels and were able to export sugars when the supply in carbohydrate exceeded the needs for metabolism. In our study, this transition matched decreases in mycelium growth, sporulation and infection efficiency when the number of source leaves exceeded that of sink leaves. When it was not the case, early in the growing season (like for experiment 1), the infection efficiency was not affected by leaf age, and only sporulation decreased for the two basal leaves. The correspondence between the sink to source transition and susceptibility to powdery mildew were once identified on leaves from Cabernet Sauvignon cuttings by autoradiography after $^{14}CO_2$ labeling (Merry et al., 2013). Our study provided some clues about the ontogenic resistance process by decomposing the sequential development of the pathogen (infection rate, colony growth and sporulation), which converges toward a specific age-related transition in the receptivity of the leaf tissues. The complete life cycle of the fungus (up to sporulation) is restricted to sink tissue (small amount of sugar), while the first steps (infection, colony growth) can extend later. Based on these experiments for different environmental conditions and two varieties, we can accurately predict the susceptibility of the leaf with its age as a predictor: a leaf aged on average 13.3 days had a very high probability (0.8) of being susceptible, while this probability dropped to 0.5 one week later.

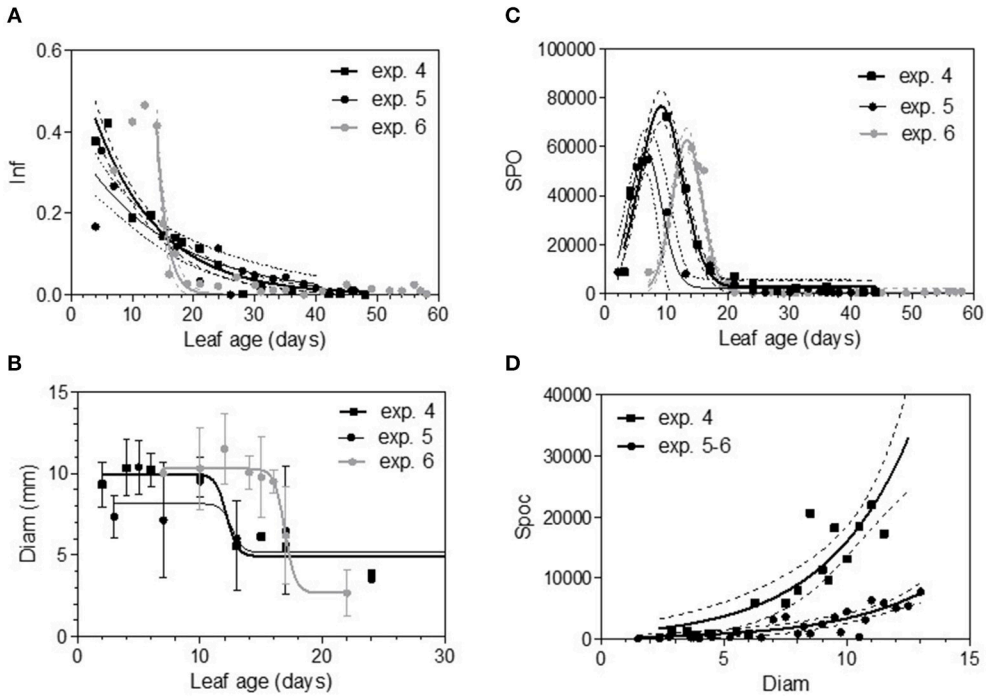

FIGURE 5 | Infection efficiency rate (Inf) **(A)**, colony diameter (Diam) **(B)**, and sporulation (number of spores produced per cm² of infected leaf disc) (Spo) **(C)** as a function of leaf age and sporulation per colony (Spoc) as function of colony diameter **(D)** for Merlot experiments. Plain lines correspond to the fitted models M1 **(A)**, M2 **(B)**, M3 **(C),** and M4 **(D)** in **Table 5**. Dashed lines correspond to the 95% confidence bands on the models, and bars correspond to the standard deviation.

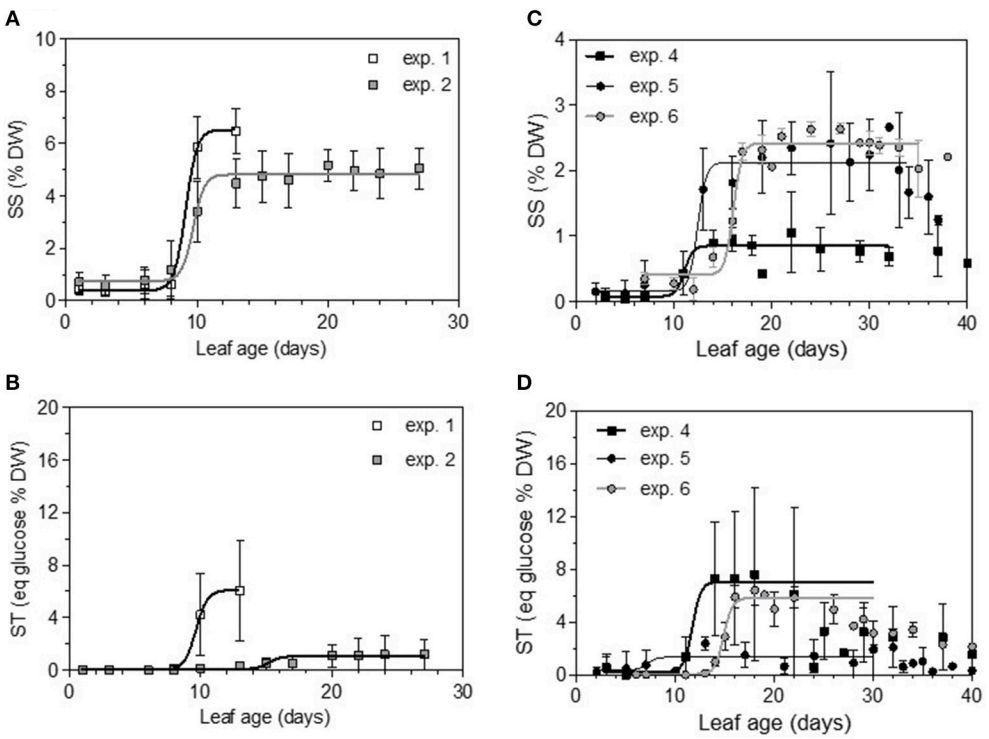

FIGURE 6 | Soluble sugars (SS) and complex sugar (ST) concentrations expressed as percentages of leaf disc dry weight and as a function of leaf age for the two first dates of sampling on Cabernet Sauvignon **(A,B)** and Merlot **(C,D)**. Bars indicate standard deviations.

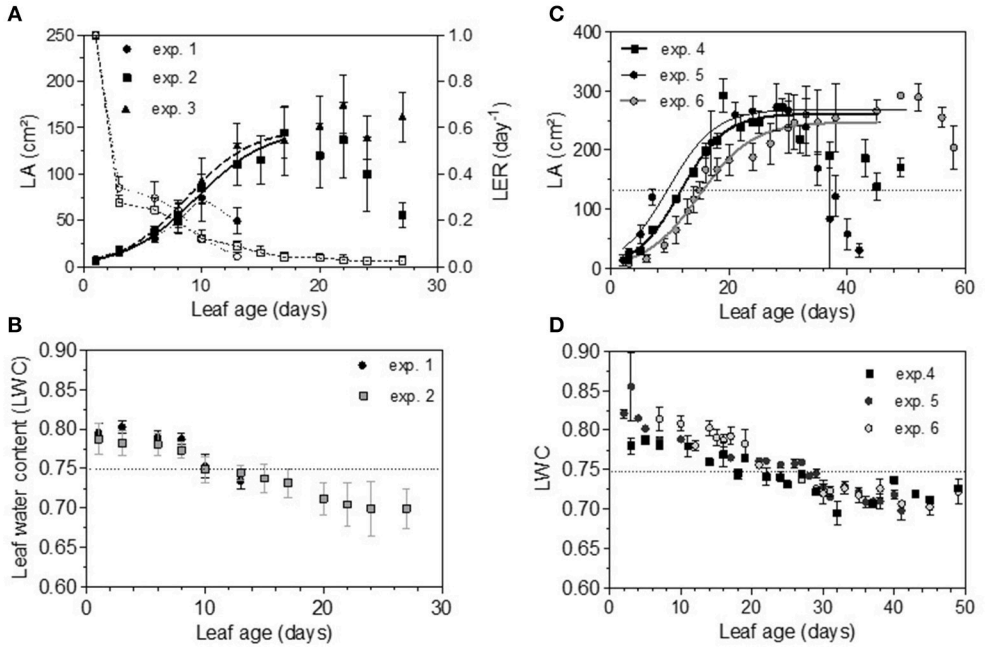

FIGURE 7 | Evolution of leaf area (LA), leaf extension rate (LER) (dashed lines) and leaf water content (LWC) for Cabernet Sauvignon **(A,B)** and for Merlot **(C,D)**. Bars indicate standard deviations.

Decreases in incidence and severity of powdery mildew with leaf age or development stage were also identified on strawberry (Carisse and Bouchard, 2010) and were reported to be a robust and biologically consistent process with a response consistent across cultivars and isolates employed and between the various sites tested (Asalf et al., 2014). Regarding pea powdery mildew, a resistance gene involved in post-penetration cell death and a reduction in percentage penetration success in mature leaves confers complete resistance in the field under high temperatures or on mature leaves (Fondevilla et al., 2006). On *Eucalyptus grandis*, all of the steps of the development of the rust *Puccinia psidii*—germination, appressorium formation, penetration and sporulation—were altered with increased leaf age (Xavier et al., 2015). For other pathosystems, the susceptibility can increase with leaf age, as is the case for another rust, *Melampsora larici populina*, which is more aggressive on mature leaves of poplar (Maupetit et al., 2018). The authors observed an increase in uredia (colony) size and a higher sporulation rate with increased LPI and lower sporulation capacity. In this case, pathogen traits were not correlated with leaf sugar, but there was a negative correlation with phenolic content, which was higher in younger leaves. On pea, detached stipules were more receptive *to Mycosphaerella pinodes* as soon as visual senescence was observed (Richard et al., 2012).

Which Factors Are Involved in the Variation of the Ontogenic Resistance Process?

Our results attest to the repeatability of ontogenic resistance on leaves during vegetative growth for two susceptible cultivars. However, our results only explained 61% of disease variation. These variations can be linked to sampling shoots with differences in the implementation age of the ontogenic resistance process or between years/cultivars with variations in disease level. To explain variation between years, one parsimonious hypothesis is that it is based on differences in isolate aggressiveness. Indeed, a strong difference in sporulation for the same colony diameter was observed for different years. Variations between shoots and experiments depend on factors with effects on the sink-to-source status of the leaf, such as exposure to light before field sampling, crop load or even leaf damage. The transition to leaf resistance is, however, clearly related to the timing of the sink-to-source status rather than to the final level of glucose attained. Variations were also observed when leaves encountered a cold temperature, which slowed the physiological processes and delayed the timing of ontogenic resistance establishment (such as in experiment 6). We also observed that infection efficiency was not significantly different for the first leaves that emerged early in the season, which could emphasize the particular status of these first expanding leaves for which the source of assimilates used for growth first comes from retranslocation from the parent vine (Keller, 2015). Using ^{14}C tracer, it has been shown that, at the 5-leaf stage shoot, only the first basal leaf is able to export assimilates to the youngest one, and at the 6-leaf stage, two to three basal leaves behave as sources (Yang and Hori, 1980). The experiments were conducted on a hybrid of Labrusca, but this outcome was consistent with what we observed. Indeed in our first experiment on Cabernet Sauvignon, only the two basal leaves being in the transition from sink to source showing significantly less sporulation. This should enhance infection success when epidemics start very early in the season and surely contributes to their particularly damaging effects.

Although infection efficiency is very low on old leaves, it is not always null. We do not know the impact of these rare infections considering that they were not sporulating at the time

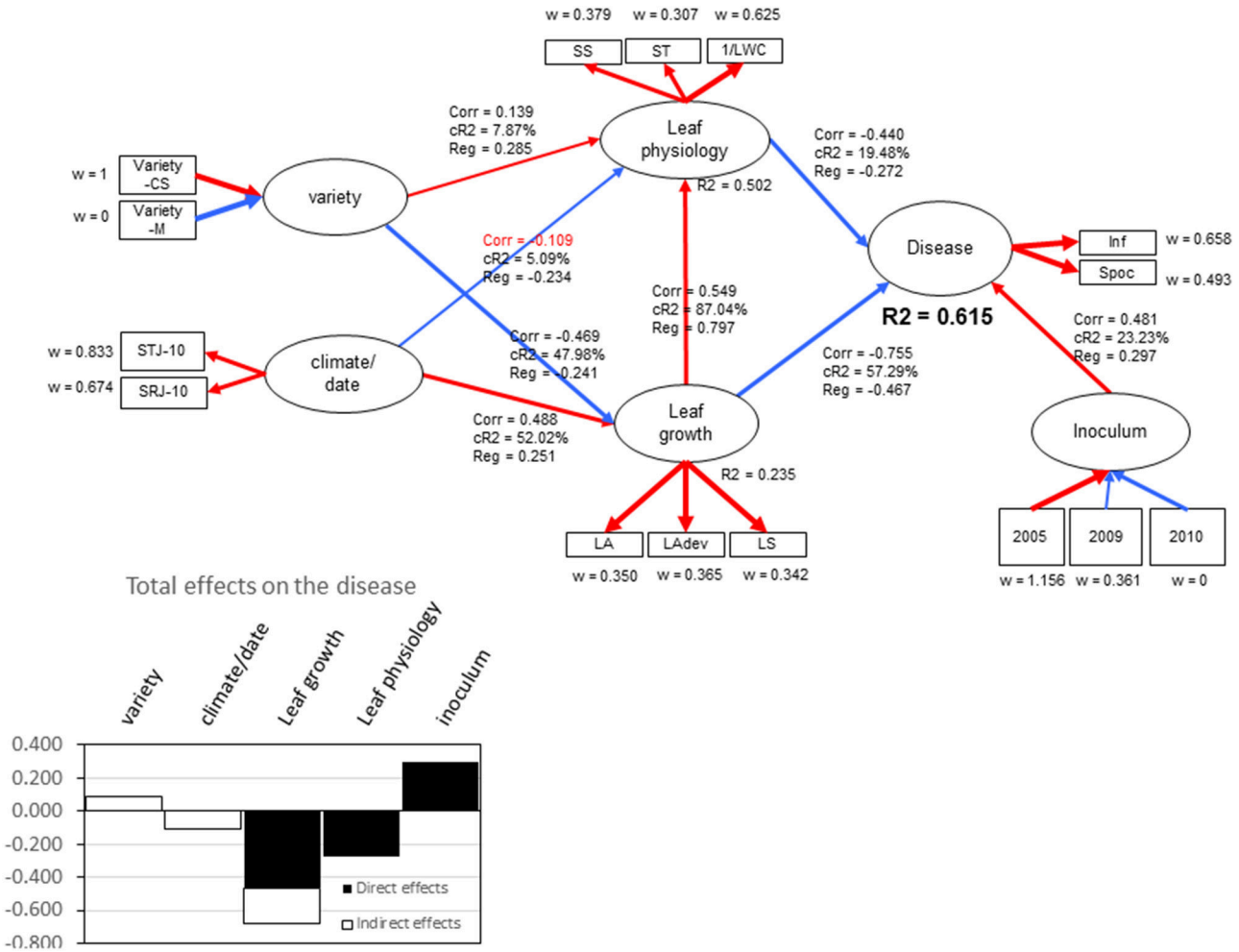

FIGURE 8 | Output of partial least squares path modeling for the two years of experiments describing the relationships between the endogenous latent variable "disease" to the other latent exogenous variables "Leaf growth," "Leaf Physiology," "Inoculum," "Variety," and "Climate/date." Corr indicates the correlation coefficient between two latent variables, CR2 indicates the relative contribution of exogenous latent variables to endogenous one, Reg indicates the regression coefficient, R^2 indicates the regression coefficient between two latent variables, and w indicates the outer weights yielding the covariances between the manifest variable and its inner latent variable. Blue lines indicate negative correlations, and red lines indicate positive correlations.

of assessment. In the pathosystems of apple/apple scab, diffuse colonies and mycelium that formed on old leaves continued to grow (Li and Xu, 2002), and these authors wondered whether these diffuse colonies could sporulate later in the season and become a source of mycelium for the formation of pseudothecia. On grapevines, we did not exclude that the translocation of carbohydrates from old leaves to berries during grape ripening would not modify leaf susceptibility or allow rare infected spores to continue their development and affect late colonies. This phenomenon has already been observed for other pathosystems, as especially demonstrated in the case of hermaphrodite plants, such as papaya (*Carica papaya* L.). Female fruit-bearing plants are susceptible to *Oidium caricae* on old leaves and fruit, whereas male plants are not attacked (Jarvis et al., 2002). These authors have advanced hypotheses of the shunting of assimilates from leaf to fruit to explain the differences. However, we could not observe any modification of ontogenic resistance processes after bunch closure (late July) on Merlot.

What Hypotheses Can Be Advanced to Explain the Process of Ontogenic Resistance Observed on Old Leaves?

Role of Sugar

The increase in carbohydrate concentration in old leaves could be involved in the activation of secondary metabolism. Soluble carbohydrates are known to control the expression of various metabolic and plant defense-related genes (Koch, 1996; Rolland et al., 2006), and high sugar content can also suppress fungus degradation enzymes, such as grape chitinase (Saito et al., 2011). Powdery-mildew diseases have already been classified as "high-sugar resistance" pathogens (Vanderplank,

1984), indicating reversal of susceptibility to high levels of sugars. The relationship between sugar amounts and osmotic pressure might also be involved (Koroleva et al., 2002). Increased osmotic pressure can challenge the pathogen during the first step of infection, slowing tissue colonization by limiting the process of penetration of secondary haustoria. This scenario is consistent with our observed reduction of colony diameter on old leaves. Increased osmotic pressure was hypothesized to explain the greater resistance of mature leaf epidermal cells to other powdery mildews on apple (Cimanowski and Millikan, 1970) and peach (Schnathorst and Weinhold, 1957; Weinhold and English, 1964).

Activation of the PTI

Transcriptome and proteome analyses showed that the susceptible variety Cabernet Sauvignon is able to initiate basal defense mechanisms (Fung et al., 2008; Fekete et al., 2009; Marsh et al., 2010). Transcriptome analyses of leaves (Dufour et al., 2016) also revealed overexpression of defense genes (phenylalanine ammonialyase, stilbene synthase, anthocyanidin synthase, chitinase, lipase) on Cabernet Sauvignon leaves at ages of 15 and 20 days, compare to leaves at ages of 7 and 10 days, only after powdery mildew inoculation (unpublished data). For young expanding leaves, a high rate of cellular reactions of plant defense might be energetic and, for the carbohydrates, its consumption too costly (Bethany et al., 2014). MLO genes, known as "powdery mildew susceptibility genes," might be involved in this regulation. It was hypothesized that adapted powdery mildew species release effectors that, by combining with specific MLO proteins, could suppress the host PTI (plant triggered immunity) in the young leaves (Dry et al., 2010). One hypothesis explaining ontogenetic resistance is that changes occur in the old leaves in the expression or activity of the MLO genes with the consequence of restoring the PTI (Qiu et al., 2015).

Constitutive Defenses

The transition in the trophic statute of the leaf bound up with development can also trigger the establishment of constitutive defenses to infection: cuticle thickness in *Lactuca sativa*, (Schnathorst, 1959) and *Prunus persica* (Weinhold and English, 1964); or the synthesis of antimicrobial compounds (Tattersall et al., 1997; Salzman et al., 1998). Precocious events of infection progress, such as germ tube initiation and appressorium differentiation, require physical or chemical cues (Muller and Riederer, 2005). Variations in cuticular waxes (quality and amount) during ontogenic development could be an inhibiting factor, consistent with the lower rate of conidium germination on old leaves that we observed. Constitutive defenses and PTI can be both active in source leaves.

How Can Ontogenic Resistance Be Used in Epidemic Management?

Given the repeatability of the results, it is unlikely that the susceptibility of young leaves can be reduced without significant cost for the plant. Our results clearly demonstrated that powdery mildew takes advantage of the compromise that the plant must make between growth and defense (Bethany et al., 2014). Even if it is tempting to think that new genome editing techniques will allow for the easy knockout of genes, such as MLO, the effect of these knockouts on the physiology of the plant remain unknown (Acevedo-Garcia et al., 2014; Malnoy et al., 2016). The rate of both primary and secondary leaf appearance can, however, be slowed by the winegrower, hence reducing the proportion of available susceptible young tissues per unit of time. Indeed, agronomical practices, such as cover-cropping and the use of a vigor-controlling rootstock, can decrease the rate of leaf appearance and consequently disease level (Calonnec et al., 2009; Schnee et al., 2011; Valdes-Gomez et al., 2011). Simulations have shown that a reduction in grapevine vigor, through a decrease in both the numbers and the rates of secondary leaf appearance, can slow epidemics (Burie et al., 2011; Mammeri et al., 2014). Other practices, such as thinning of old leaves, will decrease the photosynthesis of younger leaves, thereby potentially delaying their ontogenic resistance, whereas shoot topping of younger leaves does not impact leaf photosynthesis per unit of leaf area (Petrie et al., 2003). Consequently, thinning might be less favorable to increasing leaf resistance than shoot topping, without considering the potentially positive effect of light on tissue receptivity (Zahavi and Reuveni, 2012). Other cultural practices, such as minimal pruning, which results in increased shoot numbers, reduce leaf and shoot size, and more synchronous leaves emergence (Poni et al., 2000), could allow the plant to escape disease by simultaneously causing all leaves to behave as a source. Such cultural practices could also be used to enhance the resistance of varieties with specific resistance genes. It would be interesting to revisit the theory of grapevine balance using tools of genetics and physiology in a general context of dieback and climate change, in which yields are sought, while maintaining control of pathogens that are very deleterious, such as mildews, is a prerequisite. Coupling functional structural grapevine physiology (Weinhold and English, 1964) and pathogen development models (Calonnec et al., 2008) would help to better understand crop susceptibility under various environmental conditions and complex canopies, while early protection of the foliage, which allows for desynchronizing of the disease cycle and the crop cycle toward a higher percentage of resistant leaves, should be preferred.

CONCLUSIONS

Our results revealed a clear correlation between the appearance of grapevine leaf ontogenic resistance and the leaf transition state from sink to source. The soluble and complex sugars, leaf water content and leaves' extension rate constitute indicators of a change in the metabolic processes and are indirect markers of tissue age-related resistance. From a practical point of view, the additional effects of ontogenic resistance modification through crop management and resistant cultivars should be explored to obtain better control of powdery mildew epidemics in

sustainable agriculture (Calonnec et al., 2013a). Moreover, the integration of this developmental process into a grapevine disease management program requires reconsideration of fungicide spraying with regard to the formatting of organ susceptibility windows.

AUTHOR CONTRIBUTIONS

AC: head of the research programme, data analyses, writer. JJ: experimental technician. PV: collaborator for physiology data analysis and experimentation. SS: post-doctoral student, experimenter, writer.

FUNDING

This study was supported by a grant from the Agence Nationale de la Recherche program SYSTERRA (ANR-08-STRA-04) and by the Aquitaine Regional Council.

SUPPLEMENTARY MATERIAL

The Supplementary Material for this article can be found online at: https://www.frontiersin.org/articles/10.3389/fpls.2018.01808/full#supplementary-material

Supplementary Figure S1 | Scheme of the experimental design.

REFERENCES

Acevedo-Garcia, J., Kusch, S., and Panstruga, R. (2014). Magical mystery tour: MLO proteins in plant immunity and beyond. *New Phytol.* 204, 273–281. doi: 10.1111/nph.12889

Ando, K., Hammar, S., and Grumet, R. (2009). Age-related resistance of diverse cucurbit fruit to infection by *Phytophthora capsici*. *J. Am. Soc. Horticult. Sci.* 134, 176–182.

Asalf, B., Gadoury, D., Tronsmo, A., Seem, R., Dobson, A., Peres, N., et al. (2014). Ontogenic resistance of leaves and fruit, and how leaf folding influences the distribution of powdery mildew on strawberry plants colonized by *Podosphaera aphanis*. *Phytopathology* 104, 954–963. doi: 10.1094/PHYTO-12-13-0345-R

Baillod, M., and Baggiolini, M. (1993). Les stades repères de la vigne. *Revue Suisse de Viticulture, d'Arboriculture et d'Horticulture* 25, 7–9.

Bethany, H., Yao, J., Montgomery, B., and Yang He, S. (2014). Growth-defense tradeoffs in plants: a balancing act to optimize fitness. *Mol. Plant* 7, 1267–1287. doi: 10.1093/mp/ssu049

Burie, J. B., Langlais, M., and Calonnec, A. (2011). Switching from a mechanistic model to a continuous model to study at different scales the effect of vine growth on the dynamic of a powdery mildew epidemic. *Ann. Bot.* 107, 885–895. doi: 10.1093/aob/mcq233

Calonnec, A., Burie, J.-B., Langlais, M., Guyader, S., Saint-Jean, S., Sache, I., et al. (2013a). Impacts of plant growth and architecture on pathogen processes and their consequences for epidemic behaviour. *Eur. J. Plant Pathol.* 135, 479–497. doi: 10.1007/s10658-012-0111-5

Calonnec, A., Cartolaro, P., and Chadoeuf, J. (2009). Highlighting features of spatiotemporal spread of powdery mildew epidemics in the vineyard using statistical modeling on field experimental data. *Phytopathology* 99, 411–422. doi: 10.1094/PHYTO-99-4-0411

Calonnec, A., Cartolaro, P., Naulin, J. M., Bailey, D., and Langlais, M. (2008). A host-pathogen simulation model: powdery mildew of grapevine. *Plant Pathol.* 57, 493–508. doi: 10.1111/j.1365-3059.2007.01783.x

Calonnec, A., Cartolaro, P., Poupot, C., Dubourdieu, D., and Darriet, P. (2004). Effects of *Uncinula necator* on the yield and quality of grapes (*Vitis vinifera*) and wine. *Plant Pathol.* 53, 434–445. doi: 10.1111/j.0032-0862.2004.01016.x

Calonnec, A., Schnee, S., Cartolaro, P., and Langlais, M. (2011). Modelling the effect of the grapevine growth and susceptibility on the dynamics of a powdery mildew epidemic. *IOBC/WPRS Bull.* 67, 123–130.

Calonnec, A., Wiedemann-Merdinoglu, S., Delière, L., Cartolaro, P., Schneider, C., and Delmotte, F. (2013b). How reliable are leaf bioassays for predicting disease resistance on fruit: a case study on grapevine resistance to downy and powdery mildew. *Plant Pathol.* 62, 533–544. doi: 10.1111/j.1365-3059.2012.02667.x

Carisse, O., and Bouchard, J. (2010). Age-related susceptibility of strawberry leaves and berries to infection by *Podosphaera aphanis*. *Crop Protect.* 29, 969–978. doi: 10.1016/j.cropro.2010.03.008

Cartolaro, P., and Steva, H. (1990). Maîtrise de l'oïdium en laboratoire. *Phytoma* 419, 37–40.

Cimanowski, J., and Millikan, D. (1970). Resistance of apple to powdery mildew and its relationship to osmotic activity of the cell sap. *Phytopathology* 60, 1848–1849. doi: 10.1094/Phyto-60-1848

Deliere, L., Cartolaro, P., Leger, B., and Naud, O. (2015). Field evaluation of an expertise-based formal decision system for fungicide management of grapevine downy and powdery mildews. *Pest Manag. Sci.* 71, 1247–1257. doi: 10.1002/ps.3917

Delière, L., Miclot, A. S., Rey, P., and Calonnec, A. (2010). Efficacy of fungicides with various modes of action in controlling the early stages of an *Erysiphe necator*-induced epidemic. *Pest Manag. Sci.* 66, 1367–1373. doi: 10.1002/ps.2029

Delp, C. (1954). Effect of temperature and humidity on the grape powdery mildew fungus. *Phytopathology* 44, 615–626.

Develey-Rivière, M., and Galiana, E. (2007). Resistance to pathogens and host developmental stage: a multifaceted relationship within the plant kingdom. *New Phytologist* 175, 405–416. doi: 10.1111/j.1469-8137.2007.02130.x

Deytieux-Belleau, C., Geny, L., Roudet, J., Mayet, V., Doneche, B., and Fermaud, M. (2009). Grape berry skin features related to ontogenic resistance to *Botrytis cinerea*. *Eur. J. Plant Pathol.* 125, 551–563. doi: 10.1007/s10658-009-9503-6

Doster, M. A., and Schnathorst, W. C. (1985). Effects of leaf maturity and cultivar resistance on development of the powdery mildew fungus on grapevines. *Phytopathology* 75, 318–321. doi: 10.1094/Phyto-75-318

Dry, I., Feechan, A., and Anderson, C. (2010). Molecular strategies to enhance the genetic resistance of grapevines to powdery mildew. *Aust. J. Grape Wine Res.* 16, 94–105. doi: 10.1111/j.1755-0238.2009.00076.x

Dufour, M.-C., Magnin, N., Dumas, B., Vergnes, S., and Corio-Costet, M.-F. (2016). High-throughput gene-expression quantification of grapevine defense responses in the field using microfluidic dynamic arrays. *BMC Genomics* 17:957. doi: 10.1186/s12864-016-3304-z

Fekete, C., Fung, R. W. M., Szabo, Z., Qiu, W. P., Chang, L., Schachtman, D. P., et al. (2009). Up-regulated transcripts in a compatible powdery mildew-grapevine interaction. *Plant Physiol. Biochem.* 47, 732–738. doi: 10.1016/j.plaphy.2009.03.006

Ficke, A., Gadoury, D. M., and Seem, R. C. (2002). Ontogenic resistance and plant disease management: A case study of grape powdery mildew. *Phytopathology* 92, 671–675. doi: 10.1094/PHYTO.2002.92.6.671

Fondevilla, S., Carver, T. L. W., Moreno, M. T., and Rubiales, D. (2006). Macroscopic and histological characterisation of genes er1 and er2 for powdery mildew resistance in pea. *Eur. J. Plant Pathol.* 115, 309–321. doi: 10.1007/s10658-006-9015-6

Fung, R. W. M., Gonzalo, M., Fekete, C., Kovacs, L. G., He, Y., Marsh, E., et al. (2008). Powdery mildew induces defense-oriented reprogramming of the transcriptome in a susceptible but not in a resistant grapevine. *Plant Physiol.* 146, 236–249. doi: 10.1104/pp.107.108712

Gadoury, D. M., Cadle-Davidson, L., Wilcox, W. F., Dry, I. B., Seem, R. C., and Milgroom, M. G. (2012). Grapevine powdery mildew (Erysiphe necator): a fascinating system for the study of the biology, ecology and epidemiology of an obligate biotroph. *Mol. Plant Pathol.* 13, 1–16. doi: 10.1111/j.1364-3703.2011.00728.x

Gee, C. T., Gadoury, D. M., and Cadle-Davidson, L. (2008). Ontogenic resistance to Uncinula necator varies by genotype and tissue type in a diverse collection of *Vitis* spp. *Plant Dis.* 92, 1067–1073. doi: 10.1094/PDIS-92-7-1067

Gomez, L., Bancel, D., Rubio, E., and Vercambre, G. (2007). The microplate reader: an efficient tool for the separate enzymatic analysis of sugars in plant tissues - validation of a micro-method. *J. Sci. Food Agric.* 87, 1893–1905. doi: 10.1002/jsfa.2924

Hayes, M. A., Feechan, A., and Dry, I. B. (2010). Involvement of abscisic acid in the coordinated regulation of a stress-inducible hexose transporter (VvHT5) and a cell wall invertase in grapevine in response to biotrophic fungal infection. *Plant Physiol.* 153, 211–221. doi: 10.1104/pp.110.154765

Hugot, K., Aime, S., Conrod, S., Poupet, A., and Galiana, E. (1999). Developmental regulated mechanisms affect the ability of a fungal pathogen to infect and colonize tobacco leaves. *Plant J.* 20, 163–170. doi: 10.1046/j.1365-313x.1999.00587.x

Jarvis, W. R., Gubler, W. D., and Grove, G. G. (2002). "Epidemiology of powdery mildews in agricultural pathosystems," in *The Powdery Mildews, a Comprehensive Treatise*, eds R. Bélanger, R. Bushnell, A. Dik, T. Carver (St. Paul, MN: APS Press), 169–199.

Keller, M. (2015). *The Science of Grapevines: Anatomy and Physiology*. London: Academic Press; Elsevier. doi: 10.1016/B978-0-12-419987-3.00007-8

Kennelly, M. M., Gadoury, D. M., Wilcox, W. F., Magarey, P. A., and Seem, R. C. (2005). Seasonal development of ontogenic resistance to downy mildew in grape berries and rachises. *Phytopathology* 95, 1445–1452. doi: 10.1094/PHYTO-95-1445

Koch, K. E. (1996). Carbohydrate-modulated gene expression in plants. *Annu. Rev. Plant Physiol. Plant Mol. Biol.* 47, 509–540. doi: 10.1146/annurev.arplant.47.1.509

Koroleva, O. A., Tomos, A. D., Farrar, J., and Pollock, C. J. (2002). Changes in osmotic and turgor pressure in response to sugar accumulation in barley source leaves. *Planta* 215, 210–219. doi: 10.1007/s00425-002-0744-2

Lannou, C. (2012). Variation and selection of quantitative traits in plant pathogens. *Ann. Rev. Phytopathol.* 50, 319–338. doi: 10.1146/annurev-phyto-081211-173031

Lebon, G., Wojnarowiez, G., Holzapfel, B., Fontaine, F., Vaillant-Gaveau, N., and Clément, C. (2008). Sugars and flowering in the grapevine (*Vitis vinifera* L.). *J. Exp. Bot.* 59, 2565–2578. doi: 10.1093/jxb/ern135

Leinhos, G. M. E., Gold, R. E., Duggelin, M., and Guggenheim, R. (1997). Development and morphology of Uncinula necator following treatment with the fungicides kresoxim-methyl and penconazole. *Mycol. Res.* 101, 1033–1046. doi: 10.1017/S0953756297003651

Li, B., and Xu, X. (2002). Infection and development of apple scab (*Venturia inaequalis*) on old leaves *J. Phytopathol.* 150, 687–691. doi: 10.1046/j.1439-0434.2002.00824.x

Malnoy, M., Viola, R., Jung, M. H., Koo, O. J., Kim, S., Kim, J. S., et al. (2016). DNA-free genetically edited grapevine and apple protoplast using CRISPR/Cas9 ribonucleoproteins. *Front. Plant Sci.* 7:1904. doi: 10.3389/fpls.2016.01904

Mammeri, Y., Burie, J. B., Langlais, M., and Calonnec, A. (2014). How changes in the dynamic of crop susceptibility and cultural practices can be used to better control the spread of a fungal pathogen at the plot scale? *Ecol. Modell.* 290, 178–191. doi: 10.1016/j.ecolmodel.2014.02.017

Marsh, E., Alvarez, S., Hicks, L. M., Barbazuk, W. B., Qiu, W. P., Kovacs, L., et al. (2010). Changes in protein abundance during powdery mildew infection of leaf tissues of Cabernet Sauvignon grapevine (*Vitis vinifera* L.). *Proteomics* 10, 2057–2064. doi: 10.1002/pmic.200900712

Maupetit, A., Larbat, R., Pernaci, M., Andrieux, A., Guinet, C., Boutigny, A.-L., et al. (2018). Defense compounds rather than nutrient availability shape aggressiveness trait variation along a leaf maturity gradient in a biotrophic plant pathogen. *Front. Plant Sci.* 9:1396. doi: 10.3389/fpls.2018.01396

Merry, A. M., Evans, K. J., Corkrey, R., and Wilson, S. J. (2013). Coincidence of maximum severity of powdery mildew on grape leaves and the carbohydrate sink-to-source transition. *Plant Pathol.* 62, 842–850. doi: 10.1111/j.1365-3059.2012.02691.x

Molitor, D., and Berkelmann-Loehnertz, B. (2011). Simulating the susceptibility of clusters to grape black rot infections depending on their phenological development. *Crop Protect.* 30, 1649–1654. doi: 10.1016/j.cropro.2011.07.020

Montero, F. J., de Juan, J. A., Cuesta, A., and Brasa, A. (2000). Nondestructive methods to estimate leaf area in *Vitis vinifera* L. *HortScience* 35, 696–698.

Muller, C., and Riederer, M. (2005). Plant surface properties in chemical ecology. *J. Chem. Ecol.* 31, 2621–2651. doi: 10.1007/s10886-005-7617-7

O'Connell, R. J., and Panstruga, R. (2006). Tete a tete inside a plant cell: establishing compatibility between plants and biotrophic fungi and oomycetes. *New Phytol.* 171, 699–718. doi: 10.1111/j.1469-8137.2006.01829.x

OIV (2018). *Distribution of the World's Grapevine Varieties. Focus 2017*. Paris: OIV—International Organization of Vine and Wine.

Petrie, P. R., Trought, M. C. T., Howell, G. S., and Buchan, G. D. (2003). The effect of leaf removal and canopy height on whole-vine gas exchange and fruit development of *Vitis vinifera* L. Sauvignon Blanc. *Funct. Plant Biol.* 30, 711–717. doi: 10.1071/FP02188

Poni, S., Intrieri, C., and Magnanini, E. (2000). Seasonal growth and gas exchange of conventionally and minimally pruned Chardonnay canopies. *Vitis* 39, 13–18.

Qiu, W. P., Feechan, A., and Dry, I. (2015). Current understanding of grapevine defense mechanisms against the biotrophic fungus (*Erysiphe necator*), the causal agent of powdery mildew disease. *Hortic. Res.* 2:15020. doi: 10.1038/hortres.2015.20

Richard, B., Jumel, S., Rouault, F., and Tivoli, B. (2012). Influence of plant stage and organ age on the receptivity of *Pisum sativum* to *Mycosphaerella pinodes*. *Eur. J. Plant Pathol.* 132, 367–379. doi: 10.1007/s10658-011-9882-3

Rolland, F., Baena-Gonzalez, E., and Sheen, J. (2006). Sugar sensing and signaling in plants: conserved and novel mechanisms. *Ann. Rev. Plant Biol.* 675–709. doi: 10.1146/annurev.arplant.57.032905.105441

Saito, S., Odagiri, M., Furuya, S., Suzuki, S., and Takayanagi, T. (2011). Inhibitory effect of chitinases isolated from Semillon grapes (*Vitis vinifera*) on growth of grapevine pathogens. *J. Plant Biochem. Biotechnol.* 20, 47–54. doi: 10.1007/s13562-010-0025-2

Salzman, R. A., Tikhonova, I., Bordelon, B. P., Hasegawa, P. M., and Bressan, R. A. (1998). Coordinate accumulation of antifungal proteins and hexoses constitutes a developmentally controlled defense response during fruit ripening in grape. *Plant Physiol.* 117, 465–472. doi: 10.1104/pp.117.2.465

Schnathorst, W. (1959). Resistance in lettuce to powdery mildew related to osmotic value. *Phytopathology* 49, 562–571.

Schnathorst, W., and Weinhold, A. (1957). An osmotic mechanism for resistance to powdery mildew in lettuce and Peach (Abstract). *Phytopathology* 47:533.

Schnee, S., Jolivet, J., and Calonnec, A. (2011). Consideration of dynamical plant-pathogen interactions for an improved management of powdery mildew epidemics in grapevine. *IOBC/WPRS Bull.* 67, 131–138.

Schultz, H. (1992). An empirical model for the simulation of leaf appearance and leaf area development of primary shoots of several grapevine (*Vitis vinifera* l.) canopy-systems. *Sci. Hortic.* 52, 179–200. doi: 10.1016/0304-4238(92)90020-D

Scott, P. (2008). *Physiology and Behaviour of Plants*. Wiley, J. and Sons.

Takam Soh, P., Ndoumbè-Nkeng, M., Sache, I., Ndong Nguema, E. P., Gwet, H., and Chadoeuf, J. (2012). Development stage-dependent susceptibility of cocoa fruit to pod rot caused by *Phytophthora megakarya*. *Eur. J. Plant Pathol.* 135, 363–370. doi: 10.1007/s10658-012-0092-4

Tattersall, D. B., vanHeeswijck, R., and Hoj, P. B. (1997). Identification and characterization of a fruit-specific, thaumatin-like protein that accumulates at very high levels in conjunction with the onset of sugar accumulation and berry softening in grapes. *Plant Physiol.* 114, 759–769. doi: 10.1104/pp.114.3.759

Tenenhaus, M., Esposito Vinzi, V., Chatelinc, Y., and Lauro, C. (2005). PLS path modeling. *Comput Statist Data Analy.* 48, 159–205. doi: 10.1016/j.csda.2004.03.005

Valdés-Gómez, H., Araya-Alman, M., Pañitrur De la Fuente, C., Verdugo-Vásquez, N., Lolas, M., Acevedo-Opazo, C., et al. (2017). Evaluation of a decision support strategy for the control of powdery mildew (*Erysiphe necator* [Schw.] Burr.) in grapevine in the central region of Chile. *Pest Manag. Sci.* 73, 1813–1821. doi: 10.1002/ps.4541

Valdes-Gomez, H., Gary, C., Cartolaro, P., Lolas-Caneo, M., and Calonnec, A. (2011). Powdery mildew development is positively influenced by grapevine vegetative growth induced by different soil management strategies. *Crop Protect.* 30, 1168–1177. doi: 10.1016/j.cropro.2011.05.014

Vanderplank, J. (1984). "Sink-induced loss of resistance and high-sugar disease processes and biotrophy," in *Disease-Resistance in Plants,* ed J. Vanderplank (London: Academic press), 107–121.

Weinhold, A., and English, H. (1964). Significance of morphological barriers and osmotic pressure in resistance of mature peach leaves to powdery mildew. *Phytopathology* 54, 1409–1414.

Xavier, A. A., Costa da Silva, A., da Silva Guimaraes, L. M., Matsuoka, K., Hodges, C. S., and Alfenas, A. C. (2015). Infection process of *Puccinia psidii*

in Eucalyptus grandis leaves of different ages. *Trop. Plant Pathol.* 40, 318–325. doi: 10.1007/s40858-015-0043-7

Yang, Y.-S., and Hori, Y. (1980). Studies on retranslocation of accumulated assimilates in 'delaware' grapevines III. Early growth of new shoots as dependent on accumulated and current year assimilates. *Tohoku J. Agric. Res.* 31, 120–129.

Zahavi, T., and Reuveni, M. (2012). Effect of grapevine training systems on susceptibility of berries to infection by *Erysiphe necator*. *Eur. J. Plant Pathol.* 133, 511–515. doi: 10.1007/s10658-012-9938-z

Zufferey, V. (2016). Leaf respiration in grapevine (*Vitis vinifera* 'Chasselas') in relation to environmental and plant factors. *Vitis* 55, 65–72. doi: 10.5073/vitis.2016.55.65-72

Zufferey, V., Murisier, F., and Schultz, H. R. (2000). A model analysis of the photosynthetic response of *Vitis vinifera* L. cvs riesling and chasselas leaves in the field: I. Interaction of age, light and temperature. *Vitis* 39, 19–26. Available online at: https://ojs.openagrar.de/index.php/VITIS/article/view/4599

Conflict of Interest Statement: The authors declare that the research was conducted in the absence of any commercial or financial relationships that could be construed as a potential conflict of interest.

frontiers in Plant Science

ORIGINAL RESEARCH
published: 19 December 2018
doi: 10.3389/fpls.2018.01841

A Trade-Off Between Sporangia Size and Number Exists in the Potato Late Blight Pathogen *Phytophthora infestans*, and Is Not Altered by Biotic and Abiotic Factors

*Nicolas Mariette, Alexander Kröner, Romain Mabon, Josselin Montarry, Bruno Marquer, Roselyne Corbière, Annabelle Androdias and Didier Andrivon**

INRA, UMR1349 Institute for Genetics, Environment and Plant Protection, Le Rheu, France

The negative relationship between offspring size and number is a classic example of trade-off between life-history traits, reported many times in animal and plant species. Here, we wanted to ascertain whether such a trade-off occurred in the oomycete *Phytophthora infestans*, and whether it was impacted by biotic and abiotic factors. We thus conducted three infection experiments under controlled conditions and measured the number and the size of sporangia (asexual propagules) produced on potato by different *P. infestans* isolates. In all experiments, we observed a negative relationship between sporangia size and number, demonstrating the existence of a trade-off. Moreover, although the potato host cultivar, temperature and host of origin (tomato or potato) all affected sporangia number, sporangia size or both, none of these biotic and abiotic factors did change the trade-off. Therefore, the trade-off between sporangia size and number could maintain the polyphenism for these traits in *P. infestans* populations, and favors the coexistence of distinct reproductive strategies within this species. Our results emphasize the relevance to focus on the relationship between offspring size and number in other fungal plant pathogens, as well as to study the impact of offspring size on fitness-linked traits (virulence and disease lesion development) in these organisms.

Keywords: fitness, life-history traits, plant pathogen, reproductive strategies, *Solanum tuberosum*

OPEN ACCESS

Edited by:
Michele Perazzolli, Fondazione Edmund Mach, Italy

Reviewed by:
Remco Stam, Technische Universität München, Germany
Daolong Dou, Nanjing Agricultural University, China

***Correspondence:**
Didier Andrivon
didier.andrivon@inra.fr

Specialty section:
This article was submitted to Plant Microbe Interactions, a section of the journal Frontiers in Plant Science

Received: *13 July 2018*
Accepted: *27 November 2018*
Published: *19 December 2018*

Citation:
Mariette N, Kröner A, Mabon R, Montarry J, Marquer B, Corbière R, Androdias A and Andrivon D (2018) A Trade-Off Between Sporangia Size and Number Exists in the Potato Late Blight Pathogen Phytophthora infestans, and Is Not Altered by Biotic and Abiotic Factors. Front. Plant Sci. 9:1841. doi: 10.3389/fpls.2018.01841

INTRODUCTION

The widely accepted trade-off concept states that an organism cannot simultaneously maximize all traits involved in fitness, owing to dilemmas in resource allocation (Law, 1979). According to this theory, any beneficial change in one trait will unavoidably have a detrimental effect on another trait (Anderson and May, 1982; Stearns, 1989). The net result is a negative correlation between traits that mobilize the same resources. The trade-off concept has a prominent importance in evolutionary biology, as it can explain how the adaptation of populations to new environments can be constrained and how life-history strategies can evolve (Rausher, 1984; Roff, 1992). Trade-offs between fitness components are of central importance in plant pathogens, as they could limit their evolutionary potential (Lannou, 2012; Laine and Barres, 2013) and may thus be exploited to engineer durable control strategies (Quenouille et al., 2013; Brown, 2015).

Since they are key to determining fitness, trade-offs involving reproductive traits, especially the one between offspring size and number, have received the most attention in the scientific literature (Stearns, 1989; Roff, 2002; Begon et al., 2006). The trade-off between offspring size and offspring number is based on the hypothesis that, for a given total reproductive investment, if most resources are devoted to the production of many offspring individuals, each of them will have limited lower share of the reproductive investment (Begon et al., 2006). If this trade off exists (that is, if resources available for reproduction are constrained), reproductive strategies should range along a continuum, from the production of few large offsprings to the production of many small ones (Timi et al., 2005). This size-number trade-off was first advocated by Lack (1947) with experiments on clutch-size in birds, and has been subsequently observed in many animals (Charnov and Ernest, 2006; Walker et al., 2008) and plants (Werner and Platt, 1976; Jakobsson and Eriksson, 2000; Linkies et al., 2010).

The size-number trade-off could also be found in plant parasites, especially oomycetes and fungi. For such sporulating organisms (with spores as asexual propagules), producing large spores should indeed be more energetically costly than producing small spores, but may increase spore viability or infectious ability. Although trade-offs involving spore production on one hand and other life-history traits such as latent period (Pariaud et al., 2013), virulence (Thrall and Burdon, 2003; Montarry et al., 2010) or transmission success rate (Pasco et al., 2016) on the other hand, were observed in various plant pathogens, very few studies have investigated the existence of a trade-off between spore size and number (Delmotte et al., 2014). Fortunately, the advent of new techniques and equipments for counting and measuring thin particles like spores now make the exploration of such a trade-off possible.

As in all pathogenic interactions, the development of a disease caused by a plant pathogen is strongly influenced by both abiotic environment and host genotype (Laine, 2007; Wolinska and King, 2009; Clément et al., 2010; Delmotte et al., 2014). As a consequence, these factors can also have an impact on the shape and even the direction of the correlation between life-history traits in pathogens. Hence, fitness costs can differ among environments (e.g., temperature) as observed in the fungal pathogen *Podosphaera plantaginis* (Laine, 2008). Likewise, some studies reported shifts of life-history correlations in plant pathogens, depending on the cultivars tested (Huang et al., 2010; Susi and Laine, 2013). These data thus stress that it is crucial to take into account sufficient variation in both the host and the parasite, by measuring life-history traits in different environments, to draw conclusions on the status of a life-history trade-off in a plant pathogen.

Here, we aimed to investigate the existence of a trade-off between offspring number and size in the oomycete *Phytophthora infestans*, and the impact of some biotic and abiotic factors on this eventual trade-off. Infamous for having triggered the Irish Great Famine in the 1840s, *P. infestans* is the causing agent of late blight in solanaceous species and is responsible for significant losses in both potato and tomato crops (Fry et al., 2015). This pathogen is particularly suitable for exploring trade-offs, as it can be isolated and maintained as axenic cultures on artificial media whereas miniature biotests performed in controlled conditions can be used for the assessment of life-history traits of the pathogen, particularly those linked to spore formation (Montarry et al., 2010). We thus conducted three experiments under controlled conditions in which we measured the size and number of sporangia (*i.e.*, asexual spores) produced by *P. infestans* isolates after artificial inoculations on potato leaflets. In each experiment, we changed one factor [host resistance level, temperature, or the host of origin (tomato or potato)] which could impact the trade-off. We measured the effect of these factors on both sporangia size and number, analyzed the relationships between these two traits and compared them within each set of conditions.

MATERIALS AND METHODS

We conducted three inoculation experiments of *P. infestans* isolates on detached potato leaflets in which we measured the size and the number of sporangia produced by the pathogen. Different biotic and abiotic parameters – host resistance level, temperature and host of origin (tomato or potato) – were modified in these experiments. The experimental protocols used for these experiments were mostly similar but contained some slight differences (**Table 1**).

Isolate Collections

Single-lesion isolates were established and maintained as axenic cultures on pea agar medium as previously described (e.g., Montarry et al., 2010). Briefly, each single-lesion isolate was obtained by placing a fragment of infected leaf tissue on tuber slices of the susceptible potato cultivar Bintje. After incubation at 15°C in growth chambers for four to eight days, pure cultures were established by transferring the hyphal tips growing through the slices to sterile pea agar and subsequently maintained at 15°C in darkness by serial transfers on fresh pea agar.

In the first experiment, we used 119 isolates sampled in commercial potato fields of western France during late blight

TABLE 1 | Protocol specificities applied for each experiment lead during the study.

	Experiment 1	Experiment 2	Experiment 3
Inoculum concentration	5×10^4 sporangia·mL^{-1}	5×10^4 sporangia·mL^{-1}	3×10^4 sporangia·mL^{-1}
Potato cultivars	• Bintje • Robijn • Möwe	Bintje	Bintje
Thermal regimes	15/18°C (day/night)	• 10°C • 14°C • 18°C	15/18°C (day/night)
Time of the sporangia collection	3 days after latent period	3 days after latent period	5 days after inoculation
No. independent replicates	1	2	2

epidemics of 2014 (Mariette, 2016). All isolates were tested on three potato cultivars: Bintje, Robijn, and Möwe. These cultivars do not bear race-specific resistance genes but differ in levels and components of partial resistance to late blight: Bintje is the reference susceptible cultivar to *P. infestans* commonly used in European laboratories, whereas the partially resistant Robijn and Möwe notably reduce spore production of the pathogen (Clément et al., 2010). In the second experiment, 16 western French isolates sampled in 2013 were tested on the potato cultivar Bintje under three thermal regimes: 10, 14, and 18°C. This temperature range was chosen because it covers the biological activity of *P. infestans* (Maziero et al., 2009). The third experiment included 21 isolates sampled either on potato (11) or tomato (10), in French and Algerian crops from 2013 to 2015, and were tested on the potato cv. Bintje.

Plant Material

Three potato cultivars (Bintje, Robijn, and Möwe) and one tomato cultivar (Marmande) were used. Certified seed tubers of the potato cultivars were obtained from the INRA Biological Resource Center BrACySol (Ploudaniel, France), whereas commercial standard seed of the tomato cultivar was used.

Plants were grown in pots filled with 1:1:1 sand-peat-compost mixture placed in a glasshouse regulated at 15–20°C (night/day temperatures) with 16 h of photoperiod. Once a week, plants were watered with a nutrient solution (Hakaphos; NPK 15/10/15). For the inoculum preparation and life-history traits measurements, leaflets of similar size were picked from the median area of 6- to 8-week-old plants.

Inoculum Preparation

Prior the assessment of their life-history traits and in order to restore pathogenicity possibly lost in axenic cultures (Jinks and Grindle, 1963), *P. infestans* isolates were first inoculated onto detached leaflets of the original host species: the potato cv. Bintje and the tomato cv. Marmande for potato and tomato isolates, respectively. For this purpose, droplets of sporangial suspensions, prepared from 3- to 4-week-old pea agar cultures by flooding with sterile water and scrapping the colony surface, were deposited on the lower (abaxial) side of detached leaflets kept on the empty lids of inverted Petri dishes containing 10 g L^{-1} water agar and acting as humid chambers. After 7 days of incubation at 18/15°C (day/night temperature) and 16-h day length, newly formed sporangia were collected from infected leaflets by gently shaking in sterile water. Sporangia were then counted using a hemocytometer, adjusted to a final concentration of 3×10^4 or 5×10^4 sporangia mL^{-1}, depending on the experiment (**Table 1**), and then kept at 4°C for 2 h to promote zoospore release.

Inoculation

Sporangial suspensions were inoculated onto a potato leaflet, except in the second experiment where three leaflets of potato cv. Bintje were inoculated due to the three thermal regimes tested (**Table 1**). To this end, leaflets were placed, abaxial face up, onto the empty lids of inverted Petri dishes containing 10 g L^{-1} water agar. A 20-µL droplet of the prepared sporangial suspension was then deposited on the center of the leaflet. The Petri dishes were kept in clear boxes and incubated in climate chambers regulated at thermal conditions desired (**Table 1**) with a 16 h photoperiod.

Life-History Traits Measurements

Three days after the formation of the first sporangia – checked by daily observations under a magnifying glass – or 5 days after inoculation (depending on the experiment, **Table 1**), newly formed sporangia were washed from each leaflet in 10 mL Isoton II (saline buffer; Beckman Coulter, Villepinte, France). Suspensions were kept in glass tubes at −20°C until the counting of sporangia number (SN) produced using a Coulter Z2 counter (Beckman Coulter) equipped with a 100-µm aperture tube. Sporangia size (SS) was determined under a microscope fitted with a camera and using the image analysis software Histolab® v8.1.0 (Microvision Instruments, Evry, France). For this purpose, drops of the sporangial suspension were placed under the microscope and we used the camera measurement software to determine length and width of 100 randomly chosen sporangia. These measures allowed to calculate sporangia volumes, assuming a revolution ellipsoid shape for each sporangium (Philibert et al., 2011) by applying the standard equation $\frac{4\pi}{3} * \frac{length}{2} * \left(\frac{width}{2}\right)^2$.

Statistical Analyses

All analyses were performed using the statistical software R v. 3.4.4 (R Core Team, 2017) and the significance threshold was fixed at $\alpha = 0.05$. We first compared SS and SN of *P. infestans* isolates tested on different potato cultivars (experiment 1) and at different temperatures (experiment 2) using analysis of variance (ANOVA) followed by Tukey's honestly significant difference *post hoc* comparisons. For the comparisons between isolates sampled on potato and tomato (experiment 3), we applied a Student *t*-test. When necessary, SS and SN were log-transformed to achieve assumptions of homoscedasticity and normality. For the three tested modalities (potato cultivar, temperature and host of origin), each *P. infestans* isolate was regarded as a biological repetition. Then, we investigated the relationship between SS and SN for each modality tested in the three experiments using Pearson correlations and linear regressions (where SS and SN were log-transformed). To test whether slopes of regression lines differed between modalities within each experiment, variation in SS was analyzed by mean of analysis of covariance (ANCOVA) with SN as the covariate and host cultivar, temperature or host of origin as the factor. In the first experiment implying 119 isolates, phenotypic measurements were made only once on each of them as the large number of tested individuals allowed a good assessment of significance. In the case of experiments 2 and 3, we compared data obtained from the two independent replicates and, as results showing no significant differences (*i.e.*, the criterion was statistically fulfilled or rejected), data from both experiments were pooled, reanalyzed and represented graphically.

RESULTS

Impact of Biotic and Abiotic Factors on *P. infestans* Life-History Traits

In experiment 1, potato cultivar had a significant effect on SS of *P. infestans* isolates (ANOVA, $F_{2,352} = 3.58$, $P = 0.029$), with bigger sporangia produced on Bintje than on Robijn as revealed by Tukey *post hoc* tests (**Table 2**). Likewise, a significant effect of potato cultivar on SN was detected (ANOVA, $F_{2,352} = 158.48$, $P < 0.001$), with the highest number of sporangia produced on Bintje, then on Robijn, when the lowest number of sporangia was observed on Möwe (**Table 2**). In the second experiment, SS was significantly impacted by temperature (ANOVA, $F_{2,91} = 54.804$, $P < 0.001$): the lower the temperature, the bigger the sporangia (**Table 2**). In this experiment, temperature also had a significant effect on SN (ANOVA, $F_{2,91} = 106.31$, $P < 0.001$) with in this case, an increase of SN with increasing temperatures (**Table 2**). In experiment 3, no significant effect of isolate origin was detected on SS [$t(40) = 1.63$, $P = 0.111$; **Table 2**], nor on SN [$t(40) = 1.81$, $P = 0.079$; **Table 2**].

Relationship Between Life-History Traits

In experiment 1, significant negative relationships between SS and SN of *P. infestans* isolates were detected in the tests conducted on potato cultivars Bintje ($r = -0.36$, $P < 0.001$; **Figure 1**), Robijn ($r = -0.49$, $P < 0.001$; **Figure 1**), and Möwe ($r = -0.48$, $P < 0.001$; **Figure 1**). ANCOVA revealed no significant interaction between host cultivar and SN (**Table 3**), indicating that the relationship between SS and SN did not significantly differ among potato cultivars. Likewise, in the second experiment, the relationship between SS and SN was significantly negative at 10°C ($r = -0.70$, $P < 0.001$; **Figure 2**), 14°C ($r = -0.62$, $P < 0.001$; **Figure 2**), and 18°C ($r = -0.68$, $P < 0.001$; **Figure 2**). Again, this relationship did not significantly differ among temperatures, since no significant interaction between temperature and SN was detected by ANCOVA (**Table 3**). Finally, in experiment 3, SS and SN were also negatively correlated and this relationship was significant for isolates sampled on both potato ($r = -0.57$, $P = 0.006$; **Figure 3**) and tomato ($r = -0.58$, $P = 0.007$; **Figure 3**). As in the other two experiments, no significant interaction was revealed by ANCOVA between 'origin' and SN (**Table 3**), indicating that the SS-SN relationship was not significantly different between tomato and potato isolates.

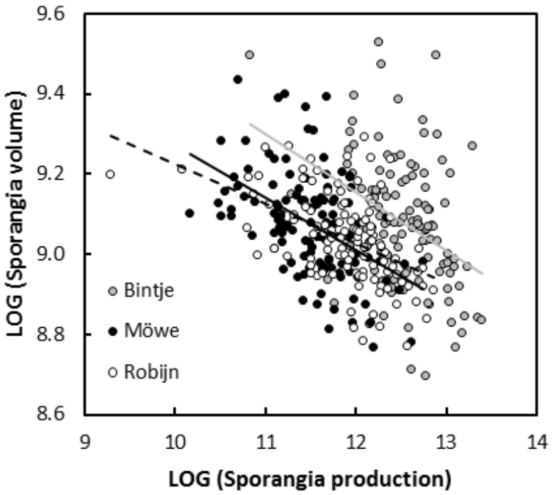

FIGURE 1 | Relationship between size and number of sporangia produced by 119 *P. infestans* isolates after inoculations on potato cultivars Bintje, Möwe, and Robijn (experiment 1). All variables were LOG-transformed. For sporangia produced on Bintje, the linear regression is represented by a continuous gray line ($y = 10.89–0.14\times$, $R^2 = 0.13$, $P < 0.001$), for sporangia produced on Möwe, the linear regression is represented by a continuous black line ($y = 10.58–0.13\times$, $R^2 = 0.23$, $P < 0.001$), and for isolates inoculated on Robijn, the linear regression is represented by a dotted black line ($y = 10.22–0.10\times$, $R^2 = 0.24$, $P < 0.001$).

TABLE 2 | Mean values (SE) of sporangia size and sporangia number measured in the three experiments for each tested factor (potato cultivar, temperature, and host of origin).

		Sporangia size (μm^3)			Sporangia number (No. sporangia/leaflet)		
Exp. 1	Bintje	8871	(138)	a	3.01×10^5	(10591)	a
	Möwe	8814	(108)	ab	1.10×10^5	(4984)	c
	Robijn	8477	(85)	b	1.64×10^5	(6753)	b
Exp. 2	10°C	7265	(204)	a	9.07×10^4	(6259)	c
	14°C	6169	(143)	b	2.10×10^5	(12247)	b
	18°C	4965	(91)	c	3.89×10^5	(8768)	a
Exp. 3	Potato	8650	(275)	a	1.32×10^5	(18493)	a
	Tomato	8011	(430)	a	9.56×10^4	(17792)	a

Different letters in a column indicates significant differences between means within an experiment at a 0.05 threshold (Tukey HSD or Student-t-tests).

TABLE 3 | Summary of analyze of covariance (ANCOVA) for testing the effects of biotic and abiotic factors on the relationship between size and number of sporangia produced by *P. infestans* isolates.

Source of variation	*df*	Mean Sq	*F*
Experiment 1			
SN	1	1.19	77.730***
Cultivar	2	0.35	22.856***
SN × Cultivar	2	0.02	1.003
Error	351	0.02	
Experiment 2			
SN	1	0.72	72.610***
Temperature	2	0.05	4.854**
SN × Temperature	2	0.00	0.099
Error	90	0.01	
Experiment 3			
SN	1	0.43	19.036***
Origin	1	0.21	9.419**
SN × origin	1	0.00	0.044
Error	38	0.02	

*In the models, potato cultivar (experiment 1), temperature (experiment 2), and host of origin (experiment 3) were rated as factors, sporangia production (SP) as the covariate and sporangia size as the response variable. Statistical significances are indicated as follow (**$P < 0.01$ and ***$P < 0.001$). Sporangia size and sporangia number were LOG-transformed.*

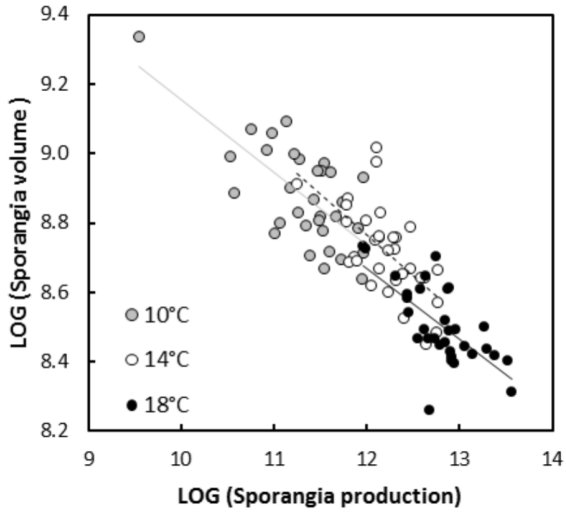

FIGURE 2 | Relationship between size and number of sporangia produced by 16 *P. infestans* isolates after inoculations on potato cultivar Bintje at 10, 14, and 18°C (experiment 2). All variables were LOG-transformed. For sporangia produced at 10°C, the linear regression is represented by a continuous gray line ($y = 11.25–0.21\times$, $R^2 = 0.49$, $P < 0.001$), for sporangia produced at 14°C, the linear regression is represented by a dotted black line ($y = 11.58–0.23\times$, $R^2 = 0.39$, $P < 0.001$) and for isolates inoculated at 18°C, the linear regression is represented by a continuous black line ($y = 11.14–0.21\times$, $R^2 = 0.46$, $P < 0.001$).

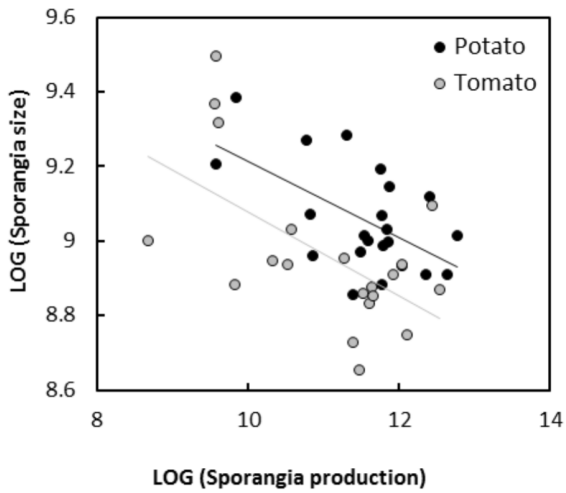

FIGURE 3 | Relationship between size and number of sporangia produced by 21 *P. infestans* isolates sampled on potato or tomato after inoculations on potato cultivar Bintje (experiment 3). All variables were LOG-transformed. For sporangia produced by potato isolates, the linear regression is represented by a continuous black line ($y = 10.23–0.10\times$, $R^2 = 0.32$, $P = 0.006$) and for sporangia produced by tomato isolates, the linear regression is represented by a continuous gray line ($y = 10.20–0.11\times$, $R^2 = 0.34$, $P = 0.007$).

DISCUSSION

The trade-off between offspring number and offspring size has been intensely studied and well characterized in animals and plant species (Werner and Platt, 1976; Charnov and Ernest, 2006; Walker et al., 2008). Here, we report that it also applies to a microorganism pathogenic to plants, potato late blight oomycete pathogen *P. infestans*: higher offspring numbers (in this case, asexual sporangia) correlates in this species with smaller offspring size. This trade-off has been seldom investigated in plant pathogens, even though a similar finding was reported in another plant pathogenic oomycete, the grapevine downy mildew pathogen *Plasmopara viticola* (Delmas et al., 2014). Such a trade-off is thus probably present in other sporulating parasites.

Interestingly, we have found significantly negative relationships between SS and number for all the modalities tested in our study, and with similar slopes within each experiment. Since host cultivar, temperature and isolate origin (potato or tomato) are important factors for the fitness of an almost obligate pathogen such as *P. infestans* (Andrivon et al., 2013), we could have supposed that these biotic and abiotic environmental variables could have altered the shape of the trade-off. Indeed, previous studies focused on plant pathogens reported for instance that host could modulate trade-offs, like those implying infectivity and transmission (Susi and Laine, 2013) or virulence and lesion size (Huang et al., 2010). Therefore, the stability of the trade-off relationship between SS and SN in *P. infestans* across a range of biotic and abiotic environments suggest that this trade-off is constitutive in this species, and might be exploited in control strategies of late blight epidemics.

The stability of the trade-off relationship over the range of environments tested is all the more remarkable that the environmental factors investigated strongly impacted one or both of the life history traits involved in the trade off. In fact, we showed that sporangia production of *P. infestans* was strongly host-dependent, confirming earlier observations made in this species (Clément et al., 2010) and more generally in a range of fungal and oomycete parasites (Hardham and Hyde, 1997; Delmotte et al., 2014). Interestingly, we also showed a clear effect of potato cultivars on SS, with smaller sporangia on Robijn – especially compared to Bintje. A similar observation was reported in *P. viticola* (Delmotte et al., 2014) and *Venturia inaequalis* (De Gracia et al., 2015), suggesting a possible selection by host on this trait among sporulating plant pathogens. Regarding temperature, the thermal optimum for *P. infestans* development is around 18–20°C (Mizubuti and Fry, 1998; Mariette et al., 2016), and spore production quickly decreases beyond this. In our second experiment, sporangia were much less numerous at the lowest temperatures, but they were bigger. This phenomenon could be due to the longer latent period of the pathogen at low temperatures (Maziero et al., 2009; Mariette et al., 2016), leading to more time for sporangia formation. Finally, we observed that isolates sampled on tomato produced less sporangia on the potato cultivar Bintje than those sampled on potato, confirming the host specialization previously highlighted in *P. infestans* (Oyarzun et al., 1998; Kröner et al., 2017).

By preventing an organism to simultaneously maximize all traits involved in fitness, trade-offs can equalize fitness across individuals, genotypes, or species with different reproductive strategies, leading to the maintenance of phenotypic diversity

(Roff, 1992). For instance, Héraudet et al. (2008) suggested that the trade-off between latent period and spore production in *H. arabidopsidis* may explain why the latent period remains variable in nature and did not achieve a uniformly minimal value. The constraint of total reproductive effort imposing a trade-off in the size and number of sporangia in *P. infestans*, as observed in our study, could therefore maintain variability for these life-history traits within populations of this pathogens. This tends to be confirmed with the large range of sporangia production values generally reported amongst isolates of single *P. infestans* populations (e.g., Montarry et al., 2008b, 2010; Mariette et al., 2016). Moreover, the polyphenism of life-history traits values imposed by a trade-off can lead to the emergence of various life-history strategies (Roff, 1992). This can be crucial in pathogens highly dependent on their environmental variations, as different life-history strategies can explain the coexistence of genetically differentiated clades, in complete or partial reproductive isolation, within single plant pathogen species (Montarry et al., 2008a).

Here, we report that a trade-off between number and size of asexual spores occurred in an important oomycete plant pathogen, *P. infestans*, and that its shape was not affected by different biotic and abiotic factors. It would be interesting to know the relationship between asexual spore number and size in other fungal plant pathogens as trade-offs (and their shape) can play a key role in evolutionary outcomes of these organisms (Kamo et al., 2007). Nevertheless, it is far from being the case at present, because if the production of the asexual propagules (spore or sporangia) is a trait extensively studied in fungal plant pathogens (Hardham and Hyde, 1997; Montarry et al., 2010), their size is still often ignored. Yet, the size of fungal propagules may be an important trait for different aspects of their fitness. The infection efficiency should be higher for large spores as they are supposed to have more resources available for hyphal growth (Bässler et al., 2015). Likewise, SS in oomycetes could also impact their indirect germination (formation of zoospores) as suggested by investigations on *P. viticola* showing that larger sporangia produced more zoospores (Delmas et al., 2014). Conversely, small spores might have higher aerial dispersal abilities and could therefore tend to deposit further to the source than larger ones (Norros et al., 2014). Nevertheless, owing to the lack of empirical evidences, the link between asexual spore size and such fitness aspects remain uncertain (De Gracia et al., 2015). Further research efforts on this topic are thus needed and it would be particularly crucial to study the impact of offspring size on virulence or disease lesion development in fungal plant pathogens. Besides, a future way of research in plant pathogens could be to not only limit on the trade-off between number and size of offspring but, as recommended by Begon et al. (2006), to look for a trade-off between the number of offspring and their individual fitness.

DATA AVAILABILITY STATEMENT

The datasets generated for this study will be found on data.inra.fr (doi: 10.15454/BB0WJN).

AUTHOR CONTRIBUTIONS

RM, AA, BM, NM, and AK performed the experiments according to a protocol elaborated jointly by RC and DA. NM and AK analyzed the data. NM, JM, RC, and DA wrote the text and prepared the figures. All authors edited the paper and have approved the current version.

ACKNOWLEDGMENTS

A part of this work presented in this paper first appeared in the NM thesis, which can be accessed online (see the reference list). We gratefully acknowledge the financial support by INRA ACCAF Metaprogramme (CLIF project) and ARIMnet (PoH-MED project; KBBE 219262/ANR). We also warmly thank Prof. Zouaoui Bouznad and Sihem Belkhiter (ENSA, Algiers) for providing Algerian isolates and Mathilde Bodiou for help with the sampling of *P. infestans* isolates. We express our thanks to E. Rolland and C. Piriou for their help with isolate maintenance and biological experiments. We are grateful to the INRA Genetic Resources Center BrACySol of Ploudaniel for providing the plant material used in the tests. NM was supported by a Ph.D. project cofunded by INRA and ACVNPT (Association des Créateurs de Variétés Nouvelles de Pomme de Terre) through a CIFRE grant (Conventions Industrielles de Formation par la Recherche). AK was supported by a post-doctoral grant funded under the ARIMnet PoH-MED project.

REFERENCES

Anderson, R. M., and May, R. M. (1982). Coevolution of hosts and parasites. *Parasitology* 85, 411–426. doi: 10.1017/S0031182000055360

Andrivon, D., Montarry, J., Corbière, R., Pasco, C., Glais, I., Marquer, B., et al. (2013). The hard life of *Phytophthora infestans*: when trade-offs shape evolution in a biotrophic plant pathogen. *Plant Pathol.* 62(Suppl. 1), 28–35. doi: 10.1111/ppa.12164

Bässler, C., Heilmann-Claussen, J., Karasch, P., Brandl, R., and Halbwachs, H. (2015). Ectomycorrhizal fungi have larger fruit bodies than saprotrophic fungi. *Fungal Ecol.* 17, 205–212. doi: 10.1016/j.funeco.2014.06.005

Begon, M., Townsend, C. R., and Harper, J. L. (2006). *Ecology, From Individuals to Ecosystems*, 4th Edn. Oxford: Blackwell Publishing.

Brown, J. K. M. (2015). Durable resistance of crops to disease: a Darwinian perspective. *Annu. Rev. Phytopathol.* 53, 513–539. doi: 10.1146/annurev-phyto-102313-045914

Charnov, E. L., and Ernest, S. K. M. (2006). The offspring-size/clutch-size trade-off in mammals. *Am. Nat.* 167, 578–582.

Clément, J. A. J., Magalon, H., Pellé, R., Marquer, B., and Andrivon, D. (2010). Alteration of pathogenicity-linked life-history traits by resistance of its host *Solanum tuberosum* impacts sexual reproduction of the plant pathogenic oomycete *Phytophthora infestans*. *J. Evol. Biol.* 23, 2668–2676. doi: 10.1111/j.1420-9101.2010.02150.x

De Gracia, M., Cascales, M., Expert, P., Bellanger, M. N., Le Cam, B., and Lemaire, C. (2015). How did host domestication modify life history traits of its pathogens? *PLoS One* 10:e0122909. doi: 10.1371/journal.pone.0122909

Delmas, C. E. L., Mazet, I. D., Jolivet, J., Delière, L., and Delmotte, F. (2014). Simultaneous quantification of sporangia and zoospores in a biotrophic oomycete with an automatic particle analyzer: disentangling dispersal and infection potentials. *J. Microbiol. Methods* 107, 169–175. doi: 10.1016/j.mimet.2014.10.012

Delmotte, F., Mestre, P., Schneider, C., Kassemeyer, H. H., Kozma, P., Richart-Cervera, S., et al. (2014). Rapid and multiregional adaptation to host partial resistance in a plant pathogenic oomycete: evidence from European populations of *Plasmopara viticola*, the causal agent of grapevine downy mildew. *Infect. Genet. Evol.* 27, 500–508. doi: 10.1016/j.meegid.2013.10.017

Fry, W. E., Birch, P. R. J., Judelson, H. S., Gruenwald, N. J., Danies, G., Everts, K. L., et al. (2015). Five reasons to consider *Phytophthora infestans* a reemerging pathogen. *Phytopathology* 105, 966–981. doi: 10.1094/PHYTO-01-15-0005-FI

Hardham, A. R., and Hyde, G. J. (1997). Asexual sporulation in the Oomycetes. *Adv. Bot. Res.* 24, 353–398. doi: 10.1016/S0065-2296(08)60079-8

Héraudet, V., Salvaudon, L., and Shykoff, J. A. (2008). Trade-off between latent period and transmission success of a plant pathogen revealed by phenotypic correlations. *Evol. Ecol. Res.* 10, 913–924.

Huang, Y. J., Balesdent, M. H., Li, Z. Q., Evans, N., Rouxel, T., and Fitt, B. D. L. (2010). Fitness cost of virulence differs between the AvrLm1 and AvrLm4 loci in *Leptosphaeria maculans* (phoma stem canker of oilseed rape). *Eur. J. Plant Pathol.* 126, 279–291. doi: 10.1007/s10658-009-9539-7

Jakobsson, A., and Eriksson, O. (2000). A comparative study of seed number, seed size, seedling size and recruitment in grassland plants. *Oikos* 88, 494–502. doi: 10.1034/j.1600-0706.2000.880304.x

Jinks, J. L., and Grindle, M. (1963). Changes induced by training in *Phytophthora infestans*. *Heredity* 18, 245–264. doi: 10.1038/hdy.1963.29

Kamo, M., Sasaki, A., and Boots, M. (2007). The role of trade-off shapes in the evolution of parasites in spatial host populations: an approximate analytical approach. *J. Theor. Biol.* 244, 588–596. doi: 10.1016/j.jtbi.2006.08.013

Kröner, A., Mabon, R., Corbière, R., Montarry, J., and Andrivon, D. (2017). The coexistence of generalist and specialist clonal lineages in natural populations of the Irish Famine pathogen *Phytophthora infestans* explains local adaptation to potato and tomato. *Mol. Ecol.* 26, 1891–1901. doi: 10.1111/mec.14004

Lack, D. (1947). The significance of clutch size. *Ibis* 89, 302–352. doi: 10.1111/j.1474-919X.1947.tb04155.x

Laine, A. L. (2007). Pathogen fitness components and genotypes differ in their sensitivity to nutrient and temperature variation in a wild plant-pathogen association. *J. Evol. Biol.* 20, 2371–2378. doi: 10.1111/j.1420-9101.2007.01406.x

Laine, A. L. (2008). Temperature-mediated patterns of local adaptation in a natural plant-pathogen metapopulation. *Ecol. Lett.* 11, 327–337. doi: 10.1111/j.1461-0248.2007.01146.x

Laine, A. L., and Barres, B. (2013). Epidemiological and evolutionary consequences of life-history trade-offs in pathogens. *Plant Pathol.* 62, 96–105. doi: 10.1111/ppa.12129

Lannou, C. (2012). Variation and selection of quantitative traits in plant pathogens. *Annu. Rev. Phytopathol.* 50, 319–338. doi: 10.1146/annurev-phyto-081211-173031

Law, R. (1979). Optimal life histories under age-specific predation. *Am. Nat.* 114, 399–417. doi: 10.1086/283488

Linkies, A., Graeber, K., Knight, C., and Leubner-Metzger, G. (2010). The evolution of seeds. *New Phytol.* 186, 817–831. doi: 10.1111/j.1469-8137.2010.03249.x

Mariette, N. (2016). Traits de vie, Adaptation et Pouvoir Invasif de Lignées Clonales de Phytophthora infestans, Agent du Mildiou de la Pomme de Terre. Ph.D. Thesis, Agrocampus Ouest, Rennes.

Mariette, N., Androdias, A., Mabon, R., Marquer, B., Corbière, R., Montarry, J., et al. (2016). Local adaptation to temperature in populations and clonal lineages of the Irish potato famine pathogen *Phytophthora infestans*. *Ecol. Evol.* 6, 6320–6331. doi: 10.1002/ece3.2282

Maziero, J. M. N., Maffia, L. A., and Mizubuti, E. S. G. (2009). Effects of temperature on events in the infection cycle of two clonal lineages of *Phytophthora infestans* causing late blight on tomato and potato in Brazil. *Plant Dis.* 93, 459–466. doi: 10.1094/PDIS-93-5-0459

Mizubuti, E. G. S., and Fry, W. E. (1998). Temperature effects on developmental stages of isolates from three clonal lineages of *Phytophthora infestans*. *Phytopathology* 88, 837–843. doi: 10.1094/PHYTO.1998.88.8.837

Montarry, J., Cartolaro, P., Jolivet, J., and Willocquet, L. (2008a). Genetic structure and aggressiveness of *Erysiphe necator* populations during grapevine powdery mildew epidemics. *Appl. Environ. Microbiol.* 74, 6327–6332. doi: 10.1128/AEM.01200-08

Montarry, J., Glais, I., Corbière, R., and Andrivon, D. (2008b). Adaptation to the most abundant host genotype in an agricultural plant-pathogen system – potato late blight. *J. Evol. Biol.* 21, 1397–1407. doi: 10.1111/j.1420-9101.2008.01557.x

Montarry, J., Hamelin, F. M., Glais, I., Corbière, R., and Andrivon, D. (2010). Fitness costs associated with unnecessary virulence factors and life history traits: evolutionary insights from the potato late blight pathogen *Phytophthora infestans*. *BMC Evol. Biol.* 10:283. doi: 10.1186/1471-2148-10-283

Norros, V., Rannik, U., Hussein, T., Petäjä, T., Vesala, T., and Ovaskainen, O. (2014). Do small spores disperse further than large spores? *Ecology* 95, 1612–1621.

Oyarzun, P. J., Pozo, A., Ordonez, M. E., Doucett, K., and Forbes, G. A. (1998). Host specificity of *Phytophthora infestans* on tomato and potato in Ecuador. *Phytopathology* 88, 265–271. doi: 10.1094/PHYTO.1998.88.3.265

Pariaud, B., Berg, F., Bosch, F., Powers, S. J., Kaltz, O., and Lannou, C. (2013). Shared influence of pathogen and host genetics on a trade-off between latent period and spore production capacity in the wheat pathogen. *Puccinia triticina*. *Evol. Appl.* 6, 303–312. doi: 10.1111/eva.12000

Pasco, C., Montarry, J., Marquer, B., and Andrivon, D. (2016). And the nasty ones lose in the end: foliar pathogenicity trades off with asexual transmission in the Irish famine pathogen *Phytophthora infestans*. *New Phytol.* 209, 334–342. doi: 10.1111/nph.13581

Philibert, A., Desprez-Loustau, M. L., Fabre, B., Frey, P., Halkett, F., Husson, C., et al. (2011). Predicting invasion success in pathogenic fungi from species traits. *J. Appl. Ecol.* 48, 1381–1390. doi: 10.1111/j.1365-2664.2011.02039.x

Quenouille, J., Montarry, J., Palloix, A., and Moury, B. (2013). Farther, slower, stronger: how the plant genetic background protects a major resistance gene from breakdown. *Mol. Plant Pathol.* 14, 109–118. doi: 10.1111/j.1364-3703.2012.00834.x

R Core Team (2017). *R: A language and environment for statistical computing*. Vienna: R Foundation for Statistical Computing.

Rausher, M. D. (1984). Tradeoffs in performance on different hosts: evidence from within- and between-site variation in the beetle *Deloyala guttata*. *Evolution* 38, 582–595. doi: 10.1111/j.1558-5646.1984.tb00324.x

Roff, D. A. (1992). *The Evolution of Life Histories: Theory and Analysis*. New York, NY: Chapman and Hall.

Roff, D. A. (2002). *Life History Evolution*. Sunderland, MA: Sinauer Associates, Inc.

Stearns, S. C. (1989). Trade-offs in life-history evolution. *Funct. Ecol.* 3, 259–268. doi: 10.2307/2389364

Susi, H., and Laine, A. L. (2013). Pathogen life-history trade-offs revealed in allopatry. *Evolution* 67, 3362–3370. doi: 10.1111/evo.12182

Thrall, P. H., and Burdon, J. J. (2003). Evolution of virulence in a plant host–pathogen metapopulation. *Science* 299, 1735–1737. doi: 10.1126/science.1080070

Timi, J. T., Lanfranchi, A. L., and Poulin, R. (2005). Is there a trade-off between fecundity and egg volume in the parasitic copepod *Lernanthropus cynoscicola*? *Parasitol. Res.* 95, 1–4.

Walker, R. S., Gurven, M., Burger, O., and Hamilton, M. J. (2008). The trade-off between number and size of offspring in humans and other primates. *Proc. R. Soc. B Biol. Sci.* 275, 827–834. doi: 10.1098/rspb.2007.1511

Werner, P. A., and Platt, W. J. (1976). Ecological relationship of co-occurring goldenrods (Solidago. Compositae). *Am. Nat.* 110, 959–971. doi: 10.1086/283120

Wolinska, J., and King, K. C. (2009). Environment can alter selection in host–parasite interactions. *Trends Parasitol.* 25, 236–244. doi: 10.1016/j.pt.2009.02.004

Conflict of Interest Statement: The authors declare that the research was conducted in the absence of any commercial or financial relationships that could be construed as a potential conflict of interest.

frontiers in Microbiology

ORIGINAL RESEARCH
published: 30 August 2019
doi: 10.3389/fmicb.2019.01969

Responses to Hydric Stress in the Seed-Borne Necrotrophic Fungus *Alternaria brassicicola*

*Guillaume Quang N'Guyen[1†], Roxane Raulo[2], Muriel Marchi[1], Carlos Agustí-Brisach[3], Beatrice Iacomi[4], Sandra Pelletier[1], Jean-Pierre Renou[1], Nelly Bataillé-Simoneau[1], Claire Campion[1], Franck Bastide[1], Bruno Hamon[1], Chloé Mouchès[1], Benoit Porcheron[5], Remi Lemoine[5], Anthony Kwasiborski[1], Philippe Simoneau[1] and Thomas Guillemette[1]**

[1] Institut de Recherche en Horticulture et Semences – UMR 1345, INRA, Université d'Angers, Agrocampus-Ouest, SFR 4207 QUASAV, Angers, France, [2] Université de Lille, INRA, ISA, Université d'Artois, Université du Littoral Côte d'Opale, EA 7394 - ICV - Institut Charles Viollette, Lille, France, [3] Departamento de Agronomía, ETSIAM, Universidad de Córdoba, Córdoba, Spain, [4] Department of Plant Sciences, University of Agronomic Sciences and Veterinary Medicine of Bucharest, Bucharest, Romania, [5] Equipe "Sucres & Echanges Végétaux-Environnement," UMR CNRS 7267 EBI Ecologie et Biologie des Interactions, Université de Poitiers, Poitiers, France

Alternaria brassicicola is a necrotrophic fungus causing black spot disease and is an economically important seed-borne pathogen of cultivated brassicas. Seed transmission is a crucial component of its parasitic cycle as it promotes long-term survival and dispersal. Recent studies, conducted with the *Arabidopsis thaliana*/*A. brassicicola* pathosystem, showed that the level of susceptibility of the fungus to water stress strongly influenced its seed transmission ability. In this study, we gained further insights into the mechanisms involved in the seed infection process by analyzing the transcriptomic and metabolomic responses of germinated spores of *A. brassicicola* exposed to water stress. Then, the repertoire of putative hydrophilins, a group of proteins that are assumed to be involved in cellular dehydration tolerance, was established in *A. brassicicola* based on the expression data and additional structural and biochemical criteria. Phenotyping of single deletion mutants deficient for fungal hydrophilin-like proteins showed that they were affected in their transmission to *A. thaliana* seeds, although their aggressiveness on host vegetative tissues remained intact.

Keywords: hydrophilins, plant pathogenic fungus, seed transmission, dehydration, *Alternaria brassicicola*

OPEN ACCESS

Edited by:
Christophe Le May, Agrocampus Ouest, France

Reviewed by:
Syama Chatterton, Agriculture and Agri-Food Canada (AAFC), Canada
Antoine Gravot, University of Rennes 1, France

****Correspondence:***
Thomas Guillemette
thomas.guillemette@univ-angers.fr

†Present address:
Guillaume Quang N'Guyen, Département de Biologie, PROTEO, Institut de Biologie Intégrative et des Systèmes, Université Laval, Pavillon Charles-Eugène-Marchand, Québec, QC, Canada

Specialty section:
This article was submitted to Plant Microbe Interactions, a section of the journal Frontiers in Microbiology

Received: *18 September 2018*
Accepted: *09 August 2019*
Published: *30 August 2019*

Citation:
N'Guyen GQ, Raulo R, Marchi M, Agustí-Brisach C, Iacomi B, Pelletier S, Renou J-P, Bataillé-Simoneau N, Campion C, Bastide F, Hamon B, Mouchès C, Porcheron B, Lemoine R, Kwasiborski A, Simoneau P and Guillemette T (2019) Responses to Hydric Stress in the Seed-Borne Necrotrophic Fungus Alternaria brassicicola. Front. Microbiol. 10:1969. doi: 10.3389/fmicb.2019.01969

INTRODUCTION

The fungus *Alternaria brassicicola* causes black spot disease and is an economically important seed-borne pathogen of Brassicaceae species. This necrotrophic fungus strongly depends on seed transmission process for its long-term survival and dispersal (van den Bosch et al., 2010). However, fungal and plant factors that impact seed transmission are still poorly described. Such knowledge is crucial to propose strategies for improving the seed health, which remains a major issue for seed companies. Recent studies conducted with the *Arabidopsis thaliana*/*A. brassicicola* pathosystem showed that the level of susceptibility of the fungus to water stress strongly influenced its seed transmission ability. For instance, two osmosensitive fungal mutants, defective for the class III Histidine kinase (HK) AbNik1 (Pochon et al., 2013) and the MAP kinase AbHog1 (unpublished result), respectively, were highly jeopardized in their ability to colonize

seeds. Consistently, Iacomi-Vasilescu et al. (2008) had previously reported that *A. brassicicola* spontaneous phenylpyrrole resistant mutants with non-functional class III HK were found to be strongly impaired in their ability to infect radish seeds in field conditions, indicating that a functional high osmolarity pathway is required for efficient infection of seeds. Pochon et al. (2013) also showed that two dehydrin-like proteins were required for effective seed colonization by *A. brassicicola*. During colonization of maturing seeds, the fungi are exposed to severe water and osmotic constraints, and their ability to cope with such stresses is probably a key factor that determines their transmission to seeds.

The strategies to withstand low water availability have been mainly investigated in some organisms called anhydrobiotes belonging to kingdoms of bacteria, fungi and plants, which have the ability to resist desiccation, i.e., to survive to nearly total dehydration (Calahan et al., 2011; Dupont et al., 2014). Various mechanical, structural and oxidative constraints are induced during dehydration, which may lead to damage to membranes, proteins and DNA. Studies in the yeast *Saccharomyces cerevisiae* have shown that the protective system is based on a set of constitutive and inducible mechanisms. For instance, the synthesis of polyols occurs to maintain the osmotic balance. In yeast, the major polyol concerned with osmotic adjustment is glycerol and its synthesis, and hence its intracellular accumulation, is under control of the high osmolarity glycerol (HOG) pathway mediated by phosphorylation of the HOG1 MAP kinase. Some other molecules, such as heat shock proteins, hydrophilins or the non-reducing disaccharides trehalose and sucrose have been identified to be synthesized during desiccation and may be involved in preserving native protein structures or stabilizing membranes (Gadd et al., 1987; Garay-Arroyo et al., 2000; Sales et al., 2000; Tapia and Koshland, 2014).

Hydrophilins are a group of proteins that are present in organisms such as plants, fungi and bacteria, and that are biochemically defined as glycine-rich and highly hydrophilic disordered proteins. They are assumed to be involved in cellular dehydration tolerance, even if their specific role is still unclear. In *Sa. cerevisiae*, 12 genes, whose expression were induced in response to water deficit, encode proteins with specific hydrophilin characteristics (Garay-Arroyo et al., 2000). The deletion (or disruption) and overexpression of these genes showed that only some of them contributed to the desiccation tolerance of yeast (Dang and Hincha, 2011; López-Martínez et al., 2012; Rodríguez-Porrata et al., 2012). A first beneficial effect of hydrophilins on yeast viability during water deficit may be due to their antioxidant capacity which minimizes the accumulation of cellular ROS (López-Martínez et al., 2012). Another role of hydrophilins would be the protection of enzymes and the stabilization of membranes during drying (Sales et al., 2000; Goyal et al., 2005; Reyes et al., 2005). In virtue of their structural plasticity, which is due in part to the presence of disordered regions, hydrophilins may act as molecular shields or directly interact with various molecular partners (Tunnacliffe and Wise, 2007).

Except for the yeast hydrophilins, very little information is available on the presence and role of this class of proteins in filamentous fungi. To date, most studies have focused on a particular class of fungal hydrophilins called dehydrins. Dehydrin-encoding genes were first identified in *Tuber borchii* during searches for genes controlling fruiting body maturation or conidial dormancy (Abba' et al., 2006). Then, Wong Sak Hoi et al. (2011, 2012) identified three dehydrin-encoding genes in *Aspergillus fumigatus*. Two of them were found to be involved in the protection against oxidative, osmotic and pH stress and the third dehydrin regulated freezing tolerance. A farnesol-induced dehydrin-like protein, that contributed to the high tolerance of resting conidia against oxidative and heat stress, was also identified in *Aspergillus nidulans* (Wartenberg et al., 2012). In *A. brassicicola*, three proteins harboring the typical asparagine-proline-arginine (DPR) signature pattern and sharing the characteristic features of fungal dehydrin-like proteins have been identified (Pochon et al., 2013). The expression of these genes was found to be regulated by the AbHog1 mitogen-activated protein kinase (MAPK) pathway. Phenotyping of single deletion mutants showed that dehydrin-like proteins have an impact mainly on oxidative stress tolerance and on conidial survival upon exposure to high and freezing temperatures. Moreover, a double deletion mutant was strongly affected with respect to conidiation and showed a highly compromised pathogenicity with a lower aggressiveness on *Brassica oleracea* leaves and a reduced capacity to be transmitted to *Arabidopsis* seeds via siliques. These results support the importance of dehydrin proteins and, more globally, of hydrophilins, with respect to the ability of *A. brassicicola* to efficiently accomplish key steps of its pathogen life cycle.

To identify new fungal molecular determinants that may be involved in the silique and seed infection process, the present study aimed at analyzing the transcriptomic and metabolomic responses of *A. brassicicola* exposed to water stress. Then, the repertoire of putative hydrophilins in this fungus was established based on expression data and structural and biochemical criteria. Finally, functional approaches were initiated to investigate the role of some of these putative hydrophilins.

RESULTS

Application of Water Stresses

Several preliminary tests were conducted to evaluate the level of stress for each treatment applied to fungal cells. Considering that the reference strain is naturally tolerant to water stress (Iacomi-Vasilescu et al., 2008), we additionally analyzed the effect of treatments on three mutant strains (Δ*abnik1*, Δ*abhog1* and Δ*absch9*) derived from the wild-type Abra43 strain, for which we hypothesized a higher sensitivity to water stress. As expected, the Abra43 reference strain exhibited high sorbitol tolerance with only 5% inhibition at a concentration of 1.2 M. At this concentration, a higher susceptibility was observed for the mutant strains (**Table 1**), confirming that the application of such a concentration indeed constitutes a stress for the fungal cells. In the same way, when a drastic decrease in relative humidity (RH) was applied to the germlings, no significant difference in mortality between the treated and the silica gel-free conditions was observed for the reference strain. On the contrary, the results

TABLE 1 | Susceptibility of *Alternaria brassicicola* wild-type, Δ*Abnik1*, Δ*Abhog1* and Δ*Asch9* strains to sorbitol and desiccation stresses.

Strains	% growth inhibition Sorbitol (1.2 M)	Mortality rate after 4 days of desiccation
WT	5 ± 2	5 ± 2
Δ*Abnik1*	29 ± 4	98 ± 2
Δ*Absch9*	48 ± 5	35 ± 5
Δ*Abhog1*	39 ± 4	98 ± 1

Each condition was tested in triplicate and the experiments were repeated twice. Values are means of biological repetitions and represent the percentage growth inhibition under stress conditions compared with standard growth conditions.

showed a very high susceptibility of Δ*abnik1* and Δ*abhog1* to the desiccation stress, while the *AbSch9* mutant exhibited an intermediate susceptibility (**Table 1**).

Based on these results, we chose to analyze the responses of the fungus when exposed to 1.2 M sorbitol for 0.5 and 2 h and when exposed to desiccation stress for 1 and 4 h. Regarding the latter stress, the chosen times implied that germlings exposed to silica gel beads were subjected to a RH value of 1% while control germlings were harvested at RH values of 70% and 90%, respectively.

In addition, we analyzed other phenotypic characteristics of these mutants: the susceptibility to oxidative stress (exposure to 10 mM H_2O_2 and 20 mM menadione), the ability to transmit to the *A. thaliana* seeds and the aggressiveness on cabbage leaves. Δ*abnik1* and Δ*abhog1* mutants were more susceptible to oxidative stress, and, consistently, had reduced ability to colonize *A. thaliana* seeds compared to the wild-type strain (**Table 2**). The Δ*absch9* mutant was not susceptible to oxidative stress and its seed transmission capacity was not altered. Compared to seed transmission capacity, the ability of leaf infection was not or less dependent on the sensitivity of fungal genotypes to oxidative stress, since Δ*abnik1* and Δ*absch9* strains did not have reduced aggressiveness on cabbage leaves.

Modulation of Fungal Transcriptomes in Response to Water Stress

In order to identify potential effectors of the response of *A. brassicicola* to dehydration stress, we first focused on the analysis of the transcriptional response in germinating conidia exposed to previously defined water stress (i.e., exposure to sorbitol 1.2 M for 0.5 and 2 h and exposure to silica gel beads for 1 h and 4 h). Each treated sample was compared to control sample and, thus, we produced four transcriptome data sets (each set was obtained from three biological replicates). We used *A. brassicicola* Nimblegen microarrays bearing one probe for each of the 10 633 ORFs predicted in the *A. brassicicola* automatically annotated genome database (JGI Genome Portal[1]). Only probes with a *P*-values ≤ 0.05 and a log2 ratio ≥ 0.7 or ≤ -0.7 were considered as differentially expressed. The numbers of genes that were induced or repressed under each condition, together with a summary of those regulated in more than one condition, are shown in **Figure 1**. To validate our microarray results, the regulation of several genes by sorbitol or silica gel exposure was confirmed by quantitative PCR (**Supplementary Figure S1**).

Our data showed that, for all the treatments, with the exception of the 4 h-silica gel (4 h-desiccation) treatment, the number of up-regulated and down-regulated genes was less than 500 and 300, respectively. Most of these genes were found to be regulated in more than one condition, 37 were found to be induced in all 4 stress conditions while none were found to be repressed. The 4h-desiccation stress led to more profound transcriptomic modifications since 578 and 917 were induced or repressed compared to control condition, respectively. Moreover, this transcriptomic response seemed rather specific since more than 800 genes (268 up-regulated and 601 down-regulated genes) were specifically regulated after the fungus was exposed to this constraint. It should be noted that 157 genes, that were induced by the sorbitol exposure, were repressed following the silica gel treatment.

The GO enrichment analyses showed that the enriched GO terms were not generally shared within the gene sets representative of each type of treatment (sorbitol or desiccation) (**Figure 2**). One exception was the GO categories corresponding to the response to oxidative and osmotic stresses, which were enriched in all the lists of induced genes. Another configuration was that enriched categories emerging from the 4h-desiccation up-regulated genes were also enriched categories emerging from the down-regulated gene lists after sorbitol exposure. These results seem to point out that the two types of treatment did not cause the same effects at the cellular level and induced quite different transcriptomic responses.

Enriched categories emerging from genes regulated following silica gel exposure were mainly related to the translation process, mitochondrial functions, and carboxylic acid and amino acids metabolic processes. Within the up-regulated genes, the main enriched GO terms identified in the sorbitol data sets were predominantly associated with a response to oxidative stress and to sugar metabolic process. Within the sorbitol repressed gene list, enriched GO terms referred to a wider range of cellular processes such as gene expression (**Figure 2**).

Metabolomic Responses to Water Stress

As several enriched GO categories emerging from transcriptomic data were linked to amino acid metabolism and catabolism, we investigated whether the response to water stress in *A. brassicicola* resulted in an alteration of the cellular content in amino acids. Regardless of the hydric stress applied, the total amino acid concentrations were significantly lower for the treatments conditions compared to the control conditions (Welch test *P*-value = $5.955E^{-08}$, **Supplementary Figure S2**). Indeed, considering the 24 amino acids and derivatives that were quantified in this study, the mean ratio of amino acid concentration in the treated conditions compared to the respective controls decreased significantly for 17 and 12 amino acids (9 in common), regardless of time exposure for the sorbitol and the desiccation treatment, respectively (**Figure 3A**). Amino acid profiles that were differentially less accumulated compared to controls were quite similar after 0.5 and 2 h of sorbitol exposure with 9 shared amino acids (over 13). Glutamine,

[1]https://genome.jgi.doe.gov/Altbr1/Altbr1.home.html

TABLE 2 | Other phenotypic characteristics of kinase mutants considered in this study.

Fungal strains (origin)	Susceptibility to oxidants		Seed transmission efficiency	Symptom development on leaves
	H_2O_2 (2.5 mM)	Menadione (5 mM)		
WT	22.2 ± 2	34,2 ± 3		
Δ*abNik1* (Dongo et al., 2009)	54.2 ± 5[a]	64.5 ± 6 [a]	– (Pochon et al., 2012)	0 (Pochon et al., 2012)
Δ*abHog1* (Joubert et al., 2011)	79.5 ± 6 [a]	84.5 ± 2 [a]	– (This study)	– (Joubert et al., 2011)
Δ*abSch9* (this study)	11 ± 3 [a]	21 ± 1 [a]	0 (This study)	0 (This study)

Values were obtained in this study and are means of three biological repetitions and represent the percentage growth inhibition under stress conditions compared with standard growth conditions. [a]indicates a significant difference between the mutant and the Abra43 WT parental isolate (Student's t-test, $P < 0.01$). The abilities of fungal strains to transmit to Arabidopsis thaliana seeds and to develop necrosis on leaves were evaluated in this study or in indicated references, depending on the mutant; 0: unchanged comparing to the wild-type; –: decrease of the ability compared to the wild-type.

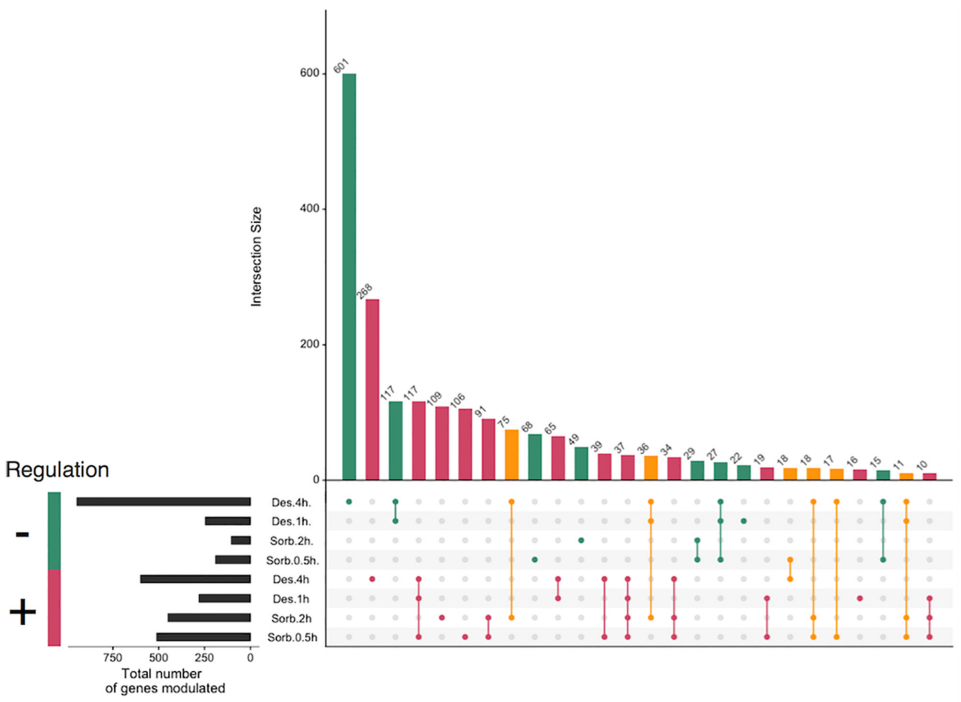

FIGURE 1 | Global modulation of gene expression in *Alternaria brassicicola* in response to applied treatments. Sorbitol and desiccation treatments were compared to non-treated cultures at two time points 0.5 h, 2 h and 1 h, 4 h, respectively. Genes with a *P*-values ≤0.05 and a log2 ratio ≥0.7 or ≤–0.7 were considered as differentially expressed. Intersection with less than 10 genes were omitted. Colors displayed regulation compared to the control; red = up-regulated in all conditions, green = down-regulated in all conditions, orange = opposite regulation according to the considered condition.

glutamate, alpha alanine, lysine and arginine concentration explained 70% [187.8/270.0 $\mu mol.g^{-1}$ DW (dry weight)] and 78% (156.3/199.8 $\mu mol.g^{-1}$ DW) of the amino acid variations for the sorbitol treatment at 0.5 and 2 h, respectively. For the 4 h desiccation condition, glutamine, GABA, alpha alanine and lysine explained 70% (134.7/194.6 $\mu mol.g^{-1}$ DW) of the amino acid variations. No significant concentration differences were observed for the 1 h desiccation treatment.

Then, we focused on sugar content, since their intracellular accumulation is a well-known protective mechanism to cope with the water constraints (Dupont et al., 2014). Eight saccharides and sugar alcohols were quantified in treated and control conditions (**Figure 3B**). The total concentration of those compounds was found to be significantly different only in the case of comparison between sorbitol-treated and untreated conditions (Welch test *P*-value = $2.05E^{-5}$, **Supplementary Figure S2**) regardless of the time exposure. Unexpectedly, we observed a strong accumulation of some sugars (arabitol, trehalose, mannitol) in the control of the desiccation condition. This result could explain that no significant difference on the sugar cellular contents was observed between treated and untreated samples, except for an arabitol accumulation after a 4 h-treatment.

As expected, glycerol was accumulated in fungal cells exposed to sorbitol. Two other polyols, arabitol and dulcitol, were also strongly accumulated under these conditions. Conversely, the amounts of other polyols and the disaccharide trehalose were lower in cells treated with sorbitol than in untreated conditions.

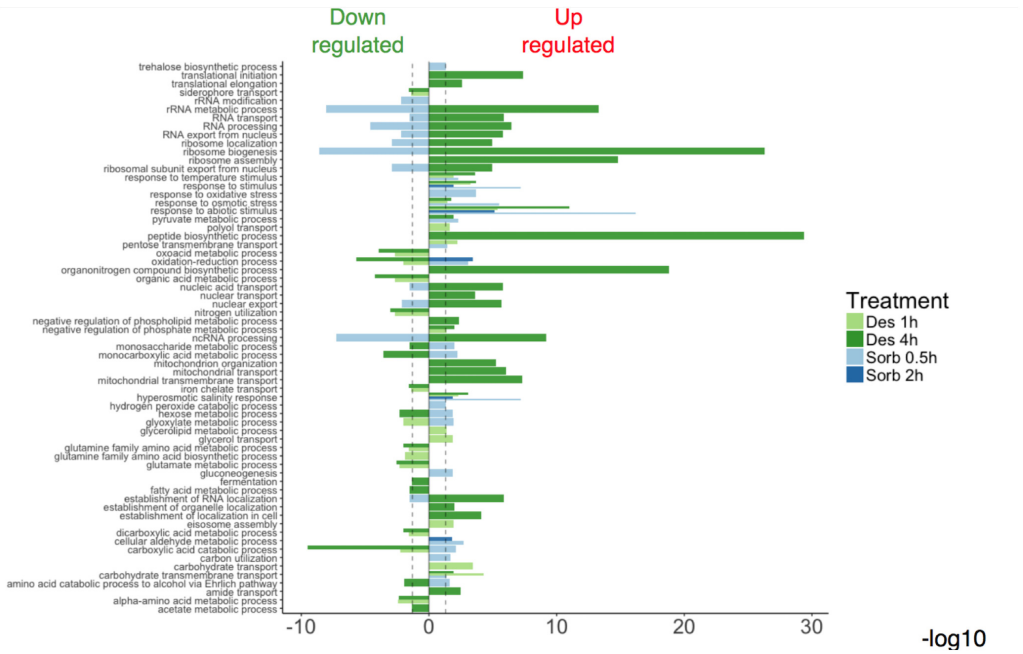

FIGURE 2 | Relevant Gene Ontology Biological Process (GO-BP) enrichments obtained from modulated gene sets after exposure to water stresses.

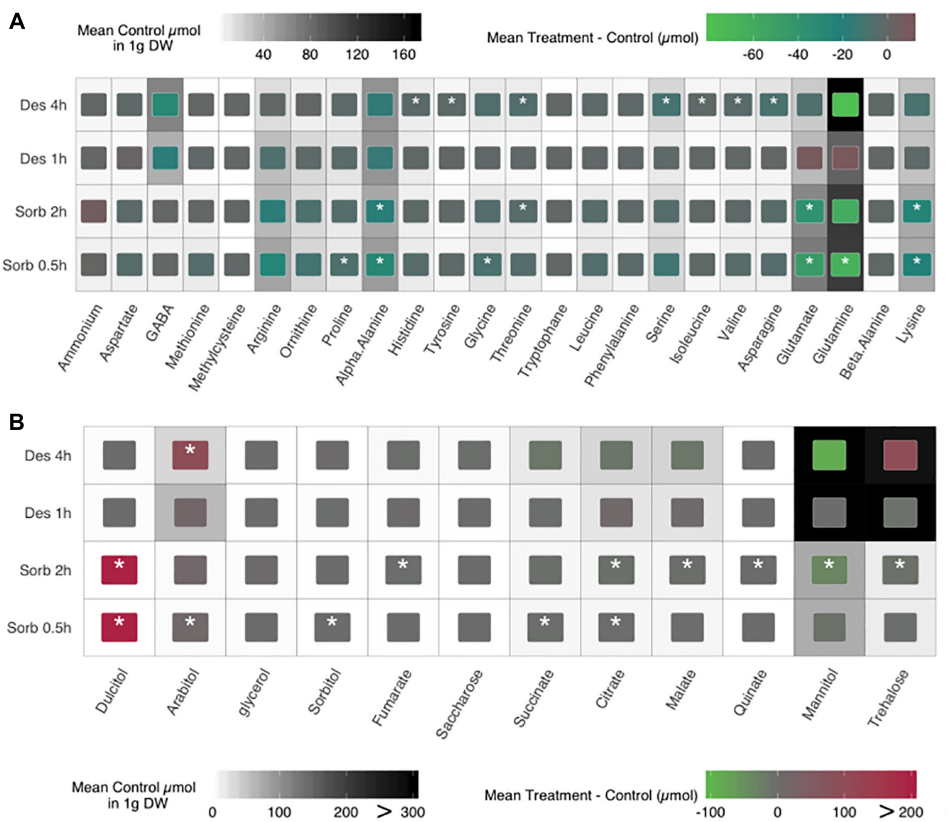

FIGURE 3 | Impact of sorbitol and desiccation treatments on amino acid **(A)**, saccharides and sugar alcohols **(B)** contents of fungal cultures. The heat map background displays the mean control contents. Internal colored boxes display the mean difference between treatments and controls. Quantifications were performed from three separate samples. Asterisks indicate a significant difference between the mutant and the parental isolate (Welch test, $*p \leq 0.05$).

Hydrophilins Identification Through *in silico* Analysis

Hydrophilins could be defined as glycine-rich, highly hydrophilic disordered proteins. This criterion was used to search in *A. brassicicola* for putative hydrophilins among the whole protein set deduced from the recently published genome of *A. brassicicola* strain Abra43 (12,456 entries, Belmas et al., 2018). A total of 732 predicted proteins with an average hydrophilicity above one (GRAVY index lower than −1) were first selected and analyzed for their glycine content. The 210 predicted proteins with at least 8% glycine were retained and subjected to secondary structure prediction analysis. Almost three quarters of them (165) were predicted to adopt a coil configuration over more than 50% of their length. After removing mis-annotated and incomplete proteins and those that had an obvious match upon Blast analysis with proteins of known functions (except "stress response"), a final set of 107 candidate hydrophilins (c.a. 0.9% of the whole predicted proteome) was selected (**Table 3**). Interestingly, among proteins that had physicochemical features of hydrophilins but were discarded after Blast analysis, several displayed similarities with proteins involved in nucleic acids metabolic processes (**Supplementary Table S1**). Each of the 107 candidate hydrophilins was characterized by an index of significance, calculated based on the following formula: [- (gravy index −1) X (% G – 8) X (% rc – 50)] X 100, whose value varied from 3 to 36.512. Six putative homologs of fungal hydrophilins were found within the whole set of *A. brassicicola* hydrophilin-like proteins: HSP12 (AB01868/Abra01064 and AB10131/Abra12207), STF2 (AB03803/Abra04061) from *Sa. cerevisiae*, CON10 (AB02056/Abra00844 and AB01782/Abra01163) and CON6 (Abra02927) from *Neurospora crassa*, and the dehydrin-like proteins from *A. brassicicola* AbDhn1 (AB02513/Abra00274) and AbDhn3 (AB05365, AB05364/Abra08036). None of the other yeast hydrophilins had putative homolog in the *A. brassicicola* genome except NOP6 (AB08803/Abra04570) and WWM1 (AB05865/Abra11690) that were not selected due to a glycine content below 8% or a gravy index above −1, respectively. Similarly, due to an average hydrophilicity below the threshold value, the other *A. brassicicola* dehydrin-like protein AbDhn2 (AB08993/Abra04787) was not selected within the candidate hydrophilins set. This protein set also contains the putative homolog DNA-damage responsive DDR48 (AB03330/Abra05531) protein from yeast.

Expression of Hydrophilins During Osmotic and Hydric Stress

Then, we explored the expression pattern of genes encoding putative hydrophilins from transcriptome data sets generated after exposing germinating conidia of *A. brassicicola* to 1.2 M sorbitol and to low relative humidity (silica gel beads). These data sets were obtained using microarrays designed based on the genome of the *A. brassicicola* ATCC 96836 strain available on the JGI Genome Portal (see footnote 1). This genomic sequence contained 10,514 predicted genes and the proportion of gaps between scaffolding boards in this sequence was relatively high (estimated to 5.2% by Dang et al., 2015). As described above, the *in silico* analysis was performed from the recently published genome of *A. brassicicola* strain Abra43 (Belmas et al., 2018[2,3]), which is a higher quality sequence containing 12,456 predicted protein-coding genes. Considering these proteome differences, expression patterns were available only for 78 putative hydrophilins that matched with a predicted ORF from the ATCC 96836 strain proteome. Under these conditions, 17 of the 78 (21.8%) candidate hydrophilin genes were up-regulated by the sorbitol treatment (**Figure 4A**). For all of them, except AB03330 and AB00441, an induced expression was observed at 0.5 h (**Figure 4B**). Moreover, 13 candidate hydrophilin genes were up-regulated by the desiccation treatment, 10 of them being also up-regulated upon the sorbitol treatment. All of these proteins were named with the abbreviation "SIH" for "stress-induced hydrophilin-like" (**Table 3**).

To gain insight on the possible regulation of hydrophilin genes expression by different kinases known to regulate the osmostress response, the expression profiles of hydrophilin genes in the Δ*abhog1*, Δ*abnik1* and Δ*absch9* mutants were compared with those in the wild-type parental strain under both control condition and after exposure to sorbitol for 0.5 h (**Figure 4**). This analysis revealed that, among the sorbitol-inducible hydrophilin genes, 6 were dependent of at least two of the three kinases for their expression. Two were regulated by AbHog1 and AbNik1, two others by AbHog1- and AbSch9 and three others by AbHog1, AbNik1 and AbSch9. The gene encoding AbDhn2 was also induced by the treatment and was found Hog1-Nilk1-Sch9-dependent.

Role of Selected Hydrophilins in *A. brassicicola*

Two putative hydrophilins (AbSih3/AB01868 and Absih15/AB05148) were selected for further studies aiming to investigate their function in *A. brassicicola*. Knockout mutants deficient for AbSih3 and Absih15 (called Δ*absih3* and Δ*absih15*), respectively, were constructed by replacing the respective ORFs with a hygromycin B resistance cassette (**Supplementary Figure S3**). For each targeted gene, two replacement mutants were selected using a PCR screen and further purified by two rounds of single-spore isolation. In all further experiments, the phenotypic characters for transformants of the same genotype were not found to be significantly different and the phenotyping values that we displayed were calculated by taking into account both transformants.

Although the expression of these genes was induced in germinating conidia exposed to previously defined water stress (i.e., exposure to 1.2 M sorbitol and to silica gel beads), the knock-out approach showed that only the *AbSih3* deletion had an impact on phenotype, mainly on oxidative stress tolerance. The corresponding deficient single mutants were indeed characterized by a slightly increased susceptibility toward oxidative stress generated by exposure to menadione and H_2O_2 compared to the wild-type (**Figure 5**). No significant difference in susceptibility to other tested stresses (exposure to PEG −0.7 MPa,

[2]https://www.ncbi.nlm.nih.gov/nuccore/PHFN00000000

[3]https://bbric-pipelines.toulouse.inra.fr/myGenomeBrowser?public=1

TABLE 3 | Set of candidate hydrophilins identified from the *Alternaria brassicicola* genome sequence through *in silico* analysis.

Prot ID									
Ab43 genome	**ref genome**	**Gravy**	**Length**	**%G**	**%CC**	**Score**	**Blast**	**Stress induction**	**Proposed name**
Abra00077	AB02678	−1.11	100	11	51	34			
Abra00088	AB02665	−1.00	334	9.3	58	5		+	AbSih1
Abra00257	AB04427	−1.16	349	9.7	59	252			
Abra00274	AB02513	−1.07	408	9.1	72	172	DHN1	+	AbDhn1
Abra00844	AB02056	−1.07	114	15.8	69	1092	con10	+	AbSih2
Abra01053	AB01878	−1.02	77	15.6	62	213			
Abra01064	AB01868	−1.08	100	13	54	164	HSP12	+	AbSih3
Abra01163	AB01782	−1.17	75	17.3	54	625	con10		
Abra01374	AB01197	−1.06	124	12.9	79	791			
Abra01387	AB01185	−1.14	255	27.1	76	7186			
Abra01450	AB01144	−1.16	551	8.5	62	98			
Abra01572	AB01031	−1.10	327	10.1	60	207			
Abra01616	AB00988	−1.10	236	12.2	64	598			
Abra01703	AB00914	−1.28	849	12	72	2426			
Abra01742	AB00884	−1.07	443	9.7	54	47		+	AbSih4
Abra01976	AB00692	−1.24	486	9.5	63	474			
Abra02025	AB00652	−1.38	196	10.1	61	884			
Abra02123	AB00572	−1.04	142	9.9	59	65			
Abra02179	AB00532	−1.78	62	16.1	75	15873			
Abra02286	AB00441	−1.20	84	10.7	71	1114		+	AbSih5
Abra02383	AB00362	−1.04	1020	8.9	67	59			
Abra02582	AB00195	−1.16	120	10	66	523		+	AbSih6
Abra02745	AB10671	−1.63	323	14.6	65	6262		+	AbSih7
Abra02936	AB09442	−1.01	139	12.2	63	35			
Abra03033	AB09525	−1.02	270	11.1	61	56		+	AbSih8
Abra03243	AB04503	−1.27	122	13.9	53	474			
Abra03342	AB04427	−1.12	309	9.7	67	343			
Abra03378	AB04393	−1.44	200	19	77	13068			
Abra03462	AB04328	−1.36	340	18.5	60	3805			
Abra03538	AB04263	−1.01	358	9.8	64	28			
Abra03729	AB04091	−1.04	112	14.3	60	225			
Abra03785	AB04037	−1.21	417	10.8	63	781	PAL1		
Abra03984	AB03874	−1.33	494	10.1	71	1465			
Abra04061	AB03803	−1.13	155	9	62	153	STF2		
Abra04301	AB10372	−1.49	396	8.1	53	15			
Abra04434	AB08681	−1.04	578	19.7	63	676			
Abra04604	AB08829	−1.15	344	9	58	118			
Abra04882	AB09668	−1.20	146	8.2	52	8			
Abra05347	AB01286	−1.02	664	9.8	66	59			
Abra05531	AB03330	−1.96	314	13.7	90	21943	DDR48	+	AbSih9
Abra05532	AB03329	−1.24	397	27.2	69	8592		+	AbSih10
Abra05581	AB03281	−1.24	210	15.7	79	5253			
Abra05783	AB03114	−1.49	89	10.1	60	1026			
Abra05849	AB03052	−1.11	310	13.2	71	1180		+	AbSih11
Abra06033	AB02899	−1.06	267	9	56	34		+	AbSih12
Abra06151	AB02794	−1.14	138	16.7	68	2145		+	AbSih13
Abra06575	AB07491	−1.22	587	10.7	56	357		+	AbSih14
Abra06733	AB07371	−1.04	79	13.9	72	509			
Abra06831	AB10289	−1.08	87	24.1	87	4519			
Abra07098	AB04617	−1.15	49	8.2	69	56			
Abra07398	AB04822	−1.04	112	8.9	62	39			

(Continued)

TABLE 3 | Continued

Prot ID									
Ab43 genome	**ref genome**	**Gravy**	**Length**	**%G**	**%CC**	**Score**	**Blast**	**Stress induction**	**Proposed name**
Abra07543	AB04946	−1.41	59	8.5	64	285			
Abra07677	AB05060	−1.35	281	11.4	63	1535			
Abra07755	AB05132	−1.18	425	9.2	61	231			
Abra07777	AB05148	−1.08	132	10.6	70	437		+	AbSih15
Abra07844	AB05207/	−1.09	177	10.2	78	529			
Abra08036	AB05365 AB05364	−1.00	1314	10.3	68	7	DHN3	+	AbDhn3
Abra08116	AB05433	−1.24	383	18.5	62	3040		+	AbSih16
Abra08144	AB05453	−1.10	131	16	74	1964		+	AbSih17
Abra08312	AB01538	−1.25	178	12.4	70	2200			
Abra08733	AB06615	−1.15	265	9.1	63	216			
Abra09230	AB08588	−1.22	148	8.1	60	22			
Abra09944	AB07063	−1.55	93	8.6	53	99			
Abra09988	AB07108	−1.29	108	9.3	58	298			
Abra10303	AB09288	−1.17	233	9.4	54	97			
Abra10788	AB07911	−1.34	139	12.9	63	2186			
Abra10847	AB07968	−1.21	76	10.5	68	953			
Abra10981	AB08081	−1.13	206	8.7	51	9			
Abra11043	AB08134	−1.18	127	12.6	62	1008			
Abra11399	AB06102	−1.40	238	20.6	75	12640			
Abra11512	AB06021	−1.51	189	11.1	65	2379			
Abra11736	AB05830	−1.31	188	13.3	81	5016			
Abra11761	AB05809	−1.73	94	9.6	62	1393			
Abra12091	AB05542	−1.01	384	8.3	76	9			
Abra12172	AB05473	−1.88	224	12.1	81	11218			
Abra12188	AB10143	−1.18	326	10.4	80	1281			
Abra12207	AB10131	−1.03	101	14.9	58	186	HSP12	+	AbSih18
Abra12251	AB10094	−1.23	242	13.6	62	1522			
Abra09652		−1.27	62	11.3	72	1944			
Abra11726		−1.09	109	8.3	51	3			
Abra02927		−1.03	75	13.3	57	114	con 6		
Abra04037		−1.06	103	8.7	52	8			
Abra04374		−1.57	62	9.7	88	3709			
Abra04664		−1.14	180	14.4	62	1092			
Abra05405		−1.47	104	10.6	64	1722			
Abra06548		−1.45	164	10.4	59	971			
Abra12282		−1.46	159	12.6	60	2115			
Abra00223		−1.47	70	8.6	54	113			
Abra00730		−1.28	63	11.1	63	1126			
Abra01125		−1.01	44	9.1	79	44			
Abra02379		−1.01	73	20.5	53	41			
Abra02426		−1.67	52	13.5	57	2562			
Abra04371		−1.83	68	20.6	85	36512			
Abra04903		−1.44	69	8.7	53	93			
Abra05665		−1.05	60	8.3	65	22			
Abra06247		−1.06	51	9.8	62	131			
Abra07265		−1.56	52	9.6	71	1880			
Abra07528		−1.00	70	15.7	72	48			
Abra07587		−1.11	51	9.8	64	267			
Abra08211		−1.32	54	9.3	51	41			
Abra10089		−1.39	62	11.3	62	1552			
Abra10521		−1.52	52	9.6	71	1732			

(Continued)

TABLE 3 | Continued

Prot ID									
Ab43 genome	**ref genome**	**Gravy**	**Length**	**%G**	**%CC**	**Score**	**Blast**	**Stress induction**	**Proposed name**
Abra10564		−1.52	52	9.6	71	1732			
Abra10568		−1.40	58	8.6	72	526			
Abra11431		−1.10	52	9.6	53	47			
Abra12286		−2.04	66	10.6	69	5127			
Abra07568		−1.01	56	12.5	85	225			

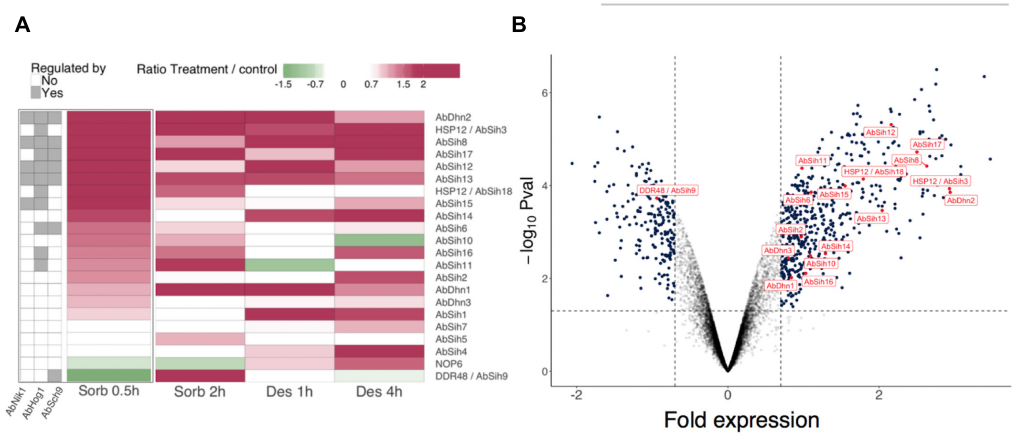

FIGURE 4 | Gene expression of *Alternaria brassicicola* hydrophilins in response to sorbitol and desiccation treatments. Sorbitol and desiccation treatments were compared to non-treated cultures at two time points 0.5 h, 2 h and 1 h, 4 h, respectively. **(A)** For each gene, numerical data were transformed into color-grid representations in which the fold gene expression induction (log2 values) is represented by a colored scale. In addition, hydrophilin gene expression were evaluated in mutant strains Δ*abnik1*, Δ*abhog1* and Δ*absch9* exposed to 1.2 M sorbitol for 0.5 h. The left part of the panel **(A)** highlights the possible regulation of hydrophilin gene expression by one or several of these protein kinases. **(B)** Volcano plot showing fold inductions of genes in the wild-type strain exposed to 1.2 M sorbitol for 0.5 h. The hydrophilin encoding genes are labeled and identified with red dots. The threshold values (*P*-values ≤0.05 and a log2 ratio ≥0.7 or ≤−0.7) are indicated by dash lines.

350 mM NaCl, 1.2 M sorbitol) was found compared to the wild-type (data not shown).

Consistently, a similar higher susceptibility to H_2O_2 of the *Sa. cerevisiae hsp12* null mutant was observed (**Figure 6**). To confirm that *AbSih3* correspond to true functional homolog of the yeast *hsp12* gene, complementation of *hsp12* mutant null mutant was carried out with relevant recombinant pYES plasmids. As shown in **Figure 6**, *AbSih3* successfully complemented the *Sa. cerevisiae hsp12* phenotypes, even if the growth of Δ*hsp12* cells expressing AbSih3 was not restored to a level comparable to that of the WT strain containing the empty vector pYES2 on media supplemented with 1 mM H_2O_2.

Then, the virulence of the *A. brassicicola* wild-type, Δ*absih3* and Δ*absih15* strains were compared on *B. oleracea* and *A. thaliana* host plants during host vegetative tissue infection or during the seed transmission process. *Brassica oleracea* leaves were inoculated with drops of conidia suspension (10^5, 10^4, or 10^3 conidia/mL). As shown in **Figure 7**, the wild-type and KO strains were all able to produce typical symptoms and their aggressiveness was not impaired. Regardless of the inoculated strain, first necrotic symptoms appeared on leaves at 3 days post-inoculation (dpi). Necrotic areas enlarged and surrounded themselves with chlorotic halos at 6 dpi. During late stages of infection, the fungus produced conidia on the surface of necrosis.

Using the model pathosystem previously described by Pochon et al. (2012) for investigating seed transmission in *Arabidopsis* plants, the ability of the hydrophilin mutants to transmit to seeds was compared with that of the wild-type. As a positive control, we also analyzed the behavior of the osmosensitive fungal mutants Δ*abnik1* and Δ*abhog1*, which were previously described as being strongly altered in their seed transmission capacity (Pochon et al., 2012). Silique inoculation with the wild-type and hydrophilin mutant strains resulted in the development of mycelium and typical lesions covered with conidia on siliques within a few days after inoculation. Seeds were then individually harvested and plated on PDA medium for a microbiological examination. As expected, a strong decrease in seed transmission rate was observed for Δ*abnik1* and Δ*abhog1* compared to the wild-type parental strain (**Figure 8**). Interestingly, the seed transmission capacity of the Δ*absch9* mutant was not altered although this strain was found to be sensitive to sorbitol and desiccation. While the deletion of *AbSih3* had a slight significant impact on seed transmission, a stronger decrease was observed for the Δ*absih15* mutant, for which the seed

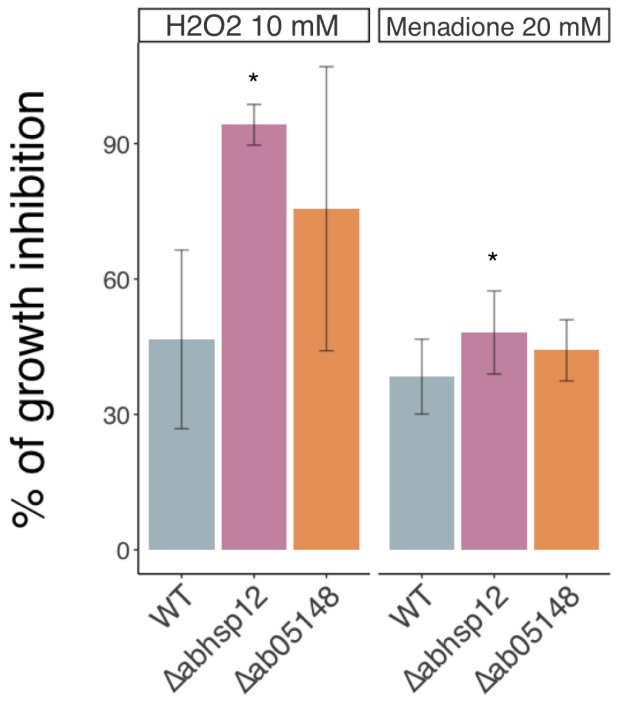

FIGURE 5 | Growth inhibition rates of the wild-type strain (WT) and hydrophilin deficient mutants in the presence of H_2O_2 (10 mM) and menadione (20 mM). The results are expressed as the percentage of inhibition in treated samples compared to the control without additive. Conidia were used to inoculate microplate wells containing standard PDB medium that was supplemented with the appropriate test substance. Growth was automatically recorded for 30 h at 25°C using a nephelometric reader (see section "Materials and Methods"). Each genotype was analyzed in triplicate and the experiments were repeated at least three times per growth condition. Error bars indicate standard deviations. Asterisks indicate a significant difference between the mutant and the parental isolate (Dunn control test, $*p \leq 0.01$).

transmission rate was reduced by a factor two compared to the wild-type strain.

DISCUSSION

The ability of *A. brassicicola* to cope with water-stress constitutes a key factor for successful seed colonization and thus accomplishment of its entire infectious cycle (Iacomi-Vasilescu et al., 2008; Pochon et al., 2012, 2013). Highly hydrophilic and disordered glycin-rich proteins containing repeated DPR-motifs called dehydrins were identified in *A. brassicicola* and might correspond to effectors of the response to water stress (Pochon et al., 2013). Based on their physicochemical features, dehydrins are considered as members of a larger protein family called hydrophilins initially described in *Sa. cerevisiae* (Garay-Arroyo et al., 2000). In an attempt to identify additional effectors of the response of *A. brassicicola* to water stress, the proteome deduced from the recently published genome of *A. brassicicola* strain Abra43 (Belmas et al., 2018) was first screened for proteins with characteristic features of hydrophilins. Candidate hydrophilins accounted for 0.9% of the whole predicted proteome. In comparison, hydrophilins represented only 0.2% of the yeast proteome (Garay-Arroyo et al., 2000) although the selection criteria were less stringent, i.e., proteins with lower glycine content were included. This difference might reflect a family expansion associated with environmental adaptation and/or fungal pathogenesis as it was proposed for other sets of proteins, e.g., secreted proteins, enzymes for secondary metabolites production (Soanes et al., 2008; Ohm et al., 2012). However, this assumption remains to be demonstrated and would require a more extensive search for hydrophilin repertoires in fungi with various lifestyles.

The fact that two of the three previously described dehydrins and additional homologs of fungal hydrophilins were included in the repertoire of candidate hydrophilins validated our screening process. Garay-Arroyo et al. (2000) proposed that hydrophilins that were not induced by water-stress conditions should not be considered as true hydrophilins. Thus, we analyzed changes in transcript levels in *A. brassicicola* germlings exposed to two kinds of water-stress: hyperosmosis (exposure to 1.2 M sorbitol) and desiccation (exposure to silica gel beads). Using gene expression array, which was designed from a previous genome sequence with a lower quality, we defined the expression patterns of 78 genes (over 107) encoding these putative hydrophilins. Twenty candidate hydrophilin genes were up-regulated either by the sorbitol treatment or by the desiccation stress, and, among them, ten were induced by both treatments. So, according to the hydrophilin definition given by Garay-Arroyo et al. (2000), we identified at least 20 hydrophilins in *A. brassicicola*. However, we can reasonably assume that their number is higher since we did not have access to the gene expression of 29 other genes encoding putative hydrophilins.

In this study, strains deficient for AbSih3 exhibited a slightly lower susceptibility to oxidative stress compared to the wild-type strain. No significant difference in susceptibility to other tested stresses (exposure to PEG, NaCl and sorbitol) was found for Δ*absih3* and Δ*absih15*. Given the large number of hydrophilins that were co-expressed in this organism, functional redundancy may occur between some of these proteins. This process would explain the scarcity of significant phenotypes that we obtained from single deficient mutants since the presence of other hydrophilin genes would compensates for the loss. For instance, AbSih3 displays high sequence similarity to AbSih18 (AB10131), and both may be considered as homologs of the *Sa. cerevisiae* HSP12 hydrophilin, even if AbSih3 only partially compensated the HSP12 loss in yeast. The existence of such a functional redundancy was also previously observed between two dehydrins AbDhn1 and AbDhn2 in *A. brassicicola*. The double mutant Δ Δ*abdhn1-abdhn2* was severely compromised in its pathogenicity while the respective single mutants were not affected (Pochon et al., 2013).

Despite this probable functional compensation, we showed here that the hydrophilins Absih3 and Absih15 could be considered as pathogenic factors since the corresponding null strains were affected in its seed transmission ability (more strongly for the Δ*absih15* strain). This result confirmed our initial assumption that an efficient fungal adaptive response to severe hydric stress conditions or to oxidative stress strongly influenced

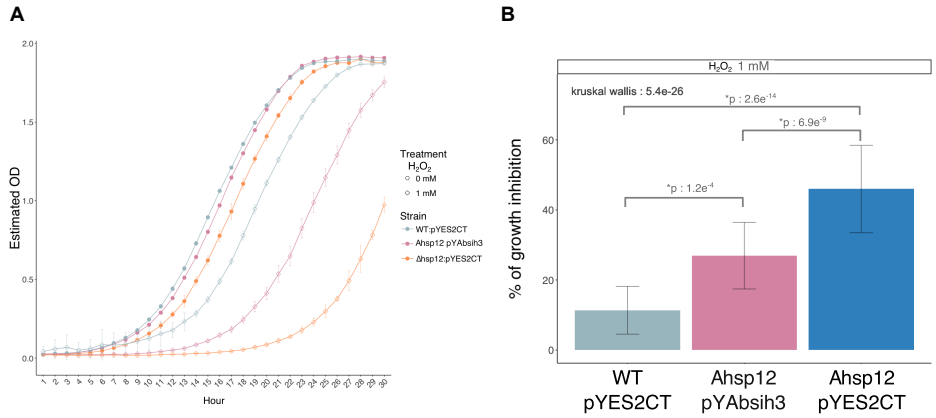

FIGURE 6 | Complementation of yeast Δ*hsp12* mutants with *AbSih3* coding sequences. **(A)** Growth curves of *Saccharomyces cerevisiae* (parental WT strain and Δ*hsp12* mutants) cells transformed with empty vector (pYES2CT) or recombinant vectors (pYAbsih3) exposed to 1 mM H_2O_2 or to water. **(B)** Comparisons of growth inhibition rates obtained for each yeast strain (Wilcoxon test, $*p < 0.001$).

FIGURE 7 | Representative symptoms at 5 dpi obtained by inoculation of wildtype, Δ*absch9*, Δ*absih3*, and Δ*absih15* on cabbage leaves. Leaves were inoculated with 5 μL drops of conidia suspension (10^5, 10^4 or 10^3 conidia/mL in water). As shown on the right side, mutants were inoculated on the right part of the central vein and compared on the same leaf with the parental strain (inoculated on the left part of the central vein). Bars = 2 cm.

the seed transmission ability. This is consistent with the fact that, during seed colonization, fungi are exposed to a gradual decrease in the water potential occurring in maturing reproductive organs and that they have to cope with this particular stress to be efficiently transmitted to seeds and complete their infection cycle. In the same vein, we showed in this study or in previous works that the class III HK AbNik1 and the MAP kinase AbHog1, two components of the high osmolarity pathway, were required for an effective seed colonization by *A. brassicicola* (Pochon et al., 2012). The Δ*absch9* mutant was also found to be sensitive to sorbitol and desiccation but, unexpectedly, its seed transmission capacity was not altered. The fact that this mutant strain did not exhibit a high susceptibility to oxidants suggested that the fungal ability to overcome oxidative stress would be an additional or the main key mechanism for an efficient seed infection process. This hypothesis is consistent with the fact that oxidative damages produced by free radical species are considered to be one of the major causes of desiccation injuries (Dupont et al., 2014).

A final point raised from these results is that several *A. brassicicola* mutants (Δ*abnik1,* Δ*absih3* and Δ*absih15)* were affected in their transmission to *A. thaliana* seeds, although their aggressiveness on host vegetative tissues remained intact. This fact confirms the specificity of some molecular mechanisms controlling transgenerational transmission of fungal pathogens (Pochon et al., 2012) and validates the strategy to gain further insight into these mechanisms for the development of specific seed disease control strategies.

In addition to the induction of genes encoding hydrophilins, we identified other metabolic clues related to the activation of an adaptive response to water stress in *A. brassicicola*. First, the cellular content in amino acids was strongly disturbed following the application of both stresses. The amino acid levels were indeed significantly reduced in treated cells compared to controls. In line with this result, several enriched GO categories emerging from transcriptomic data were linked to amino acid metabolism and catabolism. Moreover, amino acid synthesis was also found to be strongly down-regulated in response to the osmotic stress treatment in another *Dothideomycete* fungus, the wheat pathogen *Stagonospora nodorum* (Lowe et al., 2008). As reported in plants (Hildebrandt et al., 2015), the degradation of amino acids may lead to the production of an additional energetic resource, that could be useful to cope with adverse conditions, by

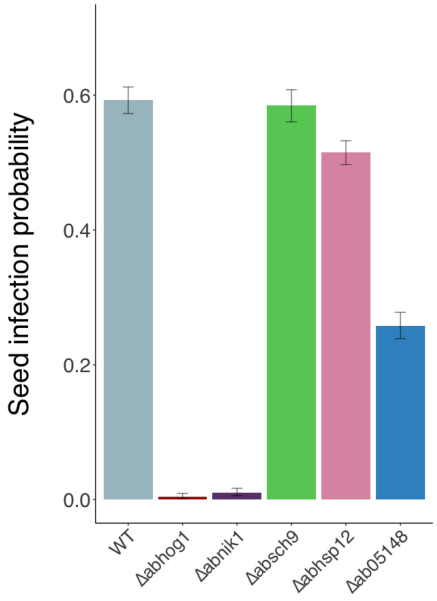

FIGURE 8 | Transmission capacity of *Alternaria brassicicola* wild-type (WT) and null strains to *Arabidopsis thaliana* seeds (Ler ecotype). The seed transmission capacity were measured as described by Pochon et al. (2012). The five youngest siliques of at least five plants were inoculated with each fungal genotype and the experiment was repeated twice. Contaminated siliques were harvested 10 dpi. After dissection, seeds were incubated separately on PDA medium for 2 days. A seed was considered contaminated when incubation resulted in typical *Alternaria brassicicola* colony development. For each inoculated fungal genotype, the seed infection probability was evaluated from at least 1000 seeds. Values represent infection probabilities with 95% confidence interval.

providing intermediates of the tricarboxylic acid cycle and finally contributing to ATP production. Moreover, the oxidation of some amino acids feeds electrons into the mitochondrial electron transport chain. Most reaction steps of the catabolic pathways occur either in the mitochondria or cytosol. Consistent with this hypothesis, several enriched GO terms referred to mitochondria organization, carboxylic acid metabolism and to oxidation-reduction process. Regarding the response to desiccation, as a GO enrichment of functions related to the genesis and transport of ribosomes and, more generally, to translation was observed, we could assume that a strong induction of the translation process would trigger a depletion of the cellular amino acid pool. So, the mechanisms leading to the decrease of the amino acid could depend on the type of applied stress.

An intriguing result from our data was that no significant difference in the amino acid concentrations was observed for the 1 h-desiccation treatment compared to the respective control. A more precise inspection showed that, for this condition, both control and treated samples showed a similar low amino acid content (**Supplementary Figure S2**). In this assay, germlings grown on cellophane were taken off from the PDA plate and directly transferred to sealed boxes (without additional agar medium) with or without silica gel beads. In the control box (without silica gel), we suspect that germlings were also exposed to a strong constraint in the early time of exposure, as a period of 4 h was required to gradually reach a RH value of about 90%. Therefore, although this experimental device triggered a specific regulation at the transcriptome level (**Figures 1**, **2**), this does not appear to be sufficient to reveal significant differences in amino acid accumulation between control and treated samples at this analysis time.

In the sorbitol-exposed samples, a strong increase in global sugar contents was observed compared to sorbitol control. Interestingly, the accumulation of non-reducing disaccharides, such as trehalose, did not seem to be favored in *A. brassicicola* germlings under the sorbitol stress conditions. On the contrary, the contents of three polyols, glycerol, arabitol and dulcitol, were mainly impacted by this stress, suggesting that they function as intracellular osmolytes to counteract the effects of decreases in the cell volume and the loss of turgor pressure (Sánchez-Fresneda et al., 2013; Dupont et al., 2014). This result was consistent with the increased sensitivity of the Δ*abhog1* mutant to osmotic stress since the MAP kinase Hog1 is known to be required for endogenous glycerol production in several fungal species (Brewster and Gustin, 2014; Hohmann, 2015). However, its involvement in the synthesis of other protective compounds, such as arabitol or dulcitol, is still unclear (Kayingo and Wong, 2005; Sánchez-Fresneda et al., 2013). Arabitol has been described as part of a set of polyols which is developed to counteract environmental challenges in several yeasts and filamentous fungi (Pascual et al., 2003; Sánchez-Fresneda et al., 2013). For instance, arabitol, and to a lesser extent glycerol, were found to accumulate in response to the osmotic stress treatment in the wheat pathogen *St. nodorum* (Lowe et al., 2008) or in the rice pathogen *Magnaporthe grisea* (Dixon et al., 1999). Conversely, the role of dulcitol in stress responses remains highly confidential and has been reported on rare occasions, for instance in the marine fungus *Cirrenalia pygmea* (Ravishankar et al., 2006).

In addition to its involvement in the synthesis of compatible solutes, we showed here that the HOG pathway, mainly regulated by the MAP kinase AbHog1 and the upstream HK AbNik1, also acted as an expression regulator of some hydrophilin encoding genes. The expression profiles of hydrophilin genes in the Δ*abhog1*, Δ*abnik1*, and Δ*absch9* mutants were indeed compared with those in the wild-type parental strain after exposure to sorbitol for 0.5 h. Of the 17 proteins that were induced under these conditions, 11 and 5 were found to be under the control of AbHog1 and AbNik1, respectively. This result, associated with the weakness of Δ*abnik1* and Δ*abhog1* to survive on reproductive organs, highlighted that the HOG pathway is a major target for controlling both the synthesis of osmolytes and hydrophilins, and thus limiting the transmission of fungal pathogens to seeds. Unexpectedly, AbDhn1 and AbDhn3 were not part of this set of HOG-regulated proteins although Pochon et al. (2013) previously reported that these two proteins (in addition to AbDhn2) were targets for the AbHog1 signaling cascade when the fungus was exposed to a saline (NaCl) stress. This suggests a possible differential regulation of hydrophilins depending on the applied constraint.

Following a 0.5 h-sorbitol exposure, six other hydrophilins were also found to be AbSch9-dependent. As a major downstream effector of the target of rapamycin (TOR) complex 1, the Sch9 protein kinase was proposed to play multiple roles in stress resistance and nutrient sensing in *Sa. cerevisiae* (Pascual-Ahuir and Proft, 2007; Huber et al., 2009). However, the functions of *Sch9* orthologs in filamentous fungi have been poorly characterized to date. In *Fusarium graminearum*, Gu et al. (2015) showed that FgSch9 served as a mediator of the TOR and HOG pathways and played important roles in regulating vegetative differentiation, secondary metabolism and stress responses. We showed here that both hydrophilins AbSih3 and AbSih15 were necessary factors for an optimal *A. brassicicola* transmission to seeds but their expression was not found to be regulated by AbSch9 (regulation by AbHog1 and AbHog1-AbNik1, respectively). This result, associated with the fact that the seed transmission capacity of the Δ*absch9* mutant was not affected, suggested that this kinase (unlike AbHog1 and AbNik1), although involved in resistance to sorbitol and desiccation, is not a major player in transgenerational transmission of fungal pathogens.

MATERIALS AND METHODS

Strains and Culture Conditions

The *A. brassicicola* wild-type strain *Abra43* used in this study was previously described (Sellam et al., 2007). For routine culture, *A. brassicicola* was grown and maintained on potato dextrose agar (PDA). The genome of *Abra43* strain was recently published and is available following this link https://bbric-pipelines.toulouse.inra.fr/myGenomeBrowser? (Carrere and Gouzy, 2017).

For transcriptomic analyses, exposure to sorbitol (osmotic stress) or to low relative humidity (desiccation stress) were achieved as follows. Conidia were first incubated for 24 h on cellophane disks overlaid on solid PDA medium. Germlings and the underlying cellophanes were then taken off from the agar plate and transferred either to a second PDA medium supplemented or not with 1.2 M sorbitol for 0.5 or 2 h.

The desiccation stress was achieved by applying a drastic decrease in relative humidity (RH) to the germlings (obtained as described below) by exposure to silica gel beads in sealed boxes for 0.5 or 4 h. Immediately after deposition of germlings (and the underlying cellophanes) in boxes, a strong RH increase was observed. In the control box (without silica gel), a gradual increase up to a RH value of about 90% in 4 h was observed. With silica gel beads, the opening of the boxes resulted in a rapid RH increase up to 20% followed by a decrease to a RH value of 1% in less than 0.5 h.

To evaluate the level of stress for each treatment applied to fungal cells and considering that the reference strain is naturally tolerant to water stress (Iacomi-Vasilescu et al., 2008), we additionally analyzed the effect of treatments on three mutant strains (derived from the wild-type Abra43 strain) for which we hypothesized a higher sensitivity to water stress. Two mutant strains (Δ*abnik1* and Δ*abhog1*) were described in previous studies (Dongo et al., 2009; Joubert et al., 2011) and were deficient for genes encoding key regulators of the HOG pathway, the HK AbNik1 and the MAP kinase AbHog1, respectively. The third mutant was obtained in this study and was deficient for the kinase AbSch9, which is also known to be involved in the fungal response to osmotic constraints (Pascual-Ahuir and Proft, 2007). Under non-stress conditions, no significant differences in mycelium growth were detected in any of the tested mutants as compared to the wild-type (data not shown). To assess the impact of low RH exposure on *A. brassicicola*, viability tests were conducted on young hyphae of wild-type and mutant strains. About 200 conidia were first incubated for 24 h on cellophane disks overlaid on solid PDA medium. Then, germinated conidia were transferred for 4 days to sealed boxes containing or not silica gel beads. The cellophane membranes were then removed from the boxes and deposited again on PDA medium. The survival rate was calculated by counting the number of mycelial colonies (derived from treated or untreated germlings) after 3 days of incubation at 24°C. As previouslys reported (de Lima Alves et al., 2015; Wang et al., 2017), exposure to these two treatments induces water stress in fungal cells. Exposure of wild-type and mutant strains to 1.2 M sorbitol were performed following the procedure described below. The radial growth was calculated after 6 days of incubation.

To study hyphal growth in liquid media, conidial suspensions (10^5 conidia/mL, final concentration) were inoculated onto microplate wells containing the considered substance (10 mM H_2O_2 or 20 mM menadione) at the desired concentrations in potato dextrose broth (PDB, Difco) in a total volume of 300 μl. Fungal growth was monitored automatically over a 30 h period with a laser-based microplate nephelometer (NEPHELOstar, BMG Labtech) as described by Joubert et al. (2010). For each condition, the area under the growth curve representative of the lag phase was used to calculate the percentages of growth inhibition under stress conditions compared with standard growth conditions (PDB medium without additive), as described by Gaucher et al. (2013). At least three replicates were conducted per treatment.

RNA Extraction and Microarray Analysis

Total RNA was extracted using the nucleospin RNAplant kit (Macherey Nagel, Düren, Germany) and 400 ng were amplified using the Ambion messageAmp II (Ambion, Austin, TX, United States) according to the manufacturer's instructions. Five micrograms of amplified RNA were retro-transcribed with 400 U of Superscript II reverse-transcriptase (Invitrogen Corp., Carlsbad, CA, United States) and labeled with 1.5 mmol of Cyanine-3 (Cy3) or Cyanine-5 (Cy5) (Interchim, France) and then purified using NucleoSpin Gel and PCR Clean-up column kits (Macherey-Nagel, GmbH and Co., KG, Germany). Purified and labeled cDNA were quantified using a NanoDrop ND-1000. Corresponding Cy3- and Cy5 labeled samples (30 pmol) were combined and cohybridized to the Abra _v1.0 12 × 135K arrays on a NimbleGen Hybridization System 4 (mix mode B) at 42°C overnight. The Abra_v1.0 chip was *in situ* synthesized by Nimblegen (Madison, WI)

and contained 10,633 60-mer oligoprobes that were designed from the *A. brassicicola* automatically annotated genome database[4], containing one probe per sequence. Slides were washed, dried, and scanned at 2 μm resolution and high sensitivity with a Roche-NimbleGen MS200. DEVA Software version 1.2.1 was used to extract pair data files from the scanned images. Three biological replicates were analyzed per comparison using the dye-switch method. Statistical analyses of the gene expression data were performed using the R language, version 2.14, and the Linear Models for Microarray Analysis package (Smyth et al., 2005) from the Bioconductor project. For the preprocessing step, data were normalized by the LOWESS method. Log ratio and log intensity were calculated before differential expression analyses and performed using the lmFit function and the Bayes-moderated Student's *t*-test in a linear model for microarray analysis. Probes with *P*-value <0.05 were considered as differentially expressed. Gene expression datasets were deposited in the Gene Expression Omnibus (GEO)[5].

Quantitative PCR

Total RNA was extracted as described above. Amplification experiments were conducted as previously described (Joubert et al., 2011). The relative quantification analysis was performed using the ΔΔCt method (Winer et al., 1999). All the primer sequences used in real-time quantitative PCR are presented in the **Supplementary Table S2**.

Generation of Targeted Gene Knockout Mutants and Fusion Strains

We followed the procedure described by Pigné et al. (2017). Gene replacement cassettes were generated with the *Hph* gene cassette from pCB1636 (Sweigard et al., 1995) conferring resistance to hygromycin B. The sets of primers used to amplify the 5′ and 3′ flanking regions of each targeted gene are presented in the **Supplementary Table S2**. The replacement cassettes were used to transform *A. brassicicola* protoplasts as described by Cho et al. (2006). Primer combinations used to confirm integration of the replacement cassette at the targeted locus were presented in **Supplementary Figure S3**.

Yeast Complementation Assays

Complementation assays were performed in *Sa. cerevisiae* cells (strains: parental BY4743 Acc#Y20000, ΔHSP12 Acc#Y27070, Euroscarf, Germany) as described by Joubert et al. (2011). Sequences encoding AbSih3 were amplified by PCR with primer pairs AbSih3-Bam (5′-**GGATCC**AAAAATGACCGACGCATTCCGC-3′) – AbSih3-Eco (5′- **GAATTC**CCATTCCAAGGGCGTTTTTGG-3′). Unique BamH1-*Eco*RI restriction sites (indicated in boldface) were thus introduced at the upstream start and downstream of the coding sequences, respectively and were used to clone the PCR product into pGEM-T (Promega) and then into the yeast expression vector pYES2CT (Invitrogen) to generate the recombinant plasmid pYAbhsp12. Sensitivity to 1 mM H_2O_2 was analyzed based on microcultivation in 300 μl liquid medium. Growth in microplates was automatically recorded using a spectrophotometer (Spectrostar Nano, BMG Labtech) at 30°C.

Infection Assays

Leaf infection assays were performed on *B. oleracea* plants (var. Bartolo) as described by Joubert et al. (2011). The experiment was repeated twice and involved at least 10 leaves inoculated by each fungal genotype.

Seed infection assays and seed contamination assessments were performed as described by Pochon et al. (2012). At least five plants per fungal genotype were inoculated and the experiment was repeated twice.

Metabolic Extraction and Amino Acids and Sugar Analysis

Metabolic extractions were made on 15 mg of dry powdered samples. Procedures for methanol–chloroform–water-based extractions as well as determination of amino acid and carbohydrate contents were described by Thouvenot et al. (2015).

AUTHOR CONTRIBUTIONS

GN'G carried out the sample preparation and microarray analyses. RR, BI, and MM involved in the sample preparation for metabolic analysis and performed the quantitative PCR. NB-S carried out the yeast complementation assays. CM, MM, and CA-B involved in the construction and phenotyping of *Alternaria brassicicola* mutant strains. PS and TG conceived the study and participated in the design of the experiments as well as in the analysis of the results. RL and BP involved in sugar analyses from fungal samples. SP and J-PR involved in the gene expression analyses. CC, MM, FB, BH, AK, and BI involved in the pathological tests.

FUNDING

This research was supported in part by grants awarded by the Region des Pays de la Loire (FUNHY project). This research was also supported by post-doctoral fellowships (CA-B) provided by the University of Angers.

ACKNOWLEDGMENTS

The authors thank the Metabolic Profiling and Metabolomic (P2M2) Platform from the French public institute IGEPP for assistance during metabolic phenotyping.

SUPPLEMENTARY MATERIAL

The Supplementary Material for this article can be found online at: https://www.frontiersin.org/articles/10.3389/fmicb.2019.01969/full#supplementary-material

[4]https://genome.jgi.doe.gov/Altbr1/Altbr1.home.html

[5]https://www.ncbi.nlm.nih.gov/geo/query/acc.cgi?acc=GSE133507

FIGURE S1 | Comparison of transcript levels obtained by microarray or RT-qPCR methods. The expression of 9 genes was monitored in response to sorbitol and desiccation stresses. The fold inductions (log2 values) are presented in **(A)** and the correlation plot in **(B)**.

FIGURE S2 | Total organic contents in a 1 mg sample of dried fungal cultures sample exposed or not to sorbitol and desiccation treatments. **(A)** Total contents of amino acids. **(B)** Total content of saccharides and sugar alcohols. Colors display the treatments. Box plots show the median, 1st and 3rd quantiles ($n = 3$). *denotes a significant difference (P-value <0.001, Welsh test).

FIGURE S3 | Generation of null mutants by homologous recombination. **(A)** Schematic representation of the deleted locus in the wild-type and the replacement construct with the Hyg B resistance cassette (*Hph* gene). Arrows indicate the position of primers used for the cassette generation and for PCR screening of mutants. **(B)** Gel electrophoresis of PCR products obtained from template DNA of the wild-type, Δ*absch9*, Δ*absih3* and Δ*absih15* strains with the indicated primer pairs. Molecular sizes (kb) were estimated based on a 1 kb ladder (lane M, NEW ENGLAND BioLabs® Inc.). A supplementary PCR was done with the primer pair ITS1/ITS4 as a positive control to assess the quality of the wild-type template DNA.

TABLE S1 | List of predicted sequences from the *Alternaria brassicicola* genome exhibiting physicochemical features of hydrophilins and an obvious match upon Blast analysis with proteins of known functions.

TABLE S2 | List of primers used in this study.

REFERENCES

Abba', S., Ghignone, S., and Bonfante, P. (2006). A dehydration-inducible gene in the truffle *Tuber borchii* identifies a novel group of dehydrins. *BMC Genomics* 7:39. doi: 10.1186/1471-2164-7-39

Belmas, E., Briand, M., Kwasiborski, A., Colou, J., N'Guyen, G., Iacomi, B., et al. (2018). Genome sequence of the necrotrophic plant pathogen *Alternaria brassicicola* Abra43. *Genome Announc.* 6:e01559-17. doi: 10.1128/genomeA.01559-17

Brewster, J. L., and Gustin, M. C. (2014). Hog1: 20 years of discovery and impact. *Sci. Signal.* 7:re7. doi: 10.1126/scisignal.2005458

Calahan, D., Dunham, M., DeSevo, C., and Koshland, D. E. (2011). Genetic analysis of desiccation tolerance in *Sachharomyces cerevisiae*. *Genetics* 189, 507–519. doi: 10.1534/genetics.111.130369

Carrere, S., and Gouzy, J. (2017). myGenomeBrowser: building and sharing your own genome browser. *Bioinformatics* 33, 1255–1257. doi: 10.1093/bioinformatics/btw800

Cho, Y., Davis, J. W., Kim, K.-H., Wang, J., Sun, Q.-H., Cramer, R. A. Jr., et al. (2006). A high throughput targeted gene disruption method for *Alternaria brassicicola* functional genomics using linear minimal element (LME) constructs. *Mol. Plant Microbe Interact.* 19, 7–15. doi: 10.1094/MPMI-19-0007

Dang, H. X., Pryor, B., Peever, T., and Lawrence, C. B. (2015). The *Alternaria* genomes database: a comprehensive resource for a fungal genus comprised of saprophytes, plant pathogens, and allergenic species. *BMC Genomics* 16:239. doi: 10.1186/s12864-015-1430-7

Dang, N. X., and Hincha, D. K. (2011). Identification of two hydrophilins that contribute to the desiccation and freezing tolerance of yeast (*Saccharomyces cerevisiae*) cells. *Cryobiology* 62, 188–193. doi: 10.1016/j.cryobiol.2011.03.002

de Lima Alves, F., Stevenson, A., Baxter, E., Gillion, J. L., Hejazi, F., Hayes, S., et al. (2015). Concomitant osmotic and chaotropicity-induced stresses in *Aspergillus wentii*: compatible solutes determine the biotic window. *Curr. Genet.* 61, 457–477. doi: 10.1007/s00294-015-0496-8

Dixon, K. P., Xu, J. R., Smirnoff, N., and Talbot, N. J. (1999). Independent signaling pathways regulate cellular turgor during hyperosmotic stress and appressorium-mediated plant infection by *Magnaporthe grisea*. *Plant Cell* 11, 2045–2058. doi: 10.1105/tpc.11.10.2045

Dongo, A., Bataillé-Simoneau, N., Campion, C., Guillemette, T., Hamon, B., Iacomi-Vasilescu, B., et al. (2009). The group III two-component histidine kinase of filamentous fungi is involved in the fungicidal activity of the bacterial polyketide ambruticin. *Appl. Environ. Microbiol.* 75, 127–134. doi: 10.1128/AEM.00993-08

Dupont, S., Rapoport, A., Gervais, P., and Beney, L. (2014). Survival kit of *Saccharomyces cerevisiae* for anhydrobiosis. *Appl. Microbiol. Biotechnol.* 98, 8821–8834. doi: 10.1007/s00253-014-6028-5

Gadd, G. M., Chalmers, K., and Reed, R. H. (1987). The role of trehalose in dehydration resistance of *Saccharomyces cerevisiae*. *FEMS Microbiol. Lett.* 48, 249–254. doi: 10.1111/j.1574-6968.1987.tb02551.x

Garay-Arroyo, A., Colmenero-Flores, J. M., Garciarrubio, A., and Covarrubias, A. A. (2000). Highly hydrophilic proteins in prokaryotes and eukaryotes are common during conditions of water deficit. *J. Biol. Chem.* 275, 5668–5674. doi: 10.1074/jbc.275.8.5668

Gaucher, M., Dugé de Bernonville, T., Lohou, D., Guyot, S., Guillemette, T., Brisset, M.-N., et al. (2013). Histolocalization and physico-chemical characterization of dihydrochalcones: insight into the role of apple major flavonoids. *Phytochemistry* 90, 78–89. doi: 10.1016/j.phytochem.2013.02.009

Goyal, K., Walton, L. J., and Tunnacliffe, A. (2005). LEA proteins prevent protein aggregation due to water stress. *Biochem. J.* 388, 151–157. doi: 10.1042/BJ20041931

Gu, Q., Zhang, C., Yu, F., Yin, Y., Shim, W.-B., and Ma, Z. (2015). Protein kinase FgSch9 serves as a mediator of the target of rapamycin and high osmolarity glycerol pathways and regulates multiple stress responses and secondary metabolism in *Fusarium graminearum*. *Environ. Microbiol.* 17, 2661–2676. doi: 10.1111/1462-2920.12522

Hildebrandt, T. M., Nunes Nesi, A., Araújo, W. L., and Braun, H.-P. (2015). Amino acid catabolism in plants. *Mol. Plant* 8, 1563–1579. doi: 10.1016/j.molp.2015.09.005

Hohmann, S. (2015). An integrated view on a eukaryotic osmoregulation system. *Curr. Genet.* 61, 373–382. doi: 10.1007/s00294-015-0475-0

Huber, A., Bodenmiller, B., Uotila, A., Stahl, M., Wanka, S., Gerrits, B., et al. (2009). Characterization of the rapamycin-sensitive phosphoproteome reveals that Sch9 is a central coordinator of protein synthesis. *Genes Dev.* 23, 1929–1943. doi: 10.1101/gad.532109

Iacomi-Vasilescu, B., Bataille-Simoneau, N., Campion, C., Dongo, A., Laurent, E., Serandat, I., et al. (2008). Effect of null mutations in the *AbNIK1* gene on saprophytic and parasitic fitness of *Alternaria brassicicola* isolates highly resistant to dicarboximide fungicides. *Plant Pathol.* 57, 937–947. doi: 10.1111/j.1365-3059.2008.01864.x

Joubert, A., Bataille-Simoneau, N., Campion, C., Guillemette, T., Hudhomme, P., Iacomi-Vasilescu, B., et al. (2011). Cell wall integrity and high osmolarity glycerol pathways are required for adaptation of *Alternaria brassicicola* to cell wall stress caused by brassicaceous indolic phytoalexins. *Cell. Microbiol.* 13, 62–80. doi: 10.1111/j.1462-5822.2010.01520.x

Joubert, A., Calmes, B., Berruyer, R., Pihet, M., Bouchara, J.-P., Simoneau, P., et al. (2010). Laser nephelometry applied in an automated microplate system to study filamentous fungus growth. *Biotechniques* 48, 399–404. doi: 10.2144/000113399

Kayingo, G., and Wong, B. (2005). The MAP kinase Hog1p differentially regulates stress-induced production and accumulation of glycerol and D-arabitol in *Candida albicans*. *Microbiology* 151, 2987–2999. doi: 10.1099/mic.0.28040-0

López-Martínez, G., Rodríguez-Porrata, B., Margalef-Català, M., and Cordero-Otero, R. (2012). The STF2p hydrophilin from *Saccharomyces cerevisiae* is required for dehydration stress tolerance. *PLoS One* 7:e33324. doi: 10.1371/journal.pone.0033324

Lowe, R. G. T., Lord, M., Rybak, K., Trengove, R. D., Oliver, R. P., and Solomon, P. S. (2008). A metabolomic approach to dissecting osmotic stress in the wheat pathogen *Stagonospora nodorum*. *Fungal Genet. Biol.* 45, 1479–1486. doi: 10.1016/j.fgb.2008.08.006

Ohm, R. A., Feau, N., Henrissat, B., Schoch, C. L., Horwitz, B. A., Barry, K. W., et al. (2012). Diverse lifestyles and strategies of plant pathogenesis encoded in the genomes of eighteen Dothideomycetes fungi. *PLoS Pathog.* 8:e1003037. doi: 10.1371/journal.ppat.1003037

Pascual, S., Melgarejo, P., and Magan, N. (2003). Water availability affects the growth, accumulation of compatible solutes and the viability of the biocontrol agent *Epicoccum nigrum*. *Mycopathologia* 156, 93–100.

Pascual-Ahuir, A., and Proft, M. (2007). The Sch9 kinase is a chromatin-associated transcriptional activator of osmostress-responsive genes. *EMBO J.* 26, 3098–3108. doi: 10.1038/sj.emboj.7601756

Pigné, S., Zykwinska, A., Janod, E., Cuenot, S., Kerkoud, M., Raulo, R., et al. (2017). A flavoprotein supports cell wall properties in the necrotrophic fungus *Alternaria brassicicola*. *Fungal Biol. Biotechnol.* 4:1. doi: 10.1186/s40694-016-0029-3

Pochon, S., Simoneau, P., Pigné, S., Balidas, S., Bataillé-Simoneau, N., Campion, C., et al. (2013). Dehydrin-like proteins in the necrotrophic fungus *Alternaria brassicicola* have a role in plant pathogenesis and stress response. *PLoS One* 8:e75143. doi: 10.1371/journal.pone.0075143

Pochon, S., Terrasson, E., Guillemette, T., Iacomi-Vasilescu, B., Georgeault, S., Juchaux, M., et al. (2012). The *Arabidopsis thaliana-Alternaria brassicicola* pathosystem: a model interaction for investigating seed transmission of necrotrophic fungi. *Plant Methods* 8:16. doi: 10.1186/1746-4811-8-16

Ravishankar, J. P., Suryanarayanan, T. S., and Muruganandam, V. (2006). Strategies for osmoregulation in the marine fungus *Cirrenalia pygmea* Kohl.(Hyphomycetes). *Indian J. Geo Mar. Sci.* 35, 351–358.

Reyes, J. L., Rodrigo, M.-J., Colmenero-Flores, J. M., Gil, J.-V., Garay-Arroyo, A., Campos, F., et al. (2005). Hydrophilins from distant organisms can protect enzymatic activities from water limitation effects in vitro. *Plant Cell Environ.* 28, 709–718. doi: 10.1111/j.1365-3040.2005.01317.x

Rodríguez-Porrata, B., Carmona-Gutierrez, D., Reisenbichler, A., Bauer, M., Lopez, G., Escoté, X., et al. (2012). Sip18 hydrophilin prevents yeast cell death during desiccation stress. *J. Appl. Microbiol.* 112, 512–525. doi: 10.1111/j.1365-2672.2011.05219.x

Sales, K., Brandt, W., Rumbak, E., and Lindsey, G. (2000). The LEA-like protein HSP 12 in *Saccharomyces cerevisiae* has a plasma membrane location and protects membranes against desiccation and ethanol-induced stress. *Biochim. Biophys. Acta* 1463, 267–278. doi: 10.1016/s0005-2736(99)00215-1

Sánchez-Fresneda, R., Guirao-Abad, J. P., Argüelles, A., González-Párraga, P., Valentín, E., and Argüelles, J.-C. (2013). Specific stress-induced storage of trehalose, glycerol and d-arabitol in response to oxidative and osmotic stress in *Candida albicans*. *Biochem. Biophys. Res. Commun.* 430, 1334–1339. doi: 10.1016/j.bbrc.2012.10.118

Sellam, A., Iacomi-Vasilescu, B., Hudhomme, P., and Simoneau, P. (2007). In vitro antifungal activity of brassinin, camalexin and two isothiocyanates against the crucifer pathogens *Alternaria brassicicola* and *Alternaria brassicae*. *Plant Pathol.* 56, 296–301. doi: 10.1111/j.1365-3059.2006.01497.x

Smyth, G. K., Michaud, J., and Scott, H. S. (2005). Use of within-array replicate spots for assessing differential expression in microarray experiments. *Bioinformatics* 21, 2067–2075. doi: 10.1093/bioinformatics/bti270

Soanes, D. M., Alam, I., Cornell, M., Wong, H. M., Hedeler, C., Paton, N. W., et al. (2008). Comparative genome analysis of filamentous fungi reveals gene family expansions associated with fungal pathogenesis. *PLoS One* 3:e2300. doi: 10.1371/journal.pone.0002300

Sweigard, J. A., Carroll, A. M., Kang, S., Farrall, L., Chumley, F. G., and Valent, B. (1995). Identification, cloning, and characterization of PWL2, a gene for host species specificity in the rice blast fungus. *Plant Cell* 7, 1221–1233. doi: 10.1105/tpc.7.8.1221

Tapia, H., and Koshland, D. E. (2014). Trehalose is a versatile and long-lived chaperone for desiccation tolerance. *Curr. Biol.* 24, 2758–2766. doi: 10.1016/j.cub.2014.10.005

Thouvenot, L., Deleu, C., Berardocco, S., Haury, J., and Thiébaut, G. (2015). Characterization of the salt stress vulnerability of three invasive freshwater plant species using a metabolic profiling approach. *J. Plant Physiol.* 175, 113–121. doi: 10.1016/j.jplph.2014.11.007

Tunnacliffe, A., and Wise, M. J. (2007). The continuing conundrum of the LEA proteins. *Naturwissenschaften* 94, 791–812. doi: 10.1007/s00114-007-0254-y

van den Bosch, F., Fraaije, B. A., van den Berg, F., and Shaw, M. W. (2010). Evolutionary bi-stability in pathogen transmission mode. *Proc. Biol. Sci.* 277, 1735–1742. doi: 10.1098/rspb.2009.2211

Wang, S., Liu, Y., and Xu, J. (2017). Comparison of different drying methods for recovery of mushroom DNA. *Sci. Rep.* 7:3008. doi: 10.1038/s41598-017-03570-7

Wartenberg, D., Vödisch, M., Kniemeyer, O., Albrecht-Eckardt, D., Scherlach, K., Winkler, R., et al. (2012). Proteome analysis of the farnesol-induced stress response in *Aspergillus nidulans*. The role of a putative dehydrin. *J. Proteomics* 75, 4038–4049. doi: 10.1016/j.jprot.2012.05.023

Winer, J., Jung, C. K., Shackel, I., and Williams, P. M. (1999). Development and validation of real-time quantitative reverse transcriptase-polymerase chain reaction for monitoring gene expression in cardiac myocytes *in vitro*. *Anal. Biochem.* 270, 41–49. doi: 10.1006/abio.1999.4085

Wong Sak Hoi, J., Beau, R., and Latgé, J.-P. (2012). A novel dehydrin-like protein from *Aspergillus fumigatus* regulates freezing tolerance. *Fungal Genet. Biol.* 49, 210–216. doi: 10.1016/j.fgb.2012.01.005

Wong Sak Hoi, J., Lamarre, C., Beau, R., Meneau, I., Berepiki, A., Barre, A., et al. (2011). A novel family of dehydrin-like proteins is involved in stress response in the human fungal pathogen *Aspergillus fumigatus*. *Mol. Biol. Cell* 22, 1896–1906. doi: 10.1091/mbc.E10-11-0914

Conflict of Interest Statement: The authors declare that the research was conducted in the absence of any commercial or financial relationships that could be construed as a potential conflict of interest.

Advantages of publishing in Frontiers

OPEN ACCESS
Articles are free to read for greatest visibility and readership

FAST PUBLICATION
Around 90 days from submission to decision

HIGH QUALITY PEER-REVIEW
Rigorous, collaborative, and constructive peer-review

TRANSPARENT PEER-REVIEW
Editors and reviewers acknowledged by name on published articles

Frontiers
Avenue du Tribunal-Fédéral 34
1005 Lausanne | Switzerland

Visit us: www.frontiersin.org
Contact us: info@frontiersin.org | +41 21 510 17 00

REPRODUCIBILITY OF RESEARCH
Support open data and methods to enhance research reproducibility

DIGITAL PUBLISHING
Articles designed for optimal readership across devices

FOLLOW US
@frontiersin

IMPACT METRICS
Advanced article metrics track visibility across digital media

EXTENSIVE PROMOTION
Marketing and promotion of impactful research

LOOP RESEARCH NETWORK
Our network increases your article's readership